

Bangor University

DOCTOR OF PHILOSOPHY

Methane in two temperate coastal marine environments

Heckers, Anette Hedwig Anuschka

Award date:
1999

Awarding institution:
Bangor University

[Link to publication](#)

General rights

Copyright and moral rights for the publications made accessible in the public portal are retained by the authors and/or other copyright owners and it is a condition of accessing publications that users recognise and abide by the legal requirements associated with these rights.

- Users may download and print one copy of any publication from the public portal for the purpose of private study or research.
- You may not further distribute the material or use it for any profit-making activity or commercial gain
- You may freely distribute the URL identifying the publication in the public portal ?

Take down policy

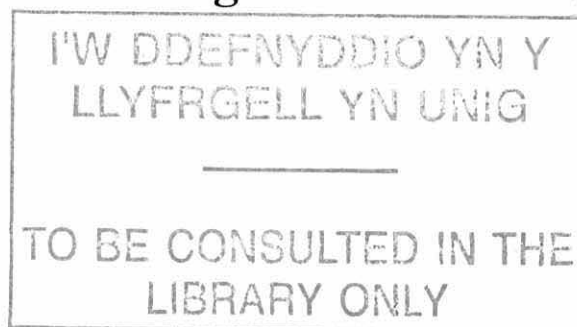
If you believe that this document breaches copyright please contact us providing details, and we will remove access to the work immediately and investigate your claim.

Download date: 09. Apr. 2024

Methane In Two Temperate Coastal Marine Environments

**A thesis submitted in accordance with the requirements of the
University of Wales for the degree of Doctor of Philosophy by**

Anette Hedwig Anuschka Heckers



**University of Wales, Bangor
School of Ocean Sciences
Menai Bridge
Ynys Môn LL59 5EY / U.K.**



Submitted: 19th September 1999 Viva voce: 2nd March 2000

Summary

Methane is the second most important greenhouse gas for which the oceans are a small but significant source. Coastal waters are usually very rich in methane, but the dynamics of production, consumption and distribution is only vaguely understood. In this project, the seasonal distribution of methane in the temperate coastal water column was studied in 1996 and 1997 at two contrasting sites off the Isle of Anglesey: the sheltered Menai Strait and the exposed area at Point Lynas. The study was based on methane concentration measurements conducted by headspace equilibration followed by gas chromatography. Although concentrations were 2- to 10-fold higher at the more sheltered location, the waters at both sites were supersaturated with methane relative to the atmosphere throughout the year (saturation ratios from 1.0 to 26.4) - which indicates a continuous source of supply. Following a fortnightly sampling programme both sites were found to display an increase in methane concentrations with temperature in the summer. However, high short-term variability in methane concentrations precludes confirmation of a 'seasonal' effect.

In an attempt to explain the distribution of water column methane in space and time potential sources and sinks were investigated for the Menai Strait. Advection of water from Liverpool Bay could account for as much as 20% of the concentration measured in the central Menai Strait, while other external sources such as the River Ogwen and treated and raw sewage discharges were only minor contributors. It was concluded that most of the Menai Strait methane was autochthonous. Methane production in the water column was only detected on one occasion. During a bloom of the heterotrophic dinoflagellate *Noctiluca scintillans* low methane production rates were observed during incubation experiments. This was the first recorded association between *Noctiluca* and methane production. It is speculated that methane is produced by bacteria that have previously been described to occur within *Noctiluca* cells (Lucas, 1982). Even during dense blooms of *Noctiluca*, however, the internal water column source for methane was calculated to be quantitatively insignificant for coastal zones.

By a process of elimination, muddy sediments were identified as the main source for methane in the water column, but the calculated diffusive flux rates were too low to account for all the methane that must be produced in the Menai Strait. The diffusive flux of methane from the sediment into the water showed no seasonal pattern.

The atmosphere is the main sink for methane from the water column. Wind was negatively correlated with methane concentrations and could account for much of the short-term variability in water column methane concentrations.

The atmospheric sink strength was estimated with three wind velocity-dependent gas exchange models. The discrepancies in estimates from different flux models were significant. Flux estimates varied by a factor of up to 7.5, with lower discrepancies at higher wind speeds. Although wind speeds were observed to be generally lower during the summer, more methane was calculated to evade the water in the summer than the winter. This suggests that the high concentrations in the summer water column must be caused primarily by increased production during the summer, and that the seasonal pattern observed in the water column is likely to be real. The fluxes to the atmosphere from Point Lynas and the Menai Strait were similar, suggesting that, despite large differences in concentrations, the source strengths at the two sites were also similar. The flux estimates demonstrated the inadequacy of existing gas exchange models as they produced different answers to the question of which of the two studied sites exported more methane to the atmosphere.

Although the broad features of the dynamics of methane in the study area have been characterised it was not possible to close the mass balance budget.

2.7 Methane analysis	2-11
2.7.1 Methane extraction from seawater	2-11
2.7.2 Methane extraction from sediments	2-14
2.7.3 Separation and quantification	2-15
2.7.4 Calculations of methane concentration and saturation	2-17
2.7.5 System performance, precision and accuracy of analysis	2-20
 Chapter 3 Results	 3-1
3.1 Seasonality of methane and other parameters in the coastal zone	3-1
3.2 Short-term variability of methane concentrations in the water column	3-7
3.2.1 Variations of methane concentrations at fixed stations	3-7
3.2.2 Spatial variability	3-12
3.2.3 Temporal variability	3-16
3.3 Methane production in the water column	3-17
3.4 Methane concentrations in external sources	3-21
3.5 Methane in Menai Strait sediments	3-23
3.5.1 Seasonal distribution	3-23
3.5.2 Spatial distribution	3-29
3.6 <i>In vitro</i> study of methane metabolism in sediments	3-34
 Chapter 4 Discussion	 4-1
4.1 Spatial and seasonal distribution of methane in the water column	4-1
4.2 Sources of methane in Menai Strait waters	4-5
4.2.1 External sources of methane in the Menai Strait	4-5
4.2.2 Internal sources of methane in the Menai Strait	4-8
4.2.2.1 Pelagic sources of methane	4-8
4.2.2.2 Methane from sedimentary sources	4-22
4.3 Sinks for methane in the Menai Strait	4-33
4.3.1 <i>In situ</i> oxidation of methane	4-34
4.3.2 Loss of methane to the atmosphere	4-36
4.4 Differences between Point Lynas and the Menai Strait	4-45
4.5 Methane budget for the Menai Strait water column	4-47
4.6 Conclusions	4-49
4.7 Suggestions for future research	4-51
 References	 Ref-1

Appendix 2-1	Wind speed profiles: calculating speeds at 10 m height	A2-1
Appendix 2-2	Cross calibration of wind velocities at Point Lynas and Pen-y-Bonc	A2-2
Appendix 2-3	Calibrations for methane headspace equilibration times using passive (A) and active (B) mixing	A2-3
Appendix 2-4	GC calibrations of carrier flow rates and temperatures	A2-4
Appendix 2-5	GC calibration curve for methane	A2-5
Appendix 2-6	Precision in dependence of signal intensity	A2-6
Appendix 3-1	Raw data for the seasonal pelagic study (Chapter 3.1)	A3-1
Appendix 3-2	Raw data for the short-term variability study (Chapter 3.2)	A3-5
Appendix 3-3	Raw data for Menai Strait water incubations (Chapter 3.3)	A3-10
Appendix 3-4	Raw data for sewage incubations (Chapter 3.4)	A3-13
Appendix 3-5	Raw data for the sediment study (Chapter 3.5)	A3-14
Appendix 3-6	Raw data for the sediment incubation experiment (Chapter 3.6)	A3-18
Appendix 4-1	Diffusion into spherical particles: Derivation of equation 4.1	A4-1
Appendix 4-2	Temporal distribution of methane in sediments at stations A, B, and C	A4-3

List of Figures

Figure 1.1	Biodegradation pathways yielding methanogen substrates	1-7
Figure 1.2	Chemical methane oxidation in the clean and polluted troposphere	1-12
Figure 1.3	Smoothed global distribution of the background concentration of atmospheric methane in the marine boundary layer in a 3-D representation	1-18
Figure 1.4	A 'typical' oceanic methane depth profile	1-21
Figure 1.5	The vertical zonation of some fundamental microbial processes in marine sediments, and a 'typical' depth profile of methane and sulphate concentrations in interstitial waters	1-23
Figure 2.1	Map showing the geographic location of the two sampling sites	2-1
Figure 2.2	Map of the investigated section of the Menai Strait	2-3
Figure 2.3	Photograph showing the Menai Strait at Menai Bridge	2-4
Figure 2.4	Photograph of the volumeter	2-12
Figure 2.5	Sequence adopted to obtain repeatable volumes for the gas and liquid phases for headspace equilibration	2-13
Figure 2.6	Sample (or standard) loading and injection for GC methane separation	2-16
Figure 3.1.1	Seasonal pattern of several pelagic and atmospheric parameters for 1996 at Point Lynas and for 1996 and 1997 in the Menai Strait	3-2
Figure 3.1.2	Seasonal pattern of methane saturations in the waters of the Menai Strait in 1996 and 1997, and at Point Lynas in 1996	3-6
Figure 3.2.1	Water column methane concentration and mean daily wind speed, sea and mean daily air temperature and atmospheric methane concentration, and water height between 27 May and 12 June 1997	3-8
Figure 3.2.2	Hourly changes in methane concentrations and mean wind speeds, air and sea temperatures, and atmospheric methane concentrations, and tidal heights on 7 July 1997 between 0725 and 1925 GMT	3-10
Figure 3.2.3	Short-term changes in water column methane concentrations, current speed and direction, and sea temperature and atmospheric methane concentrations on 22 August 1997 over five hours in the Menai Strait off Penmon	3-11
Figure 3.2.4	Map of the NW-Menai Strait showing the station numbers for the spatial variability studies	3-13
Figure 3.2.5	Methane concentrations in the water column at transect stations 1 to 5, 6 to 15, and 16 to 22	3-14

Figure 3.2.6	Depth profiles of methane concentrations in the water column at stations 23, 24 and 25 on 28 July 1997, and at St. George's Pier on 13 June 1996	3-15
Figure 3.2.7	Changes in water column methane concentrations during a 150 minutes drift study on the Menai Strait on 9 July 1997	3-16
Figure 3.3.1	Methane concentrations in live and control samples of unconcentrated and concentrated Menai Strait water during 48 hour incubation experiments	3-18
Figure 3.4.1	Methane concentrations in live and control incubations of raw and treated sewage	3-22
Figure 3.5.1.1	Pore water methane concentrations, temperature, and porosity at different sediment depths at station A between 7 August 1997 and 4 February 1998	3-25
Figure 3.5.1.2	Pore water methane concentrations, temperature, and porosity at different sediment depths at station B between 1 July 1997 and 4 February 1998	3-26
Figure 3.5.1.3	Pore water methane concentrations, temperature, and porosity at different sediment depths at station C between 7 August 1997 and 4 February 1998	3-27
Figure 3.5.1.4	20 cm depth-integrated pore water methane concentrations at stations A, B and C between 1 July 1997 and 4 February 1998	3-28
Figure 3.5.2.1	Sediment depth profiles of methane concentrations and porosity in a sand and a mud core	3-30
Figure 3.5.2.2	Sediment depth profiles of methane concentration, porosity and temperature in cores from the high, mid, and low shore	3-31
Figure 3.5.2.3	Methane concentrations and porosity of sediments at different depths in three neighbouring cores	3-33
Figure 3.6.1	Pore water methane concentrations in sediments incubated at 5°C, 15°C and 25°C for up to 65 days	3-35
Figure 3.6.2	Porosity in sediments incubated at 5°C, 15°C and 25°C for up to 65 days	3-36
Figure 4.1.1	Scatter plot of high-water methane concentrations and the squares of the mean daily wind speeds at Menai Bridge	4-4
Figure 4.2.1	Scatter diagrams showing the relationship between water temperature and methane concentration at Point Lynas and in the Menai Strait	4-11

Figure 4.2.2	Scatter diagrams showing the relationship between oxygen and methane concentrations in the Menai Strait and at Point Lynas	4-12
Figure 4.2.3	Effect of varying particle-associated oxygen consumption rates on the minimum diameter of a spherical particle with an anaerobic centre at different diffusion rates	4-17
Figure 4.2.4	Idealised methane profiles in sediments assuming various combinations of diffusion, production, and consumption of methane from the main deep production layer upward	4-24
Figure 4.2.5	Seasonal pattern in methane flux rates from muddy sediments at Menai Bridge	4-31
Figure 4.3.1	Model of methane exchange across the sea/atmosphere interface	4-38
Figure 4.5.1	Total methane budget for the Menai Strait water column in 1997	4-48

List of Tables

Table 1.1	1985 atmospheric concentrations, relative radiative forcing and lifetimes of major greenhouse gases, and their relative contributions to global warming in 1985 and to greenhouse forcing added during the 1980s	1-2
Table 1.2	Production processes and origins of source material for the three known forms of methanogenesis	1-4
Table 1.3	Sum reactions and energy yields from glucose oxidation, sulphate reduction, and some important methanogenic processes	1-8
Table 1.4	Estimates of net methane emissions and global methane consumption from natural and anthropogenic sources and sinks add up to give a measure for gross global production of methane	1-19
Table 1.5	Estimates of methane emissions from the oceans	1-21
Table 3.1.1	Mean daily wind speeds at the two meteorological stations in the Menai Strait and at Point Lynas. Mean annual, summer and winter values are given, where available with their standard deviations	3-3
Table 3.1.2	Mean monthly wind speeds at Pen-y-Bonc near Point Lynas and at the School of Ocean Sciences by the Menai Strait	3-3
Table 3.1.3	Means and standard deviations of overall and separated summer and winter atmospheric methane concentrations at Point Lynas in 1996 and above the Menai Strait in 1996 and 1997	3-5
Table 3.3.1	Sampling dates and water fractions for methane incubation experiments	3-19
Table 3.4.1	Methane concentrations in the Ogwen River, local tap water, and in treated and raw sewage	3-21
Table 3.5.1.1	Dates of core sampling at stations A, B and C	3-23
Table 3.5.1.2	Mean saturation ratios of methane at different depths in sediments of stations A, B and C	3-24
Table 3.5.1.3	Depth of maximum pore water methane concentrations at stations A,B and C on different dates, and the mean depth of maximum methane	3-28
Table 3.6.1	R ² -values, associated probabilities and numbers of paired observation for simple linear relationships between methane and sediment porosity in sediments incubated at three temperatures and analysed after four different incubation periods	3-37

Table 4.1.1	Surface water methane saturation ratios at different sampling locations and dates, and months of peak methane saturations from various literature sources	4-1
Table 4.1.2	Methane concentration ranges or rates of concentration changes for seasonal and various types of short-term variability	4-3
Table 4.1.3	Pearson's correlation coefficient between methane and the square of wind velocity over fifteen days.	4-4
Table 4.2.1	Pearson's correlation coefficients between methane and several biological, physical and chemical parameters at Point Lynas and in the Menai Strait	4-10
Table 4.2.2	Minimum particle diameter with anoxic centre calculated for different summer and winter rates of particle-associated oxygen consumption, and for minimum and maximum external oxygen concentrations in the Menai Strait	4-16
Table 4.2.3	Oxygen diffusion coefficients reported for various matrices	4-16
Table 4.2.4	Mean sediment porosity, sediment diffusion coefficient for methane, methane concentration gradient between production and surface layer, and diffusive flux of methane out of the sediments at various dates from the three stations in the Menai Bridge mudflats	4-26
Table 4.2.5	Mean methane diffusion flux rates and ranges out of the sediments at different locations in the sea	4-27
Table 4.2.6	Pearson's correlation coefficients, numbers of observations and significance at the 5% level of the relationship between pore water methane concentrations and sediment porosity	4-30
Table 4.2.7	Pearson's correlation coefficients, numbers of observations and significance at the 5% level of the relationship between pore water methane concentrations and sediment temperature	4-32
Table 4.2.8	Calculated 20 cm depth-integrated methane content in cores incubated at different temperatures and for different lengths of time	4-32
Table 4.3.1	Aerobic oxidation rates, concentrations and relative oxidation rates of methane in oxygenated coastal surface sea waters at different geographic locations and during different months	4-34
Table 4.3.2	Reports of methane sea-air flux estimates with the models used for studies at a number of sites	4-39
Table 4.3.3	Two-monthly mean wind velocities at the meteorological stations at the School of Ocean Sciences and Pen-y-Ffridd, and mean methane concentration differences	4-42

Table 4.3.4	Two-monthly mean methane transfer velocities for the central Menai Strait calculated using the models developed by Sebacher <i>et al.</i> 1983, Liss and Merlivat, 1986, and Wanninkhof, 1992	4-42
Table 4.3.5	Two-monthly mean methane flux estimates for the central Menai Strait as predicted from different models	4-42
Table 4.4.1	Two-monthly mean wind velocities and mean methane concentration differences at Point Lynas	4-45
Table 4.4.2	Two-monthly mean methane transfer velocities for Point Lynas calculated with the models developed by Sebacher <i>et al.</i> 1983, Liss and Merlivat, 1986, and Wanninkhof, 1992	4-45
Table 4.4.3	Two-monthly mean methane flux estimates for Point Lynas as predicted from different models	4-45
Table 4.4.4	1996 methane flux rates from the Menai Strait and Point Lynas calculated with three different models, and the ratio between the flux rates from the two sites	4-46
Table 4.5.1	Mean methane concentrations and flux rates in the Menai Strait in 1997	4-47
Table 4.5.2	Area, volume and flow rates of Menai Strait water, flow rates of sewage and the River Ogwen, and area estimate for muddy sediments	4-47

Glossary of Terms

A	Arrhenius constant
b	Distance (cm) from the centre of a spherical particle
B.P.	Before the present time
c	Rate of particle associated oxygen consumption ($\mu\text{moles dm}^{-3} \text{ s}^{-1}$)
C	Carbon
C ₁	Containing one carbon atom
C _{dil}	Molar methane concentration in diluting water
C _{eq}	Molar methane concentration in equilibrium with the atmosphere
C _G '	Molar methane concentration in headspace gas after equilibration
C _{G(atm)}	Molar methane concentration in atmosphere
C _{int}	Molar methane concentration in interstitial water
C _{sludge}	Molar methane concentration of the sludge in the syringe
C _w	Molar methane concentration in water
C _w '	Molar methane concentration in water phase after equilibration
Chl a	Chlorophyll a concentration
CFC	Chlorofluorocarbons
CH ₄	Methane
CMDL	Climate Monitoring and Diagnostics Laboratory
CO ₂	Carbon dioxide
CV	Coefficient of variation
D _{Msea}	Diffusion coefficient of methane in sea water ($\text{cm}^2 \text{ s}^{-1}$)
D _{Msed}	Diffusion coefficient of methane in sediments ($\text{cm}^2 \text{ s}^{-1}$)
D _{Mwater}	Diffusion coefficient of methane in distilled water ($\text{cm}^2 \text{ s}^{-1}$)
D _O	Diffusion coefficient of oxygen ($\text{cm}^2 \text{ s}^{-1}$)
DCR	Dark community respiration
DF	Degrees of freedom
DMS	Dimethylsulphide
DMSP	Dimethylsulphoniopropionate
e	Void ratio of sediments
E _a	Activation energy for diffusion of methane in water (kJ mol^{-1})
F _{CH₄}	Methane flux density ($\text{mol cm}^{-2} \text{ h}^{-1}$)
FID	Flame ionisation detector
GC	Gas chromatograph

GCP	Gross community production
GF/F	Glass fibre filter
GMT	Greenwich mean time
G_s	Particle specific gravity
$HgCl_2$	Mercuric chloride
IR	Infrared
J_M	Diffusive methane flux through sediment-water interface ($\mu\text{mol m}^{-2} \text{d}^{-1}$)
k	Kilo- (10^3) von Kármán constant
k_{sw}	Transfer velocity for methane through sea water (cm h^{-1})
LM	Liss-Merlivat (1986) model of gas exchange
M	Molarity (number of moles per dm^3)
M_G	Methane concentration in sample headspace (ppmv/v)
M_{STD}	Methane concentration in a certified gas standard (vol/vol)
m	Milli- (10^{-3})
m_D	Mass of dry saline sediment sample (g)
m_{dil}	Mass of diluting water (g)
m_{int}	Mass of interstitial water in sediment sample (g)
m_P	Mass of dry particles in sediment sample (g)
m_W	Mass of water in syringe filled with sediment sludge (g)
MMO	Methane monooxygenase
N	Nitrogen Number of observations
N_2O	Nitrous oxide
$NAD^+/NADH$	Nicotinamide adenine dinucleotide, a hydrogen transfer coenzyme used in redox reactions
NCP	Net community production
NO_x	Nitrogen oxides
NOAA	National Oceanic and Atmospheric Administration
n	Porosity, Nano- (10^{-9})
O_2	Oxygen
O_3	Ozone
O_b	Oxygen concentration ($\mu\text{mol dm}^{-3}$) at distance b from particle centre
O_c	Oxygen concentration ($\mu\text{mol dm}^{-3}$) in particle centre
O_{ex}	Oxygen concentration ($\mu\text{mol dm}^{-3}$) in external matrix

OH	Hydroxyl radical
P	Pressure (Pa or N m ⁻²)
PA _G	Integrated peak area of sample headspace
PA _{STD}	Integrated peak area of methane standard
PLOT column	Porous layer open tubular (GC) column
POC	Particulate organic carbon
POM	Particulate organic matter
PON	Particulate organic nitrogen
Phaeo	Phaeopigment concentration
p	Pico- (10 ⁻¹²)
	Probability
ppbv	Parts per billion on volume basis (10 ⁻⁹)
ppmv	Parts per million on volume basis (10 ⁻⁶)
pptv	Parts per trillion on volume basis (10 ⁻¹²)
p _w	Saturation water vapour pressure (Pa or N m ⁻²)
r	Pearson's correlation coefficient
ra	Radius (cm) of a spherical particle
R	Molar gas constant (=8.132 N m K ⁻¹ mol ⁻¹)
R ²	Square of Pearson's correlation coefficient
rRNA	Ribosomal ribose nucleic acid
RO-water	Reverse osmosis water
S	Salinity
SE	Standard error
SD	Standard deviation
SF ₆	Sulphur hexafluoride
SHB	Sebacher, Harris and Bartlett (1983) model of gas exchange
SOS	School of Ocean Sciences
Sc	Schmidt number
T	Temperature (°K)
	T-value
t	Temperature (°C)
Tg	Tera gram (10 ¹² g)
UCES	Unit of Coastal and Estuarine Studies
UV	Ultraviolet
u	Wind speed (m s ⁻¹)
u ₁₀	Wind speed at 10 m above ground/sea surface (m s ⁻¹)

u_f	Friction velocity
u_z	Wind speed at height z above ground/sea surface (m s^{-1})
V	Volume of water saturated sediment sample (dm^3)
∇^2	Laplace operator
V_A	Volume of water in syringe filled with sludge (dm^3)
V_G	Volume of headspace gas (dm^3)
V_P	Volume of particle material in sediment sample (dm^3)
V_v	Volume of void spaces in sediment (dm^3)
V_w	Volume of water or sludge (dm^3)
W	Wanninkhof (1992) model of gas exchange
z	Depth (cm) or height (m)
z_0	Roughness length (m)
β	Bunsen solubility coefficient
$\beta_{in\ situ}$	Bunsen solubility coefficient under <i>in situ</i> conditions
μ	Micro- (10^{-6})
θ	Sediment tortuosity
ω	Moisture content of sediment

*It isn't important to come out on top,
What matters is to be the one who comes out alive.*

Bertholt Brecht (1898-1956)

Acknowledgement

Doing a Ph.D. is not easy! To complete this challenge I relied on the help and support of others in matters of intellect, instrumentation, emotional well being and - alas - finance. The most vital support came from my parents, who suffered through their second Ph.D.s with me and acted as emotional and financial crutches whenever I called on them. Also my sister Caroline listened compassionately and patiently to all my troubles. Sorry for all the 'Blut im Ohr', Inalein!

My supervisor Professor Peter J. leB. Williams made sure that I never lost track of my time and objectives and was a most constructive and thorough proof-reader of my thesis. Dr. Carol Robinson played perhaps the most difficult role in this thesis as she had to change dynamically from being a compassionate and understanding friend to a scientific advisor, to a second supervisor during the writing of chapters 1 and 3, and back to 'just' a friend. Dr. Cliff Law, PML's chief biogas man, and his team - particularly Roger Ling - taught me many little tricks of the trade and - most importantly - to trust my own work and thoughts. I am furthermore indebted to Cliff for reading and correcting this thesis, and for enabling me to use PML's excellent facilities during the writing period. Professor Mary Scranton was an important first contact and very kindly guided a beginner via e-mail to understand headspace equilibration techniques and calculations. A grateful memory goes also to Varian's Alan Louis, who taught me the usage of GCs and was always available to discuss the particular set-up required for gas analysis.

I hold very warm memories of the support Sandra Hague gave when we sampled at Point Lynas and struggled with a periodically bad-tempered and for some time enigmatic GC. Sandie, you add colour to the School of Ocean Sciences and often lightened my 'heart of darkness'. Paul Williams, selected for his strength and young age to come and play with me in the mudflats, made a tough job easy, fast and fun. Tracy Bentley, the 'Welsh dragon' in the group, supported this project in many ways. We sampled the Menai Strait together, she kept the lab tidy, taught me the established techniques used within our group and analysed the Menai Strait POC/PON samples for me. As we became close friends during the project her support never stopped even after working hours. 'Big' Gwyn Jones navigated me safely through the Menai Strait and lent me his immense knowledge about the area - which exceeds recorded data. Malcolm Budd helped with all aspects of sea water, algal cultures and coulter counting and Vivian Ellis taught me how to analyse my POC and PON samples, and how research at SOS works.

I also want to thank the workshop lads David Gill, Elwyn Jones and Mike Jones for designing and building the volumeter and corers, and for making me feel special even in my muddy boots!

The friendly help from the library staff in securing hundreds of references is warmly acknowledged. I also want to thank all the cleaners who good-humouredly put up and away with the rather dirty habits I developed in 1997...

I am indebted to Steven Barkworth for his meteorological data and his mum for ample cups of tea at Pen-y-Bonc, to Brian Owen for the wind data from Pen-y-Ffridd, and to Dr. Des Barton for the School of Ocean Sciences' logged wind and salinity data. Dr. Rowena White helped me to identify and enumerate collected plankton samples, and whisked me off to an African paradise when my spirits needed urgent re-charging.

Dr. Dominique Lefèvre solved many of my computer mysteries. Some of my fellow-strugglers, especially Suse Kratzer, Maite Mascaro, Claudia Castellani, Tristan Sjöberg and Laura Cardenas, made useful comments and were always open for scientific and strategic discussions.

Finally I am thankful to you, Axel, for being there for me in whatever way I needed you, for encouraging, listening, understanding, proof-reading, suggesting, reminding and discussing, and for making me happy.

Thank you all.

This project was sponsored by the Research Committee of the School of Ocean Sciences.

*Although Nature has denied us much understanding,
and leaves us uncertain about many things,
She never causes error.
Error comes from our disposition to judge and decide
Even where our limitations make it impossible to judge and decide.*

Immanuel Kant
(German philosopher, 1724-1804)

*Everything has already begun before,
The first line of the first page of every novel
Refers to something that has already happened outside the book.*

Italo Calvino (1923-1985)

Chapter One

Introduction

This introductory chapter provides the context for the reported research project and outlines the importance of the research in the wider framework of biogeochemistry. The role methane plays in the environment is briefly summarised. The different processes of methane production (Section 1.2) and consumption (Section 1.3) are described, and the distribution of methane in the atmosphere and the emission sources and sinks are quantified (Section 1.4). Specific emphasis is given to the methane distribution and budget in the marine environment. Finally the aim and specific objectives for this thesis are stated.

1.1 The role of methane in the environment

Methane is the simplest organic molecule and exists under the conditions presently found on Earth mainly in a gaseous state and also in the form of clathrate deposits. As a relatively insoluble gas, most free methane rises from its terrestrial, aquatic or deep-Earth production sites into the atmosphere. In the atmosphere methane is the most abundant hydrocarbon and plays an influential and complex role in climate control, both as a greenhouse gas and as a constituent of the atmospheric ozone cycle.

The Earth's climate is ultimately dependent upon incoming solar radiation and upon a set of non-conservative, radiatively active gases and particles which control the trapping of this energy (Shine *et al.*, 1990; Houghton *et al.*, 1992). Energy from the sun enters the Earth's atmosphere as short-wave ultraviolet (UV) radiation, of which approximately one third is reflected back into space while two thirds are absorbed by the atmosphere and the planet surface (Ramanathan, 1988; Houghton *et al.*, 1992). For the climate to be in equilibrium, the absorbed solar energy must be balanced by outgoing thermal energy, which is emitted in the form of long-wave infrared (IR) radiation. The outgoing IR radiation is in part absorbed and thus trapped by particles and gases - such as water vapour, carbon dioxide (CO₂), methane (CH₄), nitrous oxide (N₂O), tropospheric ozone (O₃) and lately by a number of man-made chlorofluorocarbons (CFCs) (Shine *et al.*, 1990). There is a discrepancy in the absorption and emission of thermal energy by these radiatively active constituents resulting from different temperature dependencies

of the two processes (for more detail see Dickinson and Cicerone, 1986). The captured energy is thought to result in an increase in temperature in the lower Earth atmosphere, a process referred to as the greenhouse effect (Shine *et al.*, 1990). Historically, the Earth's natural greenhouse effect is believed to have resulted in a temperature regime that provided favourable and relatively stable conditions for the evolution of life. The extent to which the decrease or increase in atmospheric greenhouse gas concentrations causes changes in global climate, however, is still debated (Cicerone, 1988).

Besides water vapour, carbon dioxide and the array of CFCs, methane is the next most important greenhouse gas when considering abundance, relative radiative forcing (*i.e.* the radiative forcing of methane relative to carbon dioxide on a molecule-per-molecule basis) and atmospheric lifetime (Table 1.1).

Table 1.1 1985 atmospheric concentrations, relative radiative forcings, and present atmospheric lifetimes of the major greenhouse gases, and their respective relative contributions to global warming in 1985 and to greenhouse forcing added during the 1980s.

Gas	1985 concentration *	Radiative forcing ‡	Present life-time (year) †	1985 warming contribution †	1980s added forcing †
CO ₂	345 ppmv	1	230	71 %	57 %
CH ₄	1.7 ppmv	21	7 *	9 %	12 %
N ₂ O	0.3 ppmv	206	160	3 %	6 %
CFCs	0.2-0.4 ppbv	>10,000	15 – 120	10 %	25 %

(Sources: * Dickinson and Cicerone, 1986; † Lashof and Ahuja, 1990; ‡ Shine *et al.*, 1990; *Tyler, 1991)

Analysis of air bubbles from polar ice cores, which contain past atmospheres, has shown that atmospheric methane concentrations have increased more than any other natural greenhouse gas, from pre-industrial concentrations of about 0.7 μ -atmospheres (Rasmussen and Khalil, 1984) to 1.84 μ -atmospheres in 1994 (Simmonds *et al.*, 1996) at an annual rate of increase of approximately 1% (Rasmussen and Khalil, 1981a; Rasmussen and Khalil, 1984; Steele *et al.*, 1987; Pearman and Fraser, 1988; Stevens and Engelkemeir, 1988; Khalil and Rasmussen, 1990). This increase has been attributed mainly to human activities and population growth (Rasmussen and Khalil, 1984; Houghton and Woodwell, 1989; Hogan *et al.*, 1991). Other greenhouse gases have also been increasing due to human activities. This so-called man-enhanced greenhouse effect may be leading to climate warming at a scale that may be damaging to our socio-economic and cultural structures and is potentially destabilising for the present global ecosystem. The scale of increase of atmospheric methane over the past 200 years is extraordinary, as ice core studies have revealed that the atmospheric methane concentrations only varied between 0.35 and

0.8 μ -atmospheres over the 161,000 years prior to industrialisation (Rasmussen and Khalil, 1984; Cicerone, 1988). During glacial periods atmospheric methane concentrations were around 0.35 μ -atmospheres and rose to 0.65 μ -atmospheres during interglacial times (Cicerone, 1988).

Methane is constantly produced and released into the atmosphere, but concentrations remain relatively stable due to removal processes. Methane oxidation processes in the atmosphere indirectly influence the concentrations of stratospheric water vapour, tropospheric ozone, carbon monoxide and some CFCs (Cicerone and Oremland, 1988; Crutzen, 1991). This is described in greater detail in section 1.3. The indirect feedback effects, caused by atmospheric methane oxidation, that could support or mitigate global warming, might be of a similar importance for the Earth's climate as the effect of methane as a greenhouse gas.

During atmospheric methane oxidation, over 10^9 tonnes of oxygen are removed annually from the atmosphere. As a sink for oxygen, methane helps to avoid a build-up of atmospheric oxygen concentrations, which could otherwise enhance the emergence of landscape fires worldwide (Lovelock, 1982). The contribution of methane oxidation to the sink strength of oxygen is, however, very small. Respiration consumes annually approximately 10^{11} tonnes of oxygen, one hundred times more than is removed by methane oxidation.

Methane is thus important in the climatic system of our planet. It is furthermore of significance in the biogeochemistry of life.

In the dominant photosynthesis-based food chain, methane is a final breakdown product of the anaerobic biodegradation process and is thus an anaerobic equivalent of carbon dioxide. In anaerobic ecosystems the production of methane can furthermore remove free hydrogen (=interspecies hydrogen transfer) which would otherwise destroy the conditions under which fermenting bacteria produce the substrates methanogens require (Bryant *et al.*, 1967; Ianotti *et al.*, 1973; Mah *et al.*, 1977; Rudd and Taylor, 1980; Ward and Winfrey, 1985; Boone, 1991).

Methane producers are considered to have played an important role in the evolution of life. They are among the oldest surviving life forms (Hahn, 1982), and might well have been the most important decomposers before free oxygen became abundant in the atmosphere. There is genetic evidence that methane producing organisms were the host partner in the hypothesised endosymbiotic development of the eukaryotic cell (Martin and Müller, 1998), the cell line that gave rise through the protists to all multicellular plants and animals.

In the 1970s, oceanographers discovered warm and hot hydrothermal vents at the spreading centres of the deep ocean floor, through which various compounds from deep within the Earth enter the water. These vents are characterised by dense populations of large and unusual fauna (Spiess *et al.*, 1980). Also cold, often pockmark-shaped, gas seeps were discovered, which exist worldwide and are often, but not always (Dando *et al.*, 1991), characterised by unusual biological activity (Hovland and Judd, 1988; Judd and Hovland, 1992). These vents emit gases which are thought to originate in part from abiotic production processes in the deep Earth (Gold and Soter, 1980; Jannasch and Mottl, 1985), and in part from biological production close to the surface using substrates emitted from deep below (Baross *et al.*, 1982; Jannasch and Mottl, 1985; Laier *et al.*, 1992). Methane is often an abundant gas in these emissions (Lilley *et al.*, 1982; Martens and Klump, 1984; Laier *et al.*, 1992; Dando *et al.*, 1994). Microbial methanogenesis from geothermal carbon dioxide and hydrogen represents a chemosynthetic mechanism of primary production (Lilley *et al.*, 1982; Jones *et al.*, 1983; Jannasch and Mottl, 1985). The abiotic and biogenic methane is used by methane oxidising bacteria - referred to as methanotrophs. Both methanogenesis and methanotrophy in hydrothermal vent systems therefore form the base of a light- and surface-independent food chain (Jones *et al.*, 1983; Jannasch and Mottl, 1985; Brooks *et al.*, 1987; Kochevar *et al.*, 1992; Ward and Kilpatrick, 1993).

Methane is thus involved in numerous chemical processes and in the production and consumption of various molecular species in the atmosphere. It is an important greenhouse gas, is suggested to have played an important role in the early evolution of life, is an end product of the anaerobic biodegradation of organic material, and fuels a photosynthesis-independent food-chain in hydrothermal vent systems.

1.2 Methane production

Three general production processes are known to lead to the formation of methane: a.) the biological production of methane from a variety of C₁-substrates by a group of archaeobacteria, b.) the thermogenic production of methane from complex organic matter, and c.) the abiogenic production from inorganic source materials (Table 1.2).

Table 1.2 Production processes and origins of source material for the three known forms of methanogenesis.

	Production process	Source material
Biogenic	Microbial biodegradation	Organic
Thermogenic	Thermal biodegradation	Organic
Abiogenic	Deep Earth and interstellar thermal production	Inorganic

Biogenic production of methane

Scientific investigations into methane and its microbiological production began in the mid-19th century. While 'combustible air' emanating from aquatic muds was first scientifically reported in 1776 by the Italian physicist Alessandro Volta (in Wolfe, 1993), it was not until 1868 that Béchamp, a student of Louis Pasteur's, discovered the microbial basis of methane production. The substrate requirements of methane producing bacteria were first studied by Söhngen in 1906. Barker isolated the first methane producing bacterial culture in 1936, and the first pure culture was prepared in 1947 by Schnellen (in Oremland, 1988).

Only a few species of bacteria are capable of methane production - referred to as methanogenesis - and are called methanogens. They are morphologically very diverse and occur in a variety of sizes and forms such as rods, cocci, spirilla, sarcina or flattened plates. They comprise motile and nonmotile strains which are often Gram-positive but can also be Gram-negative or Gram-variable (Bryant, 1974; Kandler and Hippe, 1977).

Common to all methanogens, but not quite unique, is a blue-green fluorescing electron carrier, coenzyme F₄₂₀ (Cheeseman *et al.*, 1972), which allows their tentative identification using fluorescence microscopy (Doddema and Vogels, 1978). Biochemically, methanogens differ greatly from the majority of bacteria. The cell walls of methanogens for example do not contain the peptidoglycans characteristic of other bacteria, but consist of group-specific lipids such as isoprenoids or squalenes (DeRosa *et al.*, 1977; Kandler and Hippe, 1977; Kandler and König, 1978; Holzer and Oró, 1979; Tornabene *et al.*, 1979; Comita and Gagosian, 1983; Smith and Floodgate, 1992). Therefore methanogens are insensitive to antibiotics that block peptidoglycan synthesis in other bacteria (Hilpert *et al.*, 1981). Since some of these unusual cell wall lipids were found in rocks dating back to the Archean (> 2.7 x 10⁹ years B.P.), methanogens may belong to the oldest surviving organisms on Earth (Hahn, 1982). Sequence analysis of their 16S ribosomal ribose nucleic acid (rRNA) shows methanogens to be genetically distinct from other bacterial groups (Fox *et al.*, 1977). The characteristic differences of methanogen cells from the typical bacterial cell justify the taxonomic re-evaluation of methanogens as organisms that are nowadays classified as belonging to a heterogeneous kingdom, shared only with halophiles and thermoacidophiles. The kingdom 'Archaea' or 'Archaeobacteria' is thus separated from the prokaryotic eubacteria as well as the eukaryotes (Balch *et al.*, 1979). Archaeobacteria are believed to have evolved from a very ancient divergence in the cell lines of early prokaryotic life forms (Balch *et al.*, 1977; Kandler and König, 1978).

Most methanogens require a low reducing potential (E_h below -0.33 V) and a circumneutral pH range to grow (Conrad, 1989; Valentine *et al.*, 1994). They are also strict anaerobes and most

strains are thought to die when exposed to even low concentrations of oxygen due to an irreversible disassociation of their F_{420} -hydrogenase enzyme complex (Robertson and Wolfe, 1970; Oremland, 1988). There is, however, evidence that some methanogens may be able to withstand even long periods of exposure to oxygen without losing their viability (Zehnder and Wuhrmann, 1977; Kiener and Leisinger, 1983). For example, unbuffered suspensions of starved cells from three of five tested methanogen species withstood exposure to laboratory air for up to 30 hours without reducing the numbers of colony forming units (Kiener and Leisinger, 1983). This tolerance could allow methanogens to travel between anaerobic sites. Methanogens rely on an aerobic bacterial consortium, which utilises oxygen to function and survive, and thereby create and maintain the anaerobic methanogen habitat.

A thriving aerobic and anaerobic bacterial consortium is also important for methanogens because it breaks down the complex organic detritus molecules into the simple C_1 -substrates methanogens require (Figure 1.1). Methanogens metabolise only a relatively limited suite of simple substrates to provide them with carbon and energy for growth. Since the work of Söhngen in 1906, formate, acetate and the combination of hydrogen with carbon dioxide have been known to be methanogen substrates (in Oremland, 1988). Also methanol, which is produced during the anaerobic decomposition of plant pectins (Schink and Zeikus, 1980), and methylated amines, breakdown products of the algal osmoprotectant glycine betaine (Kniefel, 1979), have been identified as methanogen substrates (Hippe *et al.*, 1979). In 1986 Kiene and co-workers found that some methanogens also grow well on reduced methylated sulphur compounds such as dimethylsulphide (DMS), dimethyldisulphide and methane thiol, degradation products of the algal osmoregulatory compound dimethylsulphio-propionate (DMSP). Also carbon monoxide has been described to serve as a substrate for some methanogens, but its oxidation yields very little energy and is thus considered unimportant as a methanogen substrate (Daniels *et al.*, 1977). While a few methanogen strains can grow on most of the mentioned substrates (Mah *et al.*, 1977; Mah, 1980), many are very specific and will only grow on one or two groups of substrates (König and Stetter, 1982; Sowers and Ferry, 1983).

The temperature range for methanogen activity is broad, ranging at least from 0°C in glacier ice (Berner *et al.*, 1975) to 85°C in hydrothermal vents (Zeikus and Wolfe, 1972; Stetter *et al.*, 1981; Jones *et al.*, 1983). Most methanogens are mesophilic with temperature optima around 35°C.

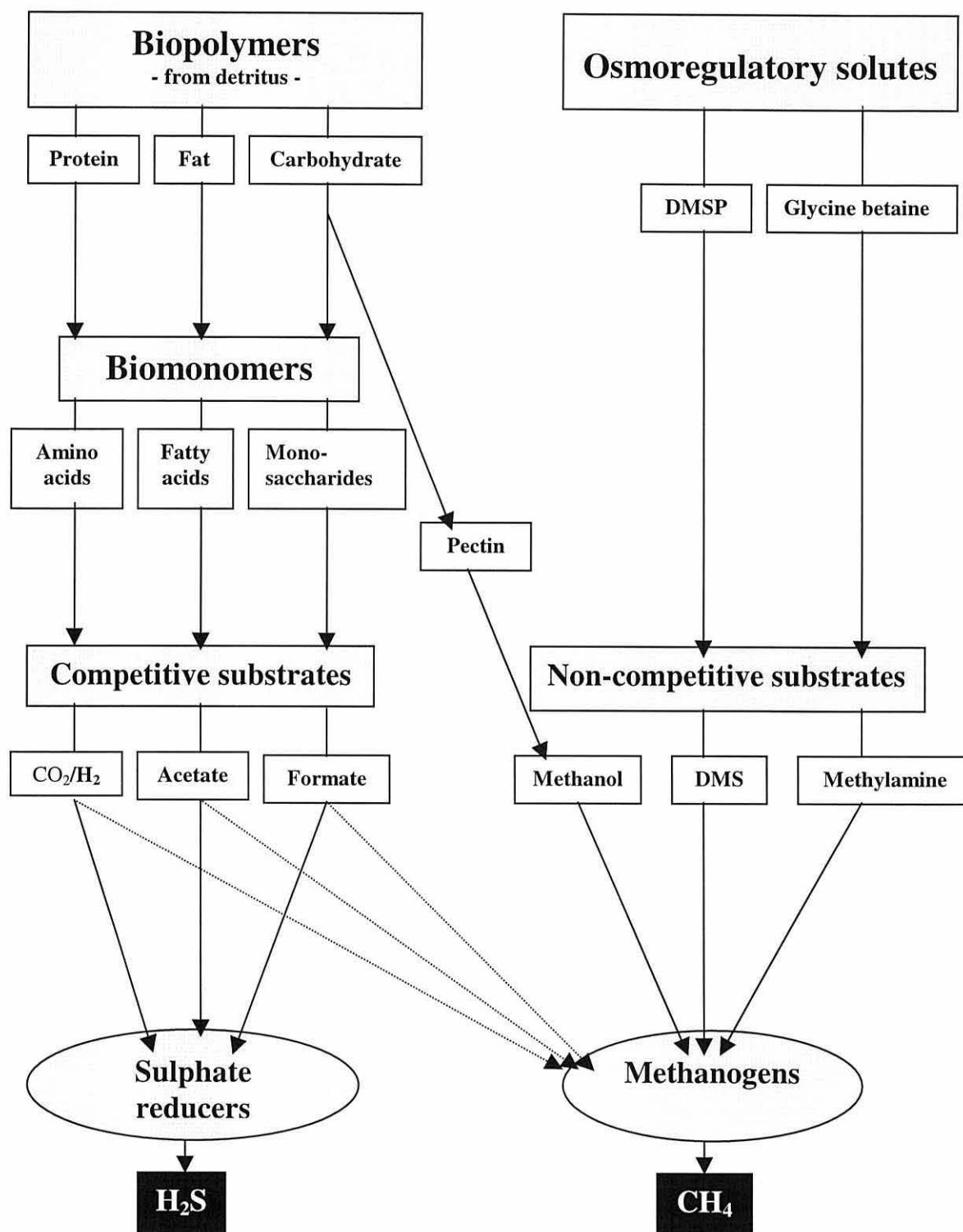


Figure 1.1 Biodegradation pathways yielding methanogen substrates. In sulphate rich environments, competitive substrates are mostly utilised by sulphate reducers. Of the carbon dioxide/hydrogen substrate only the hydrogen is competed for by both groups. The carbon dioxide is utilised solely by methanogens.

The different substrate-dependent methanogenic pathways yield varying quantities of energy (Table 1.3, reactions 3 to 8) but compare unfavourably to the energetic gains, for example from acetate oxidation by sulphate reduction or from aerobic oxidation (Table 1.3, reactions 1 and 2). Due to this, the doubling time for growth is generally long (Large, 1983) and can be up to nine

days for *Methanotherix soehngeni* (Zehnder *et al.*, 1980). Only thermophilic methanogens can have very rapid doubling times. The thermal vent strain *Methanococcus jannaschii* has been reported to duplicate in 26 minutes at 85°C (Jones *et al.*, 1983).

Table 1.3 Sum reactions and energy yields from glucose oxidation (1), sulphate reduction from acetate (2), and important methanogenic processes (3-8).

		Reaction	ΔG (kJ mol ⁻¹)
1	$C_6H_{12}O_6 + 6 O_2$	$\rightarrow 6CO_2 + 6H_2O$	-2874
2	$CH_3COOH + H_2SO_4$	$\rightarrow 2 CO_2 + H_2S + H_2O$	-57
3	CH_3COOH	$\rightarrow CH_4 + CO_2$	-36
4	$(CH_3)_2S + H_2O$	$\rightarrow 1.5CH_4 + 0.5 CO_2 + H_2S$	-74
5	$4(CH_3)_3NH^+ + 6H_2O$	$\rightarrow 9CH_4 + 3CO_2 + 4NH_4^+$	-76
6	$4CH_3OH$	$\rightarrow 3CH_4 + CO_2 + 2H_2O$	-106
7	$4HCOO^- + 2H^+$	$\rightarrow CH_4 + CO_2 + 2HCO_3^-$	-119
8	$4H_2 + CO_2$	$\rightarrow CH_4 + 2H_2O$	-130

Source: 1: Siewing (1980); 2: Schönheit *et al.* (1982); 3-8: Oremland (1988) and Müller *et al.* (1993)

The oxygen sensitivity and the specific substrate requirements of methanogens restrict their occurrence to substrate-rich anaerobic environments such as waterlogged soils (freshwater and marine sediments, marsh soils, wetlands, rice paddies), the intestinal tracts of animals, landfill sites, rubbish dumps and sewage plants (Zeikus, 1977). To a lesser extent methanogens also occur inside detrital particles, anoxic waters, anaerobic wetwood of trees infected with soil bacteria (Zeikus and Ward, 1974), and in the anaerobic dental plaque of primates (Kemp *et al.*, 1983). The strengths of the different sources are described in the budget (Section 1.4.2).

In sulphate-rich anaerobic environments such as marine sediments methanogens are commonly outcompeted by sulphate reducing bacteria which utilise some of the same substrates, particularly acetate and hydrogen (Figure 1.1) (Martens and Berner, 1974; Sansone and Martens, 1981; Sørensen *et al.*, 1981; Martens, 1982; Whiticar, 1982; Lovley and Klug, 1983; King *et al.*, 1983; Ward and Winfrey, 1985; Schmaljohann, 1996). Sulphate reducers outcompete methanogens because they have a higher substrate affinity (Kristjansson *et al.*, 1982; Lovley *et al.*, 1982; Schönheit *et al.*, 1982; Robinson and Tiedje, 1984) and are more energy efficient than methanogens (Table 1.3) (Claypool and Kaplan, 1974; Zehnder, 1978; Lovley *et al.*, 1982; Stanier *et al.*, 1987). In sulphate-rich anaerobic environments therefore only those methanogens can thrive which use substrates not commonly utilised by sulphate reducers, such as methanol (Oremland *et al.*, 1982; King, 1984a), methylated amines (Oremland *et al.*, 1982; Sowers and Ferry, 1983; King, 1984b; Cynar and Yayanos, 1991; Sieburth, 1993) or DMS (Kiene *et al.*,

1986; Oremland *et al.*, 1989) (Figure 1.1). In marine sediments the majority of biogenic methane, however, appears to be produced below the sulphate reducing zone where sulphate concentrations are low (Cappenberg, 1974; Bernard, 1979; Whiticar, 1982; Schmaljohann, 1996). Although the majority of methanogens are thought to live in the upper few meters and thus the youngest deposits of the sediment column, low concentrations of viable methanogens and methanogenic activity have been detected as deep as 750 m in the groundwaters of the Caspian Depression (Belyaev and Ivanov, 1983). The rate of methanogenesis at these depths - as in other oligotrophic environments - appears to be substrate-limited (Ward and Winfrey, 1985).

Methanogens occur within the digestive tracts of a variety of animals, particularly herbivorous mammals, xylophagous (= wood eating) insects, and herbivorous fish and zooplankton. In herbivorous mammals such as cows, goats and sheep they live in large numbers in the rumen, and in horses and rabbits in the caecum. Here the ingested cellulose, which the mammals themselves cannot digest, is biodegraded by a consortium of anaerobic bacteria. Also about one-third of the adult human population harbours methanogens in their large bowel and faeces and thus emit methane (Nottingham and Hungate, 1968). The hindgut regions of scarab beetles, cockroaches (Bracke *et al.*, 1979) and termites (Zimmermann *et al.*, 1982; Odelson and Breznak, 1983; Seiler *et al.*, 1984; Sugimoto *et al.*, 1998) are inhabited by active methanogens, and termites particularly are considered to be a globally significant source for atmospheric methane (Zimmermann *et al.*, 1982; Seiler *et al.*, 1984; Sugimoto *et al.*, 1998). Relatively little research has been carried out with respect to methanogens in the digestive tracts of marine animals. These might, however, hold the explanation to what has been termed the oceanic 'methane paradox', the anaerobic production of methane in oxygenated waters (Scranton and Brewer, 1977; Ward *et al.*, 1987; Scranton and McShane, 1991). Oremland (1979) found viable methanogens within the gut portion of two fish species and also in a mixed coastal plankton sample dominated by copepods. Sieburth (1987) demonstrated the existence of viable methanogens within the oxygenated water column when he found methane to be produced in anaerobically incubated water samples. More recently, Bianchi *et al.* (1992) and Marty (1993) proved the presence of viable methanogens associated both with copepods and their faecal pellets. In 1994 DeAngelis and Lee brought direct evidence for methane production in oxygenated water associated with one of three tested species of herbivorous copepods.

Methanogens have also been found to live as endosymbionts in anaerobic protozoans (van Bruggen *et al.*, 1983; Fenchel and Finlay, 1991; 1992), in anoxic hypersaline environments (Giani *et al.*, 1984), in hot springs (Stetter *et al.*, 1981) and within hydrothermal vents (Jones *et al.*, 1983).

Thermogenic production of methane

Thermogenic methane from fossil organic origins is derived chiefly from the remains of ancient plant material. There is evidence that in the past - particularly during the lush Carboniferous (360 - 280 million years B.P.) and Jurassic (215 - 145 million years B.P.) periods - large amounts of the abundant flora was - once dead - buried in such a way that it was not completely decomposed by bacterial action but much tissue remained well preserved. This typically happens in oxygen-depleted environments such as swamps, flooded forests and sheltered lake- and seabeds. As this material is buried to increasing depths and mixed with silts and muds, it becomes progressively more compressed, whereby the water and fluid by-products are expelled upwards. Increasing temperatures and pressures 'pressure-cook' the compacted organic detritus and thereby crack the complex structures to yield oil and gas. The type of original organic matter and the degree of maturity determine the type of hydrocarbon that is formed. Methane is mainly derived from wood buried to greater depths than required for oil or wet (C₂-C₇) gas (Floodgate and Judd, 1992). Driven by buoyancy forces or diffusion within pore water (Kross, 1989), methane slowly rises (Mackenzie and Quigley, 1988) through the porous source rock until it either is trapped by an impermeable layer of rock (*e.g.* clay, cemented sandstone or salts) and accumulates, or seeps into water or atmosphere.

Abiogenic production of methane

As methane has been found to occur on planets such as Mars and Venus where no signs of past or present life could be detected (Houghton *et al.*, 1990), a production pathway not based on biologically produced source substrates is thought to exist. For over 20 years scientists have speculated upon the occurrence of methane from abiotic sources deep within our planet. After several publications in Russia in the 1970s suggesting mantle methane of a different origin (*e.g.* Galimov, 1973 (in Russian) in Gutsalo, 1982), Gold and Soter (1980) formulated the deep Earth gas hypothesis which suggests an abiotic and possibly primordial origin for various hydrocarbon gases. The hypothesis is based on a variety of observations from different scientific disciplines ranging from interstellar investigations, earthquake studies, hydrocarbon research and the analysis of the isotopic composition of methane from volcanic and hydrothermal origin.

In 1994 Sugisaki and co-workers reported the successful uncatalysed synthesis of methane from carbon monoxide and hydrogen by shock waves, thereby yielding a possible production process for interstellar methane. Deep-Earth methane, however, is thought to be formed in the crust and upper mantle from carbon monoxide and hydrogen using thermal energy (Schoell, 1980). Evidence for the existence of abiotic methane emanating from the Earth's mantle and crust increases steadily, but remains speculative (Sugisaki and Mimura, 1994; Kenney, 1995; Sugisaki and Mimura, 1995). Deep earth gas then rises slowly upwards driven by buoyancy forces and is

either trapped in gas reservoirs within the mantle of our planet or seeps along seated faults through to the Earth surface and enters *e.g. via* volcanic eruptions or hot hydrothermal vent emissions into oceans or atmosphere (MacDonald, 1983; Ivanov *et al.*, 1993).

1.3 Methane consumption

Methane has two major degradation pathways: it is chemically oxidised in the atmosphere, and consumed by methanotrophic bacteria.

Chemical oxidation of methane

Chemical methane oxidation in the troposphere - mainly at low altitudes in low latitudes - accounts for about 85-90% of atmospheric methane destruction and is the most important methane sink (Cicerone and Oremland, 1988; Badr *et al.*, 1992). Most methane is eventually converted into carbon dioxide (Badr *et al.*, 1992). Tropospheric methane oxidation is initiated by the relatively slow reaction (Vaghjiani and Ravishankara, 1991) with the hydroxyl radical (OH) and occurs in several stages. The tropospheric concentration of hydroxyl determines the rate of methane oxidation and is therefore an important determinant of the strength of the atmospheric methane sink. Tropospheric hydroxyl concentrations show strong diurnal, seasonal and latitudinal fluctuations. This is because hydroxyl is the product of the photodissociation of tropospheric ozone by UV light and the subsequent reaction of the electronically excited oxygen atom with water vapour (Crutzen, 1987). The hydroxyl radical is a key scavenger which does not only oxidise methane but also cleans the atmosphere from various pollutants and other greenhouse gases such as carbon monoxide and CFCs. Methane thus competes with these gases for the hydroxyl radical, so that the speed of methane oxidation and the size of the atmospheric methane sink are partly dependent on the concentrations of other gases in the troposphere (Thompson and Cicerone, 1986; Pearman and Fraser, 1988). This relationship is complicated by the fact that presently about 25% of all tropospheric carbon monoxide is the product of methane oxidation (Badr *et al.*, 1992), and that tropospheric OH concentrations are rising partly due to the destruction of ozone in the stratosphere (Bekki *et al.*, 1994; Fuglestad *et al.*, 1994).

There are two slightly different pathways for tropospheric methane oxidation (Figure 1.2) depending on the magnitude of tropospheric pollution with nitrogen oxides (NO_x) (Crutzen, 1987; Cicerone and Oremland, 1988; Badr *et al.*, 1992). In clean air, with nitrogen oxide concentrations below 10 pptv, methane is oxidised to carbon dioxide with an average destruction of 3.5 hydrogen-containing molecules of various types (OH, H, HO₂) and of 1.7 ozone molecules per methane molecule (Crutzen, 1987). In polluted air the oxidation of one methane molecule

results in the production of 0.5 hydrogen-containing molecules and of 3.7 molecules of ozone (Crutzen, 1987). The tropospheric destruction of methane thus influences tropospheric ozone concentrations in a complex manner. Chemical methane oxidation is furthermore an important source for tropospheric water vapour.

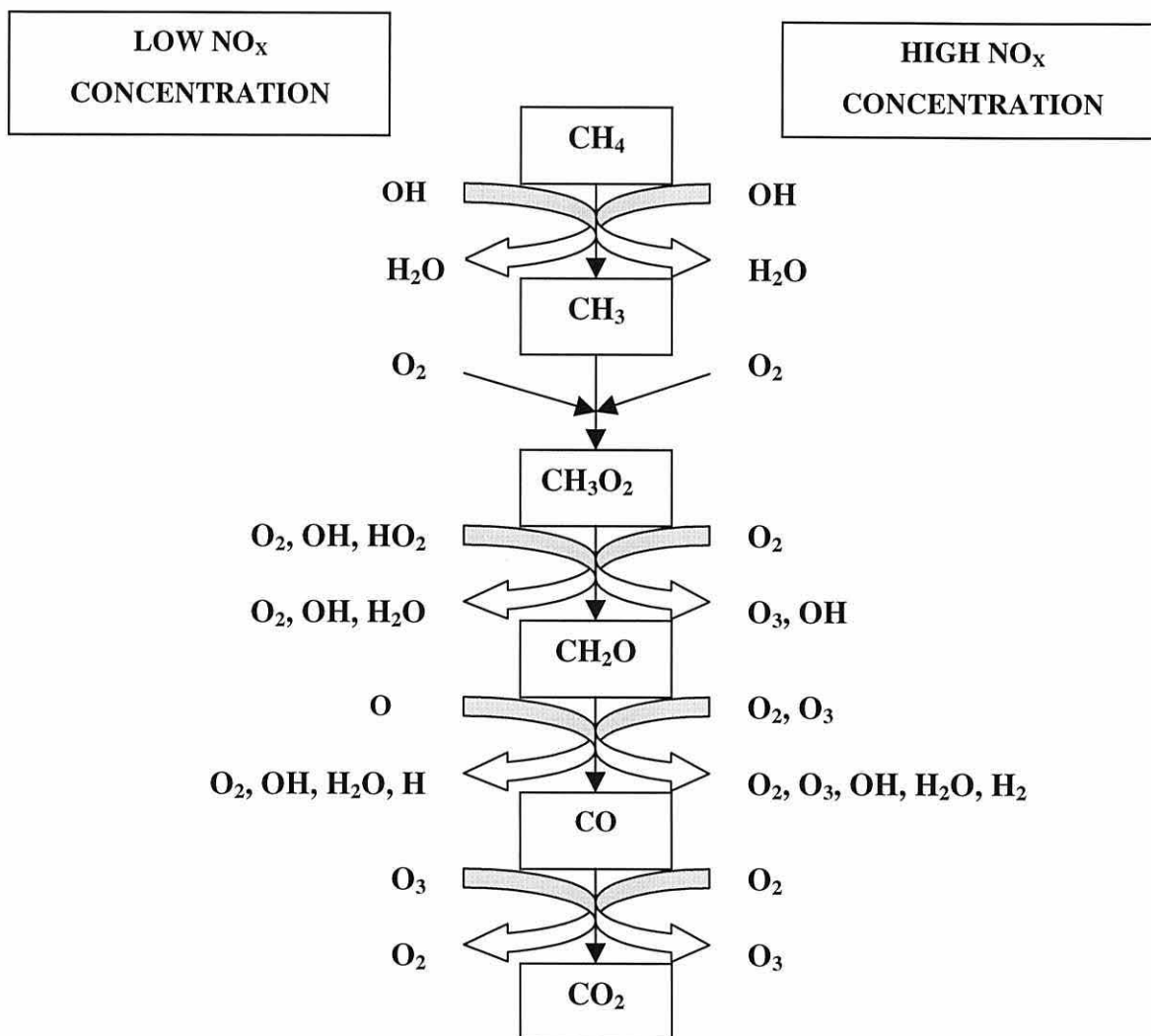


Figure 1.2 Chemical methane oxidation in the clean (left) and polluted (right) troposphere. (From: Badr *et al.*, 1992).

Approximately 10% of all tropospheric methane is transported higher up into the stratosphere, where most of it is oxidised to carbon dioxide and water (Cicerone and Oremland, 1988). Stratospheric methane can also react with chlorine, whereby the chlorine-catalysed destruction of stratospheric ozone is terminated (Badr *et al.*, 1992). Stratospheric methane oxidation is furthermore considered to have produced about half of today's stratospheric water vapour (Ehrlich, 1990). A very small fraction of stratospheric methane rises beyond the stratosphere into the mesosphere, where it is photolytically destroyed by very short wavelength UV light (Cicerone and Oremland, 1988).

Biological oxidation of methane

The activity of methanotrophs was first reported by Kaserer in 1905. The first pure culture of methanotrophs was isolated in 1906 by Söhngen from the leaves and stems of the freshwater macrophyte *Elodea* growing on methane-rich sediments.

Methanotrophs are characterised by their ability to grow on methane as their sole source for carbon and energy. While anaerobic methane oxidation has been observed, all known methanotrophs are aerobic bacteria. At least three different genetic, phenotypic and phylogenetic types of aerobic methanotrophs have been identified. These are defined as type I, type X and type II depending on morphology, membrane arrangements, resting stages, assimilation pathways for biomass synthesis and ability to fix carbon dioxide autotrophically (Whittenbury *et al.*, 1970; Anthony, 1982; Green, 1992).

While there are obligate methanotrophs, many can facultatively utilise other substrates *e.g.* methanol (Sieburth *et al.*, 1987). Methane is oxidised in a multi-step process to eventually yield carbon dioxide *via* methanol, formaldehyde and formate:



The oxidation of methane requires a relatively high activation energy because the symmetrical, non-polarised tetrahedron structure of the methane molecule is very stable. Methanotrophs therefore use a biological catalyst to overcome the high activation energy. The methanotroph-specific methane monooxygenase (MMO) enzyme oxidises methane using molecular oxygen and the hydrogen transfer coenzyme NADH to form methanol, water and NAD^+ (Anthony, 1982). Methylfluoride inhibits the MMO enzyme and can thus be used as a specific methanotroph inhibitor (Oremland and Culbertson, 1992).

Aerobic methanotrophs have a high requirement for combined inorganic nitrogen (Rudd *et al.*, 1976; Kiene, 1991; Lees *et al.*, 1991; Topp and Hanson, 1991). Their methanotrophic activity can be enhanced by light as this increases oxygen concentrations due to photosynthetic production (King, 1990). Others, however, found light to inhibit the oxidation rate (Sieburth *et al.*, 1987; Scranton *et al.*, 1993). Where there is sufficient oxygen and dissolved inorganic nitrogen, methanotrophy has often been found to be roughly proportional to the concentration of methane and the rate of methanogenesis (Reeburgh and Heggie, 1977; Sansone and Martens, 1978; Ward *et al.*, 1987; Ward and Kilpatrick, 1990; Kiene, 1991; Amaral and Knowles, 1995). Such a positive relationship, however, was not found in all studies (*e.g.* Griffiths *et al.*, 1982).

Methanotrophs live in aerobic soils (Seiler *et al.*, 1984; Whalen and Reeburgh, 1990; Mosier *et al.*, 1991; Dörr *et al.*, 1993), marine sediments (*e.g.* Oremland and Culbertson, 1992), and also within the oxic layer of freshwater and sea water (Lidstrom, 1983; Sieburth *et al.*, 1987; Ward and Kilpatrick, 1990). In sea water, methane oxidation rates are about one order of magnitude smaller than in marine sediments or in freshwater lakes (Griffiths *et al.*, 1982). Oxidation rates commonly increase close to oxic-anoxic interfaces (Rudd and Taylor, 1980; Ward and Kilpatrick, 1990; Whalen and Reeburgh, 1990) where methanotrophs act as biofilters limiting and modulating methane emissions (King, 1990a; Oremland and Culbertson, 1992).

The occurrence of anaerobic methane oxidation is now generally accepted although the processes and organisms involved remain enigmatic (Reeburgh, 1976; Martens and Berner, 1977; Reeburgh and Heggie, 1977; Bernard, 1979; Kosiur and Warford, 1979; Reeburgh, 1980; Hoehler *et al.*, 1994; Blair and Aller, 1995; Burns, 1998). There have been many reports from incubation experiments both in enrichment cultures (Panganiban *et al.*, 1979) and in the field showing that $^{14}\text{CH}_4$ oxidation to $^{14}\text{CO}_2$ occurs within anaerobic marine sediments (Kosiur and Warford, 1979; Reeburgh, 1980; Devol, 1983; Alperin and Reeburgh, 1985; Iversen and Jørgensen, 1985). It has also been demonstrated that this process is biological (Alperin and Reeburgh, 1985; Iversen *et al.*, 1987). Since sulphate is the only apparent oxidant in such environments, anaerobic methane oxidation has been theoretically linked with sulphate reduction by sulphate reducing bacteria (Reeburgh, 1976; 1980; 1982; Devol and Ahmed, 1981). A causal link between sulphate reduction and anaerobic methane oxidation is supported by the observation that anaerobic methane oxidation is an important process in anaerobic saline environments (Reeburgh and Heggie, 1977; Henrichs and Reeburgh, 1987; Niewöhner *et al.*, 1998) but seems to be absent from anaerobic but sulphate-depleted freshwater sediments (Reeburgh and Heggie, 1977; Alperin and Reeburgh, 1985). The rates of anaerobic methane oxidation and sulphate reduction were furthermore found to peak roughly simultaneously at the sulphate reduction / methane production transition zone (Reeburgh, 1980; Devol, 1983; Iversen and Jørgensen, 1985; Niewöhner *et al.*, 1998). Carbon-isotopic evidence also suggests that anaerobic sulphate reduction and methane oxidation are coupled at the base of the sulphate reduction zone (Burns, 1998).

The organisms responsible for anaerobic methane oxidation remain unknown. In cultures of sediment bacteria, both methanogens (Zehnder and Brock, 1979) and sulphate reducers (Davis and Yarbrough, 1966) were found to be capable of anaerobic methane oxidation, but at rates that fell short of explaining the observed *in situ* rates. Anaerobic methane oxidation was furthermore not affected by specific inhibitors of sulphate reduction or methane production (Alperin and Reeburgh, 1985). Field and laboratory studies suggest that methane is anaerobically oxidised by

a consortium of methanogens, which are hypothesised to operate in reverse and oxidise methane, in conjunction with sulphate reducing bacteria, which are thought to remove hydrogen and thereby make it unavailable for methanogenesis (Hoehler *et al.*, 1994). Hinrichs *et al.* (1999) recently found strong evidence suggesting that methane is consumed by sedimentary archaeobacteria that are phylogenetically only peripherally related to known methanogens.

In most environments, methane production exceeds methane consumption, so that net production of methane occurs and methane is emitted to the atmosphere (Zehnder and Brock, 1980). There are, however, examples of net methane oxidation which, for example, occur in anoxic sea water (Lidstrom, 1983; Iversen *et al.*, 1987).

1.4 Methane distribution and budget

Concentrations of methane measured at different times and in different places are a result of the dynamics between production and consumption processes and various physical, chemical and biological distribution parameters. The origin of atmospheric methane is therefore not easy to determine, thus rendering the production of a reliable global methane budget difficult. Measuring net emission and oxidation rates of methane from specific environments and extrapolating these to global emissions produces uncertain estimates. The isotopic composition of both the carbon and the hydrogen atoms in methane, however, were found to vary with source materials, production pathways, oxidation processes and time since production. The isotopic composition of methane can therefore indicate its origin and history.

In this section, a brief explanation of the isotopic composition of methane with different origins and histories is followed by a summary of the global methane budget. Finally, the cycling and budget of methane in the marine environment is introduced.

1.4.1 Isotopic composition of methane: an indicator for its origin and history

Carbon occurs in three different isotopic forms as ^{12}C , ^{13}C and ^{14}C . While the former two are stable, ^{14}C is a labile isotope with a half-life of 5,730 years. It is formed by a series of reactions initiated by cosmic ray proton collisions in the upper atmosphere (Broecker and Peng, 1982, p. 238) and is incorporated first into atmospheric carbon dioxide and from there *via* photosynthesis into organic matter. Thus, the level of ^{14}C in organic material can be used to determine the time that has passed since it was generated. The contribution of ^{14}C is therefore used to distinguish between fossil methane that contains no ^{14}C and is called radiocarbon dead and recently produced biogenic methane with ^{14}C levels close to modern carbon.

The ratio of stable carbon isotopes can vary due to kinetic fractionation processes or due to isotopic exchanges when chemical processes move towards isotopic equilibrium (Tyler, 1991). Stable carbon isotope ratios are in many cases source-specific and are thus used to fingerprint gases. They hold information on the formation, consumption and release mechanisms of methane. Measured stable carbon isotope ratios are related to those of a standard marine limestone derived substance called Pee Dee belemnite carbonate (PDB) and then referred to as $\delta^{13}\text{C}$ (Craig, 1957). Negative $\delta^{13}\text{C}$ values indicate ^{13}C depletion, which is typically caused by ^{12}C isotopes being kinetically preferred, as they require less activation energy than the heavier ^{13}C isotopes. Due to kinetic isotope fractionation biogenic methane is generally depleted in ^{13}C relative to the PDB standard, with typical $\delta^{13}\text{C}$ values of -60 to -80 . Thermogenic methane on the other hand tends to be heavier, with $\delta^{13}\text{C}$ values somewhere between -20 and -60 . Abiogenic methane is characterised by the heaviest ratio with $\delta^{13}\text{C}$ values of -15 to -18.2 (Cicerone and Oremland, 1988; Ivanov *et al.*, 1993). Many sources, however, have overlapping and seasonally and spatially variable $\delta^{13}\text{C}$ ranges. This is partly because $\delta^{13}\text{C}$ is influenced by the $\delta^{13}\text{C}$ of the organic source material and by the microbial production pathway (Burke *et al.*, 1988; Tyler, 1991; Martens *et al.*, 1992).

The isotopic composition of the produced methane is later altered by oxidation processes. Both chemical and biological methane oxidation favour the lighter ^{12}C isotopes (Cantrell *et al.*, 1990; Chanton *et al.*, 1992) whereby ^{13}C enriched methane remains, relative to the originally produced methane. Also transport of methane from its sedimentary production site through macrophytes to the atmosphere slightly alters the stable carbon isotope ratio and typically depletes it of ^{13}C (Stevens and Engelkemeir, 1988; Chanton *et al.*, 1992).

Hydrogen isotope ratios ($^1\text{H}:^2\text{H}$) in methane molecules also vary according to their origin and production pathways but show an even larger overlap than the stable carbon isotope ratios (Schoell, 1980). In biogenic methane the deuterium content is used to distinguish between continental and marine origin (Schoell, 1983). Some methane sources with overlapping $\delta^{13}\text{C}$ signals have different hydrogen isotope ratios. Therefore all carbon and hydrogen isotope values of methane are commonly combined, *e.g.* in a refined crossplot diagram, to better identify the source of methane (Schoell, 1980; Woltemate *et al.*, 1984). Often geological and chemical clues are required as support to determine the origin and previous fate of methane.

1.4.2 Global methane distribution and budget

Many assumptions and generalisations have to be made in order to draw up a global methane budget from a relatively sparse collection of data. The strengths and even the identities of various atmospheric methane sources remain ill-defined (Piccot *et al.*, 1996). The study of global methane distribution and its budget must begin with the concentrations in the atmosphere before considering the individual emission sources and sinks.

Atmospheric methane concentrations

One of the most recent estimates for the mean global atmospheric methane concentration was given as 1.84 μ -atmospheres for 1994 (Simmonds *et al.*, 1996). There are large deviations from the global mean value both in time and space (*e.g.* Khalil and Rasmussen, 1983; Lammers and Suess, 1994). As shown in Figure 1.3, there is an inter-hemispheric gradient in tropospheric methane concentrations. The southern hemisphere has a lower mean methane concentration than the northern hemisphere with the steepest gradient in the northern low-latitude region (Lamontagne *et al.*, 1974; Ehhalt and Schmidt, 1978; Houghton *et al.*, 1990; Fung *et al.*, 1991; Steele *et al.*, 1992). This inter-hemispheric gradient already existed in pre-industrialised times (Rasmussen and Khalil, 1984) and is thought to be due to primarily land-based natural methane sources. Vertically methane appears to decrease with increasing altitude (Ehhalt and Heidt, 1973) which has been suggested to correlate well with atmospheric lifetime (Bridgman, 1990). Atmospheric methane concentrations show a seasonal pattern with general increases in the colder winter months (Rasmussen and Khalil, 1981b; Fung *et al.*, 1991; Steele *et al.*, 1992). In the southern hemisphere this seasonality is simpler and better defined (Figure 1.3) and is thought to be caused by the seasonally increased photochemical production of methane oxidising hydroxyl radicals (Steele and Lang, 1991; Prinn, 1994). In the northern hemisphere, where the seasonal pattern is more complex, seasonality is thought to be a result of interactions between seasonal sources and sinks (Steele *et al.*, 1992).

As mentioned earlier, the atmospheric concentration of methane has varied over time and has more than doubled since industrialisation. The rate of increase, however, has begun to fall from 1% per annum to about 0.7% between 1984 and 1990 (Steele *et al.*, 1992). In the early 1990s the rate of increase dropped even further, particularly in the northern hemisphere (Dlugokencky *et al.*, 1994; Novelli *et al.*, 1994). Approximately 30 to 50% of this is thought to be caused by stratospheric ozone depletion, which allows more UV radiation to enter the troposphere and thereby more hydroxyl radicals to be produced (Bekki *et al.*, 1994; Fuglestvedt *et al.*, 1994). Other explanations for the slowing in the growth rate of atmospheric methane include a.) decreased emissions from fossil fuels particularly in the former Eastern Block due to reduced industrial activity and improved environmental controls (Steele *et al.*, 1992; Dlugokencky *et al.*, 1994), b.) reduction in tropical biomass burning in 1992 (Rudolph, 1994), c.) enhanced mixing

of stratospheric, low-methane air into the troposphere due to temperature dependent circulation changes after the eruption of Mount Pinatubo in June 1991 (Schauffler and Daniel, 1994), d.) changes in methane oxidation rates due to changes in tropospheric temperature (Rudolph, 1994), and e.) reductions in methane emissions from temperature dependent northern wetlands as a response to decreased surface temperatures after the Mount Pinatubo eruption (Dlugokencky *et al.*, 1994). If the Mount Pinatubo eruption was in a significant part responsible for the recent decrease in the growth rate of atmospheric methane, it can be speculated that the mixing ratios of methane will increase progressively with time as the effects of the volcano eruption decline.

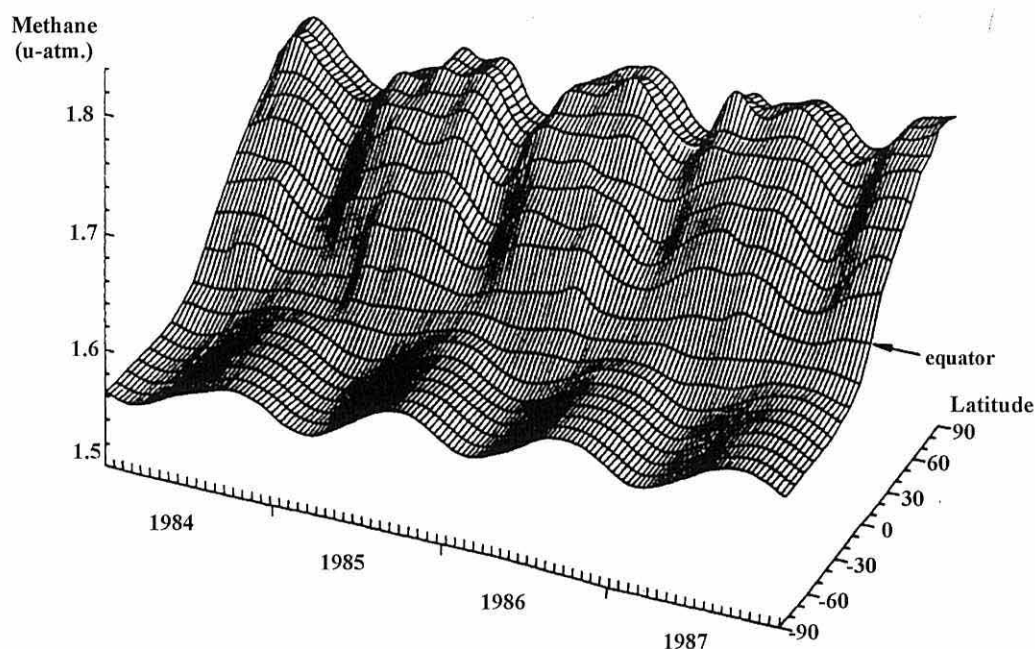


Figure 1.3 Smoothed global distribution of the background concentration of atmospheric methane in the marine boundary layer in a 3-D representation. (After: Fung *et al.*, 1991).

Methane sources and sinks

While methane is produced in oxygen-depleted sub-surface layers of our planet, methane oxidation generally takes place either in layers above the production sites or in the atmosphere. Transport from the production to the consumption locations is thus important in determining the rate and quantity of methane emissions to the atmosphere. Methane transport occurs by one of four mechanisms: 1.) by diffusion along concentration gradients, 2.) by bubble ebullition if production rates exceed the saturation threshold of the soil water (Reeburgh, 1982; Devol *et al.*, 1988; Schütz *et al.*, 1991), 3.) by plant-mediated transport through plant tissue (Schütz *et al.*, 1991) or 4.) by advection. The mobility across sediment-water, water-air and sediment-air interfaces is co-determined by the degree of turbulence created by currents or winds (Sebacher *et al.*, 1983; Liss and Merlivat, 1986; Wanninkhof, 1992).

Several estimated global methane budgets have been published which vary in some details but generally agree in their overall scales (*e.g.* Cicerone and Oremland, 1988; Watson *et al.*, 1990; Fung *et al.*, 1991; Müller, 1992). The large remaining uncertainties about the exact source and sink strengths are in most cases caused by the problems of extrapolating global emissions from measurements with large spatial and temporal variability.

Table 1.4 Estimates of net methane emissions and global consumption (in Tg CH₄ y⁻¹) from natural (N) and anthropogenic (A) sources (+) and sinks (-) add up to give a measure for gross global methane production. (From Reeburgh *et al.*, 1993).

Source (+) / sink (-)	Net emissions	Global consumption	Global production
+N Wetlands	115	27	142
+N Termites	20	24	44
+N Oceans / freshwater	10	75	85
+N Methane hydrates	5	5	10
+A Fossil fuels	75	18	93
+A Animals	80	0	80
+A Rice paddies	100	477	577
+A Biomass burning	55	0	55
+A Landfills	40	22	62
Total sources	500		
- Chemical oxidation	-450	-	-
- Soil consumption	-10	40	40
Total sinks	-460	688	
Total global production			1188

The total global gross production of methane is believed to amount to around 1188 Tg CH₄ y⁻¹, (Reeburgh *et al.*, 1993), which has been calculated by adding the estimates for annual net atmospheric emissions of methane to the annual global methane consumption (Table 1.4). As can be seen in Table 1.4, the total methane emissions into the atmosphere per year are nearly balanced by the annual net oxidation of atmospheric methane. The annual excess emissions of 40 Tg CH₄ lead to the approximate 1% increase in global atmospheric methane concentrations. Table 1.4 also shows that approximately 60% of all methane that is originally produced is biologically oxidised by methanotrophs before it reaches the atmosphere (Reeburgh *et al.*, 1993). For the oceans it is nearly 90% (Table 1.4).

The natural sources of atmospheric methane are presently smaller than the anthropogenically caused or enhanced sources (Table 1.4). The contribution of methane from fossil sources to the atmospheric pool has been estimated to lie somewhere between 10 and 33% based on ¹⁴C isotope studies (Ehhalt, 1976; Lowe *et al.*, 1988). Whether the relative contribution of fossil methane

has increased in the industrialised period can only be speculated, as, to the author's knowledge, no ^{14}C isotope studies have yet been conducted on past atmospheres preserved in ice cores.

Large quantities of methane are currently stored underground in gas and also within oil and coal reserves. More than 20% of this methane is thought not to be of fossil but of biogenic origin (Rice and Claypool, 1981). The contribution of thermogenically produced methane from abiotic source material to these reserves is unknown, but some scientists have argued that these dwarf all other methane reserves (Gold and Soter, 1980; Evans, 1996). Also, methane hydrates keep methane locked up underground. Methane hydrates are crystalline ice like structures of methane and water formed under high pressures and low temperatures both in terrestrial and marine environments. Large quantities of methane hydrates have been identified within the upper few hundred meters of Arctic and deep-oceanic sediments (Floodgate and Judd, 1992; Dickens *et al.*, 1997). The solid hydrates often overlie zones of free gas, which they effectively prevent from seeping into the water or atmosphere (Dando and Hovland, 1992; Dickens *et al.*, 1997). These free methane reserves beneath hydrates can contain more methane than the hydrates themselves (Dickens *et al.*, 1997). Approximately 10^3 Tg of methane are thought to be deposited beneath terrestrial permafrost regions, in sediments of the Arctic continental shelf and in cold ocean sediments at the bottom of the continental slope (Kvenvolden, 1988). It has been suggested that global warming might result in the gradual or sudden defrosting of these hydrates and the release of large quantities of methane (Cicerone and Oremland, 1988; Kvenvolden, 1988). At the end of the last glaciation, the rapid melting of gas hydrates has been suggested to have contributed to the fast warming of the climate (Nisbett, 1990).

1.4.3 Methane distribution and budget in the marine environment

As can be calculated from the data in Table 1.4, only about 2% of all methane that is emitted into the atmosphere originates from the single largest ecosystem on Earth – the ocean. This appears not to be due to low methane production but to efficient microbial methane oxidation processes within the marine environment (Reeburgh *et al.*, 1993; Iversen, 1996). The global ocean contributes approximately 7% to the gross methane production and 11% to the gross methane consumption (from Table 1.4), rendering it globally the second largest natural methane production site and the largest natural biological methane consumption system.

The environmental conditions in the sea are believed to have been relatively stable for a long time, which might explain why the very close and efficient cycling of methane between marine methanogens and methanotrophs has become established.

The emission estimates for the ocean are primarily based on concentration measurements made at different locations and times. Depending on the measurements used and the extrapolations and corrections applied, other scientists have suggested different emission rates (Table 1.5) from the one shown in Table 1.4 (Ehhalt, 1974; Lambert and Schmidt, 1993; Hovland *et al.*, 1993).

Table 1.5 Estimates of methane emissions (in Tg CH₄ y⁻¹) from the oceans (Iversen, 1996).

Total emissions	Coastal emissions	Oceanic emissions	Source
4.7 – 20.7	0.7 – 14	4 – 6.7	Ehhalt, 1974
50 – 60	47 – 56	3 – 4	Lambert & Schmidt, 1993
	8 – 65		Hovland <i>et al.</i> , 1993

Oceanic waters are generally slightly supersaturated with methane relative to atmospheric concentrations with surface concentrations usually between 1.8 to 3.9 nM (Swinnerton *et al.*, 1969; Lamontagne *et al.*, 1973; Jones, 1991). They often - but not always - show a spatially continuous subsurface peak somewhere between 30 and 150 m before concentrations begin to decrease with increasing depth to reach undersaturation at depths around 250 to 2,000 m (Swinnerton *et al.*, 1969; Brooks and Sackett, 1973; Brooks *et al.*, 1973; Lamontagne *et al.*, 1974; Scranton and Brewer, 1977; Scranton and Farrington, 1977; Traganza *et al.*, 1979; Conrad and Seiler, 1988; Owens *et al.*, 1991; Bianchi *et al.*, 1992; Cynar and Yayanos, 1992; Ward, 1992; Ward and Kilpatrick, 1993; Tilbrook and Karl, 1995; Patra *et al.*, 1998). The decrease in methane in the deeper layers of the water column is thought to be caused by biological methane oxidation (*e.g.* Patra *et al.*, 1998). A 'typical' open ocean profile is shown in Figure 1.4.

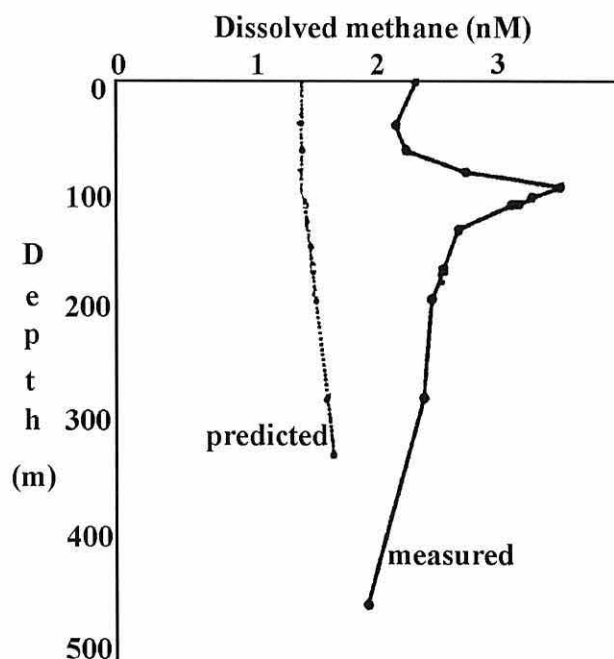


Figure 1.4 A 'typical' oceanic methane depth profile (After: Scranton and Brewer, 1977).

Several scientists calculated that the surface methane supersaturation and subsurface maximum can only rarely be explained by advection or lateral transport of methane from a sedimentary production site alone but that *in situ* production of methane within the oxygenated water column must contribute (Scranton and Brewer, 1977; Burke *et al.*, 1983; Owens *et al.*, 1991; Tilbrook and Karl, 1995). They suggested that methane might be produced by phytoplankton or other as yet unidentified methane producers, and/or by methanogens living in anaerobic microsites in the water column. Evidence was collected showing occasional correlations between subsurface methane and zooplankton (Traganza *et al.*, 1979; Patra *et al.*, 1998) or chlorophyll concentrations (Brooks *et al.*, 1981; Patra *et al.*, 1998).

The most likely sites for anaerobic methanogenesis within the oxygenated water column are the guts of fish (Oremland, 1979) or zooplankton (Oremland, 1979; Cynar and Yayanos, 1991; Bianchi *et al.*, 1992; Marty, 1993; DeAngelis and Lee, 1994), and the inside of detrital particles such as faecal pellets (Burke *et al.*, 1983; Sieburth, 1987; 1988; 1991; Conrad and Seiler, 1988; Bianchi *et al.*, 1992; Karl and Tilbrook, 1994). Sieburth (1987) suggested that *in situ* methanogenesis occurs throughout the oxygenated water column in microparticulates, which accumulate in the upper ocean pycnocline creating the methane maximum. Oxygen-tolerant methanogens have been detected in the water column, which utilise non-competitive substrates such as methylamines (MAs) or methylated sulphur compounds (Sieburth, 1987; 1993; Sieburth *et al.*, 1993b). Such oxygen-tolerance may explain how anaerobic methanogens can survive in the oxic water column, where they have to travel between anaerobic sites. The origin of methane produced in the oxygenated waters of the ocean remains uncertain to this day.

In anoxic waters - as found in the deep Cariaco Trench off Venezuela, in anoxic marine fjords, and in the Black Sea - methane levels do not decrease steadily with depth but increase below the oxic-anoxic interface where methanogenesis occurs (Atkinson and Richards, 1967; Ward *et al.*, 1987; Reeburgh *et al.*, 1991; Scranton *et al.*, 1993; 1995). Rates of methanotrophy, however, are also much higher in the anaerobic zone than the aerobic layer (Lidstrom, 1983).

Coastal areas are generally richer in methane and despite their small spatial contribution to the global ocean appear to be much more important methane emission sites than the open ocean (Table 1.5) (Griffiths *et al.*, 1982; Cynar and Yayanos, 1992; Lambert and Schmidt, 1993; Tilbrook and Karl, 1995; Bange *et al.*, 1996; Patra *et al.*, 1998). The coastal concentrations of methane reported to date show a large variability with values ranging from 2 to 8,000 nM (Sansone and Martens, 1978; Lambert and Schmidt, 1993; Schmaljohann, 1996). This is not

surprising, as there is a large spatial and temporal variability in the inputs of organic carbon both from terrestrial sources and from *in situ* primary production.

The main methane production sites in coastal areas are anoxic sediments, where methane production occurs mainly at depths below the sulphate reduction zone (Figure 1.5) (*e.g.* Martens and Klump, 1984; Iversen and Jørgensen, 1985; Crill and Martens, 1986; Schmaljohann, 1996).

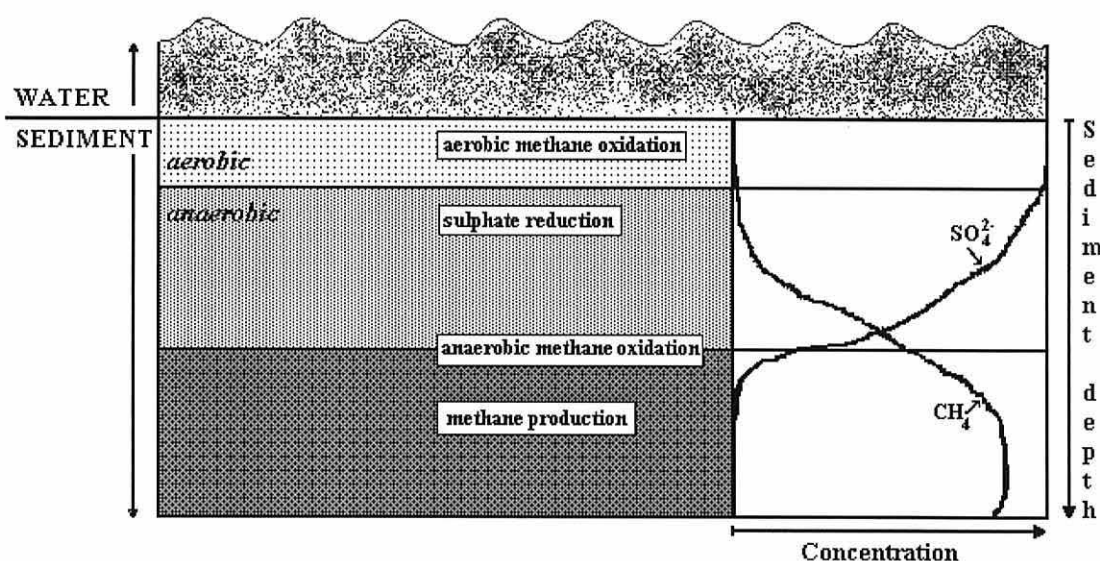


Figure 1.5 The vertical zonation of some fundamental microbial processes in marine sediments, and a 'typical' depth profile of methane and sulphate concentrations in interstitial waters.

Very little of the methane produced in the sediments ever reaches the water column as most of it is consumed by methanotrophs (Figure 1.5). Only if it can bypass the methane-oxidising zone - *e.g.* via ebullition where very high production rates occur - does a significant quantity of methane enter the water and atmosphere (Chanton and Martens, 1988). This occurs commonly in organically very rich sediments (Chanton *et al.*, 1989), which are often characterised by high sedimentation rates. Aerobic microbial methane oxidation, which is quite well understood and extremely important in freshwater systems, occurs only in the water column and the very narrow oxic zone at the sediment surface. It is generally considered not to be very important in the marine system. The rates of aerobic methanotrophy in the sediments have been found to be highly variable and to range from 0 to 6,250 $\mu\text{mol dm}^{-3} \text{d}^{-1}$ (King, 1990b; Topp and Hanson, 1991; Iversen, 1996; Schmaljohann, 1996). In water aerobic methane oxidation rates depend for example on surrounding concentrations of oxygen and dissolved inorganic nitrogen, and were found to vary between 0.0004 and 17 $\mu\text{mol dm}^{-3} \text{d}^{-1}$ (Sansone and Martens, 1978; Scranton and Brewer, 1978; Griffiths *et al.*, 1982; Fenchel *et al.*, 1995). The dominant methane consumption

process in the marine environment is the enigmatic process of biological anaerobic methane oxidation, which occurs mainly at the lower boundary of the anoxic sulphate reduction zone of marine sediments (Figure 1.5) (Reeburgh, 1980; Devol, 1983; Alperin and Reeburgh, 1985; Iversen and Jørgensen, 1985; Henrichs and Reeburgh, 1987; Blair and Aller, 1995; Niewöhner *et al.*, 1998), but also in anoxic water columns. Up to 97 % of all methane produced within the sediment is thought to be oxidised anaerobically before it can leave the sediment (Iversen and Jørgensen, 1985). The maximum rates of anaerobic methane oxidation occur in the sulphate-methane transition zone, where rising methane is consumed at typical anaerobic oxidation rates of 0.01 to 34 $\mu\text{mol dm}^{-3} \text{ d}^{-1}$, giving rather uniform integrated rates of 0.8 to 1.8 $\mu\text{mol m}^{-2} \text{ d}^{-1}$ (Devol, 1983; Alperin and Reeburgh, 1985; Iversen and Jørgensen, 1985). The rapid oxidation results in methane concentrations decreasing rapidly above the transition zone. The methane emissions from anoxic water basins are also generally low as methane oxidisers consume most of the methane that has been produced (Rudd and Hamilton, 1975; Ward *et al.*, 1987; Scranton, 1988; Reeburgh *et al.*, 1991). Only episodic events such as storms can lead to the sudden and at times very substantial release of methane from such environments (Ward and Kilpatrick, 1990; Scranton *et al.*, 1993).

There appear to be seasonal increases in methane concentrations in warmer months in temperate coastal waters (De Laune *et al.*, 1983; Bange *et al.*, 1994; Bates *et al.*, 1996; Bange *et al.*, 1998). In polar, partly ice-covered waters methane was found to reach peak concentrations at the end of the winter. The ice appears to trap gases and thus to be responsible for the winter accumulation of methane (Kling *et al.*, 1992; Lammers *et al.*, 1995).

Summarising, on a global scale the oceans are not a major source for atmospheric methane. The distribution of methane in the marine environment varies horizontally and vertically, and methane concentrations are often higher in the warmer months. Coastal waters are richer in methane than oceanic waters. While the surface layers are generally supersaturated with methane relative to the atmosphere due to partly unexplained production processes, there is commonly undersaturation at greater depths. Most methane is produced in anaerobic sediments below the sulphate reduction zone, but is consumed mainly by anaerobic methane oxidation processes before it can reach the water column.

A science which hesitates to forget its founders is lost.
 Attributed to A.N. Whitehead (1861-1947)

1.5 Study aim and objectives

This study was carried out to enhance our understanding of methane dynamics in coastal waters and to enlarge the scarce data base of measurements of methane concentrations in this complex environment. Methane concentration measurements were used to investigate the seasonality and eventually to budget the net methane cycling in the Menai Strait.

The specific objectives were:

1. To establish the seasonal behaviour of methane in temperate coastal waters
2. To study the different potential methane sources in the Menai Strait:
 - a) net methane production in coastal waters
 - b) methane additions from external sources
 - c) methane from sediments
3. To investigate the potential sinks of methane in the Menai Strait:
 - a) net methane consumption in coastal waters
 - b) methane loss due to external sinks (*e.g* the atmosphere)
4. To budget the annual fluxes of methane from the sediments through the water into the atmosphere of the Menai Strait.

*Laboratorium est oratorium.**Joseph Needham (1900-1995)*

Chapter Two

Study Site Description and Methodology

2.1 Study site description

The study was conducted at two coastal eastern Irish Sea sites located off the Isle of Anglesey in North Wales (Figure 2.1). The seasonal behaviour of methane in both the pelagic and the sedimentary marine environment was investigated in the Menai Strait at Menai Bridge while at Point Lynas only the pelagic system was studied.

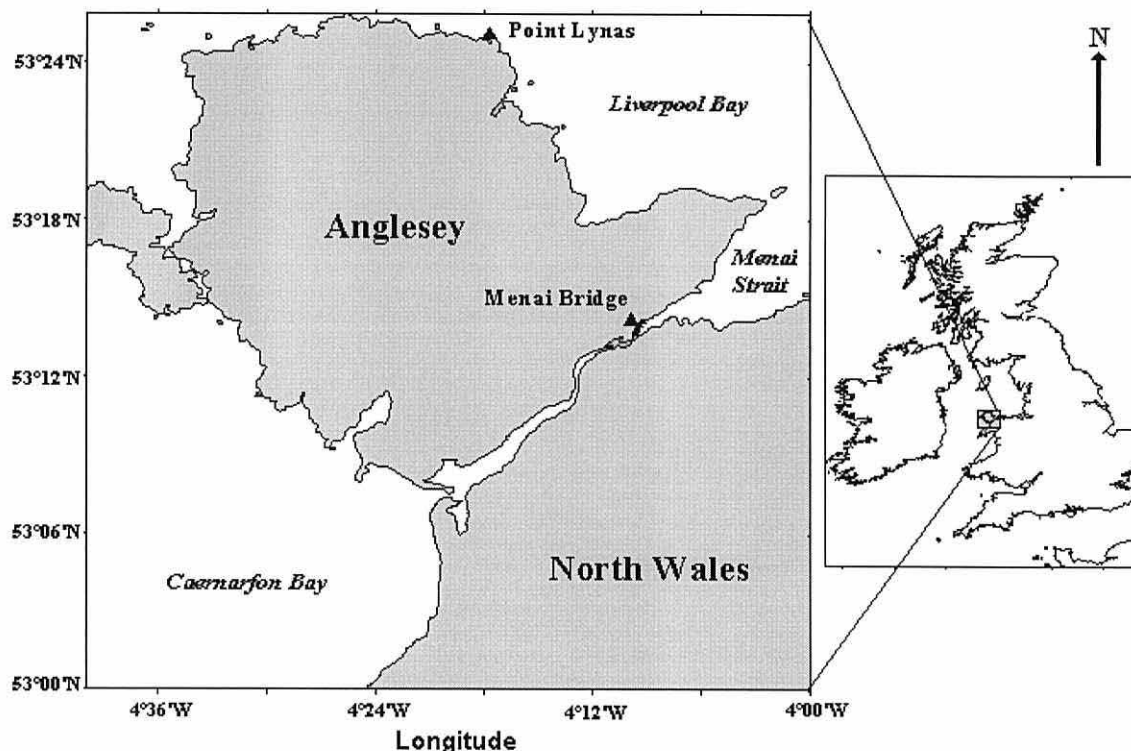


Figure 2.1 Map showing the geographic location of the two sampling sites (▲) at Point Lynas and the Menai Strait.

The Menai Strait

The Menai Strait is a turbulent, shallow stretch of water dividing the Isle of Anglesey from the northern Welsh mainland (Figure 2.1). Its limits are arbitrarily drawn between Penmon Point, Puffin Island and Penmonmawr in the northeast and Abermenai Point and Fort Belan in the southwest.

Altogether the Menai Strait is approximately 25 km long, has a mean width of 800 m and a mean depth of about 5 m. Its deepest point of 22 m below chart datum lies just southwest of the Britannia Bridge (Figure 2.2). The mean spring and neap tidal ranges at Menai Bridge are 6.6 m and 3.4 m respectively, but vary through the Strait depending on mean water depths (Admiralty Tide Tables, Vol.I).

In the northeast the Menai Strait is very wide and shallow. Therefore the tidal currents here are weak so that sandy sediments have been deposited. At low tide the extensive sandbanks of the Lavan Sands are exposed (Figure 2.2). Only the sediments of the deeper shipping channel consist of coarser particles and shell fragments (Ali, 1992). The Strait becomes progressively narrower and reaches its most narrow point of 250 m by Menai Bridge village. Here the tidal currents are very strong and the substratum is mainly composed of rocks and boulders with very little loose sediments. There are, however, several sheltered embayments along the banks of the Strait where tidal currents are low and where muddy areas have developed (Figure 2.2). Between the Telford Bridge and the Britannia Bridge lie the Swellies, which are very narrow and shallow and thus experience the strongest tidal currents in the Strait. The bottom of this turbulent stretch is solid rock. Beyond the Swellies the Strait begins to deepen and widen again forming the sandy Traeth Gwyllt and two more large sandy bays further to the southwest. In the southwest the Strait ends in a 400 m narrow exit between Abermenai Point and Ford Belan.

The tidal pattern in the Menai Strait is complex. The tide enters first from Caernarfon Bay in the south and runs northwards. During this time the tidal wave flows around Anglesey and enters the Strait from Liverpool Bay in the north. The two tidal currents meet normally in the Swellies. Tidal flow velocities are very high, reaching up to 150 cm s^{-1} for the southwesterly flow at spring tides, and 80 cm s^{-1} for water flowing from Caernarfon Bay (Harvey, 1968; Simpson *et al.*, 1971). These strong currents result in a generally well-mixed water column. The stronger southwesterly tidal current causes a residual flow with a mean velocity of approximately 15 cm s^{-1} from Liverpool Bay towards Caernarfon Bay ($= 800 \text{ m}^3 \text{ s}^{-1}$ at spring and $330 \text{ m}^3 \text{ s}^{-1}$ during neap tides) (Harvey, 1968). The flushing time of Liverpool Bay coastal water through the Strait is thus in the order of two days (Harvey, 1968). In general the water in the Menai Strait is considered typical of northeastern coastal Irish Sea waters (Jones and Spencer, 1970).

Several small rivers flow into the Strait from the mainland (Figure 2.2). Sewage inputs have altered dramatically during the sampling period. Until January 1997 eleven sewage treatment works treated only about 28% of the $29,000 \text{ m}^3$ of sewage discharged daily into the Strait. The remaining $21,000 \text{ m}^3 \text{ d}^{-1}$ were discharged untreated through several outfalls (NRA Bangor, 1993).

Since January 1997, a modern central sewage treatment plant has been in action at Treborth that will eventually treat over 85% of Menai Strait sewage. Its single outfall is located to the southwest of the Britannia Bridge (Figure 2.2). During the sampling season in 1997 it treated about $10,600 \text{ m}^3 \text{ d}^{-1}$. Menai Bridge sewage, however, had not been connected to the Treborth works during the 1997 sampling period but was still discharging an average of $925 \text{ m}^3 \text{ d}^{-1}$ of raw sewage (Environment Agency Ref: AN/285) through five small outfalls.

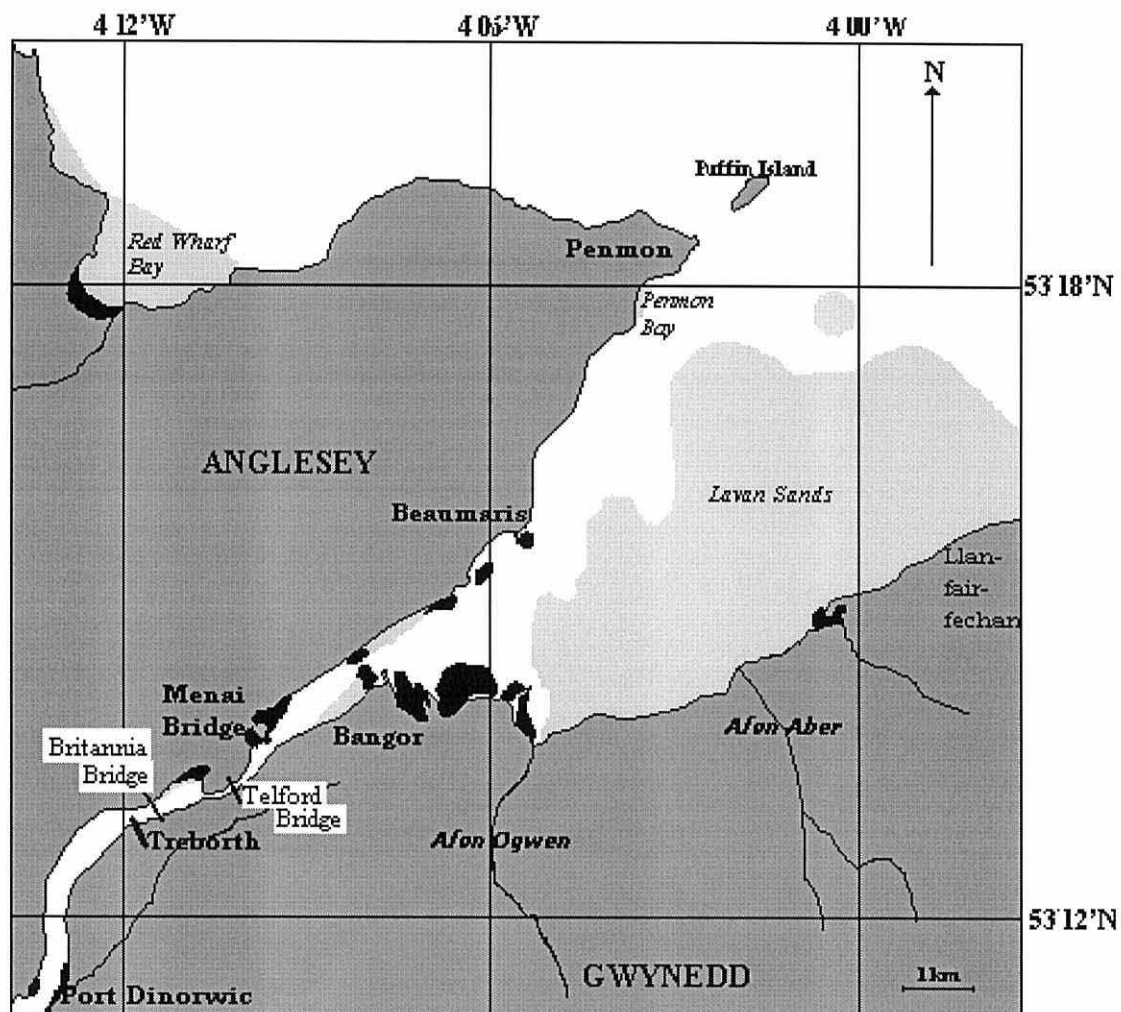


Figure 2.2 Map of the investigated section of the Menai Strait with black areas marking muddy and light grey areas sandy areas.
(Sources: Ordnance survey map 1464 (1986), Ali (1992), and observations).

Seasonal water sampling was conducted from St. George's Pier in Menai Bridge. Here the water is considered to be of mid-stream Strait quality although slack water may linger for longer and back eddies can form when tidal currents are high (Harvey, 1972). Water collected here generally originates from Liverpool Bay. Caernarfon Bay water only reaches Menai Bridge with the northeasterly tide if spring tides are assisted by very strong south-westerly winds (Harvey, 1972).

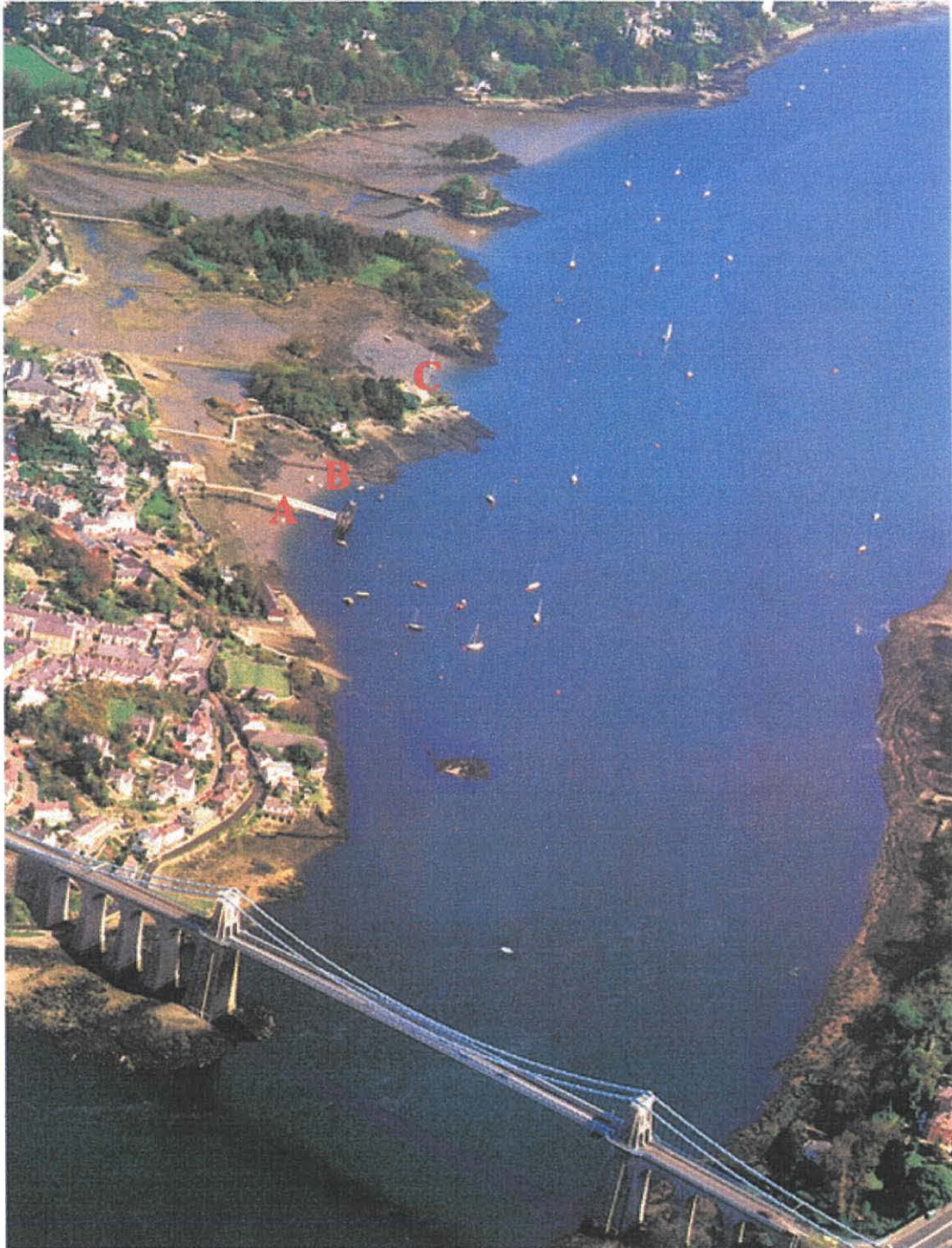


Figure 2.3 Photograph showing the Menai Strait at Menai Bridge (Photo: D. Roberts).
*A, B and C are the sites from where the seasonal sediment samples were collected.
Seasonal water sampling was conducted off St George's Pier by station A.*

Point Lynas

Point Lynas is positioned at the north-eastern corner of Anglesey (Figure 2.1). It is a very exposed, steep rocky shore with a jetty. The bottom beneath the platform and in the wider bay was found to be rocky with areas of very coarse sand and shell fragments. The net current movements around Anglesey are clockwise. Point Lynas water thus originates from the Amlwch area. No larger inhabitation is situated within the direct vicinity of Point Lynas, and only one small raw sewage outfall from Llanelian is positioned about 1km west of the sampling point. The water at Point Lynas is generally considered unpolluted (NRA statement 3/EQ/TS/63/NT).

2.2 Sampling programme

A variety of studies were undertaken to investigate first the distribution and then the potential sources and sinks of methane in coastal waters.

The seasonal distribution of methane in the coastal water column was investigated at two different sites on Anglesey. At both locations methane concentrations were measured during high tide at fixed stations in the water column at Point Lynas and in the Menai Strait on nineteen occasions between March and November 1996 at approximately fortnightly intervals. Concurrent measurements of atmospheric methane concentrations, water temperature, salinity, wind speeds, particulate organic carbon and nitrogen concentrations, chlorophyll and phaeopigment concentrations, and oxygen productivity rates were determined at both sites. To obtain an initial indication for the scale of interannual variability at one site, methane concentrations and auxiliary parameters were measured at thirty-four occasions during a second season in the Menai Strait.

To evaluate the significance of such periodic sampling, the short-term variability of water column methane concentrations at fixed sampling stations was investigated. The variability encountered at the fixed sampling stations was studied by measuring the changes in methane concentrations over a diurnal tidal cycle and over a fortnightly spring-neap tidal cycle. An attempt was then made to separate the spatial and the temporal components of the measured variability as this might help to identify the sources and sinks of coastal methane. Spatial variability was established through transect and depth profile measurements of methane. Temporal changes were quantified by measuring methane concentrations at short intervals in one water mass in the Menai Strait.

Potential sources and sinks for water column methane were investigated and quantified in three different studies in the Menai Strait. First, methane production within the oxygenated Menai Strait water column was investigated by incubating water for two days at fortnightly intervals. Second, the inputs of methane from outside the Menai Strait were quantified by measuring methane concentrations in the River Ogwen, and in treated and untreated sewage samples. The third and last investigated source for water column methane was the sediment. To determine the seasonal distribution of methane in the sediments and to estimate the contribution of sedimentary methane to the water column methane pool, pore water methane concentrations were measured in Menai Strait muds at three stations at between five and nine occasions between July 1997 and February 1998. Several studies were conducted to establish the magnitude of the spatial variability of methane in sediments. Finally, a laboratory experiment was conducted to study the effect of temperature on the production of methane in sediments.

2.3 Sampling procedure

In 1996 water was pumped slowly and steadily ($\sim 3 \text{ dm}^3 \text{ min}^{-1}$) from a depth of 1 m with a hand bilge pump into a 10 dm^3 opalescent propylene aspirator and allowed to overflow twice the container volume. Within 15 minutes of sampling, the water was dispensed into various containers using silicone tubing. For methane analysis water was introduced into calibrated nominally 50 cm^3 plastic syringes with three-way stopcocks, and for production measurements into calibrated 50 cm^3 borosilicate glass bottles with ground glass stoppers. For chlorophyll, particulate organic carbon (POC), particulate organic nitrogen (PON) and salinity analyses, water was dispensed into a series of glass bottles. Care was taken to avoid introduction of air into the samples by keeping tubing bubble-free and overflowing all containers. The samples were stored in a cool, dark place until processed. If methane samples could not be analysed within the next two to three hours, they were poisoned with saturated mercuric chloride (HgCl_2 (AnalaR BDH Chemicals Ltd) - final concentration 0.5% by volume).

In 1997 water samples for methane analysis were collected directly into the syringes. The syringe body was submerged in the top 20 to 40 cm of the water column with the stopcock open. Care was taken to avoid sampling the surface microfilm by covering the syringe opening with the syringe plunger until it reached the appropriate depth. When the syringe had filled with water the plunger was introduced under water to close the filled syringe without trapping air bubbles. When samples had to be poisoned, the open syringe was lifted out of the water with the stopcock closed, HgCl_2 was added with a pipette, and the plunger was then introduced carefully. Water samples from deeper water depths for methane analyses were collected with a Niskin bottle.

Samples for incubation experiments were collected by submerging an open 5 dm³ propylene container upside down into the water to a depth of approximately 30 cm. Syringes were filled by submersion into the water filled container. Such a sampling procedure ensured that one body of water was used for all incubations of the day. Triplicate water samples and HgCl₂-poisoned controls were incubated in outside incubators under ambient light and temperature conditions for up to 48 hours. In the poisoned controls only physical but no biological processes were assumed to occur.

Water column methanogenesis – if present – occurs at a very slow rate (Scranton and Brewer, 1977; DeAngelis and Lee, 1994). The increase in methane during a 24 to 48 hour incubation period could well be too small to be detected with the available analytical system. Therefore the signal was attempted to be increased by concentrating the microplankton, and incubating these concentrated samples and their poisoned controls. Plankton was concentrated by submerging a plankton net of 53 µm mesh size from the pier or boat to a depth of about 1 m and allowing it to accumulate particles and plankton passively for three minutes. The concentrate was emptied into the 5 dm³ container, diluted 1:1 with surface sea water, and filled into syringes by submersion. The concentration factor was calculated from chlorophyll, POC and PON measurements for the normal and the concentrated samples.

Sediment samples were collected repeatedly from three different locations in Menai Bridge (stations A, B and C in Figure 2.3). Plastic corers of 40 cm length and with an inner diameter of 6 cm were pushed where possible to their entire length into recently exposed intertidal sediments at low tide and dug out. Rubber bungs were introduced to seal the corer openings and avoid turbulent exchange with air. In the laboratory, 0.5 to 1 cm thick slices of sediment were cut in 5 cm intervals for porosity and methane analysis.

Air samples were collected by filling 50 cm³ plastic syringes with air and then closing their stopcocks. Air samples were typically taken 2 m above the water or intertidal sediment surface.

2.4 Pelagic parameters

2.4.1 Sea surface temperature

Sea surface temperature was measured in degrees Celsius with a digital thermometer (Digitron Instrumentation, U.K.).

2.4.2 Salinity

In 1996 salinity was measured with a Bisset Berman laboratory salinometer model 6230. In 1997 logged salinity data were obtained from a Valeport 660DR NKIII conductivity-temperature-depth probe which was permanently deployed from a raft off Ynys Faelog 1 m above the seabed.

2.4.3 Chlorophyll and phaeopigment concentrations

Chlorophyll was measured as an estimate of phytoplankton biomass. Phaeopigment concentrations were also analysed. Chlorophyll and phaeopigments were determined after 24 hour acetone extraction of a seawater sample filtered onto a glass fibre (GF/F) filter by fluorometric analysis with a Turner 10 Design fluorometer. Method details, fluorometer calibration and calculation of results are described in Tett (1987).

The analytical precision for fluorometric chlorophyll analysis was consistently better than 2% (coefficient of variation, CV), and therefore the analysis of a single sample was considered to be adequate. The measured chlorophyll concentration therefore does not describe the natural variability, which could only be estimated with a wider sampling strategy.

2.4.4 Oxygen production rate measurements

Respiration and photosynthesis were determined from the changes in dissolved oxygen (O_2) concentrations in bottled sea water samples before and after a 24-hour dark and light incubation period. Water was dispensed into calibrated nominally 50 cm³ borosilicate bottles, allowed to overflow by two bottle volumes and carefully stoppered with ground glass stoppers. Four replicate bottles were incubated in the light and four in the dark under ambient temperature conditions. Oxygen concentrations at zero time were fixed in another four replicate bottles by adding 1 cm³ each of manganese (II) sulphate and alkaline iodine. Sulphuric acid (1 cm³) was added to re-dissolve the precipitate prior to titration. Dissolved oxygen concentrations were measured in the incubation bottles using an automated Winkler titration system. The system is based on PC-controlled titrations with standardised thiosulphate using a photometric end-point detector. The instrument used is a modernised version of the system described by Williams and Jenkinson (1982). The method precision achieved ranged from 0.07 to 0.3% (CV).

Community production and dark respiration rates were calculated as follows from the temperature corrected mean oxygen concentrations measured in the zero, light and dark bottles:

$$\text{Dark Community Respiration (DCR)} = [\text{Dark } O_2] - [\text{Zero } O_2] \quad (2.1)$$

$$\text{Gross Community Production (GCP)} = [\text{Light } O_2] - [\text{Dark } O_2] \quad (2.2)$$

$$\text{Net Community Production (NCP)} = [\text{Light } O_2] - [\text{Zero } O_2] \quad (2.3)$$

To calculate GCP, the conventional assumption was made that community respiration is unaffected by light.

2.4.5 Particulate organic carbon and nitrogen (POC/PON) concentrations

Triplicate sub-samples of sea water were filtered onto 25 mm diameter pre-combusted (4 hours at 500°C) GF/F filters and stored frozen. The sample volume filtered depended on the amount of organic particles in the water and thus varied with season and location between 0.1 and 0.8 dm³. Usually enough water was filtered to leave an even colour on the filters. Prior to analysis the frozen filters were oven-dried at 40°C and wrapped in pre-combusted aluminium discs to make small, tight balls using acetone-cleaned forceps and surfaces. The wrapped samples were stored dry in titration dishes. Standards of acetanilide (Point Lynas) or urea (Menai Strait) were prepared ranging from 0.4 to 14 µmole nitrogen (N) and 0.2 to 70 µmole carbon (C). The Point Lynas samples were analysed with a Roboprep C/N analyser, the Menai Strait samples with a Tracer Mass Spectrometer (Europa Scientific Ltd). Pre-combusted GF/F filters were analysed to establish the blank carbon in the filters to subtract from the sample results.

2.5 Sediment parameters

2.5.1 Sediment temperature

Sediment temperatures - required to calculate diffusion rates and methane saturation - were measured using a digital thermometer (Digitron Instrumentation, U.K.). The thermometer probe was kept moving slowly through the sediment during temperature measurements to achieve a steady reading. Temperature depth profiles were obtained from corers with 0.5 cm diameter holes bored into the walls at 5 cm intervals. When repeating the same measurement eight times the results showed a maximum variability of 0.3°C between the highest and lowest reading.

2.5.2 Sediment porosity

Porosity is the ratio of the volume of the void spaces in the sediment to the total sediment volume. It was established by transferring a constant volume of sediment onto pre-weighed aluminium trays, weighing the sample on a Sartorius 1265 MP electronic top-loader balance to the nearest milligram, and recording the wet weight of the sediment (m_w , g) after subtracting the weight of the tray. The samples were then oven-dried at 40°C until they reached constant weight, which was - after correction for the tray weight - noted as the saline sediment dry weight (m_D , g). Assuming that the sediment was saturated with sea water, the mass of interstitial water (m_{int} , g) can be calculated from the difference in wet and dry sediment weight:

$$m_{int} = m_w - m_D \quad (2.4)$$

The weight of the dry sediment particles (m_p , g) was calculated by correcting m_D for the salt from the evaporated interstitial water (assumption: salinity = 34).

As there was a substantial error associated with sampling a constant volume of sediment, the porosity was calculated from the moisture content of the sediment in the following way. The moisture content (ω) is the ratio of the mass of interstitial water to that of sediment particles. Before calculating porosity, the dimensionless void ratio (e), *i.e.* the relationship between the volume of the void spaces in saturated sediment (V_v , dm^3) and the particle volume (V_p , dm^3), was estimated from the moisture content multiplied by the ratio of the mass of a volume of dry particles to that of an equal volume of pure water. This so-called particle specific gravity (G_s) is assumed to be 2.65 for sand, and 2.7 for mud (Smith and Smith, 1998):

$$e = \frac{V_v}{V_p} = \omega G_s \quad (2.5)$$

Using the void ratio, the porosity (n) is calculated as:

$$n = \frac{V_v}{V} = \frac{e}{1+e} \quad (2.6)$$

where V is the volume (dm^3) of the water saturated sediment sample.

2.6 Meteorological parameters

2.6.1 Wind velocity

Wind velocity is a crucial factor as it determines the flux of methane between the ocean and the atmosphere. Wind data were obtained from meteorological stations close to the sampling sites.

The wind in the Menai Strait is highly variable due to land shielding. There are two stations close to St. George's Pier, which record wind data differently. Pen-y-Ffridd on the Bangor side of the Menai Strait collects the 'run of wind' with a cup counter anemometer at a height of 10 feet, *i.e.* the total amount of wind in whole kilometres over a 24 hour period starting from 0900 h Greenwich Mean Time (GMT). From this the mean wind velocity in m s^{-1} was calculated without a measure of variability. The School of Ocean Sciences' meteorological station in Menai Bridge has been in operation since summer 1996 and records wind velocities ten times per hour. The data were summarised to hourly averages from which a mean daily wind velocity with a measure of variability was calculated. Velocities from both sites were corrected to velocities at 10 m height above ground level using the logarithmic relationship between wind speed and height above water/ground as described in Oke (1978) (see Appendix 2-1).

There is no meteorological station at Point Lynas. The nearest one is Pen-y-Bonc on top of Parys Mountain some 5.5 km inland from Point Lynas. Here the wind velocity is measured six times a day with a hand-held Casella cup counter anemometer. A mean daily wind velocity with a variability value calculated from only six data points is not very reliable for such a dynamic parameter. Cross-calibrations were undertaken to establish the relationship between wind velocities measured at Pen-y-Bonc and Point Lynas. For this, hand-held Casella anemometer readings were recorded simultaneously at Pen-y-Bonc and Point Lynas during calm and windy conditions. The cross-calibrations suggest that the wind velocity at Pen-y-Bonc is similar to that at Point Lynas during windy days but is significantly higher during calm spells (Appendix 2-2.).

2.7 Methane analysis

The first project task was to set up a simple, reliable and inexpensive method to quantify methane concentrations in air and sea water - and subsequently in sediments - at the School of Ocean Sciences. This section outlines the general principles of the method, followed by a description of the specific set-up, and concludes with an explanation of the calculations.

Methane is analysed using gas chromatography. Whilst air and freshwater samples can be injected directly into the gas chromatograph (GC) (HMSO, 1988), this procedure is not appropriate for sea water and mud because corrosion and seizure of GC components would occur. Methane in such samples is therefore extracted into a gaseous phase before GC injection.

2.7.1 Methane extraction from sea water

Methane extraction methods endeavour to remove all or a constant fraction of methane from the water sample into a gaseous matrix. Two different extraction procedures are commonly used for water samples: the purge and trap and the headspace equilibration technique. For the purge and trap extraction technique (*e.g.* Brooks *et al.*, 1981; Lilley *et al.*, 1983), a water sample is purged for several minutes with a methane-free gas (*e.g.* nitrogen, hydrogen or helium) until all methane is removed from the sample. The purged components are then cryotrapped. Thermal desorption of the trapped gases is followed directly by GC injection. Methane extraction by headspace equilibration (Johnson *et al.*, 1990; Upstill-Goddard *et al.*, 1996) on the other hand is based on Henry's law, and uses the partitioning relationship between two phases. It thus does not remove all methane from the water sample. A known headspace volume of methane-free gas (or a gas mix of known methane concentration) is added to a known volume of water sample. Gases are allowed to equilibrate fully between the two phases before the methane content in the headspace gas is analysed with the GC. Initial methane concentrations in the water sample are calculated by

adding methane measured in the headspace and methane calculated to have remained in the water. The amount of methane left in the water phase after equilibration can be calculated using the gas specific, temperature and salinity dependent Bunsen coefficient (Yamamoto *et al.*, 1976; Wiesenburg and Guinasso, 1979).

Several alterations have been made to this extraction method, commonly a vacuum extraction with or without ultra-sonification (Swinerton *et al.*, 1962; Brooks and Sackett, 1973; Ward *et al.*, 1987; Schmitt *et al.*, 1991; Scranton and McShane, 1991; Lammers and Suess, 1994). Purge and trap extraction is the more sensitive technique but also more complicated and expensive to set up and run. As coastal waters are generally methane-rich, headspace extraction was considered adequate and thus chosen.

Experimental procedure

Water samples were taken and equilibrated in 50 cm³ hypodermic luer lock Plastipak[®] syringes (Becton Dickinson & Co. Ltd, Ireland) with plastic luer lock three-way stopcocks to open and close the syringes. Experiments showed new plastic syringes to be leak-tight for about two days if kept submerged under water, and not to absorb any methane. Older syringes, however, became progressively less gas-tight. Even new glass syringes on the other hand were found to leak gas already after two to four hours.

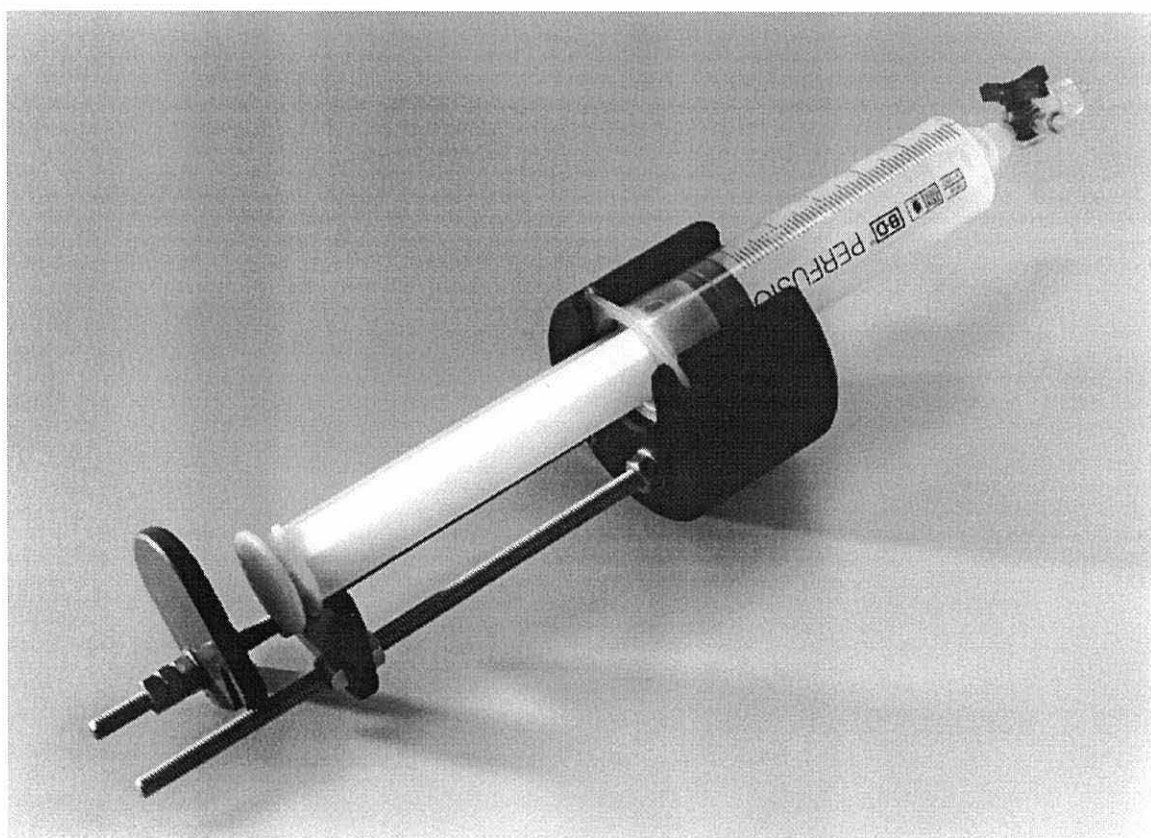


Figure 2.4 Photograph of the volumeter (Photo: D.L. Robbins).

a. SAMPLING

The diagram shows a syringe with 'wings' being used to draw water from a reservoir. The syringe is inverted, with the tip submerged in water. The atmosphere is above the water level. A 3-way stopcock is at the bottom of the syringe.

b. FITTING SYRINGE INTO VOLUMETER

The diagram shows the syringe being inserted into a volumeter body. The syringe is held in place by a limit stop groove. The volumeter body has a fixed V_W limit stop.

c. ESTABLISHING V_W

The diagram shows the stopcock open, allowing water to be expelled from the syringe. The water level in the syringe is adjusted to the V_W limit stop (fixed). Manual pressure is applied to expel excess water.

d. ESTABLISHING V_G

The diagram shows the syringe being connected to a gas carrier (Nitrogen) via a valve. The gas carrier is set to 10 ml/min. The gas is introduced into the syringe, and the gas level is adjusted to the V_G limit stop (rotatable).

Oxygen-free nitrogen, taken from the GC carrier gas line, was used as the headspace gas. Thereby no signal was obtained when injecting the headspace gas before equilibration. The

headspace gas line was connected to the three-way stopcock of the syringe (Figure 2.5 d). The syringe was still housed in the volumeter and the V_G limit stop was slid forward. The line and stopcocks were purged with nitrogen before the syringe stopcock was turned to allow headspace gas into the sample syringe (flow rate $\sim 10 \text{ ml min}^{-1}$). The pressure of the in-flowing gas gently pushed the plunger back until it hit the V_G limit stop (Figure 2.5 d). The syringe stopcock was then closed, the nitrogen flow stopped and the line disconnected from the syringe. The stopcock was opened for two to three seconds to allow pressure equilibration of the headspace with the atmosphere. Experiments (not illustrated) had shown that no detectable amounts of methane entered the syringe during the short period when the stopcock was open.

Earlier every syringe had been numbered and its V_W and V_G calibrated gravimetrically on a Sartorius 1265 MP electronic top-loader balance with deionised water at a constant temperature. The calibrations and later the equilibrations were carried out at $20 \pm 2 \text{ }^\circ\text{C}$, so that no thermal correction for the volume was required. As the syringes were not totally rigid and their fitting into the volumeter was a little loose, the filling precision was found to be $0.41 \pm 0.24 \text{ \% (CV)}$ for V_W ($N = 16$) and $0.6 \pm 0.31 \text{ \% (CV)}$ for V_G ($N = 16$).

As methane from a certain volume of water is the more concentrated the smaller a gas volume (V_G) it equilibrates into, and as the analytical precision increases with signal intensity (Section 2.7.5), the smallest possible V_G was used. Calibrations showed the injection system to have a volume of 4.12 cm^3 under experimental conditions. As the system should be flushed at least once, 8.5 cm^3 were considered the minimum V_G volume required. The syringe size allowed V_W to take up approximately 52 cm^3 .

Once the headspace gas was introduced, equilibration began. In 1996 the syringes were briefly shaken and then allowed to passively equilibrate over 3 to 4 hours submerged in water (Appendix 2-3 A). In 1997 samples were shaken. Insulating gloves were worn to avoid heat transfer to the samples. Two to three minutes of shaking proved sufficient to obtain equilibration (Appendix 2-3 B). The extraction method was altered because active equilibration reduced analysis time and furthermore improved precision (Section 2.7.5). HgCl_2 poisoning of samples for preservation was no longer required.

2.7.2 Methane extraction from sediments

The common way of extracting methane from sediments is by introducing a calibrated volume of headspace gas into a vessel containing a calibrated volume of sediment. The samples are then shaken and the headspace methane concentration is analysed with a GC. The amount of interstitial water, which contains the methane, is established gravimetrically by weighing the sediments before and after drying (Section 2.5.2 on sediment porosity).

To avoid purchasing and calibrating new gas-tight vessels, a method was designed which used the already calibrated plastic syringes and the set-up for water analysis. Sediment was taken either from the sediment surface or from a sliced core by pushing a truncated 50 cm³ syringe with an inner diameter of 2.75 cm into it. A 0.5 or 1 cm deep slice was cut off and transferred swiftly into an upside down syringe which was filled with HgCl₂ poisoned filtered sea water of determined methane concentration and which was at room temperature. The plunger was introduced without trapping bubbles. The 'sludge' (V_w) and headspace volumes (V_G) were established as for extraction from sea water using the two-stop volumeter. The interstitial water was thoroughly mixed with the poisoned water during active equilibration so that it behaved like pelagic water. The analysis was the same as for water.

The sediment porosity of the sample was determined using an aliquot sample from the same core. After methane analysis the syringe content was weighed before and after all water was evaporated. Multiplying the dry weight of the sample with the moisture content of the wet sediment yields the volume of pore water. The volume of water of determined methane content added to dilute the sediment into sludge is the difference between the total volume of water and the interstitial water. Methane added in this volume of water is subtracted from the total methane content to obtain the sample methane concentration. For calculations see section 2.7.4.

2.7.3 Separation and quantification

Air samples and the equilibrated headspace from water and sediment samples were introduced into the GC through a line that could be swept clean with nitrogen carrier gas. The sample was introduced by connecting the syringe to the line *via* a stopcock arrangement (Figure 2.6 A) and opening the syringe stopcock to the line. The headspace gas was gently pushed into the system by pressing the plunger forward until the water reached the stopcock. The headspace gas passed then through a 'Drierite' drying tube with a glass wool plug to absorb water and salts, and was from there directed *via* a 6-port 2-position 1/16" Valco valve, positioned inside the GC oven, into a loop of a calibrated volume (1 cm³). Once passed through this loop, it was vented through a long exhaust tube to the outside (Figure 2.6 A). Once all the headspace gas had been introduced, the valve was turned from the 'load' to the 'inject' position which directed the carrier gas through the loop to take the plug of headspace gas onto the separating GC column (Figure 2.6 B). A 30 m long megabore (inner diameter = 0.53 mm) porous layer open tubular (PLOT) molecular sieve column (J&W Scientific GS-Molesieve, P/N 1153632) separated methane from other hydrocarbon gases. When turning the valve, a trigger was pulled to start recording the detector readings. A carrier gas flow rate of 10 cm³ min⁻¹ and an isothermal column temperature of 30°C were found to produce the sharpest and most intense signals and also the shortest retention times (Appendix 2-4 A, B and C).

Flame ionisation detectors (FID) are draught-free blocks in which the column eluates are first mixed with hydrogen and then burnt in air. Organic compounds in the eluate, which have been separated along the GC column, become ionised during combustion and are thus converted into pulses of ions. Two electrodes near the FID flame have an electrical current flowing between them. The pulses of ions formed per unit time increase this current proportionally to the amount of volatile, ionised carbon in the eluted sample. The electrical signal is then processed and integrated to show peaks along the time axis representing the amount of carbon compounds eluted from the column at specific retention times. A computer programme integrated the peaks. Varian Star Chromatography Workstation software produced a chromatogram and a list of retention times, peak areas and half peak widths. The FID measures nearly all volatile organic compounds with very high sensitivity and over a wide range of linearity (Willett, 1987; Schomburg, 1990).

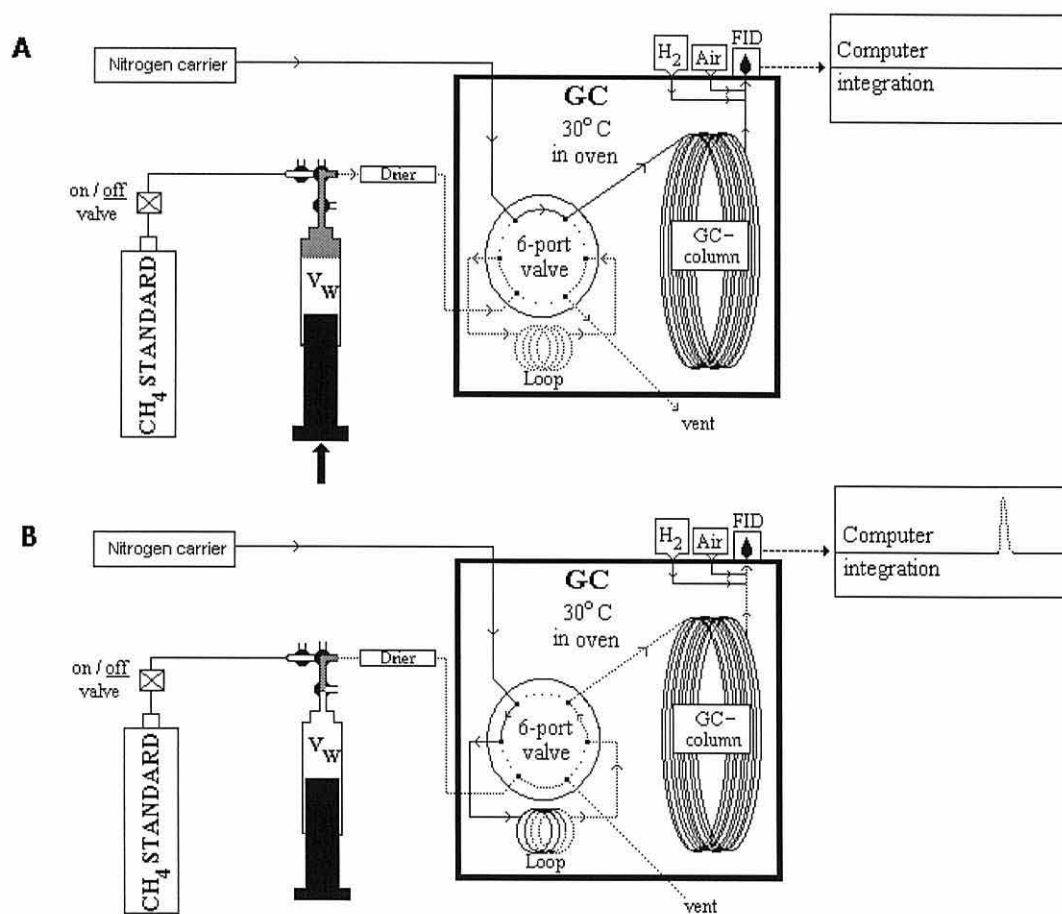


Figure 2.6 Sample (or standard) loading (A) and injection (B) for GC methane separation.

The FID set-up used flow rates of 20 cm³ min⁻¹ make-up nitrogen, 30 cm³ min⁻¹ hydrogen and 300 cm³ min⁻¹ air (Figure 2.6 A). High detector temperatures were found to increase the signal intensity (Appendix 2-4 C) and the detector temperature was therefore set at 250°C. Under these

conditions the methane retention time was 1.30 ± 0.02 minutes. Often a negative peak occurred at around 0.7 minutes, which proved to be caused by oxygen. It was used as a qualitative indication for oxygen in incubation experiments. Quantification was achieved by comparison to a certified methane standard. Calibration curves proved the FID response to be linear ($R^2 > 0.999$) over the tested range from 0.25 to 1000 μ -atmosphere (Appendix 2-5). The standard was connected directly to the injection line (Figure 2.6 A) and injected every 3 to 6 runs. On most days, no machine drift occurred and standard injections were used for estimates of GC precision.

2.7.4 Calculations of methane concentration and saturation

The following equations were employed to calculate methane concentrations and saturations in seawater, air, and sediments.

Sea water

Headspace extraction of methane distributes the methane contained in the water sample between the liquid and the - previously methane-free - gas phase. The mass balance equation of methane partition is:

$$C_w \times V_w = (C_G' \times V_G) + (C_w' \times V_w) \quad (2.7)$$

where C_w = methane concentration in initial sea water sample (mol dm^{-3})
 V_w = volume of water in syringe (dm^3)
 C_G' = methane concentration in headspace after equilibration (mol dm^{-3})
 V_G = headspace volume in syringe (dm^3)
 C_w' = methane concentration in water after equilibration (mol dm^{-3})

The distribution of the gas between the liquid and the aqueous phase is determined by the Bunsen solubility coefficient (β , v/v) such that

$$\beta = \frac{C_w'}{C_G'} \quad \text{and} \quad C_w' = \beta \times C_G' \quad (2.8)$$

As β is dimensionless it can be used also for the molar distribution.

Thus equation 2.7 may be re-written as

$$C_w \times V_w = (C_G' \times V_G) + (\beta C_G' \times V_w) = C_G' (V_G + \beta V_w) \quad (2.9)$$

Dividing by V_w gives

$$C_w = C_G' \left(\frac{V_G}{V_w} + \beta \right) \quad (2.10)$$

The Bunsen solubility coefficient may be calculated from the experimentally derived equation by Wiesenburg and Guinasso (1979):

$$\ln \beta = -60.8862 + 101.4956 \left(\frac{100}{T} \right) + 28.7314 * \ln \left(\frac{T}{100} \right) + S \left[-0.076146 + 0.04397 \left(\frac{T}{100} \right) + \left(0.006872 \left(\frac{T}{100} \right)^2 \right) \right] \quad (2.11)$$

where T = absolute temperature (K)
S = salinity

The computer software calculates the integrated area of the sample peak (PA_G) and that of a 5.15 μ -atmosphere methane standard (PA_{STD}) from GC signal peaks. The methane concentration in the injected sample is calculated as:

$$M_G = M_{STD} \times \frac{PA_G}{PA_{STD}} \quad (2.12)$$

where M_G = methane concentration in the headspace gas (μ -atmosphere)
 M_{STD} = methane concentration in the standard (= 5.15 μ -atmosphere)

The ideal gas equation is used to convert M_G to molarity:

$$C_G = M_G \times \frac{P}{RT} \times 10^{-3} \quad (2.13)$$

where P = atmospheric pressure ($N m^{-2}$) at time of injection
R = gas constant ($8.3 N m K^{-1} mol^{-1}$)
T = absolute temperature (K) at time of injection

Multiplication by 10^{-3} converts moles m^{-3} into moles dm^{-3} .

A correction was made for the water vapour that was initially present in the headspace gas but was removed prior to sample injection. The removal of water vapour from the gas will effectively increase the partial pressure of methane by $(P-p_w)/P$.

The saturation water vapour pressure (p_w , $N m^{-2}$) is calculated from the following equation from Weiss and Price (1980):

$$p_w = EXP \left[24.453 - \left(67.4509 * \left(\frac{100}{T} \right) \right) - \left(4.8489 * \ln \left(\frac{T}{100} \right) \right) - (0.000544 + S) \right] \quad (2.14)$$

The corrected form of equation (2.13) is thus

$$C_G = M_G \times \frac{P - p_W}{P} \times \frac{P}{RT} \times 10^{-3} = M_G \times \frac{P - p_W}{RT} \times 10^{-3} \quad (2.15)$$

Thus combining the above and equation (2.10) gives C_W in moles methane dm^{-3} :

$$C_W = M_G \times \frac{P - p_W}{RT} \times 10^{-3} \times \left(\frac{V_G}{V_W} + \beta \right) \quad (2.16)$$

or

$$C_W = 5.15 \times 10^{-6} \times \frac{PA_G}{PA_{STD}} \times \frac{P - p_W}{RT} \times 10^{-3} \times \left(\frac{V_G}{V_W} + \beta \right) \quad (2.17)$$

To determine the degree of saturation of methane in sea water relative to the atmosphere, one first has to calculate the hypothetical equilibrium concentration:

$$C_{eq} = C_{G(atm)} \times \beta_{in situ} \quad (2.18)$$

where C_{eq} = methane concentration (mol dm^{-3}) in equilibrium with atmosphere
 $C_{G(atm)}$ = atmospheric methane concentration (mol dm^{-3})
 $\beta_{in situ}$ = Bunsen solubility coefficient for *in situ* temperature and salinity

The saturation of methane in sea water relative to the atmosphere is obtained by dividing C_W by the equilibrium methane concentration:

$$Saturation = \frac{C_W}{C_{eq}} \quad (2.19)$$

A saturation ratio of 1 signifies saturation, of less than 1 undersaturation and of greater than 1 supersaturation.

Air

Methane in air is calculated with equation (2.12) yielding the concentration in μ -atmospheres. If required in a molar unit, the μ -atmosphere unit is converted using equation (2.15).

Sediments

Equation (2.17) provides the molarity of methane of the sludge in the syringe (V_W), made up of sediment particles, interstitial water and diluting water. To calculate the methane concentration in the interstitial water of the sediment the following measurements and corrections are made.

To estimate the total mass of water in the syringe (m_w , g), the wet weight of the sample is measured before all water is evaporated and the dry weight of the sediment (m_p , g) is determined and corrected for the weight of the salt from the evaporated water. m_w is the difference between the wet and the dry weight.

The mass of interstitial water (m_{int} , g) is determined from the dry weight of the sediment in the sample and the moisture content (ω , dimensionless) of a replicate of the original sediment sample (Section 2.5.2):

$$m_{int} = \omega * m_p \quad (2.20)$$

The mass of diluting water (m_{dil}) is then simply calculated by difference, *i.e.*:

$$m_{dil} = m_w - m_{int} \quad (2.21)$$

The mass balance equation for the diluted sample is thus:

$$C_{Sludge} \times (m_{dil} + m_{int}) = (C_{int} \times m_{int}) + (C_{dil} \times m_{dil}) \quad (2.22)$$

where C_{sludge} = Methane concentration in the sludge in the syringe (mol dm^{-3})
 C_{dil} = Methane concentration in the diluting water (mol dm^{-3})
 C_{int} = Methane concentration in the interstitial water (mol dm^{-3})

Note, the salt content is ignored in the calculation as the salinity of the diluting water and the interstitial water are close and so the density effect cancels out.

Solving equation 2.22 for C_{int} :

$$C_{int} = \frac{C_{Sludge} (m_{dil} + m_{int}) - (C_{dil} \times m_{dil})}{m_{int}} \quad (2.23)$$

2.7.5 System performance, precision and accuracy of analysis

The detection limit of the used methane system is calculated as twice the GC signal to noise ratio, and lies around 600 pM. The instrumental, random error was found to be inversely related to signal intensity and to lie between 0.06 % (CV) for 100 μ -atmosphere methane and 4.94 % for 0.25 μ -atmosphere (Appendix 2-6). Precision depends also on the type of sample injected. Gas samples (standard and air) give the most precise results, while extraction from an aqueous matrix into the headspace proved to be an additional source of error. Equilibration by passive diffusion as practised in 1996 had a precision of 4.2 ± 0.41 (CV) % ranging from 1.53 to 9 %.

The improved technique used in 1997 reduced the coefficient of variation to 2.63 ± 0.38 % (CV), ranging from 0.37 to 8.6 %. The analytical errors are due to i) occasional bubble inclusion during filling of syringes, ii) loss of supersaturation from water during filling, iii) volumetric inaccuracies during the establishment of V_w and V_G (chapter 2.6.1), and iv) to older syringes beginning to leak. Also the cleanliness of the nitrogen, the condition of the column and detector and the presence or absence of small leaks in the system influence precision.

The routinely used standard contained 5.15 μ -atmosphere methane in nitrogen (MG Gas) and had a guaranteed accuracy of 2% or 0.103 μ -atmosphere. A cross-calibration with a NOAA standard of 1.818 μ -atmosphere methane in air verified the accuracy of the MG standard.

Triplicate samples were taken for methane analysis and the variability for methane is expressed as 1 standard error (SE) where not otherwise stated.

*Science is built of facts, as a house is built of stones;
But an accumulation of facts is no more a science
Than a heap of stones is a house.*

Henri Poincaré (1854-1912)

Chapter Three

RESULTS

This chapter describes the results of a two-year investigation (March 1996 to February 1998) into the distribution, sources and sinks of methane in the coastal water column, and is divided into six sections. The first describes the seasonal patterns of methane and of several physical, particulate and production parameters in the waters at Point Lynas and in the Menai Strait. The second section investigates the small-scale variability of methane in Menai Strait waters. Part three looks at the pelagic environment as a site for methane production by investigating net production rates of methane in the water. To quantify methane inputs from external sources, methane concentrations in river water and sewage are reported in the fourth section. The fifth section studies the sedimentary distribution of methane. The final part reports on a laboratory experiment studying the effect of temperature on methane metabolism in Menai Strait sediments. All raw data are tabulated in Appendix 3.

3.1 Seasonality of methane and other parameters in the coastal zone

Very few seasonal studies of methane in coastal waters have been published. The following section reports the seasonal pattern of surface water methane concentrations in relation to other seasonal parameters measured in 1996 and 1997 in two contrasting environments: the sheltered Menai Strait and the exposed Point Lynas site. Aquatic and atmospheric methane concentrations, water temperatures, salinities, wind speeds, POC and PON, chlorophyll and phaeopigment concentrations, and community oxygen production and respiration rates were measured between March and November 1996 in both environments. All parameters but oxygen production rates and POC and PON concentrations were determined for a consecutive season in the Menai Strait.

Physical parameters

Sea water temperature

In all three seasonal studies highest water temperatures were observed late in July or early in August (Figure 3.1.1 B and H). In the Menai Strait, a higher maximum water temperature was observed in 1997 than the previous year.

Salinity

Salinity followed no obvious seasonal pattern, and remained in all three studies above 30 (Figure 3.1.1 B and H).

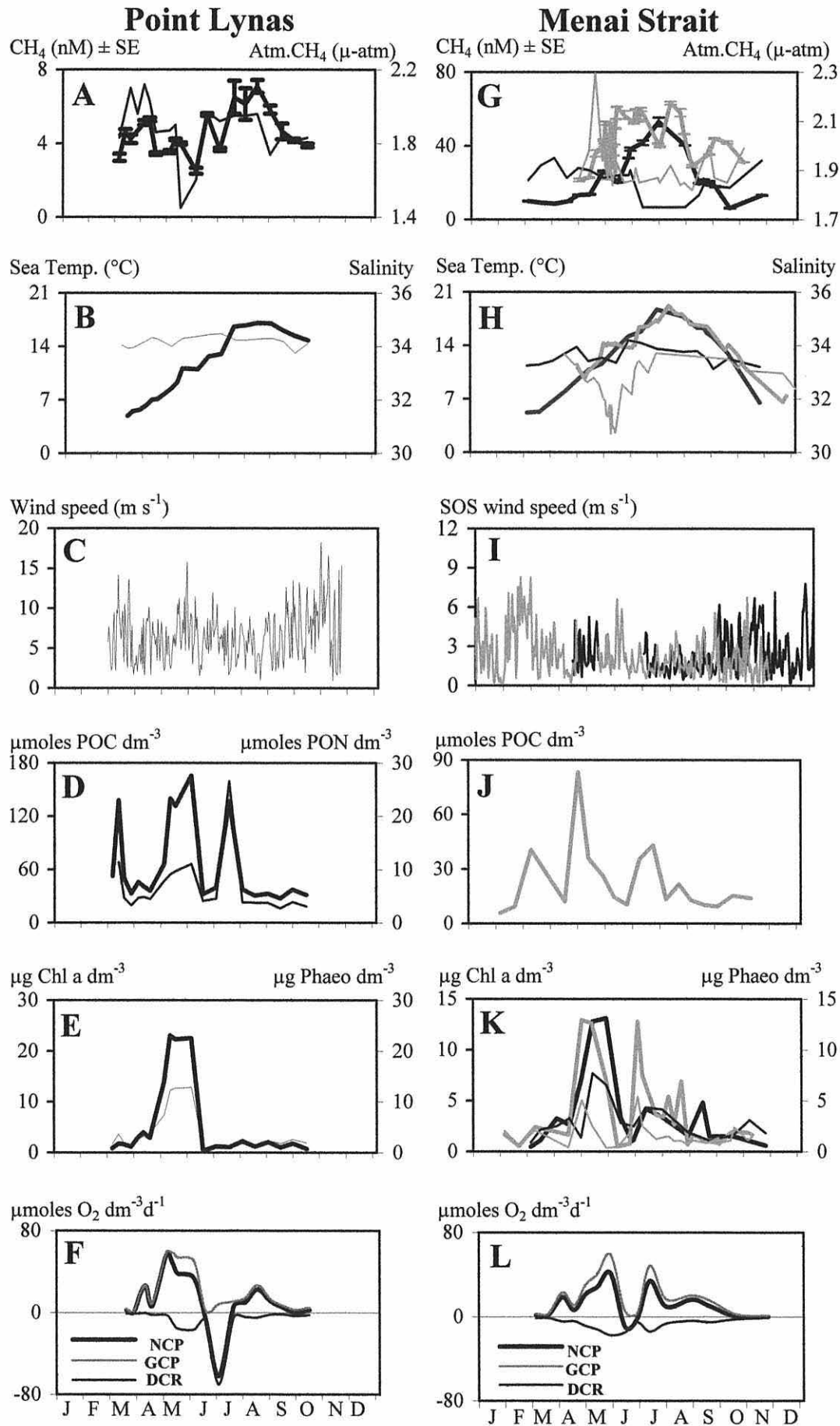


Figure 3.1.1 See next page for legend.

Figure 3.1.1 Seasonal patterns of several pelagic and atmospheric parameters for 1996 at Point Lynas (left column, graphs A – F), and for 1996 (black) and 1997 (grey) in the Menai Strait at Menai Bridge (right column, graphs G – L). Thick lines refer to the primary y-axis, thin lines to the secondary y-axis: Graphs A and G show aquatic methane concentrations (CH_4 - nM) and atmospheric methane concentrations (Atm. CH_4 - $\mu\text{-atm}$), graphs B and H water temperatures ($^{\circ}\text{C}$) and salinities, graphs C and I mean daily wind speeds (m s^{-1}), graphs D and J POC and PON concentrations (μM), graphs E and K chlorophyll (Chl a - $\mu\text{g dm}^{-3}$) and phaeopigment concentrations (Phaeo - $\mu\text{g dm}^{-3}$), and graphs F and L rates of net community production (NCP), gross community production (GCP), and dark community respiration (DCR) ($\mu\text{mol O}_2 \text{ dm}^{-3} \text{ d}^{-1}$).

Wind speed

The mean 1996 wind speeds at Point Lynas were between 2.4 and 5 fold higher than in the Menai Strait (Table 3.1.1 and Table 3.1.2). A large spatial variability was observed over the short distance (approximately 1 km) between the School of Ocean Sciences and the Pen-y-Ffridd meteorological stations. Mean wind speeds at the School of Ocean Sciences were -3 to 60% higher than at Pen-y-Ffridd (Table 3.1.1 and Appendix 3.1). At all three sites wind speeds were very variable throughout the year (Figure 3.1.1 C and I), and the mean daily wind speeds were lower in the summer than in the winter (Table 3.1.1). Lowest mean monthly wind speeds occurred in mid summer (July – August) and in spring (April) (Table 3.1.2).

Table 3.1.1 Mean daily wind speeds (m s^{-1}) at the two meteorological stations in the Menai Strait (Ocean Sciences and Pen-y-Ffridd) and at Point Lynas. The mean summer (23/05 to 22/10) and winter values (23/10 to 22/05) are given, where available, with their respective standard deviations (SD) as a measure of variability.

	Summer 1996	Winter 1996	Summer 1997	Winter 1997
Ocean Sciences	2.0 ± 1.3	2.7 ± 1.7	2.0 ± 1.3	2.8 ± 2.1
Pen-y-Ffridd	1.3	2.8	1.3	1.9
Point Lynas	6.4 ± 2.9	6.8 ± 3.8	-	-

Table 3.1.2 Mean monthly wind speeds (m s^{-1}) at Pen-y-Bonc near Point Lynas and at the School of Ocean Sciences by the Menai Strait.

	Point Lynas 1996	Menai Strait 1996	Menai Strait 1997
January	-	-	2.3
February	-	-	4.7
March	6.6	-	2.7
April	5.7	2.3	1.6
May	6.5	2.7	2.0
June	6.4	-	2.4
July	5.7	1.7	1.6
August	5.5	1.5	1.8
September	6.4	2.5	2.1
October	8.5	3.2	1.9
November	8.0	2.7	-

Particulate parameters

Particulate organic carbon and nitrogen

At both sites, POC concentrations displayed three peaks throughout the season, - in March, May and July (Figure 3.1.1 D and J). 1996 Point Lynas POC concentrations were above 1997 Menai Strait concentrations by between 30 and 570%. PON concentrations at Point Lynas followed the same pattern as POC. The July peak, however, was significantly richer in PON than the previous peaks. The mean C/N ratio at Point Lynas was 8.6 ± 2.1 . The PON measurements for the Menai Strait were disregarded because they were extremely low (Appendix 3.1) when compared to concentrations reported by Blight and co-workers (1995) for the same site in previous years, because the C/N ratio of 35 ± 14 was unusually high, and because there was suspicion that stored samples had been defrosted.

Chlorophyll and phaeopigment concentrations

Chlorophyll and phaeopigment concentrations followed very similar seasonal patterns and reached peak values in May (Figure 3.1.1 E and K). During this spring bloom the concentrations at Point Lynas were nearly double the Menai Strait concentrations. Chlorophyll and phaeopigment showed only one peak at Point Lynas, but multiple peaks in both years in the Menai Strait. In the Menai Strait both chlorophyll and phaeopigment concentrations peaked 1-3 weeks earlier in 1997 than the previous year. Phaeopigment concentrations were high relative to chlorophyll. During bloom situations phaeopigment concentrations were about 60% (1996) and 40% (1997) of chlorophyll. During the colder months, phaeopigment concentrations were close to or even higher than chlorophyll concentrations.

Production parameters

Oxygen production and respiration rates

Gross community oxygen production rates (GCP) were highest towards the end of May (Figure 3.1.1 F and L) when they preceded and overlapped with the major chlorophyll, phaeopigment, POC and PON peaks. There was a second smaller peak in mid to late summer. Spring dark community respiration rates (DCR) peaked simultaneously with or just after gross production rates. Respiration rates increased to form a second smaller peak in August in the Menai Strait, and an unusually large peak on 2 July at Point Lynas. Net community production rates (NCP) showed a positive oxygen balance in both stations throughout most of the year with maximum net oxygen production in May. During June and July net oxygen consumption occurred at times.

Methane concentrations

Atmospheric methane concentrations

Figures 3.1.1 A and G and Table 3.1.3 suggest a tendency for atmospheric methane concentrations to be slightly higher in winter than in summer at both sampling sites. Analysis with an independent non-equal two sample t-test renders this difference as insignificant for Point Lynas ($T=0.59$, $p=0.57$) and for 1997 in the Menai Strait ($T=1.85$, $p=0.14$). The difference is, however, significant at the 5% level for 1996 in the Menai Strait, where winter concentrations of atmospheric methane were higher than summer concentrations as revealed by an independent greater than two sample t-test ($T=3.27$, $p=0.003$). An increase in atmospheric methane concentrations above the Menai Strait from 1996 to 1997 is apparent (Table 3.1.3).

Table 3.1.3 Means and standard deviations (SD) of overall, and separated summer (23/05 to 22/10) and winter (23/10 to 22/05) atmospheric methane concentrations (μ -atmosphere) at Point Lynas in 1996 and above the Menai Strait in 1996 and 1997. The number of observations in each class (N) is given in brackets.

	Overall	Winter	Summer
1996 Point Lynas	1.88 ± 0.16 (N=19)	1.90 ± 0.20 (N=9)	1.86 ± 0.12 (N=10)
1996 Menai Strait	1.87 ± 0.07 (N=16)	1.91 ± 0.03 (N=7)	1.83 ± 0.06 (N=9)
1997 Menai Strait	1.92 ± 0.10 (N=33)	2.03 ± 0.16 (N=5)	1.90 ± 0.06 (N=28)

Water column methane concentration

In the Menai Strait water column methane concentrations show a distinct seasonal pattern with a broad summer peak in both years of the study (Figure 3.1.1 G). Concentrations in 1996 ranged approximately from 10 to 53 nM, and in 1997 from 13 to 63 nM. These concentration ranges equate to saturation ratios of 2.4 to 17.6 in 1996 and 3.8 to 26.4 in 1997 (Figure 3.1.2). Maximum concentrations were measured in late summer, on 29 July in 1996 and on 11 August in 1997. The 1997 methane concentrations were systematically higher than in the previous year, particularly during spring and autumn. They also showed much greater variability throughout the year. As indicated by this two year long study, however, the interannual differences in methane concentrations in the Menai Strait appear relatively small.

At the exposed Point Lynas site water column methane concentrations were nearly 10-fold lower than in the more sheltered Menai Strait, with concentrations ranging from 2.5 to 7.1 nM (Figure 3.1.1 A) and saturation ratios from 1.0 to 2.7 (Figure 3.1.2). The seasonal pattern at Point Lynas was much less clear than in the Menai Strait. As in the Menai Strait, however, the maximum concentration occurred in late summer (15 August 1996).

Because of malfunctioning analytical equipment, water samples for methane analysis taken between 17 July and 16 August 1996 were preserved with HgCl_2 , stored under cooled water and analysed in late August. HgCl_2 -poisoned samples of oceanic water, when kept cool and submerged in gas-tight containers, have been reported to remain unaltered in their methane content for several weeks (*e.g.* Scranton & Brewer, 1977). Coastal waters, however, appear to vary in their response to preservation (see changes in poisoned controls in incubation experiments in Figure 3.3.1). The reliability of the 1996 peak values therefore remains unknown. The large error bars for the 1996 summer concentrations in both environments (Figure 3.1.1 A and G) may thus result from the method of preservation.

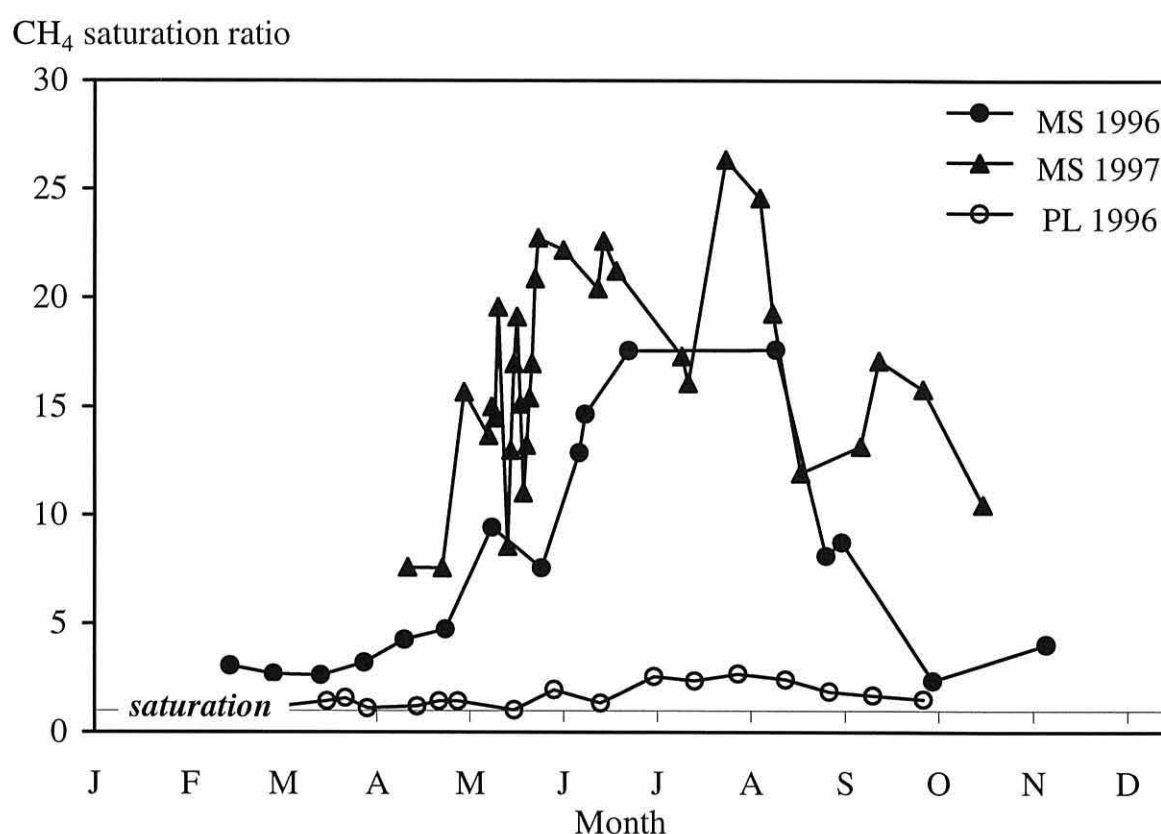


Figure 3.1.2 Seasonal pattern of methane saturation ratios in the waters of the Menai Strait at Menai Bridge (MS) in 1996 and 1997 and at Point Lynas (PL) in 1996.

The seasonal patterns of water column methane concentrations and of sea water temperature are very similar, with peak values coinciding in all three studies (Figure 3.1.1 A, B and G, H). Wind speed with its winter peaks and summer troughs shows a broadly negative relationship with water column methane concentrations (Figure 3.1.1 A, C and G, D). Chlorophyll, phaeopigment, POC and PON concentrations, oxygen productivity and respiration rates peaked at roughly the same time in spring and thus showed no systematic relationship with the seasonal behaviour of methane.

Box 3.1: Summary of ‘seasonality of methane in coastal waters’

- Methane concentrations were supersaturated throughout the sampling periods
- Methane concentrations showed a summer maximum
- Concentrations in the Menai Strait were 2 to 10 fold higher than at Point Lynas
- Methane concentrations and water temperature were positively related
- A general negative relationship between methane and wind speed was observed
- No relationship was detected between methane concentration and plankton production or particulate parameters

3.2 Short-term variability of methane concentrations in the water column

The degree of the small-scale variability of methane measured in the water column at fixed sampling stations must be known to evaluate the results of the seasonal study for which water had been sampled periodically (Section 3.1). In this section, the scale of the short-term variability at fixed sampling stations in the Menai Strait is established. An attempt is then made to deconvolute the spatial and temporal components of the variability, as this may aid to identify methane sources and sinks. The investigation proceeded in three steps.

First, the changes in water column methane concentrations at fixed sampling sites in the Menai Strait were examined a.) on an approximately daily basis over a full spring-neap tide cycle and b.) through the diurnal tidal cycle.

Then, the predominantly spatial variability of methane was investigated along three horizontal transects through different sections of the Menai Strait. Changes in methane concentration with water depth were also studied at four sites.

Finally, the temporal methane variability in one mass of Menai Strait water was investigated and quantified from a station that drifted passively on the water.

3.2.1 Variations of methane concentrations at fixed stations

Variability over a fortnightly spring-neap tidal cycle

Between 27 May and 12 June 1997 daily samples for measurements of aquatic and atmospheric methane and of water temperature were taken at St. George’s Pier within two hours of daytime high tide, when water flowed south-westwards into the net current direction. No samples were

collected on 31 May and 1 June. Daily mean meteorological data were obtained from the School of Ocean Sciences station. Neap tide was on 29 May and again on 13 June (one day after the end of the study) and spring tide on 5 June.

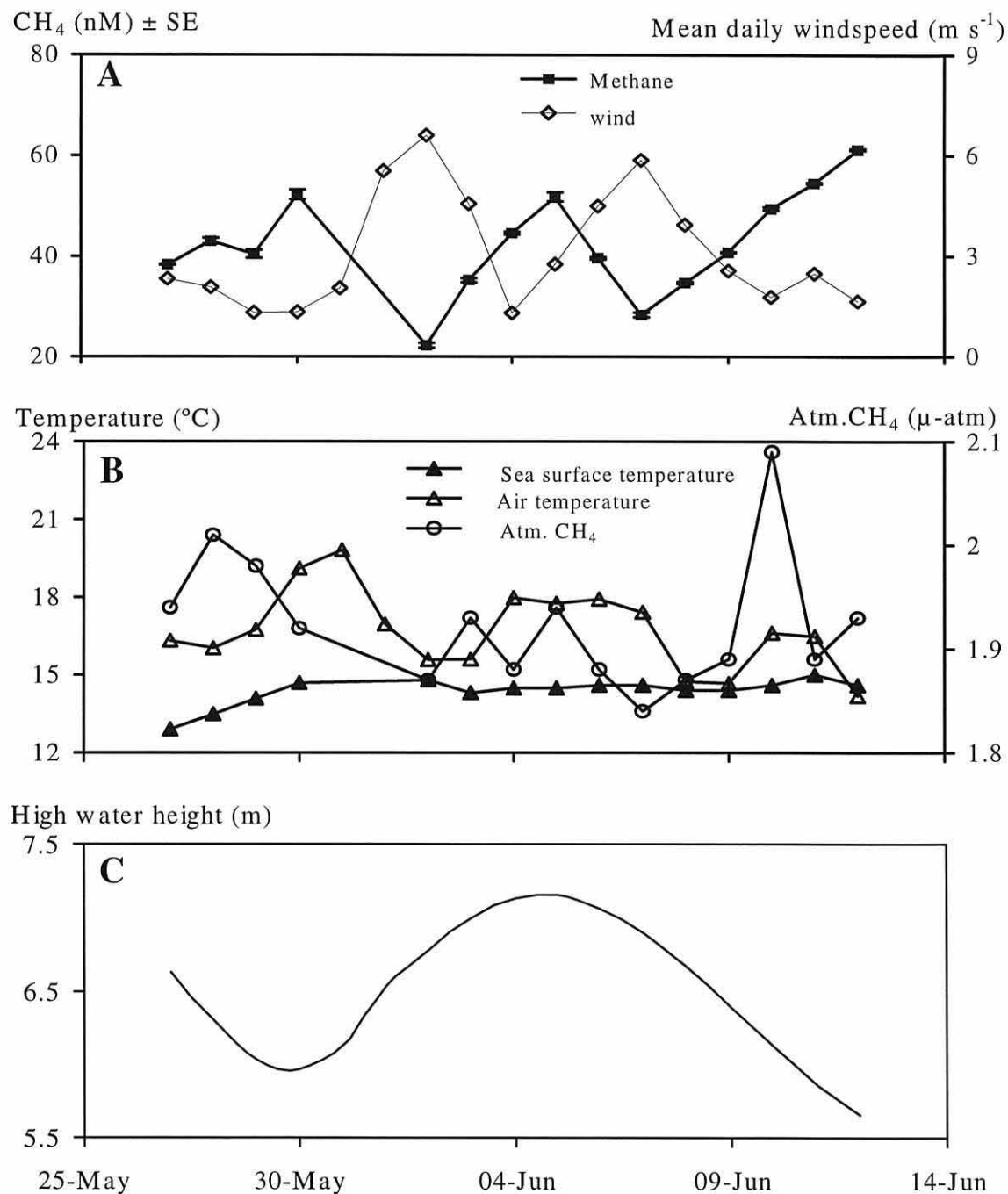


Figure 3.2.1 Water column methane concentration (CH_4 , nM) and mean daily wind velocity (m s^{-1}) (A), sea and mean daily air temperature ($^{\circ}\text{C}$) and atmospheric methane concentration ($\mu\text{-atmosphere}$) (B), and water height (meters above chart datum) (C) during high water at Menai Bridge between 27 May and 12 June 1997.

Methane concentrations in the water varied greatly during this period (Figure 3.2.1 A) with the peak concentration of 61 nM being 2.8-fold larger than the lowest concentration of 22 nM.

These changes appeared not to be related with the spring-neap tide cycle (Figure 3.2.1 C), but showed a generally negative relationship with the mean daily wind speed (Figure 3.2.1 A). This relationship appeared stronger at higher wind speeds.

Despite also displaying three peaks, the mean daily air temperature appeared to be unrelated to the pattern for water column methane (Figure 3.2.1 B). Neither sea water temperature, which increased quite gradually over the sampling period (Figure 3.2.1 B), nor atmospheric methane concentration, which showed a significant variability (Figure 3.2.1 B), displayed any relationship with the distribution of water column methane concentrations.

Variability over a diurnal tidal cycle

The stability of methane concentrations in Menai Strait water at fixed stations was investigated over a diurnal tidal cycle at St. George's Pier on 7 July 1997, and over half a tidal cycle at the northeastern entrance of the Menai Strait on 22 August 1997.

During a spring tide, on 7 July 1997, aquatic and atmospheric methane concentrations and seawater temperatures were measured hourly at St. George's Pier between 0725 and 1925 GMT. Hourly mean wind speeds and mean air temperatures over the sampling period were computed from the School of Ocean Sciences' logged meteorological data. To describe the state of the tide, tidal heights, current speeds and current directions were taken from the 1997 Menai Strait Tide Tables produced by the Unit of Coastal and Estuarine Studies (UCES) at the School of Ocean Sciences.

The water column methane concentration varied significantly during this 12 hour period between 42 and 73 nM (Figure 3.2.2 A). There was a progressive decrease in methane concentrations over the day and then a steep increase towards the evening. This pattern appears negatively related to mean hourly wind speed, as low methane concentrations occurred generally during periods of high wind speed, and high methane concentrations were measured when the wind blew less strongly (Figure 3.2.2 A). This relationship, however, was only a general trend as the lowest methane concentration occurred during not particularly strong winds (Figure 3.2.2 A).

No relationships were detected between water column methane concentrations and either the temperatures of water or air, or the atmospheric methane concentrations (Figure 3.2.2 B).

The direction of the tidal current on the other hand appeared to be related to the concentration of methane in the water at St. George's Pier. Generally, concentrations were higher when the water was flowing against its net current direction, and lower when it was flowing southwestwards

towards Caernarfon Bay (Figure 3.2.2 C). Also the tidal height appeared to be related to the methane content of the water as peak concentrations occurred during - or just after - low water (Figure 3.2.2 C).

This study thus revealed a significant variability of water column methane concentrations at St. George's Pier over the course of a few hours. Concentrations were generally lower when water was flowing into its net flow direction and when the wind was blowing strong. High concentrations occurred around low water.

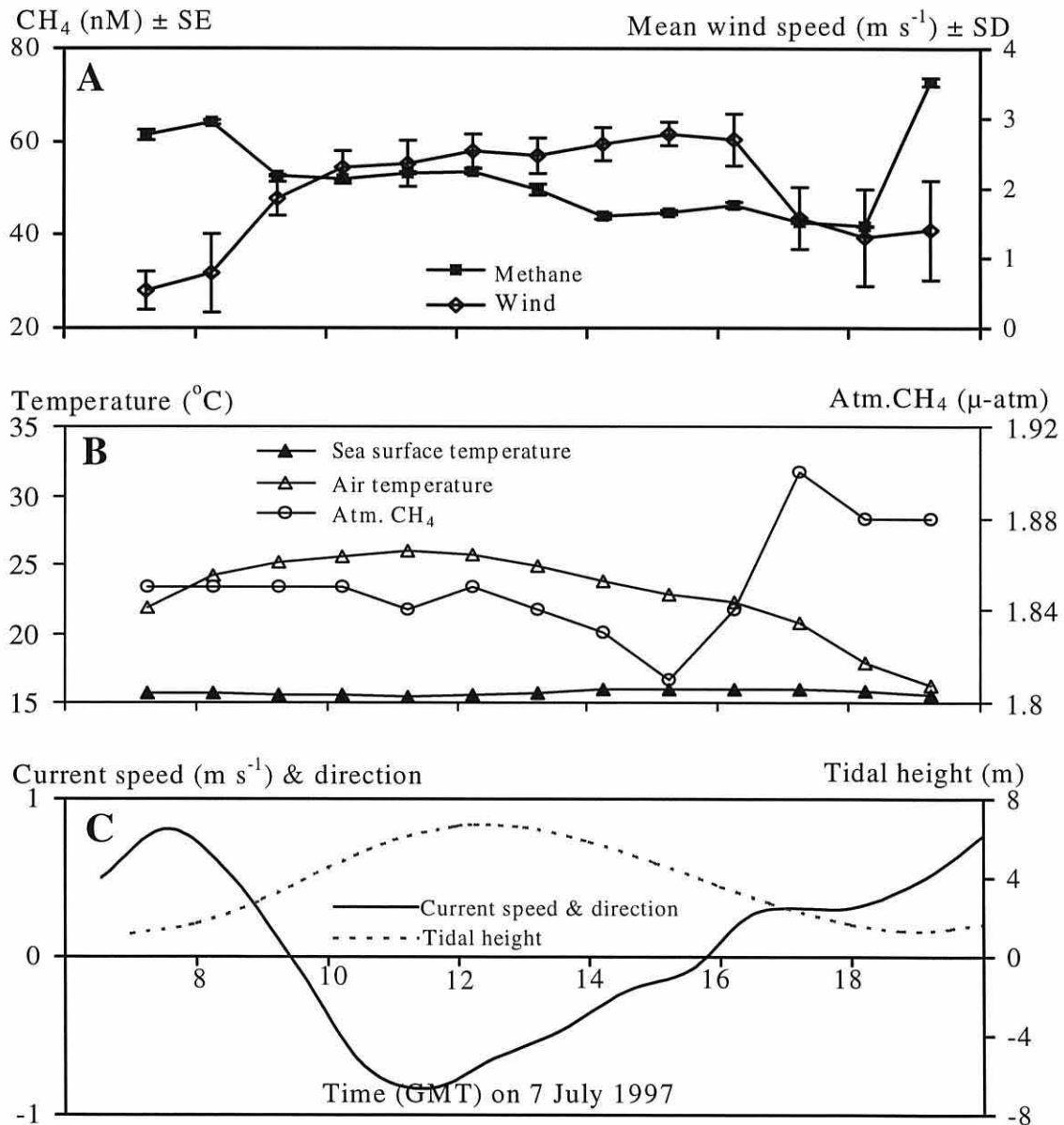


Figure 3.2.2 Hourly changes in water column methane concentrations (CH_4 , nM) and mean wind speeds (m s^{-1}) (A), air and sea temperatures ($^{\circ}\text{C}$), and atmospheric methane concentrations ($\mu\text{-atm}$) (B), and tidal heights above chart datum (m), current speeds (m s^{-1}) and current directions (+ve = towards Liverpool Bay, -ve = towards Caernarfon Bay) (C) in the Menai Strait at Menai Bridge on 7 July 1997 between 0725 and 1925 GMT.

On 22 August 1997 a similar study was conducted over half a tidal cycle from a fixed station moored at the northeasterly entrance to the Menai Strait. The aim of this investigation was to gain an indication for the variability of the methane concentration in the waters entering the Menai Strait. A boat was anchored to the southeast of Penmon Bay within the main shipping channel (53°18'071N, 04°02'165W). Samples for water column methane concentrations were taken every 20 minutes starting at 0742 GMT. Initially the tidal current was still washing water out of the Menai Strait into Liverpool Bay, but soon changed direction so that Liverpool Bay water streamed into the Strait. Sampling ended at 1232 GMT when the current was about to turn once more. Water current speed and direction were measured every 10 minutes at a depth of 71 cm with a calibrated Valeport® Braystoke type BFM002 miniature current flow meter with a 50 mm impeller. Atmospheric gas samples were collected hourly, and sea temperature was measured every 10 minutes. No wind data are available for this station, but the morning was generally calm.

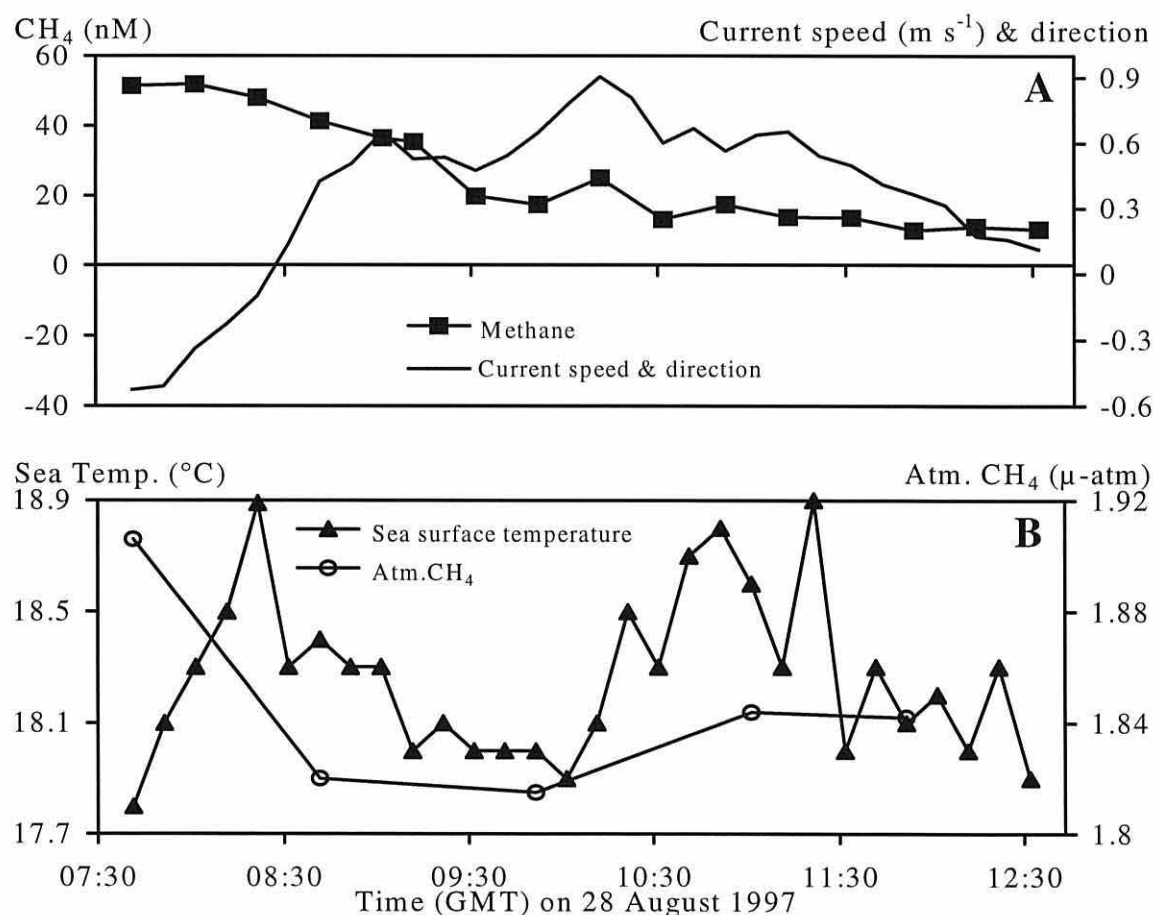


Figure 3.2.3 Short-term changes in water column methane concentrations (CH₄, nM), current speeds (m s⁻¹) and directions (-ve = current flowing from Menai Strait into Liverpool Bay, +ve = current flowing from Liverpool Bay into Menai Strait) (A) and sea temperatures (°C) and atmospheric methane concentrations (μ-atmosphere) (B) on 22 August 1997 over five hours in the main shipping channel of the Menai Strait off Penmon.

Water column methane concentrations decreased significantly from about 51 nM to 10 nM in the first three hours and remained low and relatively constant thereafter (Figure 3.2.3 A).

Neither seawater temperature nor atmospheric methane concentrations showed any relationship with the concentration of methane in the water (Figure 3.2.3 B). The direction of the current, however, seemed to be related to the methane concentration. Concentrations were generally lower when the water that flowed past the sampling station came from Liverpool Bay than when it originated from the Menai Strait (Figure 3.2.3 A). The methane concentration began to drop when the current direction turned and eventually displayed an approximately constant concentration.

In these two short tidal studies, water column methane was observed to vary significantly over short periods of time at the fixed sampling sites, with the highest concentrations being 74% (St. George's Pier) and 530% (Penmon Bay) larger than the lowest concentrations. In both cases methane concentrations appeared to be related to the direction of the current, with methane being higher in waters that have come from the southwest than those carrying Liverpool Bay water through the Menai Strait.

The variability in methane concentrations at Menai Bridge both over the daily high / low water cycle and the fortnightly spring / neap tidal cycle was large. On a daily scale the methane concentrations appeared to be related to the direction and strength of the tidal current. The results from the spring-neap cycle study did not highlight any relationship with the current strength. There was, however, a significant negative relationship between methane and wind speed.

3.2.2 Spatial variability

As there is a net current through the Menai Strait, the water sampled at St. George's Pier is continuously replaced from Liverpool Bay. The variability in the methane content of the water sampled at St. George's Pier could therefore result from different methane concentrations in advected Liverpool Bay water. In the following section an attempt was made to quantify the spatial variability throughout the northern and central parts of the Menai Strait. The horizontal and vertical components of the spatial variability are dealt with separately.

To investigate the horizontal stability of water column methane concentrations, surface water methane was measured along three transects in the Menai Strait. The vertical variability was studied by depth profiles at St. George's Pier and at three stations in the central Menai Strait.

The location of the sampling stations for the transects (stations 1 to 22) and the depth profiles (stations 23, 24 and 25) are shown in Figure 3.2.4.

Horizontal variability

Methane concentrations were found to increase by about 60 % along the first approximately 3.3 km long transect between the Telford Bridge (station 1) and Bangor Pier (station 5) (Figure 3.2.5 A). The samples had been collected on 19 May 1997 just before slack water while the water was flowing very slowly towards the northeast. The direction of this increase in concentration was reversed in the longer second transect, which was sampled on 5 June 1997 between Puffin Island (station 6) and Menai Bridge (station 15). Over the roughly 14 km of this transect, the concentrations more than tripled (Figure 3.2.5 B). The samples had been collected around high water while the current directed water from Liverpool Bay southwestwards through the Menai Strait. Both transects along the main shipping channel of the Strait thus show a high degree of spatial variability. This variability, however, is not erratic but increases constantly in current direction.

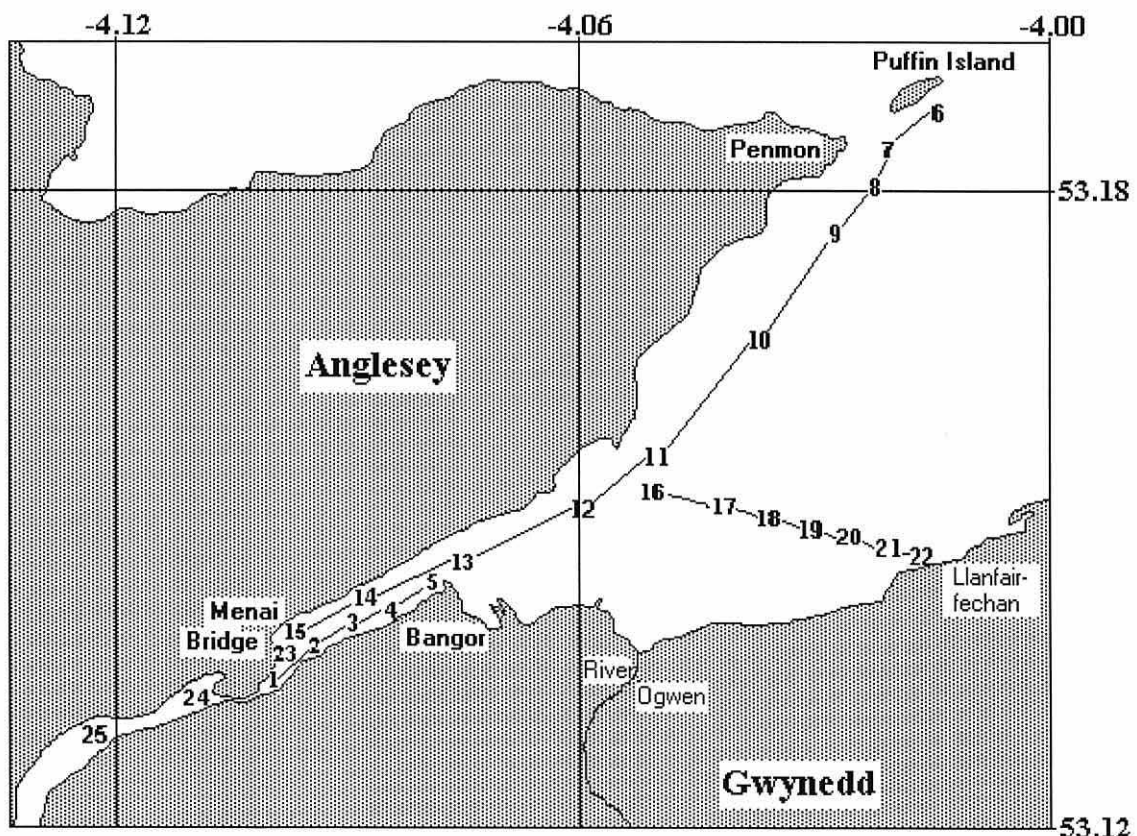


Figure 3.2.4 Map of the northwestern Menai Strait showing the station numbers for the spatial variability studies of methane concentrations in the water column. Surface water for methane analysis was sampled along horizontal transects on 19 May (stations 1-5), on 5 June (stations 6-15), and on 20 June 1997 (stations 16-22) 1997. Water samples for vertical profiles of methane at stations 23-25 were determined on 28 July 1997.

The third transect was sampled across the Lavan Sands during slack water on 20 June 1997, across the main current flow. Methane concentrations along this *circa* 5 km long transect varied 4.6 fold (Figure 3.2.5 C). The pattern of this variability was rather erratic. The highest concentration occurred at the shore station 22, where the substratum was muddy.

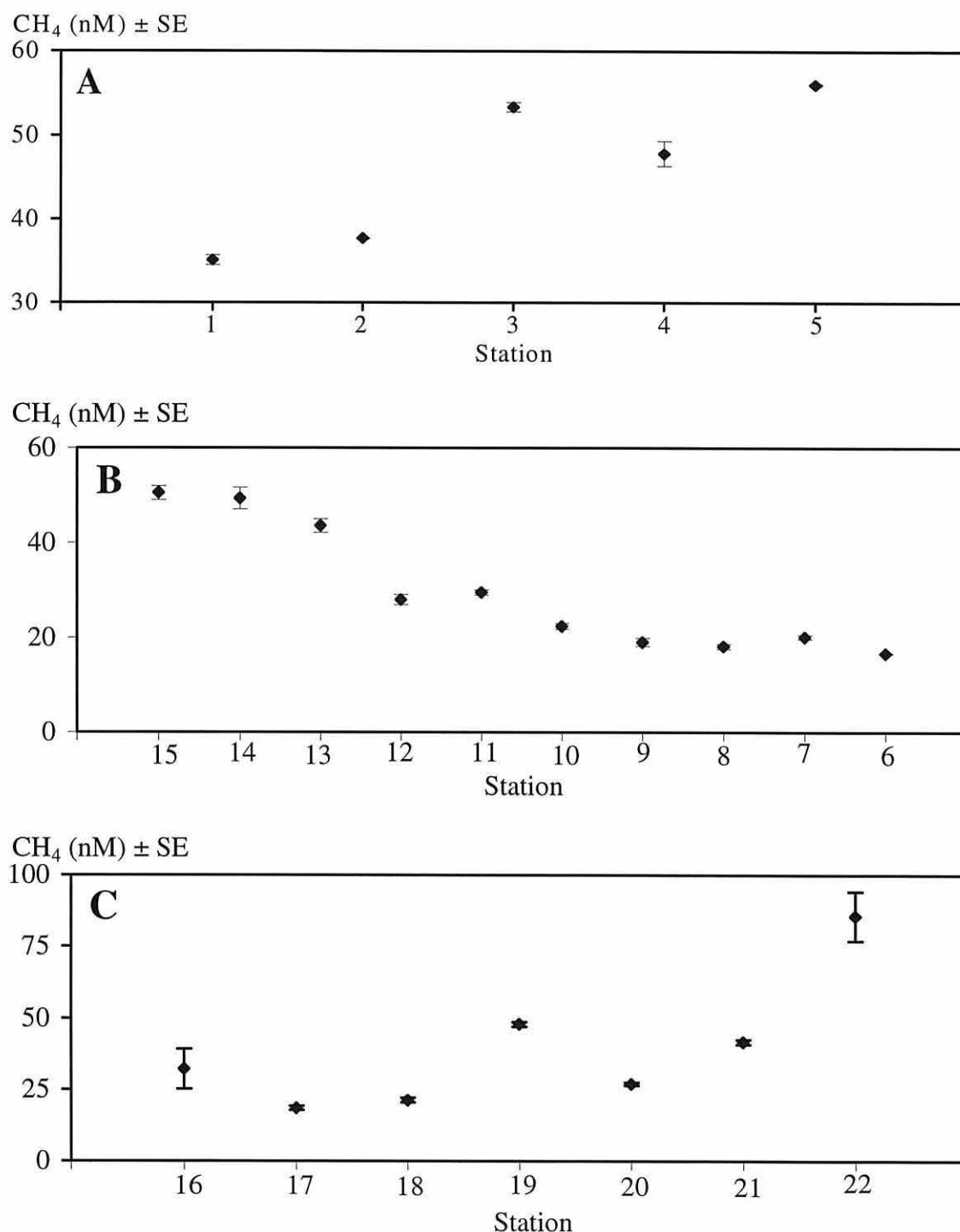


Figure 3.2.5 Methane concentrations (CH_4 , nM) in the waters at stations 1 to 5 measured on 19 May 1997 during slack water (A), at stations 6 to 15 sampled on 5 June 1997 during high tide (B), and at stations 16 to 22 at slack water on 20 June 1997 (C).

To summarise, all three transects revealed high degrees of horizontal variability in water column methane concentrations for the Menai Strait. Concentrations appeared to increase along the direction of flow through the Menai Strait. Perpendicular to the current, concentrations were more erratic. The underlying substratum might in part be related to the changes in methane concentrations.

Vertical variability

To study the vertical stability of methane in the Menai Strait, the methane concentrations at different water depths were determined at four sites: on 13 June 1996 at St. George's Pier, and on 28 July 1997 at stations 23, 24 and 25 in the central Menai Strait.

At St. George's Pier slack water methane concentrations increased by approximately 30% from the surface to the shallow ground (Figure 3.2.6). No such systematic increases were observed at the three stations in the main shipping channel, which had been sampled during high water with the current flowing towards Caernarfon Bay. As only single samples were collected at these three sites, it cannot be confirmed whether the erratic and unexpected drop in concentrations at 4 meters at station 24 was a real event or an analytical error. A slight general increase in concentrations occurred in the direction of the current from station 23 to station 25.

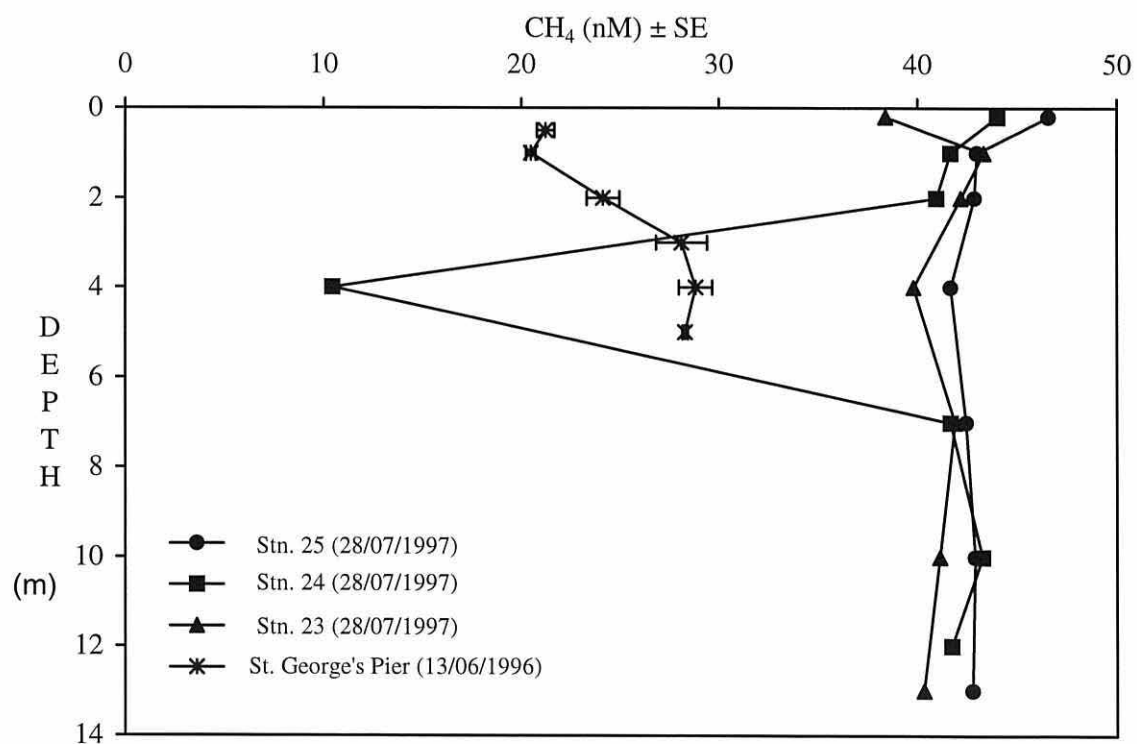


Figure 3.2.6 Depth profiles of methane concentrations (CH_4 , nM) in the water column at stations 23, 24 and 25 in the Menai Strait on 28 July 1997 half an hour before high tide, and at St. George's Pier on 13 June 1996 during slack water.

Water column methane concentrations in the central Menai Strait thus did not increase from the surface towards the bottom when the current was running fast over a rocky substratum, but increased where the water was standing over muddy sediments.

3.2.3 Temporal variability

To study time-dependent changes in methane concentrations as a body of water flows through the central Menai Strait, surface water was sampled from a passively drifting boat on 9 July 1997 in 10-minute intervals for a total period of 150 minutes. In this time the boat had drifted approximately 9 km from Bangor Pier to just north of Port Dinorwic. As the day was extremely calm (mean daily wind speed of 0.61 m s^{-1}), the boat was assumed to drift only with the tidal current, so that it is reasonable to assume that the same body of water was sampled throughout the experiment.

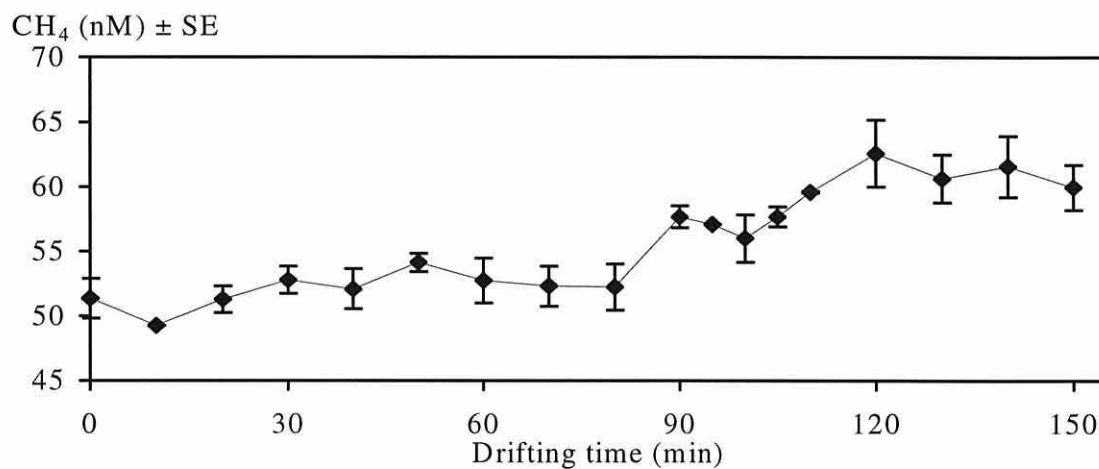


Figure 3.2.7 Changes in water column methane concentrations (CH_4 , nM) during a 150 minute drift study on the Menai Strait on 9 July 1997.

Water column methane increased by approximately 20% or 10 nM during the 2.5-hour drift (Figure 3.2.7). The rise in concentration was relatively gradual with the steepest increase after 90 minutes when the water passed beneath the Telford Bridge.

**Box 3.2: Summary of ‘short-term variability of methane
in the water column’**

- At fixed stations significant variations in methane concentrations were detected over the diurnal tidal cycle, which may be associated with current direction
- The large variability in methane concentrations over a fortnightly period revealed no systematic relationship with the spring-neap tidal cycle but was negatively related with wind
- Up to 500% horizontal variability was detected in the north-eastern and central parts of the Menai Strait
- Samples showed a 30% increase in methane concentrations with water depth in standing waters adjacent to muddy sediments. No depth-related increase was detected in flowing water above rocky substrates
- Hourly changes in methane concentrations of 8% (4 nM) were measured in the central Strait

3.3 Methane production in the water column

In the previous sections water column methane concentrations were found to increase in summer (chapter 3.1), and evidence was presented suggesting that there is methane production or release occurring somewhere within the Menai Strait (chapter 3.2). All following sections of this chapter report on investigations into potential sources of Menai Strait methane, *i.e.* methane production within the water column (this section), external methane inputs (chapter 3.4) and sedimentary methane concentrations (chapters 3.5 and 3.6).

In this section the water column is examined for its capacity to produce methane. This cannot easily be done *in situ* because coastal methane concentrations are affected by the permanent exchange of water, by the turbulence-dependent exchange of methane between the water and the atmosphere, and by the presumably variable flux rates of methane from the sediment into the water column. Bottle incubation experiments were conducted to avoid these influences. Initially only unconcentrated water samples were incubated, with mercuric chloride poisoned samples acting as controls. As no methane production was observed in these unconcentrated water samples, the larger particulate fraction of the water column, in which methanogenesis is most likely to take place within the water, was concentrated with a plankton net and also incubated.

The sampling dates and fractions of the water incubations are listed in Table 3.3.1. The incubation results are shown in Figures 3.3.1 A to K.

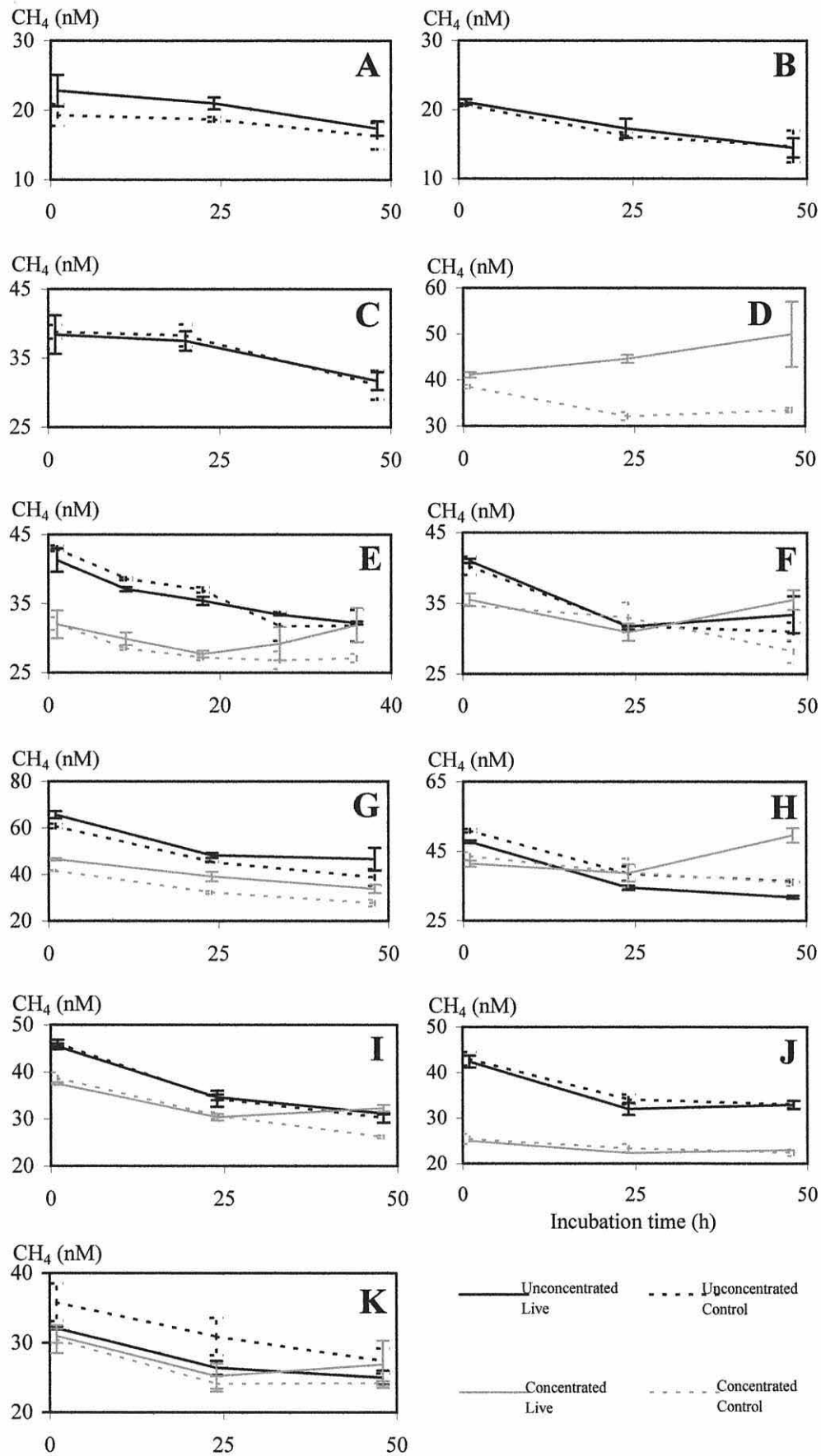


Figure 3.3.1 Methane concentrations (CH_4 , nM) in live and control samples of unconcentrated and concentrated Menai Strait water during up to 48-hour incubations under *in situ* light and temperature conditions. Lines show mean concentrations over time with standard deviations. Letter symbols refer to the sampling dates listed in Table 3.3.1. Zero times are offset by one hour.

Table 3.3.1 Sampling dates and water fractions for methane incubation experiments. The letter attributed to each date is used as an identifier in Figure 3.3.1 A to K.

Sampling date	Identifier	Unconcentrated sample	Concentrated sample
01.05.1997	A	✓	
12.05.1997	B	✓	
27.05.1997	C	✓	
09.06.1997	D		✓
02.07.1997	E	✓	✓
30.07.1997	F	✓	✓
11.08.1997	G	✓	✓
26.08.1997	H	✓	✓
29.09.1997	I	✓	✓
13.10.1997	J	✓	✓
01.11.1997	K	✓	✓

On all sampling days the incubated water was strongly supersaturated with methane. Initial methane concentrations were generally lower in concentrated than unconcentrated water samples (Figure 3.3.1). This is thought to be due to outgassing from the concentrated samples that were left standing before being sub-sampled. Both fractions had been collected simultaneously but the concentrated samples were processed after the unconcentrated water, so that there was more time for supersaturated methane to outgas. Outgassing might also account for the tendency of initial methane concentrations in live samples to be slightly above those of control samples. Control samples were generally sub-sampled into syringes after the live samples to avoid contamination of live samples with mercuric chloride.

The controls from all eleven incubation dates and both fractions displayed a loss of methane with time. This could be due to leakage of supersaturated gases from ageing syringes and/or to physical absorption of methane on detrital particles. The loss rate, however, was not constant over time.

In more than half of the incubations, live samples behaved very similarly to controls (Figures 3.3.1 A, B, C, E unconcentrated, G concentrated, H unconcentrated, I unconcentrated, J, and K) which suggests that no quantitatively relevant net methane production or consumption occurred on these days.

On several other occasions methane in live and control samples displayed a similar behaviour during the initial 24 hours of incubation but began to increase in live samples relative to controls thereafter (Figure 3.3.1 E concentrated, F concentrated, H concentrated, and I concentrated). In all the concentrated live samples in these incubations the water had become anoxic between 24 and 48 hours as indicated by the disappearance of the negative oxygen peak from the GC-chromatograms. This must have been the result of the concentration of primarily heterotrophic

organisms in the concentrated fractions that exhausted the oxygen supply in the isolated water sample. Methane production under these conditions suggests the occurrence of methanogenic particles in the particulate fraction of the water, but cannot prove methane production in the water column under *in situ* conditions.

Due to poor precision, the results remain inconclusive about the production of methane in unconcentrated water collected on 30 July and 11 August 1997 (Figure 3.3.1 F and G unconcentrated). Statistical analysis of the results using regression analysis and balanced two-factor mixed model analysis of variance (results not shown) could not detect significant methane production. In unconcentrated water oxygen was never exhausted during the short incubation periods, so that any methane production would be likely to represent *in situ* events. The results of these incubations, however, suggest that *in situ* production does not contribute significantly to methane concentrations in the oxygenated Menai Strait water column.

A definite increase in methane concentrations with incubation time in the live samples was only observed on one occasion, in the concentrated samples collected on 9 June 1997 (Figure 3.3.1 D). As the control samples on this date displayed the usual loss in methane concentrations with time, this observation strongly suggests that methane was produced in the live samples. On this day, the concentrated sample was strongly dominated (99% of non-bacterial organisms) by a large (200 to 600 μm diameter), naked, exclusively heterotrophic, luminescent and dull-reddish dinoflagellate, *Noctiluca scintillans* (MaCartney 1810). Approximately 315 *Noctiluca* cells were counted per cm^3 of the initial concentrated sample. Methane production rates, calculated from the difference between live and control samples adjusted to a shared initial concentration, were between 8.1 and 10.8 $\text{nmoles dm}^{-3} \text{ d}^{-1}$ on day one (mean = 10 $\text{nmoles dm}^{-3} \text{ d}^{-1}$), and between 7.3 and 22.6 $\text{nmoles dm}^{-3} \text{ d}^{-1}$ on day two (mean = 13.9 $\text{nmoles dm}^{-3} \text{ d}^{-1}$). Assuming this to be produced by 315,000 *Noctiluca* cells dm^{-3} , the mean methane production rate of *Noctiluca* could be in the order of 32 $\text{fmoles cell}^{-1} \text{ d}^{-1}$ on day one. As no unconcentrated water samples were obtained on that day, the natural abundance of *Noctiluca* in the Menai Strait on 9 June 1997 remains unknown. Oxygen concentrations decreased during these incubations but did not fall to anoxic conditions, as indicated by the decrease but not disappearance of the negative oxygen peak that preceded the methane peak in the GC-chromatograms. Most *Noctiluca* cells remained alive throughout the live incubations as they retained their colour while the poisoned cells in the control samples turned grey. It can thus be concluded that methane was produced under oxic conditions in water samples dominated by *Noctiluca*.

Box 3.3: Summary of ‘methane production in the water column’

- In a concentrated sample containing the dinoflagellate *Noctiluca scintillans*, methane was generated in an oxygenated water sample at low net production rates
- In all other samples no significant water column production of methane was detected during the first 24 hours while the water was oxygenated
- On several occasions the water column was found to contain viable methanogenic particles which produced methane at slow rates when oxygen became scarce

3.4 Methane concentrations in external sources

To estimate the importance of external methane inputs to the Menai Strait, methane concentrations were analysed in different waters that enter the northeastern parts of the Menai Strait. The Ogwen River, which debouches approximately 3 km east of Bangor, was sampled on 13 July 1997 about 500 m upstream from its mouth (53°13'613 N, 04°04'968W). Treated sewage was obtained from the new Treborth sewage treatment works on 3 July, and raw sewage was collected during low tide on 22 July at Menai Bridge. Tap water, the main constituent of sewage, was sampled from four different sites in Bangor and Menai Bridge on 13 and 21 July 1997.

Table 3.4.1 gives a summary of the concentrations found. Methane concentrations both in the Ogwen River and in local tap water were - although still supersaturated by a factor of 1.5 to 5.7 - approximately one order of magnitude smaller than in the main water mass of the central Menai Strait at this time of year. These waters thus do not constitute an external methane source and are on the contrary likely to dilute the methane concentrations in the Menai Strait. Both treated and raw sewage, on the other hand, were up to one order of magnitude richer in methane than the receiving Menai Strait waters and thus represent external sources.

Table 3.4.1 Methane concentrations (CH_4 , nM) and temperatures (Temp., °C) in July 1997 in, and the mean daily rates of water inputs (Vol. - $\text{m}^3 \text{d}^{-1}$) into the Menai Strait from the Ogwen River, local tap water, and treated and raw sewage.

Source	Sampling date	CH_4 (nM)	Temp. (°C)	Vol. ($\text{m}^3 \text{d}^{-1}$)
River Ogwen, Penrhyn Estate	13 July 1997	4.5 ± 0.1	16.5	~70,000*
Tap water, Bangor & Menai Bridge	13 & 21 July 1997	6.0 – 16.0	18.7	-
Treated sewage. Treborth	03 July 1997	180.8 ± 0.7	14.8	10,600
Raw sewage, Menai Bridge	22 July 1997	475.5 ± 15.8	14.3	925

*As no regular monthly/annual mean flows are available for the River Ogwen, the quoted rate was calculated from ten spot measurements taken at various times of the year by the Environment Agency Wales (ref. 1251).

To investigate the potential of sewage to produce methane once it enters the Menai Strait, live and control samples of saline dilutions of treated and untreated sewage were incubated for 24 and 48 hours respectively. Treated sewage samples were diluted with 0.2 μm filtered, UV-treated sea water to a salinity of approximately 17, and raw sewage was diluted with Menai Strait water to a salinity of about 30. The results of the incubations are shown in Figure 3.4.1.

In incubations of both raw and treated sewage methane concentrations decreased rather evenly in both the live and the control samples (Figure 3.4.1). Statistical analysis using balanced two-factor mixed model ANOVA found no significant difference in the behaviour of methane concentrations of live and control samples with time (treated sewage: $F=1.33$, $p=0.334$; raw sewage: $F=0.69$, $p=0.584$). This suggests that sewage once it enters coastal waters does not produce significant amounts of methane. The loss of methane with time, as it occurs both in live and control samples, is not due to biological but to physical or chemical processes such as absorption or leakage.

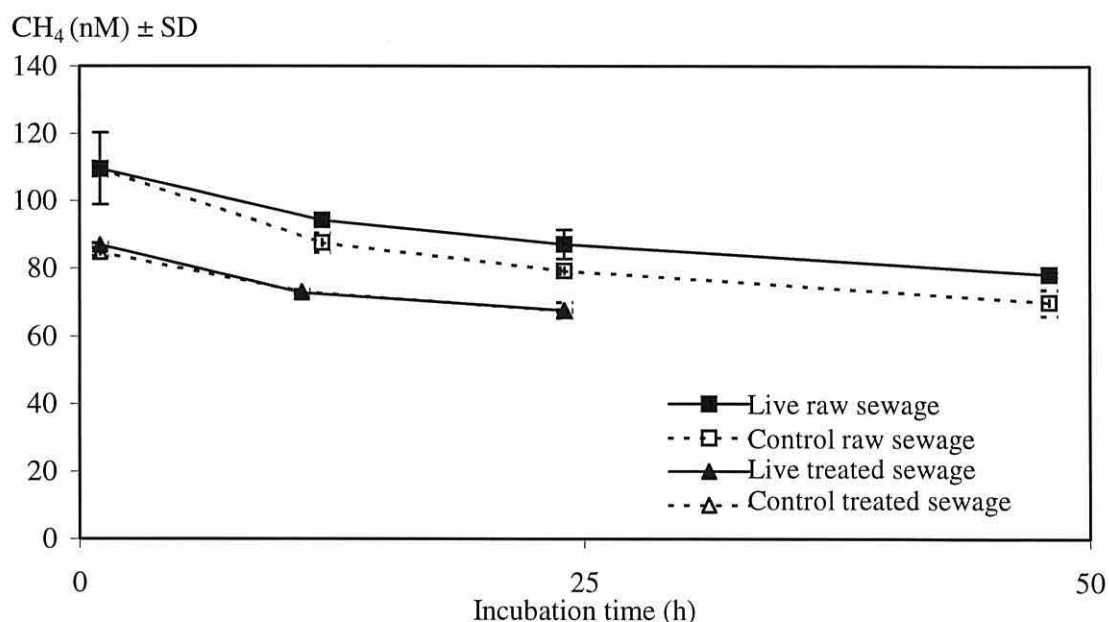


Figure 3.4.1 Methane concentrations (CH_4 , nM) in live and control incubations of raw and treated sewage collected on 3 July (treated) and 22 July (raw) 1997. Zero times are offset by one hour for improved presentation.

Box 3.4: Summary of 'methane concentrations in external sources'

- Methane concentrations in the River Ogwen are lower than in the Menai Strait
- Raw sewage was 10 fold and treated sewage 3 to 4 fold richer in methane than the receiving Menai Strait waters
- No methane production was detected in saline dilutions of either raw or treated sewage

3.5 Methane in Menai Strait sediments

In earlier sections methane concentrations in Menai Strait waters were reported to rise at fixed stations in summer (Section 3.1), and over short time scales (Section 3.2) in water flowing through the Menai Strait. As neither *in situ* production nor external sources were found to account for either of these increases in methane concentrations (Sections 3.3 and 3.4), the source strength of Menai Strait sediments was investigated. Methane is produced biogenically in the anaerobic layer of the sediment below the sulphate reduction zone. Methane produced there diffuses upwards and, if not oxidised, enters the water column. The contribution of sedimentary methane to water column concentrations can be estimated from depth profiles.

To gain an indication of the magnitude of methane entering the waters of the Menai Strait from sediments, both seasonal and spatial changes in methane concentrations in local sediments were investigated.

3.5.1 Seasonal distribution

The seasonal distribution of methane in sediments was measured to test the hypothesis that the seasonal pattern apparent in the water column originates from a sedimentary source.

Sediment cores of 20 to 30 cm depth were sampled between 1 July 1997 and 4 February 1998 from the Menai Bridge mudflats at stations A, B and C during daytime low water on the dates and times shown in Table 3.5.1.1. In the laboratory, sediment methane concentrations and porosity were analysed from 0.5 or 1cm thick sediment slices at 5cm intervals. Sediment temperature profiles were measured in neighbouring cores. The results are shown in Figures 3.5.1.1, 3.5.1.2 and 3.5.1.3. The methane distribution at different sediment depths over time are shown in Appendix 4.2.

Table 3.5.1.1 Dates of core sampling at stations A, B and C in the Menai Bridge mudflats.

Date & time (GMT)	Station A	Station B	Station C
01.07.1997 at 1340		✓	
24.07.1997 at 0750		✓	
07.08.1997 at 0800	✓	✓	✓
21.08.1997 at 0900		✓	✓
05.09.1997 at 0700	✓	✓	✓
19.09.1997 at 0720	✓	✓	✓
06.10.1997 at 0800		✓	✓
03.11.1997 at 0710	✓	✓	✓
04.02.1998 at 1030	✓	✓	✓

Sedimentary methane concentrations at stations A and B were similar and remained at all depths below 4 μM on all but one occasion at each site. Station C was richer in methane with concentrations as high as 440 μM . These concentrations translate into saturation ratios of above 1,000 for stations A and B, and of around 50,000 for station C at depths of 20 to 30 cm (Table 3.5.1.2). In the surface sediment of stations A and B, methane was approximately 75 times supersaturated, and at station C over 8,000 times (Table 3.5.1.2).

While methane concentrations in the water column peaked in early August (section 3.1), the highest methane concentrations in the sediments at station A were measured on 19 September 1997 (Figure 3.5.1.1), at station B on 4 February 1998 (Figure 3.5.1.2), and at station C on 5 September and 3 November 1997 (Figure 3.5.1.3). Maximum methane concentrations in the sediments were thus measured at different times of the year at the three stations, and were never found to coincide with maximum concentrations in the water column.

Table 3.5.1.2 Mean saturation ratios \pm standard deviations of methane at different depths in sediments of stations A, B and C in the mudflats at Menai Bridge between 1 July 1997 and 4 February 1998.

Depth (cm)	Station A	Station B	Station C
0	80 \pm 50	70 \pm 40	8,300 \pm 11,000
5	220 \pm 130	160 \pm 130	37,000 \pm 46,700
10	400 \pm 90	270 \pm 220	53,000 \pm 59,000
15	900 \pm 700	500 \pm 500	42,000 \pm 40,000
20	1,100 \pm 900	900 \pm 1,300	50,000 \pm 58,000
25	1,200 \pm 1,000	1,000 \pm 1,400	52,000 \pm 56,600
30	1,700 \pm 1,700	1,300 \pm 1,700	45,000 \pm 56,000

No seasonal pattern in sedimentary methane concentrations was discerned at any station. This can be seen more clearly from plots of depth-integrated methane concentrations for the upper 20 cm of the sediment (Figure 3.5.1.4). These depth-integrated concentrations were calculated by multiplying the mean methane concentration on a certain day with the depth of the analysed core.

The depth of maximum methane concentration appears to increase slightly in winter (Table 3.5.1.3).

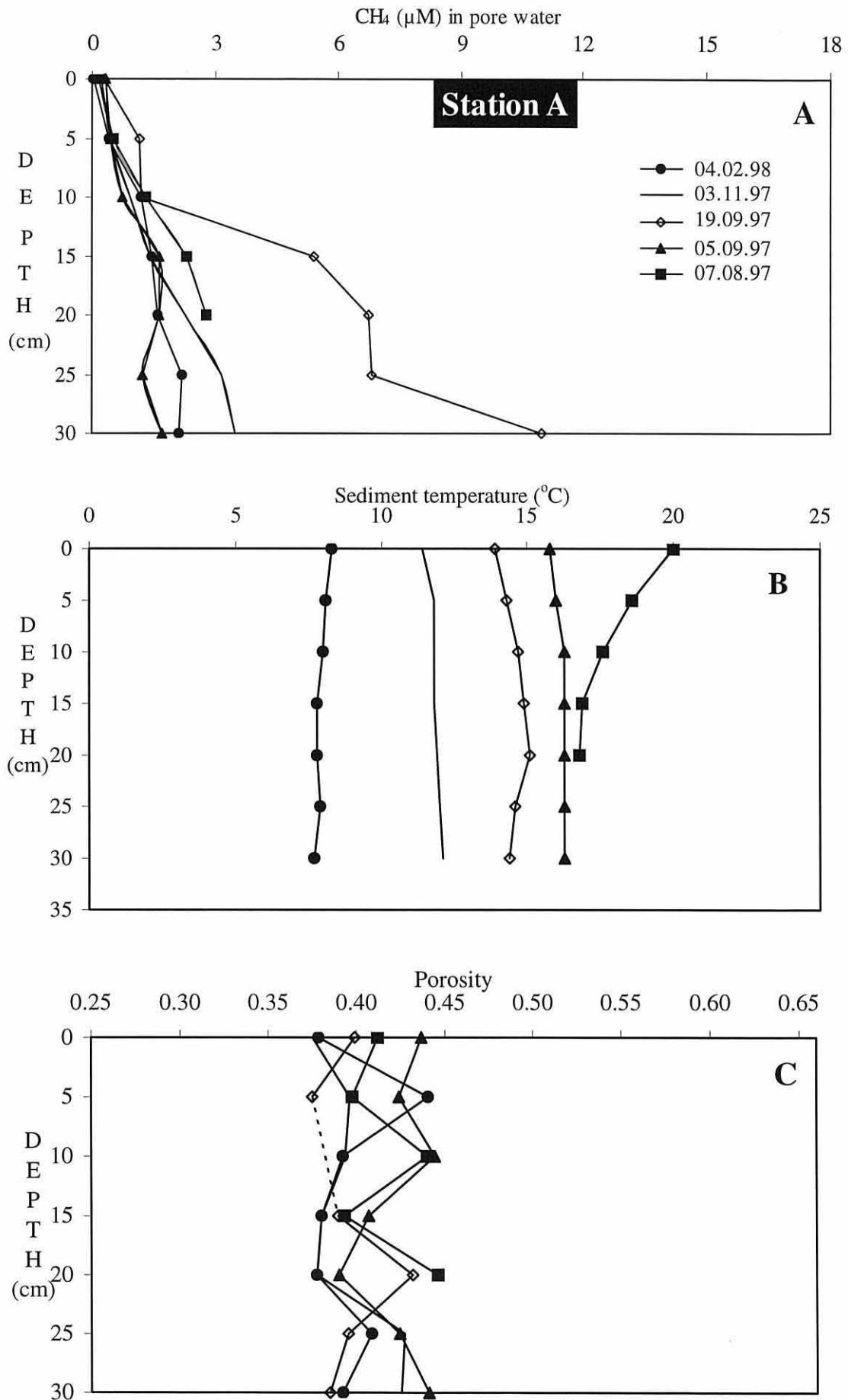


Figure 3.5.1.1 See page 3-28 for legend

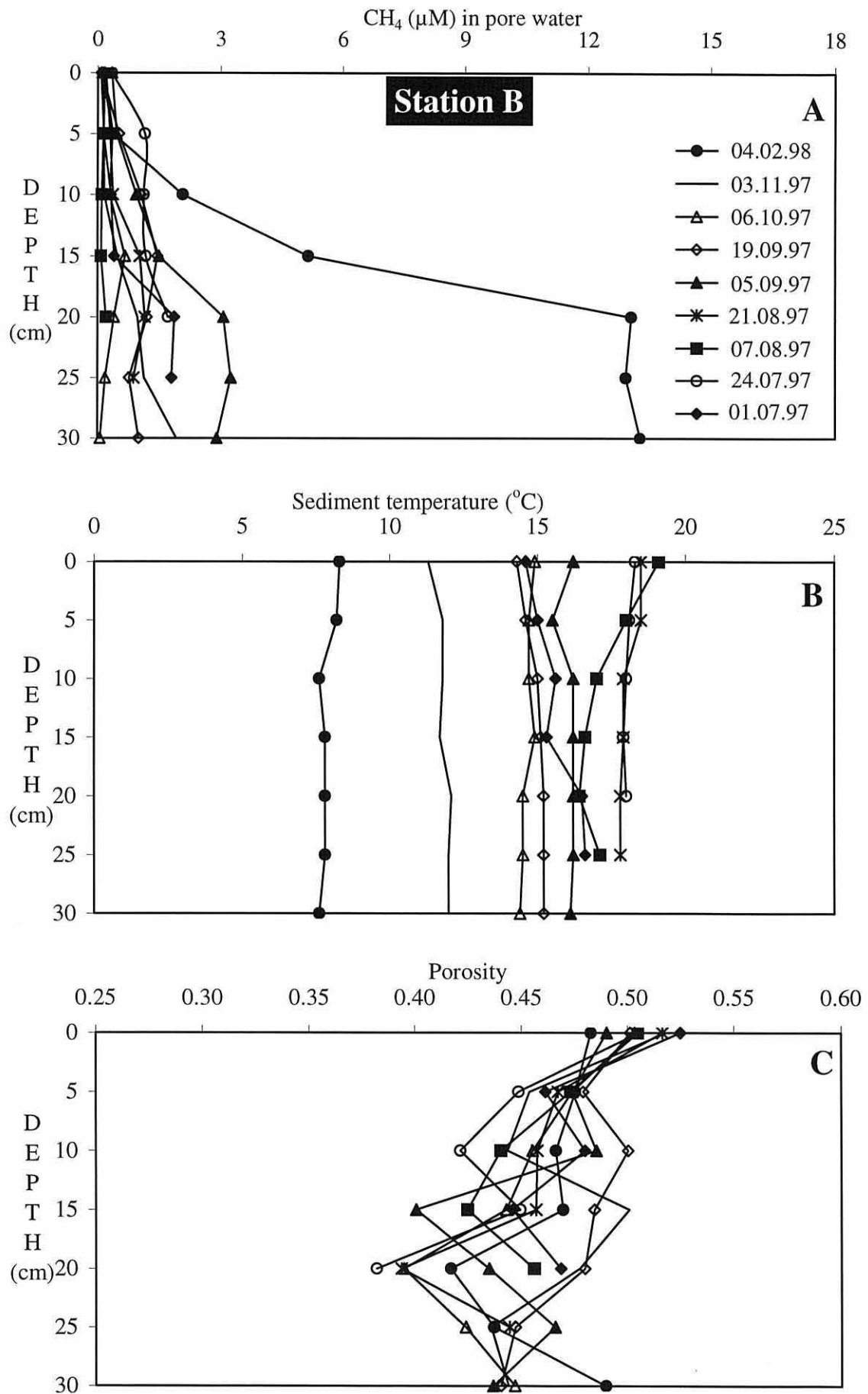


Figure 3.5.1.2 See page 3-28 for legend

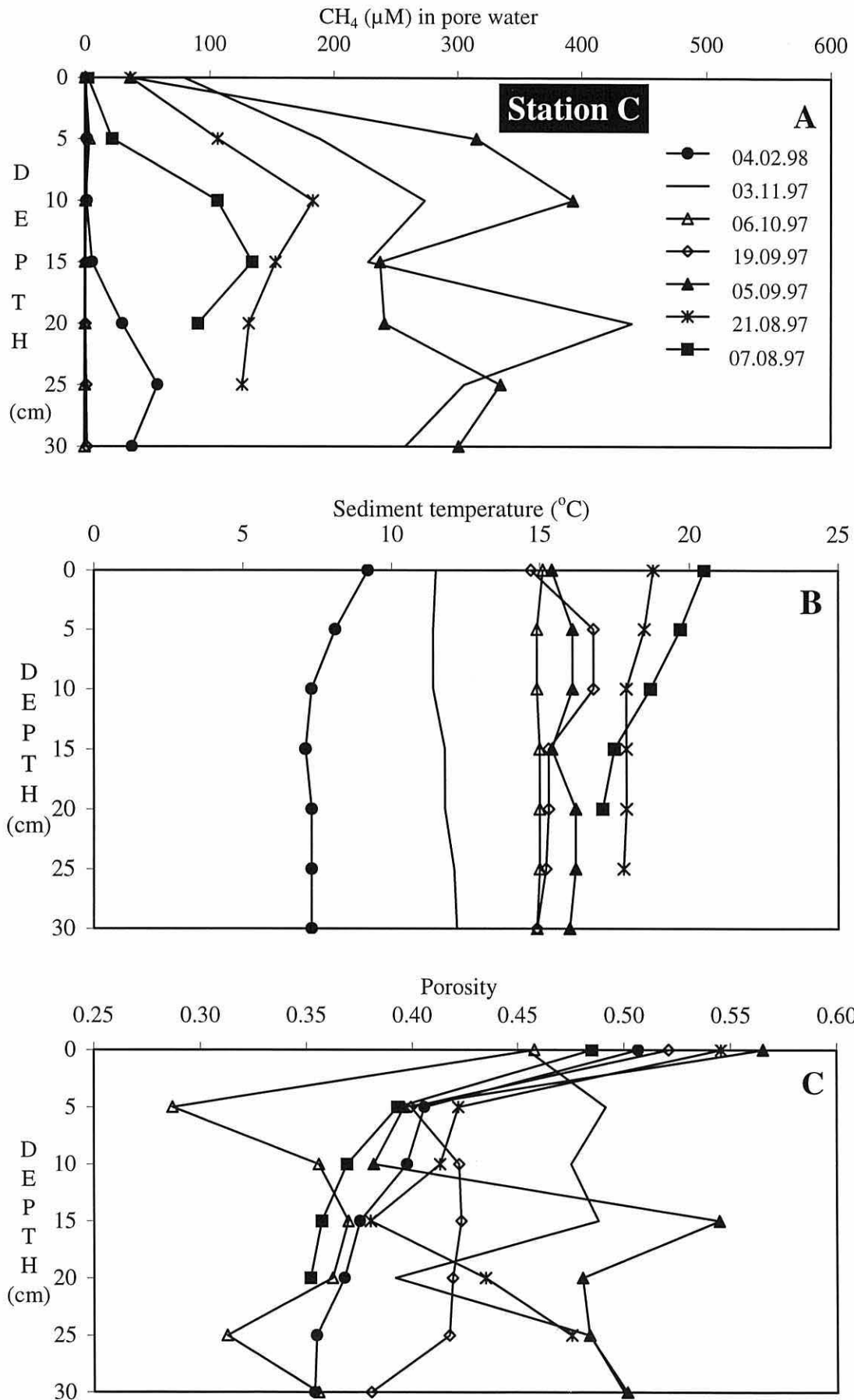


Figure 3.5.1.3 See next page for legend

Figure 3.5.1.1 Pore water methane concentration (CH_4 , μM) (A), temperature ($^{\circ}\text{C}$) (B), and porosity (C) at different sediment depths at station A in the Menai Bridge mudflats at various dates between 7 August 1997 and 4 February 1998.

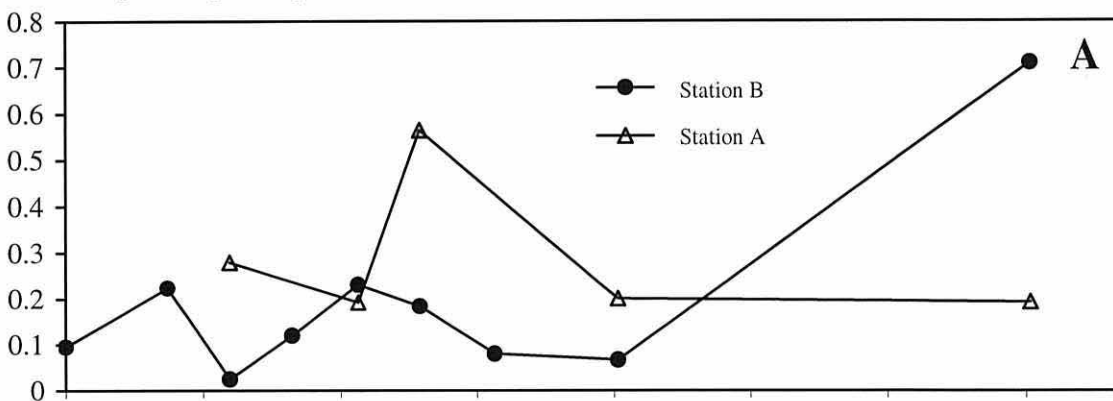
Figure 3.5.1.2 Pore water methane concentration (CH_4 , μM) (A), temperature ($^{\circ}\text{C}$) (B), and porosity (C) at different sediment depths at station B in the Menai Bridge mudflats at various dates between 1 July 1997 and 4 February 1998.

Figure 3.5.1.3 Pore water methane concentration (CH_4 , μM) (A), temperature ($^{\circ}\text{C}$) (B), and porosity (C) at different sediment depths at station C in the Menai Bridge mudflats at various dates between 7 August 1997 and 4 February 1998.

Table 3.5.1.3 Depth (cm) of maximum pore water methane concentrations at stations A, B and C on the different sampling dates, and the mean depth of maximum methane. (The total depth of sediment analysed is given in brackets).

Date	Station A	Station B	Station C	Mean
01.07.1997		20 (25)		20.0
24.07.1997		15 (20)		15.0
07.08.1997	20 (20)	20 (20)	15 (20)	18.3
21.08.1997		20 (25)	10 (25)	15.0
05.09.1997	15 (30)	25 (30)	25 (30)	21.7
19.09.1997	30 (30)	15(30)	30 (30)	25.0
06.10.1997		15 (30)	5 (30)	10.0
03.11.1997	30 (30)	30 (30)	20 (30)	26.7
04.02.1998	25 (30)	30 (30)	25 (30)	26.7

20 cm depth-integrated pore water CH_4 (mmoles m^{-2})



20 cm depth-integrated sediment CH_4 (mmoles m^{-2})

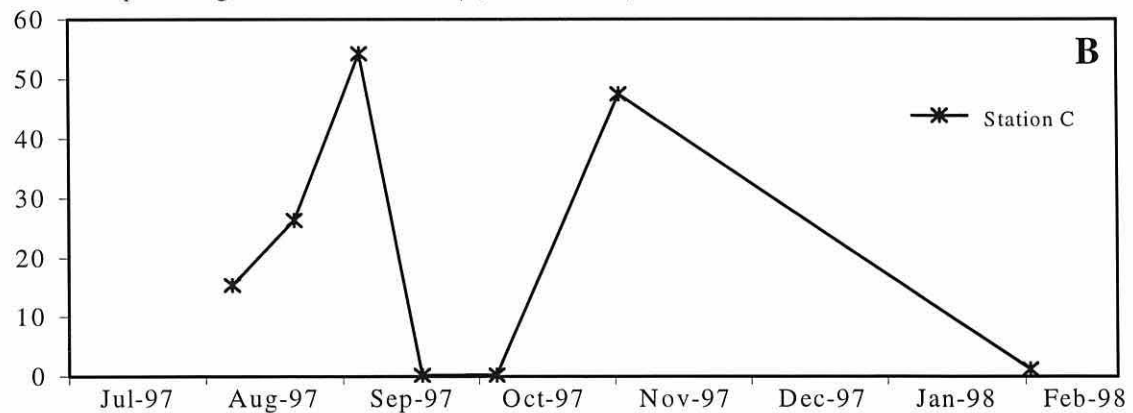


Figure 3.5.1.4 20 cm depth-integrated pore water methane concentrations (mmoles m^{-2}) at stations A, B (A), and station C (B) between 1 July 1997 and 4 February 1998.

During the nine-month sampling period the sediment temperature varied by more than 10°C at all depths (Figures 3.5.1.1 B, 3.5.1.2 B and 3.5.1.3 B), but showed no relationship with sediment methane concentrations. Further, sediment porosity appeared not to be strongly related to methane concentrations (Figures 3.5.1.1 C, 3.5.1.2 C and 3.5.1.3 C). The average porosity over all depths and dates at station A was 0.41, at station B 0.46, and at station C 0.42.

3.5.2 Spatial distribution

Sedimentary heterogeneity might markedly influence the interpretation of the seasonal sediment study reported earlier. Thus, spatial distribution of methane was investigated in different sediment types, at different shore heights in the intertidal zone, and finally in replicate cores.

Effect of sediment type on methane concentrations in sediment depth profiles

As sandy sediments cover a large part of the Menai Strait bottom, the potential of sand as a methane source for Menai Strait water was investigated and compared to the source strength of the less widely distributed mud. The mud core was collected on 1 July 1997 from the low water edge during low tide at station B in the Menai Bridge mudflats. The sand core originated from the Lavan Sands close to the low water edge west of Llanfairfechan, and was sampled on 11 July 1997. Both cores were 25cm long, were sliced in 5cm intervals and poisoned with HgCl_2 on site.

In the laboratory sediment methane concentrations and porosities were measured. The results are shown in Figure 3.5.2.1.

The mud core was richer in methane than the sand core at all depths (Figure 3.5.2.1 A) with the difference between the cores increasing with depth. The sediment surface concentration of methane in sand (35 nM) was within the concentration range measured a few days earlier in the overlying waters (18 to 86 nM, see Figure 3.2.8). The surface concentration of methane in mud (170 nM), on the other hand, was more than three fold greater than the concentrations measured the same day in overlying waters (52.5 nM, see Appendix 3.1).

At all depths sediment porosity was lower in the methane-poor sand core than in the methane-rich mud core (Figure 3.5.2.1 B), suggesting a positive correlation between methane and porosity.

The depth profiles of each core individually, however, suggest a negative relationship as porosity was generally higher in the top layers of the sediment where methane was low (Figure 3.5.2.1 B).

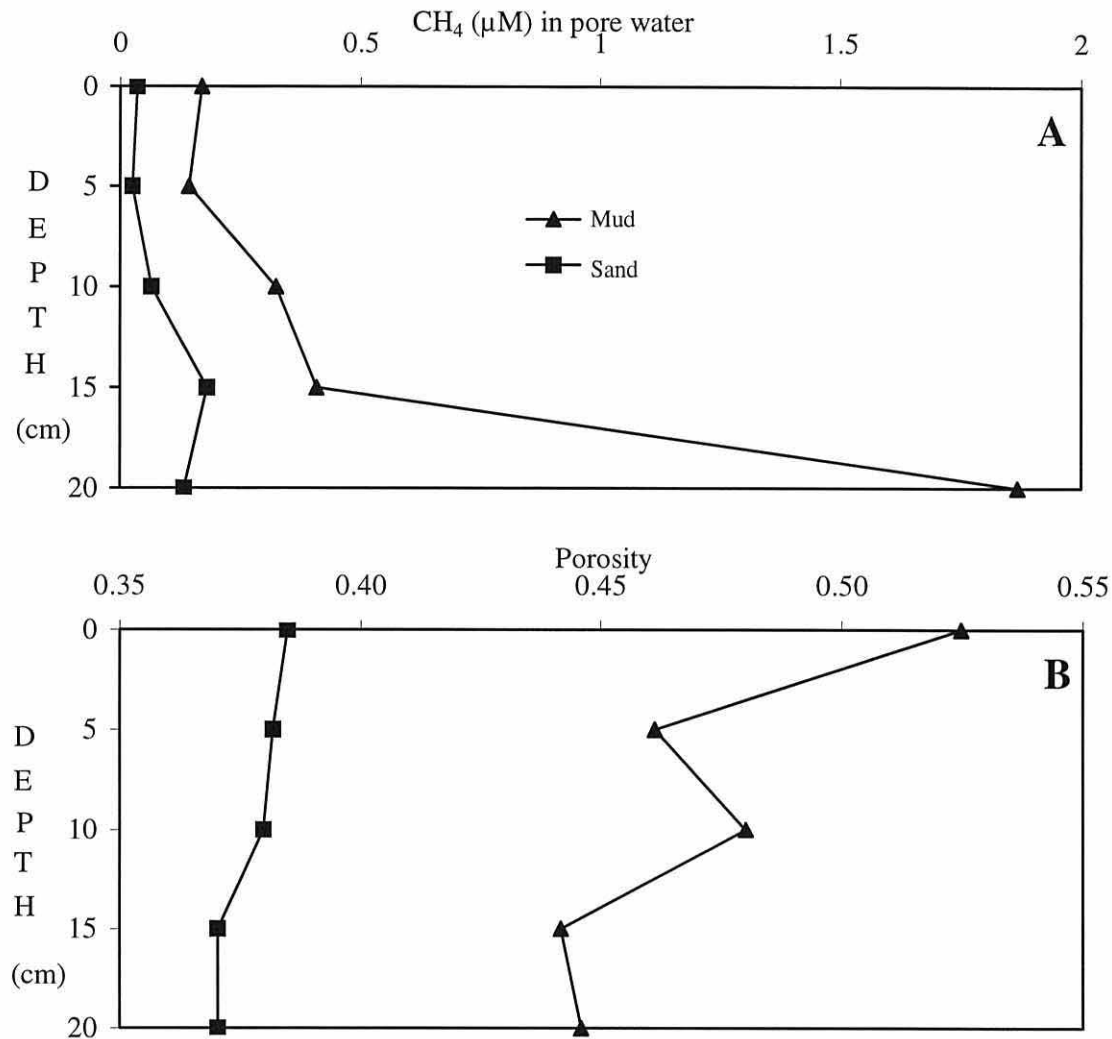


Figure 3.5.2.1 Sediment depth profiles of pore water methane concentrations (CH₄, nM) (A), and porosity (B) in a sand core from the Lavan Sands on 11 July 1997 and in a mud core from station B in the Menai Bridge mudflats on 1 July 1997.

The effect of shore height on methane concentrations in intertidal sediments

The Menai Strait is such a turbulent environment, that potentially methanogen-harbours sediments such as muds have only accumulated in sheltered areas mainly in the intertidal zone. High shore sediments are exposed for significant periods of time to air. As diffusion through gas is significantly faster than diffusion through a liquid matrix, oxygen can be expected to penetrate deeper into high shore sediments and thereby limit methanogen activity when compared to low shore sediments. The produced methane might furthermore be exchanged directly with the atmosphere so that less methane enters the water during periods of submersion. To test this hypothesis, methane concentrations at different depths were measured in sediments from the high, mid and low shore along a transect at station B in the mudflats in Menai Bridge. The high shore station was selected to experience daily sea water coverage. Cores were collected during low tide on 24 July 1997. The temperature profiles at the three sites were measured in neighbouring cores. The results are shown in Figure 3.5.2.2.

Methane concentrations in low shore sediments were at least double the mid or high shore concentrations at all depths except the surface (Figure 3.5.2.2 A). The mid shore core was richer in methane than the high shore core in the top 15 cm but not at 20 and 25 cm depth.

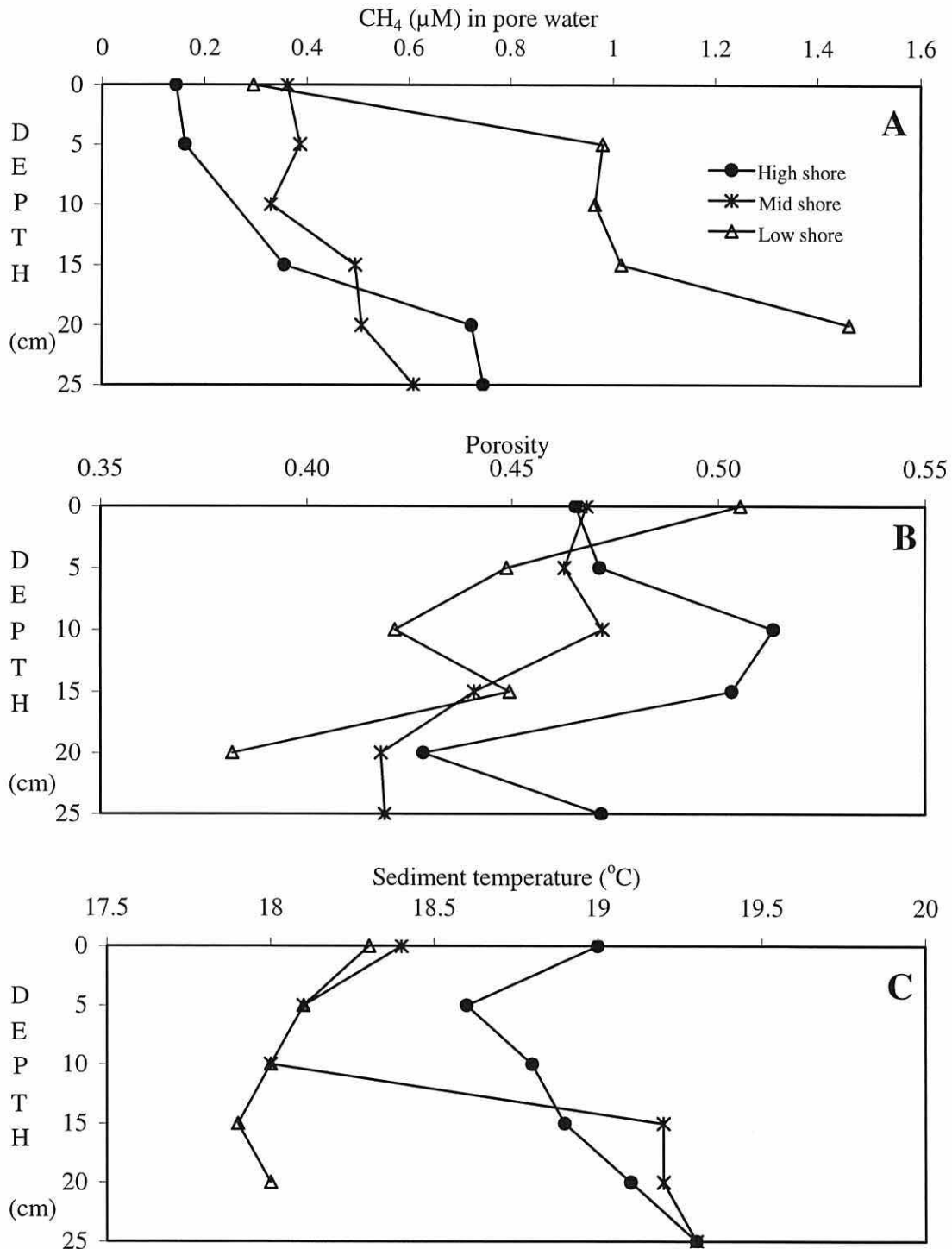


Figure 3.5.2.2 Sediment depth profiles of pore water methane concentration (CH₄, μM) (A), porosity (B), and temperature (°C) (C) in cores from the high, mid and low shore of station B sampled on 24 July 1997.

The sediment porosity was generally highest at the high shore and decreased towards the low shore (Figure 3.5.2.2 B). This suggests a negative relationship between methane concentrations and water content of the sediments.

Sediment surface temperature was highest at the high shore and lowest at the low shore (Figure 3.5.2.2 C) which might indicate a negative relationship with sedimentary methane. The depth profiles of temperature and methane concentrations, however, do not support this observation. Both the sea (17°C) and the air (16°C) temperatures at the time of sampling were below those measured in the sediments.

Small scale horizontal variability of sedimentary methane

To assess and evaluate the results from seasonal and spatial studies of methane in intertidal sediments the natural variability of methane concentrations in neighbouring sediment samples was quantified. Three 30 cm deep sediment cores were collected on 21 August 1997 within an area of 1m² at the spring low water's edge at station C in the Menai Bridge mudflats. The methane concentration and porosity therein were analysed at 5cm depth intervals. The results are shown in Figure 3.5.2.3.

The mean methane concentrations of the three sediment cores increased from the surface to a depth of 10 cm and slightly decreased thereafter (Figure 3.5.2.3 A). Maximum methane occurred in each of the three neighbouring cores at a different depth between 10 and 20 cm. The variability between the cores was large. Concentrations at equal depths were up to 3.3 fold higher in one core than another. The coefficients of variation around the mean concentrations ranged from 5 to 66 %, and were generally higher in surface sediments and in the regions of maximum concentrations than at greater depths.

The sediment porosity was higher at the surface than deeper down, while the variability did not change systematically with depth (Figure 3.5.2.3 B). Methane and porosity appeared to be negatively related in the triplicate cores.

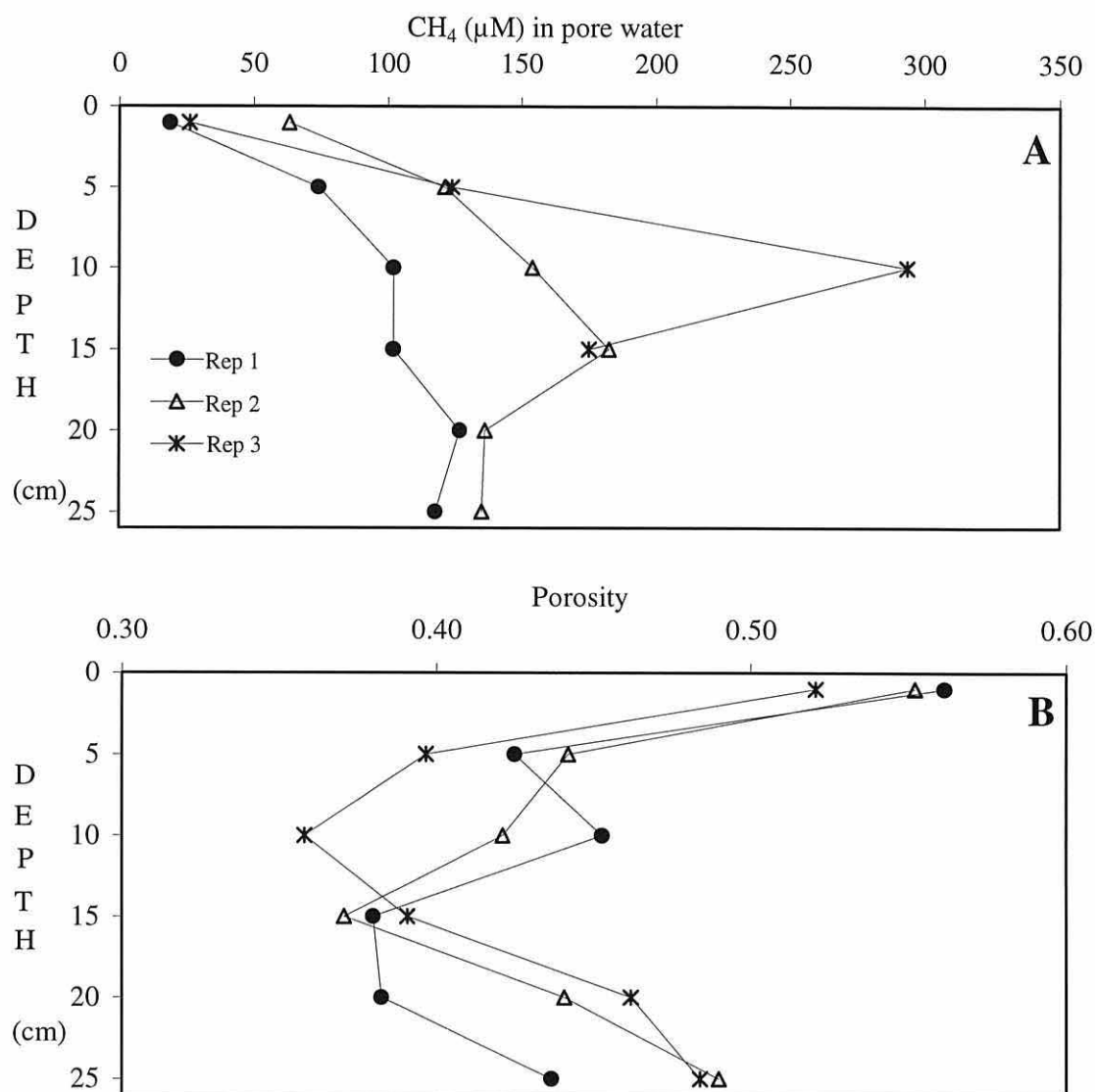


Figure 3.5.2.3 Pore water methane concentrations (CH₄, µM) (A) and porosity of sediments (B) at different depths in three neighbouring cores sampled at station C in the Menai Bridge mudflats on 21 August 1997.

Box 3.5: Summary of 'methane in Menai Strait sediments'

- Sediment methane concentrations were significantly higher in mud than in sand
- Particularly muddy sediments were generally much richer in methane than overlying waters
- Despite large variability, no systematic methane seasonality was detected in sediments
- Methane concentrations were higher in low shore intertidal sediments than further up the shore
- Methane concentrations in sediments vary greatly even over short distances
- Sediment heterogeneity of methane appeared to decrease with increasing depth

3.6 *In vitro* study of methane metabolism in sediments

An *in vitro* laboratory experiment was designed to study the effect of temperature on methane concentrations in sediments. The experiment tested the hypothesis that the seasonal increase of water column methane concentrations with temperature – as observed in section 3.1 – originated from a sedimentary methane source. As the typical Q_{10} for metabolism (*i.e.* effect of a 10°C temperature difference on enzymatic reaction rates) is usually in the range of 2 to 3, a significant difference in methane concentrations in sediments experiencing temperature differences of 10 and 20°C was expected.

Twelve sediment cores were collected with plastic corers of 25 cm length and an inner diameter of 3.9 cm at the spring low water edge of station C in the Menai Bridge mudflats on 21 August 1997. In the laboratory the cores were randomly divided into three groups of four and introduced into three incubators initially set at an approximately ambient temperature of 25°C. The top bungs of the corers were removed and sea water was added to cover the sediment. A water level of 0.5 cm above the sediment surface was kept approximately constant throughout the experiment by adding distilled water when evaporation had reduced the water volume and stirring the upper sediment layer to evenly distribute salts. The incubator temperatures were gradually cooled to their experimental temperatures of 5°, 15° and 25°C over a period of seven days. The incubator for the coolest cores was only powerful enough to cool them down to 9°C. Thereafter the cores were transferred into a ventilated cold room of 5°C, where they were kept standing upright in a container of sea water. The 15°C cores were incubated in a Julabo C F10 cooler that pumped water of 15°C through silicone tubing around the cores. The 25°C cores were kept in a Harvard / LTE Unitemp water bath filled with tap water.

After seven days of temperature adaptation, the experiment commenced on 28 August (day 1) when sediment concentrations of methane and porosities were measured at depths of 0, 5, 10, 15 and 20 cm in one core from each temperature group. The remaining cores were analysed after 20 days (16 September), 37 days (3 October) and 65 days (31 October).

Figure 3.6.1 shows the depth profiles of methane concentrations in sediments incubated at 5°C, 15°C and 25°C at the commencement of the experiment, and after 20, 37 and 65 days. Methane concentrations were lower in the 25°C cores than in cores incubated at lower temperatures. There was furthermore a general trend of methane to decrease during the incubation period at all temperatures and depths. The depth of maximum methane concentration appeared to increase with time.

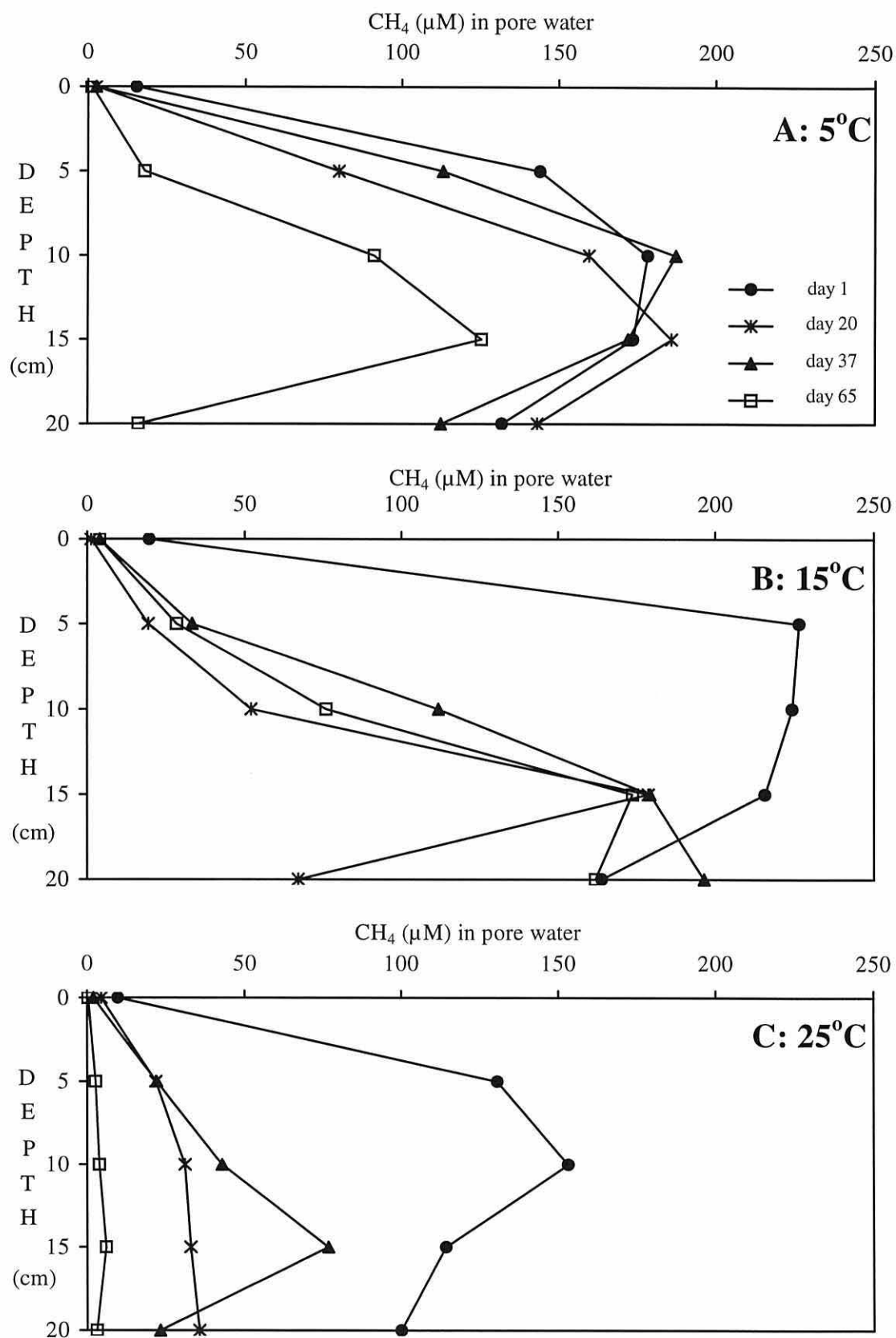


Figure 3.6.1 Pore water methane concentrations (CH_4 , μM) in sediments incubated at temperatures of 5°C (A), 15°C (B), and 25°C (C) between 28 August 1997 (day 1) and 31 October 1997 (day 65). Intermediate analysis dates were on 16 September (day 20) and 3 October (day 37).

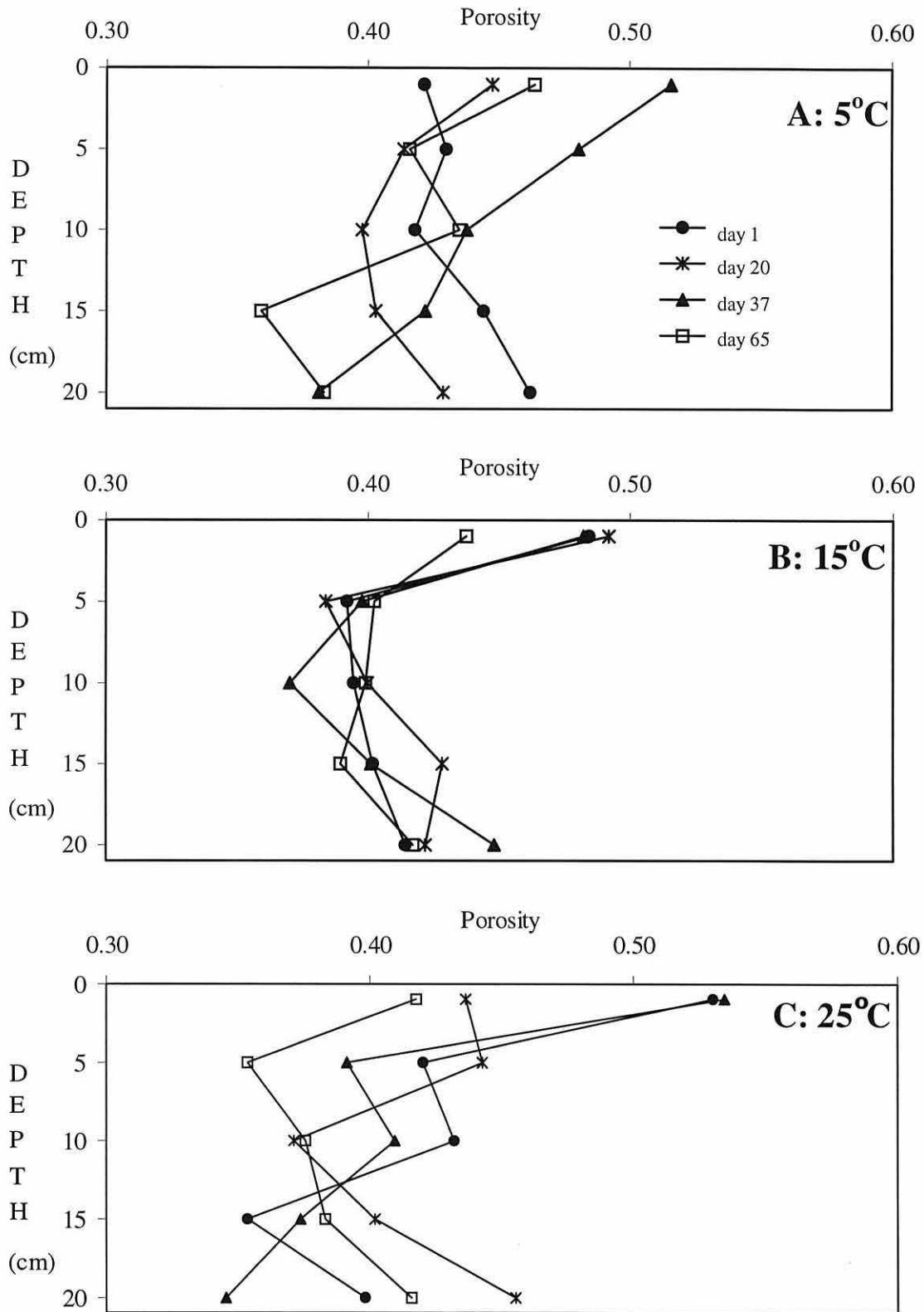


Figure 3.6.2 Sediment porosity in sediments incubated at 5°C (A), 15°C (B) and 25°C (C) on days 1, 20, 37 and 65.

The porosity profiles of the cores are shown in Figure 3.6.2 A to C. Porosity varied both with depth and from core to core with values ranging from 0.35 to 0.54. The variability between cores was largest at the surface and decreased with increasing depth. Surface sediments were generally more porous than deeper layer, and lowest porosities were measured at sediment depths of 15 and 20cm.

Sediment methane concentrations were generally not related to sediment porosity apart from on 28 August (Table 3.6.1).

Table 3.6.1 R^2 values, associated probabilities (p) and number of paired observations (N) for simple linear relationships between methane concentration and sediment porosity in sediment cores incubated at three different temperatures and analysed after four different incubation periods.

	R^2	p	N
DATA ORGANISED BY ANALYSIS DATE			
28 August 1997 (day 1)	0.363	0.018	15
16 September 1997 (day 20)	0.089	0.281	15
03 October 1997 (day 37)	0.064	0.362	15
31 October 1997 (day 65)	0.018	0.629	15
DATA ORGANISED BY TEMPERATURE			
5°C	0.077	0.237	20
15°C	0.184	0.059	20
25°C	0.033	0.447	20
ALL DATA	0.092	0.090	60

The results of a 65-day incubation of sediment cores at 5, 15 and 25°C are thus not conclusive. The variability between sampled cores is generally large (section 3.5.2) and might have masked any temperature effect.

Box 3.6: Summary of ‘study of methane metabolism in sediments’

- There was no evidence of an increase in sedimentary methane concentrations with temperature over the experimental period of 65 days.
- Sediment methane concentrations tended to decrease with time in incubated cores

*Natural science does not simply describe and explain Nature,
It is part of the interplay between Nature and ourselves.*

*Wernher Heisenberg (1901-1976)
'Physics and Philosophy'*

Chapter Four

Discussion

In this chapter the results summarised in boxes 3.1 to 3.6 are discussed on their own, are compared to published studies and put into the broader context of methane biogeochemistry in the marine environment. First, the spatial and seasonal distribution of methane in the waters of the Menai Strait and at Point Lynas are discussed. Then, the potential causes for the scale and distribution of coastal methane are discussed with particular attention to the Menai Strait. All possible sources (Section 4.2) and sinks (Section 4.3) of methane in the Menai Strait are discussed, and the results are summarised in a budget for methane in the Menai Strait in 1997.

4.1 Spatial and seasonal distribution of methane in the water column

In this section the concentrations and the spatial and temporal distribution of methane in the water column described in sections 3.1 and 3.2 are discussed.

The study showed that methane in coastal waters is heterogeneously distributed both in space and time. Concentrations between 2.5 and 85.6 nM corresponding to saturation ratios between 1.02 and 33.1 were encountered in the waters around Anglesey. Such methane saturation ratios are typical for coastal areas as can be seen by comparison with other studies (Table 4.1.1).

Table 4.1.1 Surface water methane saturation ratios at different sampling locations and dates, and months of peak methane saturations from various literature sources.

Saturation	Location	Sampling dates	Peak month	Source
1.2-239	NW Gulf of Mexico	75-76	-	Brooks <i>et al.</i> , 1981
3-290	Oregon estuaries	1979 – 1982	-	DeAngelis & Lilley, 1987
0.85-420	S-California Bight	11/89, 3/90	-	Cynar & Yayanos, 1992
1.08-2.05	Coast Arabian Sea	5/94,3/95,8/95	SW monsoon	Patra <i>et al.</i> , 1998
1.8	Black Sea	05/67	-	Lamontagne <i>et al.</i> , 1973
2-5	Black Sea	07/88	-	Reeburgh <i>et al.</i> , 1991
0.95-120	S-North Sea	03/89	-	Scranton & McShane, 1991
1.13-3.95	Baltic Sea	2/92,7/92	July	Bange <i>et al.</i> , 1994
1.05-135	S. Baltic Sea	6/94,9/96,3/97	September	Bange <i>et al.</i> , 1998
2.31	N-Aegean Sea	07/93	-	Bange <i>et al.</i> , 1996
1.46-9.74	Amvrakikos Bay	07/93	-	Bange <i>et al.</i> , 1996
1.48	Shelf E-Ionian Sea	07/93	-	Bange <i>et al.</i> , 1996
1.02-2.7	Point Lynas	3/96 to 10/96	August	This study
2.4-26.4	Menai Bridge	3/96 to 11/97	July-August	This study

Methane concentrations in coastal waters seemed to increase in the summer and be lower in the winter and spring in water sampled from fixed stations during high water at spring tides (Figures 3.1.1 A and G for 1996). A seasonal pattern with maximum summer concentrations agrees with findings reported for other coastal sites (Table 4.1.1). When the water at Menai Bridge, however, was sampled more frequently in 1997, a high degree of short-term variability became apparent (Figure 3.1.1 G for 1997). High short-term variability in dissolved methane concentrations opens up the possibility that the seasonal pattern concluded from approximately fortnightly measurements could be a chance result. To investigate this possibility, surveys were conducted to determine scales and causes of short-term variability.

On an hourly basis over a 12-hour tidal cycle methane concentrations at the fixed station at St. George's Pier were seen to vary by a factor of 1.7 (Figure 3.2.2, and Table 4.1.2), which could account for roughly half the seasonal variability measured in 1997. This variability, however, appeared to be related to the direction of the tidal current. It should thus not influence the methane concentrations measured for the seasonal study, which were always made during the same period in the tidal cycle.

The variability of methane concentrations displayed during daily measurements at high water over an entire spring-neap tidal cycle, however, was so high that it could account for nearly the entire seasonal variability (Figure 3.2.1, and Table 4.1.2). This daily variability appeared to be independent from the spring-neap tidal cycle, so that sampling at spring high water for the seasonal study will not have removed this significant source of variability, and the results from the seasonal study can be expected to entail this daily high water variability.

The variability of methane concentrations at fixed sampling sites consists of spatial and temporal components. The scales of the different types of variability are summarised in Table 4.1.2.

The purely temporal component of the variability of methane concentrations in the Menai Strait was quantified by measuring the internal changes of methane in the water column with time during *in vitro* incubations. Except during a dense *Noctiluca* bloom, no changes occurred as a result of biological activity (Figure 3.3.1). It can therefore be assumed that the short-term variability in methane concentrations at fixed sites is not caused by temporal changes in the water column. However, a maximum change in methane concentrations of 0.6 nM h^{-1} is calculated when making the conservative assumption that the loss of methane from the incubation vials with time was due to *in situ* processes (Table 4.1.2). Under this assumption the pure temporal component of the variability could account for a maximum daily loss of 15 nM methane from the water column but is not responsible for any increase in concentrations.

The variability in methane concentrations caused by the interaction of water with the environment was investigated by measuring changes in the water as it drifted for 2.5 hours over 10 km through the Menai Strait (Figure 3.2.7). A mean increase of $4 \text{ nM CH}_4 \text{ h}^{-1}$ or $1.1 \text{ nM CH}_4 \text{ km}^{-1}$ was measured to occur. As no methane was produced internally in the water, the increase must have been due to inputs of methane from the sediments while water flowed over it. The rather stepwise increase in concentrations in the current direction suggests that the sources are not homogeneously distributed. The hypothesis of a sedimentary source of methane will be explored in section 4.2.2.2.

The spatial variability of methane is great as is apparent from the large concentration differences for all seasons between the waters at Menai Bridge and Point Lynas (Table 4.1.2). The short-term spatial variability of methane in the Menai Strait was so significant over distances of a few kilometres that it exceeded the seasonal variability measured at a fixed station (Table 4.1.2). Generally methane concentrations along the Menai Strait did not vary erratically but increased into the direction of the current (Figure 3.2.5 A and B). Also the evidence from spatial variability studies thus suggests an internal sedimentary source.

The short-term variability studies suggest that the variability at the fixed sampling station at St. George's Pier will unlikely be due to temporal changes in methane concentrations. As the waters passing a fixed station can be expected to have always passed across very similar sediments before, the effects of the principally very significant spatial variability within the Menai Strait will be much reduced.

Table 4.1.2 Methane concentration ranges or rates of concentration changes for seasonal and various types of short-term (ST) variability.

Type of variability	Concentration range (nM)	Rate of concentration change
Seasonal		
Point Lynas 1996	2.5 – 7.1	
Menai Strait 1996	6.3 – 53.0	
Menai Strait 1997	21.5 – 63.2	
ST Fixed station (St. George's Pier)		
Hourly – over 12 hours	42 – 73	
Daily – over 2 weeks	22 – 61	
ST Spatial		
NE-Menai Strait along	16.6 – 50.5	2.5 nM km^{-1}
Central Menai Strait along	35 – 56	7 nM km^{-1}
Menai Strait across	18.5 – 85.5	13.4 nM km^{-1}
ST Temporal (Menai Strait)		
Incubations		$\leq 0.6 \text{ nM h}^{-1}$
Drift study	49.3 – 62.6	4 nM h^{-1} or 1.1 nM km^{-1}

Another parameter that could influence the day-to-day variability in high-water methane concentrations is the wind. A significant negative relationship was observed between the square of the wind velocity and methane (Figure 4.1.1). In general increased wind velocity increases the rate at which methane is transferred from the supersaturated sea into the atmosphere, so that lower concentrations remain in the water after a period of strong winds. The effect of wind on methane concentrations will be discussed in detail in section 4.3.2.

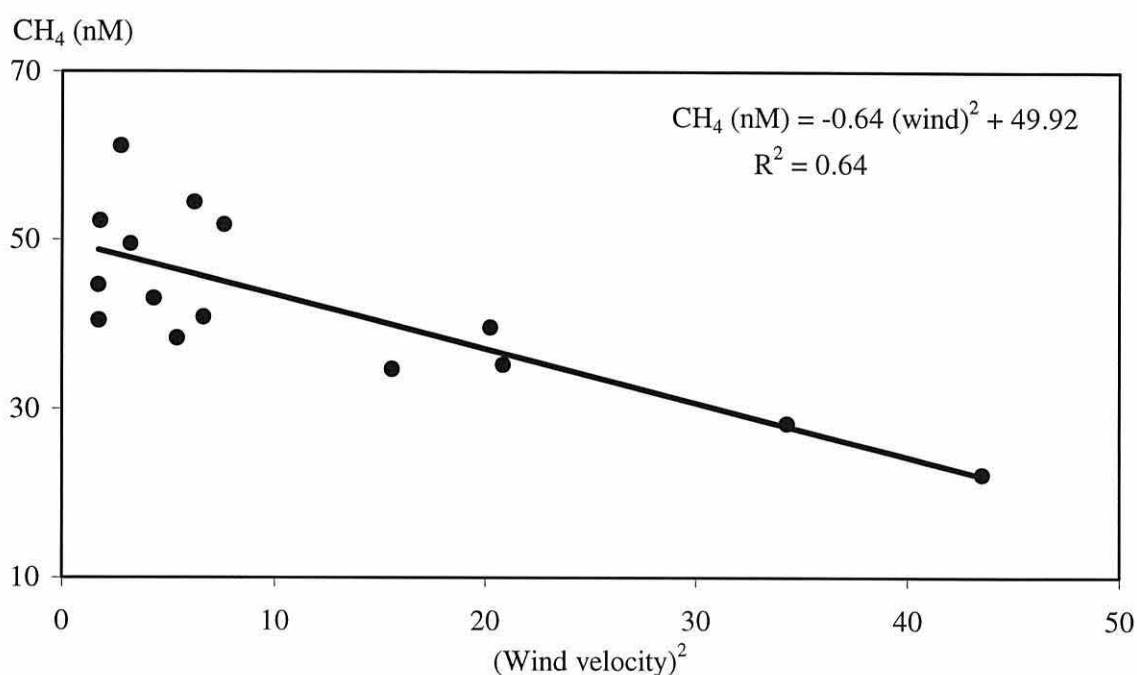


Figure 4.1.1 Scatter plot of high-water methane concentrations (CH₄, nM) and the squares of the mean daily wind speeds (m s⁻¹) between 27 May and 12 June 1997 at Menai Bridge.

At higher wind speeds this relationship was seen to be more significant than at lower wind speeds (Table 4.1.3), which may be due to the quadratic nature of the wind effect (Wanninkhof, 1992). The low wind speeds of 2 ± 0.7 (SD) m s⁻¹ during the hourly variability study (Figure 3.2.2) might account for the absence of a significant relationship between methane and wind on this occasion ($r = -0.311$), when current direction was the determining factor.

Table 4.1.3 Pearson's correlation coefficient (r) between water column methane concentrations and the square of wind velocity over fifteen occasions between 27 May and 12 June 1997. At the 5% level significant correlation coefficients are given in bold.

	r
All data (N=15)	-0.80
Low wind speeds: 1.3 to 1.8 m s ⁻¹ (N= 5)	0.54
High wind speeds: 3.9 to 6.6 m s ⁻¹ (N= 5)	-0.92

In summary, methane concentrations in coastal waters are heterogeneously distributed in space and time. A seasonal increase in methane concentrations towards the summer is discernible but could be a chance pattern as the day-to-day variability in methane concentrations is high. At St. George's Pier the short-term variability depended on current direction, spatial variability and wind. At this stage it cannot be decided whether the observed seasonal increase in methane concentrations is a representation of reality. The nature and seasonality of the different sources and sinks and their combined effects have to be discussed before a conclusion can be reached.

4.2 Sources of methane in Menai Strait waters

Coastal seawater was supersaturated with respect to atmospheric methane on all occasions during this study and also during surveys at other coastal sites (Table 4.1.1). For such continuous supersaturation to occur, methane must constantly be produced or released within the marine environment. In this section the various potential sources of methane in the temperate coastal waters of the Menai Strait are discussed in the following order: external sources (Section 4.2.1), which include advection of methane, and atmospheric, riverine and sewage inputs, and internal sources (Section 4.2.2), which considers pelagic and sediment sources.

4.2.1 External sources of methane in the Menai Strait

Methane measured in the waters of the Menai Strait does not necessarily originate there but can have been advected with inflowing water from Liverpool Bay, can have diffused into the water from the atmosphere, or might have been introduced with inflowing river water or with sewage inputs. This section discusses the magnitude of such external sources and considers the possibility that these sources could contribute to a seasonal increase in methane in the summer.

Advection of methane from Liverpool Bay

There is a net current of water that carries Liverpool Bay water in the course of approximately two days through the Menai Strait into Caernarfon Bay. Some of the methane measured in the Menai Strait will have been in the water before it entered the Menai Strait and thus be of external origin. The water that entered the Menai Strait from Liverpool Bay on 22 August 1997 had a methane concentration of approximately 10 nM (Figure 3.2.3). It thus seems that about 20% of the concentrations measured at St. George's Pier in summer could have been advected. As the concentrations in inflowing water at other times of the year are unknown, no conclusions can be drawn concerning a possible contribution to a seasonal increase in methane concentrations. As methane concentrations in sea water are usually at their highest in the summer, it is unlikely that more than 10 nM methane will be introduced into the Menai Strait at other times of the year.

Atmospheric methane input

The atmosphere is a potential source of methane in surface waters that are undersaturated, so that atmospheric methane can equilibrate into it. This has for example been observed off the coast of Peru during periods of above average atmospheric methane concentrations (Lammers and Suess, 1994), and during autumn and winter in large areas of the Pacific Ocean outside tropical latitudes (Bates *et al.*, 1996). Both the Menai Strait and Point Lynas, however, were supersaturated throughout the year and the atmosphere must thus have acted as a sink for, and not a source of methane in coastal waters.

Riverine methane input

Freshwater environments such as rivers and lakes are often very rich in methane (Lamontagne *et al.*, 1973; Wilkness *et al.*, 1978; DeAngelis and Lilley, 1987; Richey *et al.*, 1988; Scranton and McShane, 1991). This is attributed in part to anthropogenic effluents (Brooks and Sackett, 1973; Brooks *et al.*, 1981; Butler *et al.*, 1987), and in part to lateral diffusion and runoff from saturated forest and fertilised agricultural soils (Wilkness *et al.*, 1978; DeAngelis and Lilley, 1987). Some rivers such as the Amazon, the Rhine, the Hudson, the Orinoco, the Scheldt and the Peene have been found to be major contributors to methane concentrations in the receiving coastal waters (Richey *et al.*, 1988; Scranton and McShane, 1991; DeAngelis and Scranton, 1993; Jones and Amador, 1993; Bange *et al.*, 1998). It was thus important to consider the situation of riverine inputs into the Menai Strait. In the studied north-eastern and central sections of the Strait, the River Ogwen is the only river or stream of significance and brings an average daily freshwater volume of $70 \times 10^3 \text{ m}^3$ into the Strait with a total volume of about $100 \times 10^6 \text{ m}^3$. The summer methane concentrations measured close to the mouth of the Ogwen were 4.5 nM and thus approximately one order of magnitude smaller than those in the receiving waters. The river inputs will thus add methane to the Menai Strait but dilute the concentrations. As the Ogwen is small it will reduce the methane concentrations in the Menai Strait by less than 0.01%. The effect of riverine methane inputs into the Strait can thus be considered insignificant.

Sewage input

Sewage has been recognised as a globally relevant source of methane, such that it is imperative to consider the inputs of methane and methanogenic material *via* sewage into the Menai Strait. Menai Strait sewage was seen to be richer in methane than the receiving waters (Table 3.4.1) and must therefore be considered to be an external source for methane. Methane in treated sewage from the central sewage treatment plant at Treborth was, with 181 nM, only about three to four times as concentrated as the receiving waters, while raw sewage at Menai Bridge contained 476 nM of methane and was thus approximately an order of magnitude more concentrated (Table 3.4.1). The reason for the lower concentration in the treated sewage is thought to be that aeration of the activated sewage sludge during secondary treatment and again prior to discharge sweeps

much of the supersaturated methane out of the treated water into the atmosphere. The contributions of treated sewage to Menai Strait methane concentrations are greater than from raw sewage due to more than ten times greater daily discharge volumes (Table 3.4.1). Treated sewage introduces daily 1.92 moles of methane into the Menai Strait, and raw sewage about 0.44 moles. Treated sewage is discharged at a rate of $0.12 \text{ m}^3 \text{ s}^{-1}$ ($22 \text{ } \mu\text{moles CH}_4 \text{ s}^{-1}$) from a single outfall located to the south-west of the Britannia Bridge (Figure 2.2). Despite this high discharge rate, methane concentration in the water flowing through the Menai Strait did not increase at a greater rate than elsewhere in the Menai Strait (Figure 3.2.7 at 105 minutes). This is thought to be due to the high Menai Strait flow rates of $800 \text{ m}^3 \text{ s}^{-1}$ during spring high tides (Harvey, 1968). As the Menai Strait water at the discharge location at the day of the drift study contained approximately 55 nM CH_4 or $44000 \text{ } \mu\text{moles CH}_4 \text{ s}^{-1}$, the discharged sewage enlarges this by only by 0.05%. It can be speculated, however, that methane concentrations around the outfall increase significantly during slack water.

The source of methane in sewage must be associated with the contaminants as the tap water matrix was ten to eighty times less rich in methane than the sewage (Table 3.4.1). Anaerobic conditions suitable for methanogens exist in the large bowel of humans, of which approximately one-third harbour methanogens (Nottingham and Hungate, 1968). Methane in sewage will thus at least in part originate in the large bowel and enter sewage with the faeces. Also, methanogens will be contained in the sewage and might be active where anaerobic conditions exist. Net methane production, however, does not occur once sewage enters the marine environment as no increase in methane concentrations could be detected during incubations of sewage diluted with sea water (Figure 3.4.1).

Methane concentrations were only determined once for both treated and raw sewage and assumptions have to be made concerning its distribution with time. The concentrations in both treated and raw sewage will vary according to the diluting effect of rain, but the total mass of methane discharged per day can be expected to be approximately constant. Over the course of an average day methane concentrations in raw sewage might vary significantly as different activities during the day produce different types of liquid wastes. Discharges of treated sewage, on the other hand, can be assumed to be rather constant because the sewage is mixed and treated for six to eighteen hours before being released. There is no significant seasonal variability in the volumes of sewage that are processed at Treborth (personal communication: Nina Johnson from Treborth Sewage Treatment Works). Thus the input of allochthonous methane with sewage into the Menai Strait might be assumed to be constant over the year and not to give rise to a seasonal pattern in methane concentrations in Menai Strait waters.

In summary, none of the four external sources considered are likely to contribute to a seasonal increase in Menai Strait methane concentrations. Advection from Liverpool Bay was seen to be the only significant external source of methane in the Strait and to support approximately 20% of the methane in waters at St. George's Pier. Methane from sewage discharges contributes only to a minor extent and riverine methane inputs are quantitatively insignificant. The atmosphere was identified as a sink for methane.

4.2.2 Internal sources of methane in the Menai Strait

There is ample evidence from spatial and temporal variability studies of methane in the Menai Strait suggesting that most of the supersaturated methane that occurs inside the Menai Strait has been produced or released internally and was not transported to the sampling stations in advecting water currents or added with sewage or river inputs. This can be concluded from observations that methane concentrations increase steadily as water flows through the Menai Strait (Figures 3.2.5 B and 3.2.7). Also, results from the fixed station study conducted at the entrance to the Menai Strait suggest that there is significant internal production of methane. The water entering the Strait from Liverpool Bay contained rather low and constant concentrations of methane, while water that had already been in the Strait and flowed back into Liverpool Bay was richer in methane (Figure 3.2.3), which it consequently must have picked up within the Strait. In both fixed station studies there was a temporal delay in the response to changes in current direction, as the water that first flowed again in the net current direction was not 'new' water but was roughly the same water that had beforehand passed the station in the opposite direction.

Internal sources of methane must thus exist within the water column and/or within the sediment. The possibility that methane production occurs and the issues of production sites and rates will be discussed separately for these two major marine environments.

4.2.2.1 Pelagic sources of methane

Methanogenesis as a strictly anaerobic process was traditionally not considered to be possible in the oxygenated water column. There is, however, ample indirect evidence that *in situ* production of methane takes place in oxygenated surface waters. Scranton and Brewer (1977) calculated that *in situ* methane production in the order of $80 \text{ nmol cm}^{-2} \text{ yr}^{-1}$ in the top 100 m of the water column ($\equiv 22 \text{ pmol dm}^{-3} \text{ d}^{-1}$) had to occur in the western subtropical North Atlantic to account for the measured values of surface water supersaturation. Tilbrook and Karl (1995) estimated that a net methane production rate in the order of $23 \text{ pmol dm}^{-3} \text{ d}^{-1}$ had to take place to maintain surface layer supersaturation in Californian coastal waters and the North Pacific gyre. Other investigators argued that *in situ* methane production was a necessity to explain the distribution of methane at a variety of offshore sampling sites (Scranton and Farrington, 1977; Burke *et al.*, 1983; Ward *et al.*, 1987). To the author's knowledge, no direct measurements of pelagic methane production

under *in situ* conditions have yet been conducted successfully due to the low production rates. Coastal waters are characterised by significantly larger biomass and biological productivity than oceanic regions, so that the rates of pelagic methanogenesis might be higher in coastal areas and could thus be measured more readily. This was the motivation for the incubation experiments conducted in this project.

The organisms, sites and processes of pelagic methanogenesis remain subject to debate. In the following section I shall examine the possibility that methane is produced in the water column and if so where. Evidence may be gained in four ways:

- 1) Investigation of potentially causal correlations between methane concentrations and biological, physical and chemical water column parameters.
- 2) Direct demonstration of the occurrence of viable methanogenic bacteria in the water column.
- 3) The demonstration of sites or circumstances that could give rise to and maintain anoxic conditions under which methanogens could be active.
- 4) Accumulation of methane *in situ* or *in vitro* in the water column.

In the following pages, the available evidence for all four types of investigation will be discussed.

1) Correlations

In this study, no consistent correlation could be detected linking coastal methane concentrations to any of the measured biological water column parameters in either the Menai Strait or at Point Lynas (Table 4.2.1). The biological parameters all peaked during blooms in spring, when increased light availability usually allows phytoplankton to utilise the nutrients that are readily available after the winter mixing. Such algal blooms are commonly accompanied, after a slight temporal delay, by blooms of heterotrophic bacteria and zooplankton (Blight *et al.*, 1995). The lack of a consistent correlation of methane with biological parameters is supported by the literature. While occasional positive correlations between methane and indicators for algal and/or zooplankton biomass have been reported (Scranton and Farrington, 1977; Conrad and Seiler, 1988; Owens *et al.*, 1991; Cynar and Yayanos, 1991; Patra *et al.*, 1998), these did not occur in other field campaigns (Brooks *et al.*, 1981; Scranton and McShane, 1991; Lammers and Suess, 1994), and are thus not consistent.

Table 4.2.1 Pearson's correlation coefficients (r) between methane concentrations and several biological, physical and chemical parameters at Point Lynas in 1996 (PL96) and in the Menai Strait in 1996 and 1997 (MS96, MS97). Values in bold are significant at the 5% level. The number of observations is shown in brackets.

	r (PL96)	r (MS96)	r (MS97)
Chlorophyll a	-0.43 (18)	-0.03 (17)	-0.51 (12)
Phaeopigment	-0.50 (18)	0.07 (15)	-0.51 (12)
Net community production	-0.03 (16)	0.20 (14)	-
Gross community production	-0.28 (16)	0.25 (14)	-
Dark community respiration	0.30 (16)	0.28 (14)	-
POC concentration	-0.44 (18)	0.36 (10)	-0.50 (9)
PON concentration	-0.44 (18)	-	-
C/N ratio	-0.44 (18)	-	-
Temperature	0.51 (19)	0.75 (19)	0.56 (34)
Salinity	0.20 (18)	0.66 (19)	-0.05 (24)
O ₂ concentrations	-0.42 (19)	-0.84 (11)	-

The lack of a consistent relationship between biological water column parameters and methane could be due to various reasons:

- 1.) The water column is not the main source for water column methane.
- 2.) There is no causal connection between biological methane production by pelagic methanogens and the abundance and activity of other planktonic organisms.
- 3.) There is a time lag between the autotrophic production of organic material in the water column - which occurs predominantly during the spring bloom - and the arrival of suitable substrates for methane production in mid-to-late summer. A time lag of three months, however, is unlikely as the organic material that is produced in the spring bloom will either be recycled or will have sedimented long before August, when maximum methane concentrations occur.
- 4.) Wind has a marked effect on supersaturated gas concentrations as argued in section 4.1. It does not, however, affect other biological parameters in the water to a similar extent. Wind could therefore mask causal relationships between biological methane production and other biological variables. The role of wind on surface water methane concentrations will be discussed in section 4.3.
- 5.) Methanogenesis might not be associated with phytoplankton, zooplankton or bacteria as a whole, but could be species-specific. DeAngelis and Lee (1994) found that methane was produced under *in situ* surface ocean conditions in association with certain species of actively grazing copepods. While the algal food species affected the rates of production, the process itself was restricted to some copepod species. The production rates (4 to 20 pmol CH₄ copepod⁻¹ d⁻¹) were high enough to make a significant contribution to the oceanic subsurface methane maximum. Species-specific responses would result in positive correlations only where the source species dominate the plankton community.

With the available information it has not been possible to decide which - if any - of the suggestions listed above provide the true explanation for the lack of correlations between methane concentrations and biological parameters in the marine water column.

The only parameter that correlated consistently with methane was sea surface temperature (Table 4.2.1). Regression analysis found the relationship between temperature and methane to be positive and linear (Figure 4.2.1). A connection between water temperature and methane has also been observed in other seasonal studies (Bange *et al.*, 1998), and temperature has been proposed to be a driving force for the methane dynamics in temperate waters (Bates *et al.*, 1996).

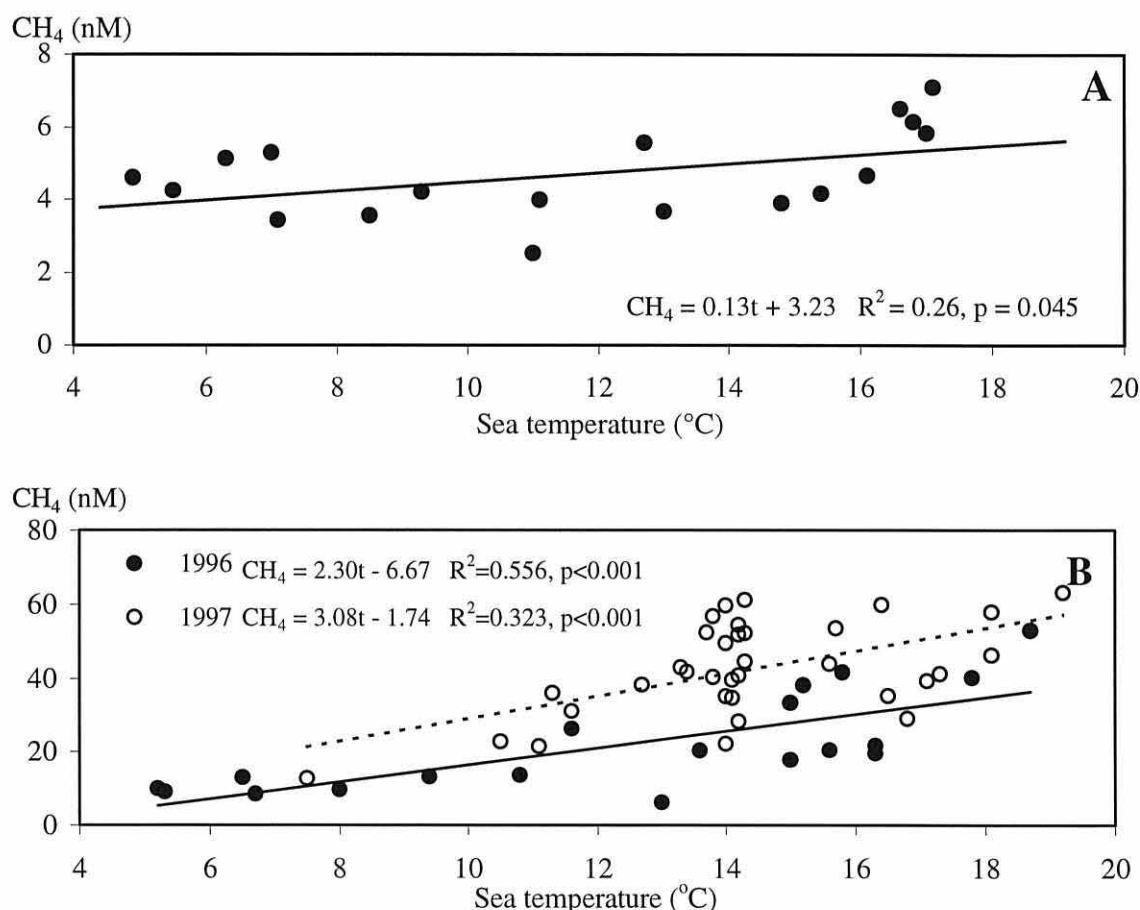


Figure 4.2.1 Scatter diagrams showing the relationship between water temperature (t , °C) and methane concentration (CH_4 , nM) in the waters at Point Lynas in 1996 (A) and in the Menai Strait in 1996 and 1997 (B).

The positive correlation with temperature could be a result of increased methanogen activity at higher temperatures. Many methanogens, however, are thermophilic and show maximum activity at temperatures well above those of temperate waters. Furthermore most biological processes - including methanotroph activity - will also increase with temperature. The cause for the correlation between methane and temperature thus remains unknown and might well be the effect temperature has on other factors, *e.g.* the oxygen concentration in the water.

At higher temperatures water is saturated at lower oxygen concentrations than in the winter, and temperature and oxygen concentrations correlate significantly and negatively at both study sites ($r = -0.78$, $N=20$ at Point Lynas and $r = -0.81$, $N=11$ in the Menai Strait in 1996). Lower oxygen concentrations in seawater might facilitate the development of anaerobic microzones within particles, as will be discussed in detail in 'Anoxic environments in the water column'. If methanogens exist in the water column and if they produce methane within anaerobic microzones, it can be speculated that more methanogenic zones exist in summer due to the reduced oxygen concentrations in the water. This could contribute to an increase in methane concentrations in summer. Negative correlations between methane and oxygen concentrations have indeed been observed in the past (Owens *et al.*, 1991), and were also found to exist in the Menai Strait (Table 4.2.1). At Point Lynas, however, no significant correlation linked methane and oxygen concentrations (Table 4.2.1).

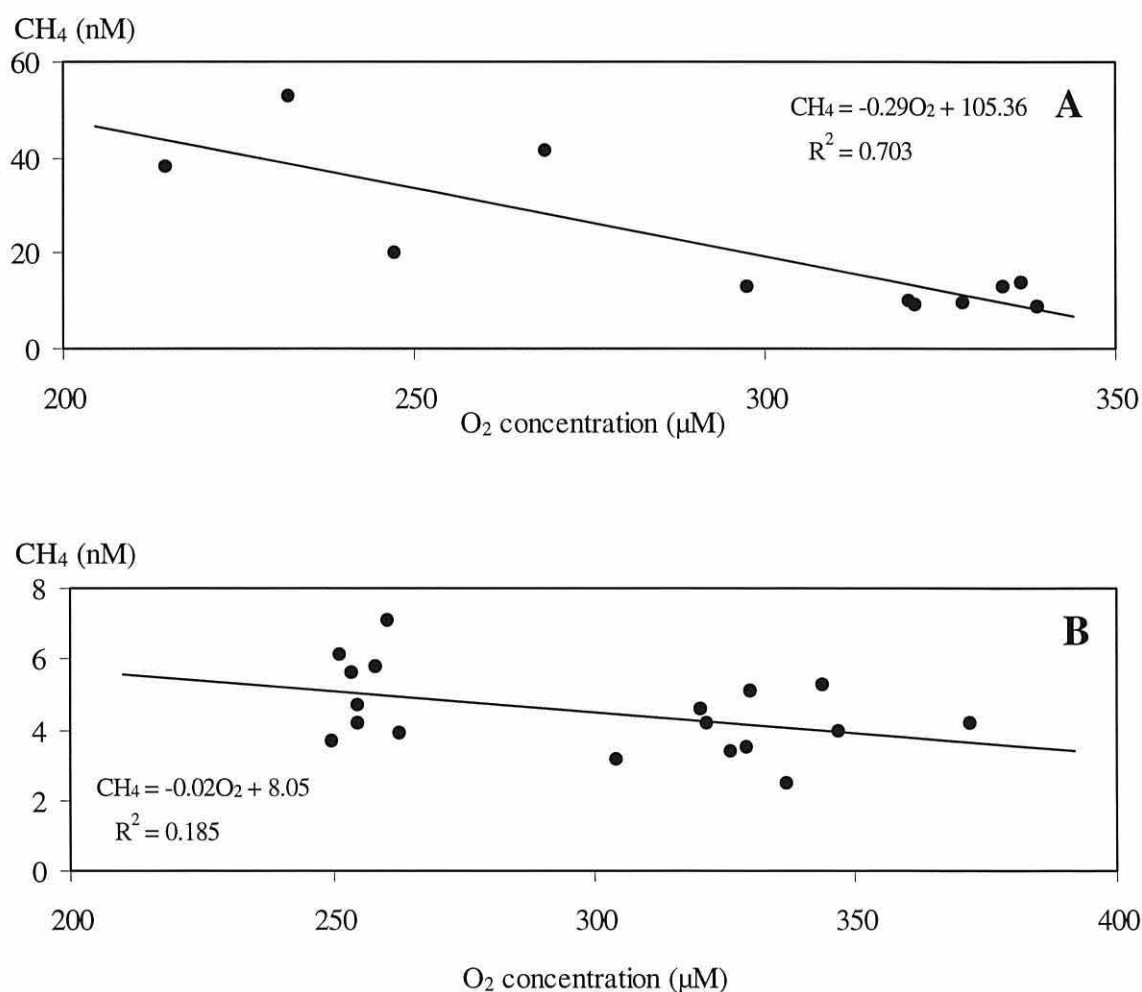


Figure 4.2.2 Scatter diagrams showing the relationship between oxygen (μM) and methane concentrations (CH_4 , nM) in the waters of the Menai Strait (A) and Point Lynas (B) in 1996.

The lack of a correlation at Point Lynas might be the result of the strong turbulence of the water column, which keeps both methane and oxygen concentrations close to saturation and could conceivably mask any causal correlation. The summer reductions in oxygen concentrations were at both sites not very dramatic and will not facilitate the development of anaerobic methanogen habitats fundamentally, as will be discussed later.

To summarise, correlations do not provide any new information about the water column as a source for methane. Sea surface temperature is the only parameter to correlate consistently with methane concentrations, while oxygen correlates with methane in the sheltered Menai Strait but not at the exposed Point Lynas site. The cause for the correlation between methane and temperature remains unknown but is suggested to be at least in part connected with the negative relationship between temperature and the oxygen concentration of the water column.

2) Occurrence of methanogens in the water column

This section considers the reported evidence for the existence of methanogens in the water column. The existence of methanogens has been investigated indirectly by measuring methane production under various artificial conditions, and directly using genetic and microbiological evidence.

The majority of the indirect evidence is based on the effect of anaerobic or substrate-enriched incubations of concentrated samples on the methane concentration. As the incubation conditions vary significantly from the *in situ* conditions in the water column and often require incubation times in excess of five weeks, the results only prove the existence of viable methanogens in the samples, but not their activity at *in situ* conditions. Oremland (1979) found methane to be produced in anaerobic incubations of mixed >164 µm plankton from San Francisco Bay and of the intestines of two different fish species. Bianchi *et al.* (1992) and Marty (1993) detected methane production in anaerobically incubated copepods, their fresh faecal pellets, and in large settling particles. These three studies strongly suggest the existence of viable methanogens in fish, in copepods and their faecal pellets, as well as in large settling particles. Whether such methanogens are active in these environments within the oxygenated water column cannot be decided from this type of study.

Sieburth (1987) found methane to be produced in aerobic cultures of Chesapeake Bay waters enriched with methylamines. Conducting incubation experiments with filtered and unfiltered samples of this culture, he discovered that these methane producers were not free-living but lived in association with particles. Using a model he then calculated that the methane producing particles must be suspended material with a diameter of 40 to 45 µm. The study thus found

methane to be produced in an aerobic but substrate-enriched environment and in association with relatively small particles. Sieburth (1987) observed that enrichment cultures lost their methanogenic activity six months after turning anaerobic, while sub-samples that were kept aerobic continued to produce methane. As substrates were provided in the cultures, this observation suggests that methanogens require their aerobic bacterial consortia to provide them with something additional to their major substrates.

Direct evidence for the existence of methanogens was brought by Cynar and Yayanos (1991) who found, enriched and characterised a strictly anaerobic, non-spore forming, methylamine and methanol utilising methanogenic bacterium from live plankton samples from the upper layer of oxygenated coastal waters. The existence of viable methanogens in the water column was confirmed by Marty (1993) who found methanogenic bacteria of high morphological diversity in anaerobically incubated, methane-producing enrichment cultures.

The recurrent presence of viable methanogens in oxygenated marine surface waters suggests at least their periodic activity in the water column. The findings support the hypothesis of association of methanogens with particles as well as zooplankton and fish. In coastal waters such as the Menai Strait, however, the existence of viable methanogens in the water column could be caused by resuspension of sedimentary particles, and was therefore not studied in this project.

3) Anoxic environments in the water column

In the last section the existence of viable methanogens in the water column was discussed. If these are the agents of methane production within oxygenated sea water they must live within anaerobic microenvironments to produce methane. Other anaerobic processes, such as sulphate-reduction, occur in oxygenated waters and also indicate the existence of anaerobic microsites (Smith and Oremland, 1987). The two most likely compartments in the pelagic zone to maintain anaerobic conditions are the centres of detrital particles and the intestinal tracts of marine animals. In the following sections, the possibility for anaerobiosis to occur in these two microsites is investigated.

Anaerobiosis within particles

For a suspended particle to contain an anoxic centre capable of harbouring anaerobic bacteria such as methanogens, all oxygen entering the particle from the surrounding seawater matrix must be completely removed during its diffusion into the centre of the particle. The removal of oxygen is achieved by the aerobic activity of the large number of bacteria that colonise particles in the surface layer of the ocean. Oxygen enters a particle by diffusion along the concentration gradient. In particles smaller than a few millimetres, molecular diffusion is the only means for the transportation of substances, because the viscosity of the water limits the size of the smallest

eddies which are responsible for turbulent diffusion to a few millimetres (Mann and Lazier, 1991). Molecular diffusion relies on the random motion of molecules as described by Fick's first law of diffusion: the mass of a substance crossing a unit area of a plane of equal concentration in unit time is proportional to the concentration gradient. The constant of proportionality is the empirically established diffusion coefficient, which has a low dependence on temperature and substrate but a high dependence on the matrix.

Under steady state conditions, *i.e.* when the rate of oxygen diffusion into the particle is balanced by the rate of oxygen consumption, the oxygen concentration in the centre of a spherical particle of radius ra (cm) is dependent on the oxygen concentration in the external seawater matrix (O_{ex} , $\mu\text{mol dm}^{-3}$), the specific oxygen diffusion coefficient (D_o , $\text{cm}^2 \text{s}^{-1}$), and the internal rate of oxygen consumption in the particle (c , $\mu\text{mol dm}^{-3} \text{s}^{-1}$). The minimum radius of a particle with an anaerobic centre can be calculated using the following equation given by Kaplan and Wofsy (1985). The derivation is given in Appendix 4.1:

$$ra = \sqrt{\frac{O_{ex} \times 6 D_o}{c}} \quad (4.1)$$

The external oxygen concentration, O_{ex} , was the only variable measured in the course of the seasonal study in the Menai Strait, and was found to vary between 215 and 339 $\mu\text{mol O}_2 \text{dm}^{-3}$ in 1996 (Appendix 3.1). Values for the internal oxygen consumption rate and the diffusion coefficient have to be estimated from the literature to calculate the minimum size of a particle with an anoxic core.

Iturriaga (1979) measured a particle-associated oxygen consumption rate (c) of 0.204 $\text{mg O}_2 \text{mg POM}^{-1} \text{d}^{-1}$ in summer and of 0.065 $\text{mg O}_2 \text{mg POM}^{-1} \text{d}^{-1}$ in winter in the top 10 m of coastal waters of the Baltic Sea. Assuming a maximum density for particles of 1 g cm^{-3} (Kaplan and Wofsy, 1985), this suggests an oxygen consumption rate within particulate matter in coastal waters of 204 $\text{g O}_2 \text{dm}^{-3} \text{POM d}^{-1}$ or 74 $\mu\text{moles O}_2 \text{dm}^{-3} \text{POM s}^{-1}$ in summer and of 65 $\text{g O}_2 \text{dm}^{-3} \text{POM d}^{-1}$ or 23.5 $\mu\text{moles O}_2 \text{dm}^{-3} \text{POM s}^{-1}$ in winter. Using these oxygen consumption values in equation 4.1, an average oxygen diffusion coefficient of $10^{-5} \text{cm}^2 \text{s}^{-1}$, and the lowest and highest external oxygen concentration encountered, the minimum diameter of a particle with an anaerobic centre is calculated to be roughly between 260 and 330 μm in summer and between 470 and 590 μm in winter (Table 4.2.2). Kaplan and Wofsy (1985) used the same source for particle-associated respiration rates and the same diffusion coefficient to calculate minimum particle sizes for productive coastal waters. They suggested the minimum diameter to be around 40 μm in fully oxygenated waters. The discrepancy in the results is caused by Kaplan and Wofsy

(1985) misquoting the original consumption rate (Iturriaga, 1979) as given per hour, while indeed it is given per day. The relationship between the oxygen consumption rate and the minimum particle size with an anoxic core is of an exponential nature (Figure 4.2.3).

Table 4.2.2 Minimum particle diameter with an anoxic centre calculated with equation 4.1 for different summer ($74 \mu\text{mol dm}^{-3} \text{ s}^{-1}$) and winter ($23.5 \mu\text{mol dm}^{-3} \text{ s}^{-1}$) rates of particle-associated oxygen consumption, and for the minimum ($215 \mu\text{M}$) and maximum ($339 \mu\text{M}$) external oxygen concentrations (O_{ex}) in the Menai Strait. The oxygen diffusion coefficient was assumed to be $10^{-5} \text{ cm}^2 \text{ s}^{-1}$.

	Min. O_{ex}	Max. O_{ex}
Winter O_2 consumption	469 μm	588 μm
Summer O_2 consumption	264 μm	332 μm

The second unknown in equation 4.1 besides the oxygen consumption rate is the oxygen diffusion coefficient through the particles. The diffusion coefficient is in principal inversely proportional to the density of the matrix (Matson and Characklis, 1976), and is furthermore influenced by the size and distribution of pores within the matrix, the complexity of the pathways and the intermolecular bonding between matrix and oxygen molecules. Within the same matrix the diffusion coefficient changes with temperature, C/N ratio and age of the matrix (Matson and Characklis, 1976). Table 4.2.3 lists oxygen diffusion coefficients for various matrices.

Table 4.2.3 Oxygen diffusion coefficients (D_O) reported for various matrices.

Matrix	D_O ($\text{cm}^2 \text{ s}^{-1}$)	Source
Water at 20°C	2.42×10^{-5}	Fair <i>et al.</i> , 1968
Water	$2.2 \times 10^{-5} (\pm 25\%)$	Matson and Characklis, 1976
Domestic waste flocs	$1.37 \times 10^{-5} (\pm 2\%)$	Matson and Characklis, 1976
Domestic-Industrial waste flocs	$1.17 \times 10^{-5} (\pm 21\%)$	Matson and Characklis, 1976
Industrial waste flocs	$8.5 \times 10^{-6} (\pm 25\%)$	Matson and Characklis, 1976
Fungal slime <i>Zooglea ramigera</i>	2.1×10^{-6}	Müller, 1966

Particles in the marine water column are of a very diverse composition (Wakeham and Lee, 1993). Consequently the diffusion coefficients through them must be variable and can only be approximated. In the literature the oxygen diffusion coefficient through marine particles has been assumed to be roughly $1 \times 10^{-5} \text{ cm}^2 \text{ s}^{-1}$ (Kaplan and Wofsy, 1985). For a particle of $40 \mu\text{m}$ to contain an anoxic core, as suggested by Sieburth (1987) for a typical methanogenic particle, the diffusion coefficient would have to be $9 \times 10^{-7} \text{ cm}^2 \text{ s}^{-1}$ during summer when internal oxygen consumption rates are high and when external Menai Strait oxygen concentrations are minimal. Such a slow diffusion rate has never been measured in a marine particle, so it seems unlikely that particles of $40 \mu\text{m}$ could maintain an anoxic centre.

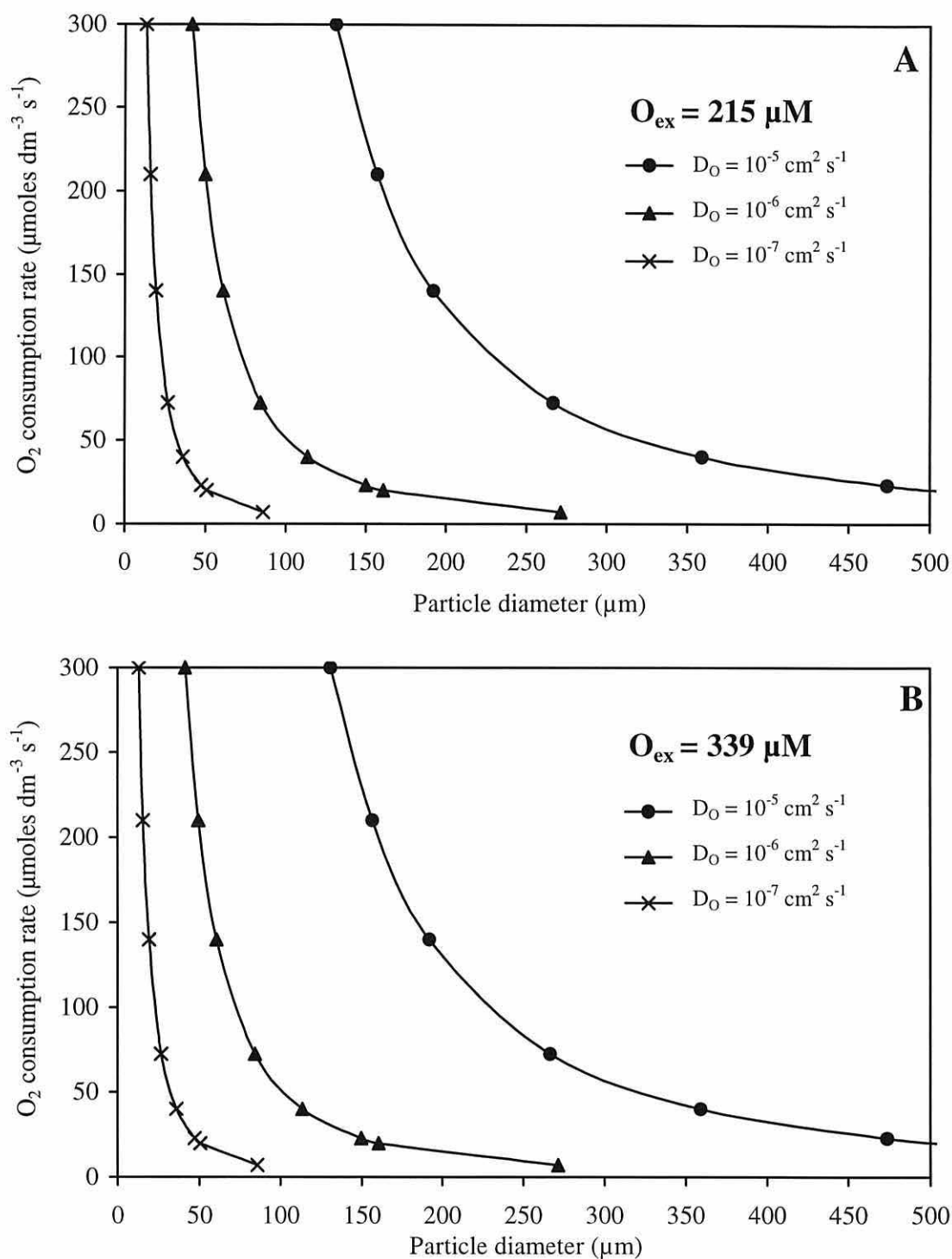


Figure 4.2.3 Effect of varying particle-associated oxygen consumption rates on the minimum diameter of a spherical particle with an anaerobic centre assuming three different diffusion rates (D_O) during minimum and maximum external Menai Strait oxygen concentrations (O_{ex}) of 215 (A) and 339 (B) $\mu\text{mol O}_2 \text{ dm}^{-3}$. Calculations were conducted using equation 4.1.

The oxygen gradient through a particle does not begin outside the particle but extends linearly through the boundary layer that surrounds the particle (Jørgensen and Revsbech, 1985). This effectively enlarges the particle in respect of its oxygen environment, so that the minimum particle size calculated with equation 4.1 is a conservative estimate and might be smaller.

In any case, in the pelagic Menai Strait environment an anaerobic microenvironment is unlikely to develop in particles with a diameter below 200 μm . Such large particles are rare in the water column. It is mainly zooplankton faecal pellets that can satisfy the size requirements for anaerobic conditions. Copepod faecal pellets of cylindrical shapes commonly range in length between 400 μm and 3 mm (Small *et al.*, 1979). Anaerobic centres could only occur in smaller particles if particle-associated oxygen consumption occurred at much greater rates and/or oxygen diffusion at slower rates than measured to-date.

There is, however, experimental evidence for the existence of anaerobic microenvironments in near-surface waters. Using microelectrodes Alldredge and Cohen (1987) found anaerobic conditions within 100 μm of the surface of a 6.2 mm long faecal pellet, which supports the minimum particle diameter estimation of 200 μm as argued above. The pellet was surrounded by a largely intact peritrophic membrane, which is thought to act as an effective oxygen diffusion barrier. In areas where the membrane was disrupted, oxygen extended further into the particle. However, Alldredge and Cohen (1987) found no evidence for anaerobic microsites within smaller faecal pellets. While these workers could not detect anaerobic microzones in marine snow, Shanks and Reeder (1993) did. Using tetrazolium salts, which on entering reduced conditions turn from a colourless solute into a coloured crystal, they found that anaerobic zones were patchily distributed throughout marine snow even in fully oxygenated waters. Often these microzones existed inside dense detrital material such as diatom frustules. Above ambient concentrations of sulphide suggested that these zones were able to sustain the anaerobic process of sulphide production. In sediments Jørgensen (1977) made similar observations of anoxic microzones of 50 to 200 μm diameter. These were scattered throughout aerobic layers and were capable of sustaining anaerobic sulphate reduction. The observations of patchily distributed anaerobic microzones paired with the findings of the diffusion barrier posed by the peritrophic membrane, suggest that the diffusion rate through some detrital materials must be extremely low, so that anaerobic conditions can develop, and that the situation within particles is much more complex and heterogenous than assumed in the models.

In summary, while theoretical calculations suggest that anaerobic conditions do not exist in particles with diameters below 200 μm , there is experimental evidence that patchily distributed pockets of anaerobic conditions do exist in particles below 200 μm . These sites might be the result of dense enveloping material with very low oxygen diffusion coefficients, and constitute potential loci for methanogenesis within the oxygenated water column.

Anaerobiosis within guts of pelagic animals

There are parts of the digestive systems of mammals which are known to be anoxic and to be capable of sustaining quite substantial numbers of actively metabolising anaerobic bacteria. It is thus very likely that herbivorous marine mammals such as baleen whales will have anaerobic compartments in their guts (Oremland, 1988). But the number of marine mammals in the water column is low and their distribution patchy and variable. Only little research has concentrated on determining whether anaerobic conditions occur in the digestive tracts of the more numerous and more evenly distributed fish and zooplankton populations. There is evidence that some copepod species from oxygenated environments harbour active methanogens and must thus contain anaerobic zones (DeAngelis and Lee, 1994). It has been suggested that intense microbial activity provides ample substrates for methanogenesis and depletes the oxygen content in parts of the digestive system and within the ingesta, *i.e.* the future faecal pellets (Sieburth, 1979). Some zooplankton experts, however, doubt that copepod guts could be permanently anaerobic because of the very short food passage times, or that enteric bacterial communities could become established in crustacean plankton which moult all but their mid-gut region regularly (personal communication: Drs David Jones and Andy Yule, University of Wales, Bangor).

It can be concluded that the available evidence is too limited and too contradictory to establish with some certainty whether anaerobic microzones exist in particles of common dimensions and animals with wide distribution.

4) Accumulation of methane within the water column

As there is evidence for the occurrence of methane-producing bacteria in certain microenvironments in the water, it was appropriate to attempt a study into whether these bacteria were actively generating methane under the natural oxygen and substrate conditions. To this end the incubations of normal surface waters were undertaken at different times of the season. The results of these experiments, however, showed no evidence for net methane production. It is very likely that even if there was net methane production, this would occur at production rates far too low to be detected with the adopted method. Oceanic methane production rates have been estimated to be in the region of $20 \text{ pmol dm}^{-3} \text{ d}^{-1}$ (Scranton and Brewer, 1977; Tilbrook and Karl, 1995), which would require a precision of about 0.05 % to be detectable. Even if coastal net production rates were much higher than those calculated for oceanic waters, it is unlikely that the method applied, with its precision of 2.6 %, would have been able to detect the difference. To increase the signal, the fractions above $53\mu\text{m}$ were concentrated before being incubated. The results from such a treatment, however, cannot be seen as representing natural conditions as they show a slightly altered community structure and too high a density. Even in these incubations, a definite increase in net methane concentration during the incubation period could only be detected on one occasion (Figure 3.3.1 D). This was during a bloom of the exclusively

heterotrophic dinoflagellate *Noctiluca scintillans* MaCartney 1810 (syn. *miliaris* Suriray 1836) where methane was produced at a rate of approximately $30 \text{ fmoles cell}^{-1} \text{ d}^{-1}$. This is the first time a dinoflagellate has been connected to methane production. As it was not a pure culture of *Noctiluca*, it cannot be proven that these dinoflagellates were the agents of methane production, but they were the overwhelmingly dominant organisms and particles in the samples. To calculate the contribution from this type of methane production to water column concentrations requires the natural abundance of *Noctiluca* in the environment. A long-term study on *Noctiluca* in the German Bight found its abundance to follow a general seasonal pattern with a maximum abundance of up to $1000 \text{ cells dm}^{-3}$ in June/July (Uhlir and Sahling, 1990). In the Menai Strait *Noctiluca* had a maximum population density of $1500 \text{ cell dm}^{-3}$ in the early 1960s (Jones and Spencer, 1970). Assuming that *Noctiluca* does produce methane, a maximum abundance of $1500 \text{ cells dm}^{-3}$ could produce $45 \text{ pmol CH}_4 \text{ dm}^{-3} \text{ d}^{-1}$. Although such production rates might contribute markedly to methane concentrations in calmer waters, they should be quantitatively insignificant in dynamic sites such as the Menai Strait, where daily variations in methane have been seen to be two to three orders of magnitude higher than the calculated production rates. In open ocean environments, however, *Noctiluca* - although generally less densely distributed - might contribute significantly to the required *in situ* methane production rate.

The process by which *Noctiluca* might produce methane remains unknown and subject to speculation. Using scanning electron microscopy, Lucas (1982) detected healthy looking intracellular bacteria in the cell cytoplasm of *Noctiluca scintillans* collected from the Menai Strait. These rod-shaped bacteria appeared to have their own cell membrane and showed no association with any internal organelles of the host cell. Intracellular bacteria are quite widespread in dinoflagellates and have been reported in a number of algal species from other classes (Gold and Pollinger, 1971) and in several protists (Van Bruggen *et al.*, 1983; Fenchel and Finlay, 1991). The role of these intracellular bacteria remains unknown, but it is proposed that the *Noctiluca* endosymbionts might be methanogens and were thus responsible for the methane production detected during the incubation of *Noctiluca*-rich waters. The conditions inside cells are strongly reducing and might well offer a suitable habitat for methanogens.

Several researchers in the past have suggested a minor involvement of other types of algae in methane production. Scranton and Brewer (1977) reported some preliminary results suggesting methane production at very low rates of around $2.4 \times 10^{-3} \text{ fmol cell}^{-1} \text{ d}^{-1}$ by the coccolithophore *Coccolithus huxleyi*. DeAngelis and Lee (1994) report trace methane formation by *Rhodomonas lens* and *Prorocentrum minimum*. It appears though that not all phytoplankton species are equally capable of the trace production of methane as *Thalassiosira weissflogii* tested negative (DeAngelis and Lee, 1994). As none of these experiments were conducted with axenic cultures, the possibility remains that not the algal organism but a contaminant produced the measured

methane. The process by which any of these algae could produce methane remains unknown. As there is genetic evidence suggesting that methanogens were the host partner in the endosymbiotic development of the eukaryotic cell (Martin and Müller, 1998), it is tangible that some eukaryotic organisms (*e.g.* some phytoplankton species) maintained the genetic information to produce methane. It has been suggested that phytoplankton cells contain rather large amounts of methane, which - similar to DMSP (Dacey and Wakeham, 1986) - is mainly released during zooplankton grazing. This is, however, unlikely, as the effect of grazers on methane concentrations has been seen to be highly dependent on the species of zooplankton (DeAngelis and Lee, 1994).

In conclusion, pelagic methanogenesis could not be detected with the available methodology, and did not contribute significantly to the methane concentrations measured in the Menai Strait. To investigate low net production rates of methane with the existing methodology one would have to conduct incubation experiments with much larger volumes of water, and concentrate the purged methane on a cryotrap. Even small differences in methane concentrations might then become detectable, as precision was seen to be positively related to methane concentration, and at 100 μ -atmospheres in the GC injection loop a precision of 0.06 % was achieved (Appendix 2-6).

Lately evidence has emerged suggesting that methane could be produced photochemically in the water column. Tilbrook and Karl (1995) observed a methane production rate of between 0.3 and 0.6 nM d^{-1} in a salt solution exposed to direct sunlight, while dark or low light incubations resulted only in random variations of methane concentrations. While photochemical production could produce an increase in concentrations in the summer when light intensity is increased and light availability prolonged, the production rates are too low to account for the high variability in methane concentrations. Photochemical methane production in the water column - if confirmed by further research - will therefore not contribute significantly to methane concentrations in the Menai Strait, but might be relevant for oceanic areas.

Instead of direct measurements of methane production *via* incubation experiments, some researchers have studied the accumulation of methane in sinking particles collected in sediment traps. The settling particles, harbouring viable methanogens (Bianchi *et al.*, 1992; Marty, 1993), were collected in hypersaline and poisoned solutions which were analysed for their methane content upon trap recovery. The results confirmed that methane is a common constituent of sinking particles. Using trap study results, Tilbrook and Karl (1995) estimated a methane input from sinking particles to the water column of the oligotrophic North Pacific gyre of at least 4 to 8 $\text{pmol dm}^{-3} \text{d}^{-1}$, *i.e.* about 15-30% of the total of $\sim 23 \text{ pmol dm}^{-3} \text{d}^{-1}$ required to sustain the surface supersaturation. The spatial variability of particle-associated methane concentrations was discovered to be large. While coastal and oceanic stations in the North Pacific showed ample particle-associated methane, areas such as Antarctica - where waters were found not to be

supersaturated with methane (Williams and Bainbridge, 1973) - were dominated by particles which were not enriched in methane (Karl and Tilbrook, 1994). Particle-associated methane concentrations were larger in surface waters and decreased with increasing water depth to zero at about 500 m (Karl and Tilbrook, 1994), supporting the theory that the in-water methane source lies in the euphotic zone. Despite the greater particle flux in inshore waters, coastal particles were generally less methane-rich than oceanic particles, which Karl and Tilbrook (1994) attributed to differences in faecal pellet composition in part due to the different food supply. This observation suggests that production of methane in the water column is a less important source in coastal waters than in the open ocean.

To summarise, the coastal water column is seen to be at best a very minor source for water column methane concentrations. While viable methanogens are known to exist in the water column, net methane production is very limited and may only be of quantitative importance in oceanic waters. In the coastal waters of the Menai Strait water column methane production does not contribute significantly to the measured methane concentrations.

4.2.2.2 Methane from sedimentary sources

In the previous sections the methane source strengths of external inputs and of internal water column production were discussed and seen to contribute only to a minor extent to the methane concentrations measured in the Menai Strait. Neither external nor pelagic sources could account for the seasonal increase in the concentrations in summer. In this section the source strength of Menai Strait sediments will be calculated and discussed. Initially the possibility of methane seeps within the Menai Strait will be considered. Then the diffusive flux rates from Menai Strait sediments will be calculated from vertical methane profiles, and the sediment contribution to methane concentrations in the Menai Strait water column will be discussed. Thereafter the horizontal variability will be considered before dealing with the seasonality of the sediment contributions of methane to the water column.

Methane seepage within the Menai Strait

As large gaseous reservoirs exist and are commercially exploited within Liverpool Bay, the possibility of seeps as origins to the observed methane distribution must be considered. The transect measurements through north-eastern and central parts of the Menai Strait (Figure 3.2.5) and also the drift study (Figure 3.2.7) found methane concentrations to increase generally rather steadily as the water moved south-westwards through the Strait. If the majority of methane, however, originated from defined seepage areas, the concentrations would be expected to increase more suddenly and perhaps to decrease again further downstream after mixing with less methane-rich waters. It thus seems unlikely that seeps contribute markedly to the methane pool in the Menai Strait. This conclusion is further supported by the observation of a seasonal increase

in methane concentrations in the summer months, while seepage rates appear to be rather constant over time (Dando *et al.*, 1994; Schuster, 1994). The spatial distribution and the existence of a seasonal pattern of methane therefore suggest that the measured methane is primarily of recent biological origin.

Methane in sediments

The profile of water column methane concentrations during slack water on 13 June 1996 above the muddy sediment at St. George's Pier showed an increase of about 7 nM (25%) from the surface to the bottom (Figure 3.2.6), which was the first indication of a significant input of methane from the sediment. No such increase, however, was observed at three stations in the central Menai Strait (Figure 3.2.6). These stations were above rocky substrates, which are unlikely to produce or release methane.

Methane concentrations in muddy sediments were found to range from 20 nM to 440 μ M (Appendix 3.5.1) which corresponds to saturation ratios of approximately 7 to 157,000. These concentrations are not particularly high for coastal sediments when compared to concentrations reported for other coastal sites. In Kiel Harbour, for example, concentrations were about two orders of magnitude higher, commonly reaching between 2 and 6 mM (Schmaljohann, 1996), while in Long Island sediment concentrations reached maximum values of around 1 mM (Martens and Berner, 1974). The mean sediment concentration of methane at depths below 20 cm in the mudflats in Menai Bridge was about 37 μ M. Muddy sediments were thus generally about three orders of magnitude richer in methane than the overlying waters, which suggests that they are a source of methane to the water column.

Vertical distribution of methane in sediments

The results show that methane is not homogeneously distributed throughout the sediment. There is a significant increase in methane with sediment depth to a zone of maximum concentrations (*e.g.* Figures 3.5.1.1, 3.5.1.2 and 3.5.1.3). This depth distribution could be a consequence of a diffusive flux of methane from a deep methane-producing sediment layer towards a less methane-rich water column. It could, however, also be a combined result of diffusion and production, of diffusion and consumption, or of diffusion, production and consumption.

The shape of the depth profile contains information about the occurrence of methane production and consumption at sediment depths above the main methane production layer. Figure 4.2.4 shows idealised depth profiles of methane for situations when molecular diffusion is the only distribution process, and when diffusion is accompanied by production or consumption of methane. If diffusion is the only process controlling the methane distribution in the upper

sediment, methane concentrations can be expected to decrease linearly from the source towards the sediment/water interface. Methane consumption in sediment layers above the production zone oxidises some of the rising methane, whereby a concave-upward distribution is created. Where methane production occurs, extra methane is added to the diffusive methane flux resulting in a convex-upward distribution curve. The depth distribution when methane production and consumption occur simultaneously depends on which of the two processes is dominant.

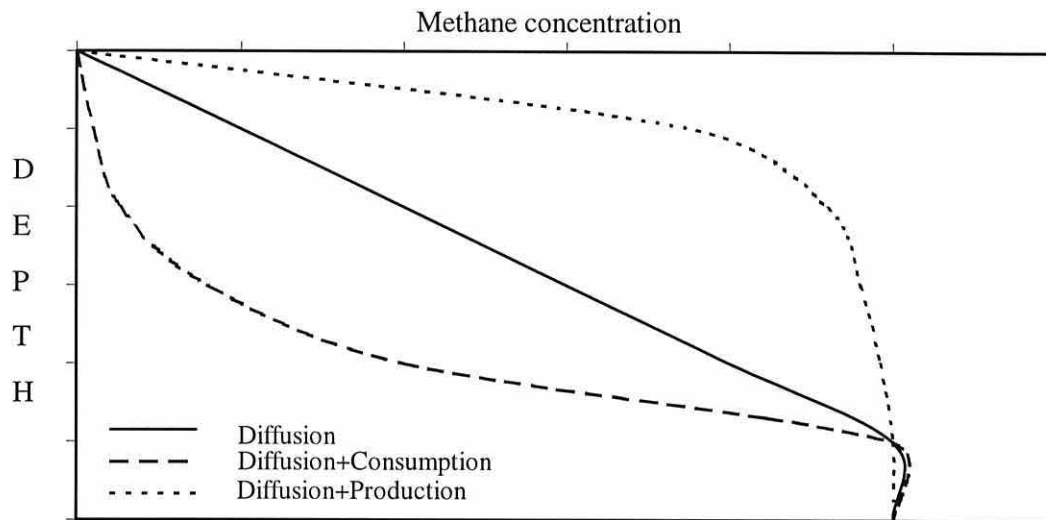


Figure 4.2.4 Idealised methane profiles in sediments assuming various combinations of diffusion, production and consumption of methane from the main deep production layer upward (After Bernard, 1979).

The methane profiles from Menai Bridge muds, as for example in the triplicate cores shown in Figure 3.5.2.3, are very difficult to interpret. While two of the three profiles appear convex in shape, which suggests some net production, the third core is slightly concave, indicating net consumption. If one wanted to use the profiles to calculate methane production and consumption rates in the upper sediment layer, as has been done (*e.g.* Barnes and Goldberg, 1976; Reeburgh, 1976; Martens and Berner, 1977; Martens, 1982), more intermediate depths would have to be analysed to get a more certain picture of the depth distribution. It appears, though, from the available sediment data, that the methane depth distribution in the mudflats is diverse, and that in the layer above the main production zone methane is both produced and consumed at rates varying from site to site and with time (Figures 3.5.1.1 A, 3.5.1.2 A, 3.5.1.3 A and 3.5.2.3).

Diffusion of methane from the major methane production layer upward, however, is a dominant process in controlling the depth distribution of methane. The contribution of the sediment to water column methane concentrations can be estimated from the depth distribution when molecular diffusion can be assumed to be the main distribution parameter.

Flux calculations

If the sediment is in a steady state without any turbulence, bioturbation or convection, the flux of methane will be driven purely by diffusion along the concentration gradient. The diffusive flux can be calculated using Fick's first law of diffusion as applied to the pore spaces in the sediments (Ullman and Aller, 1982):

$$J_M = -nD_{Msed} \frac{\partial C_{int}}{\partial z} \quad (4.2)$$

where J_M = Diffusive flux of methane across the sediment-water interface ($\mu\text{mol cm}^{-2} \text{s}^{-1}$)
 n = Porosity (mean porosity for all depths from max. CH_4 concentration upward)
 D_{Msed} = Sediment diffusion coefficient for methane ($\text{cm}^2 \text{s}^{-1}$)
 $\partial C_{int}/\partial z$ = Methane concentration gradient between the interstitial waters in the layer of methane production and those at the sediment surface ($\mu\text{mol cm}^{-3} \text{cm}^{-1}$)

To estimate the actual flux of methane across the sediment-water interface the concentration gradient between the top sediment layer and the overlying water would have to be used in equation 4.2. To provide a conservative estimate of the maximum potential for vertical diffusion of methane from the sediments, however, the flux was calculated from the concentration gradient within the sediment.

In equation 4.2 the sediment diffusion coefficient, D_{Msed} , is the only unknown. It can be estimated from the methane diffusion coefficient in sea water and the square of the geometric sediment tortuosity (Ullman and Aller, 1982):

$$D_{Msed} = \frac{D_{Msea}}{\theta^2} \quad (4.3)$$

where D_{Msea} = diffusion coefficient for methane in sea water ($\text{cm}^2 \text{s}^{-1}$)
 θ = sediment tortuosity (dimensionless)

Sediment tortuosity (θ) is the mean length of the path through the porous space between two points relative to a straight line between the same two points. As it is difficult to measure tortuosity, the linear relationship between tortuosity squared and porosity can be used to estimate θ^2 based on an empirical equation (Iversen and Jørgensen, 1993):

$$\theta^2 = 1 + f(1 - n) \quad (4.4)$$

where $f = 3$ for clay-silt sediments (*e.g.* mud) and 2 for sandy sediments.

The methane diffusion coefficient is temperature- and salinity-dependent. To account for the temperature effect in pure water, the diffusion coefficient for methane is estimated using an Arrhenius equation (Jähne *et al.*, 1987):

$$D_{Mwater} = A e^{-\frac{Ea}{RT}} \quad (4.5)$$

where D_{Mwater} = Diffusion coefficient for methane in distilled water ($\text{cm}^2 \text{s}^{-1}$)

A = Arrhenius constant ($3047 \times 10^{-5} \text{ cm}^2 \text{s}^{-1}$)

Ea = Activation energy for diffusion of methane in water ($18.36 \text{ kJ mol}^{-1}$)

R = Gas constant ($0.0083 \text{ kJ K}^{-1} \text{ mol}^{-1}$)

T = Water temperature (K)

In sea water diffusion coefficients are slightly lower than in pure water. This reduction in the coefficient is temperature-dependent and larger at lower temperatures (Jähne *et al.*, 1987). For temperatures between 5 and 35°C the diffusion coefficient for methane in sea water is estimated with the following equation:

$$D_{Msea} = D_{Mwater} \times \left(\frac{(100 + (0.1t - 8.5))}{100} \right) \quad (4.6)$$

where t = Sediment temperature (in °C).

Table 4.2.4 Mean sediment porosity (n), sediment diffusion coefficient for methane (D_{Msed} , $10^{-6} \text{ cm}^2 \text{s}^{-1}$), methane concentration gradient between production and surface layer ($\delta C_{int}/\delta z$, $\text{nmol cm}^{-3} \text{ cm}^{-1}$), and diffusive flux of methane out of the sediments (J_M , $\mu\text{mol m}^{-2} \text{d}^{-1}$) at various dates from the three stations in the Menai Bridge mudflats.

Sample site and date	n	D_{Msed}	$\delta C_{int}/\delta z$	J_M
Station A	07.08.1997	0.42	5.40	0.13
	05.09.1997	0.42	5.19	0.05
	19.09.1997	0.40	4.83	0.36
	03.11.1997	0.40	4.38	0.10
	04.02.1998	0.39	3.93	0.09
Station B	01.07.1997	0.48	5.39	0.09
	24.07.1997	0.44	5.54	0.07
	07.08.1997	0.46	5.59	0.01
	21.08.1997	0.46	5.64	0.05
	05.09.1997	0.46	5.37	0.12
	19.09.1997	0.48	5.32	0.09
	06.10.1997	0.45	5.15	0.04
	03.11.1997	0.47	4.75	0.06
	04.02.1998	0.46	4.24	0.44
Station C	07.08.1997	0.39	5.39	8.80
	21.08.1997	0.45	5.60	14.72
	05.09.1997	0.48	5.48	35.72
	19.09.1997	0.43	5.09	0.04
	06.10.1997	0.36	4.70	0.64
	03.11.1997	0.47	4.72	18.05
	04.02.1998	0.39	3.90	2.30

The diffusive flux rates of methane from the three sediment stations calculated with equation 4.2 are given in Table 4.2.4. The averaged flux rate for the five dates when measurements were available from all three stations is $9.2 (\pm 22.0 \text{ SD}) \mu\text{mol m}^{-2} \text{ d}^{-1}$, while the individual fluxes from all dates ranged from 0.01 to $81.1 \mu\text{mol m}^{-2} \text{ d}^{-1}$ (Table 4.2.4).

Such flux rates are low compared to subtidal sediments at other coastal sites but are much higher than from sediments in the abyssal plain (Table 4.2.5). As the flux rates are linearly related to the concentration gradient (Equation 4.2), the differences in flux rates are a consequence of greater concentrations and/or lower depths of maximum concentrations.

Table 4.2.5 Mean methane diffusive flux rates and ranges ($\mu\text{mol m}^{-2} \text{ d}^{-1}$) out of the sediments at different locations in the sea.

Mean Flux	Range	Location	Source
1,240	370 – 17,800	Kiel Harbour – subtidal	Schmaljohann, 1996
700	490 – 920	Cape Lookout Bight – subtidal	Boehme <i>et al.</i> , 1996
2,300		Cape Lookout Bight – subtidal	Martens and Klump, 1980
0.016	0.006 – 0.033	Gulf of Mexico – abyssal	Bernard, 1979
13.1	0.01 – 81.1	Menai Strait – intertidal	This study

The relatively low methane concentrations in the intertidal sediments in this study could be a consequence of regular aerial exposure of the majority of muddy sediments during low tide. Evidence for a reduction in methane due to exposure to air is gained from comparisons of sediment cores from different shore heights. Methane concentrations at all depths were lowest in high shore sediments which were exposed to air the longest (Figure 3.5.2.2 A). Kelley *et al.* (1995) made similar observations when they found that constantly submerged White Oak River sediments were significantly richer in methane than neighbouring but tidally exposed riverbank sediments. The cause for a decrease in methane concentrations due to contact with air is thought to be that exposed sediments can become undersaturated with water. Sediments that are partially undersaturated with water will generally experience deeper oxygen penetration, which destroys anaerobic conditions for methanogens and creates favourable conditions for aerobic methanotrophs. Thereby exposure to air would reduce methane concentrations in the sediments both by inhibiting methane production and by increasing consumption rates. As the diffusion coefficient for methane through air spaces in the sediments is several-fold greater than through water-filled spaces, it is likely that the methane flux rates in water-undersaturated sediments might also be enhanced. Faster flux rates reduce the methane concentrations remaining in the sediment. The hypothesis that methane concentrations in undersaturated sediments are lower than they would be in saturated soils is supported by a study in a Danish coastal meadow and fen (Priemé, 1994). In this study the reduced concentrations in unsaturated soils were attributed primarily to increased oxidation rates.

Low methane concentrations in sediments might in places be caused by the burrowing macrofauna that has been frequently encountered during the slicing of sediment cores. Borrowing animals can reduce net methane production because they irrigate the reducing sediments and thereby transport oxygen and sulphate deep into the sediments. In the vicinity of their borrows methane oxidation and sulphate reduction rates are therefore likely to increase while methane production might well be reduced (Martens, 1982).

The methane concentrations in the muddy Menai Strait sediments might thus be lower than in subtidal sediments at other locations because of the effect of periodic aerial exposure and due to high incidences of bioturbation. But the low methane concentrations in Menai Strait sediments render the sedimentary source too small to account for the measured water column concentrations, as will be demonstrated in section 4.5 on the methane budget of the Menai Strait water column. Therefore the possibility will be explored that the calculated flux rates could underestimate the source strength of the sediment.

The main assumption for the flux calculations is that molecular diffusion is the only transport mechanism for methane out of the sediment. This may be a reasonable assumption for periods of slack water above submerged sediments. During periods when water levels are rising or falling and when the tide is moving over the sediments, however, advective transport is likely to increase the methane flux rate. The flux would also be higher than calculated with a diffusion model if ebullition carried methane out of the sediment (Klump and Martens, 1981; Reeburgh, 1982; Devol *et al.*, 1988; Schütz *et al.*, 1991). Ebullition can be a quantitatively important process that may carry 7.5 times more methane out of sediments than diffusive fluxes (Boehme *et al.*, 1996). As bubbles were indeed observed to occasionally emerge from sediments in the Menai Bridge mudflats, the causes and effects of ebullition must be considered in greater detail. Ebullition occurs where methane exceeds the saturation threshold of the sediment and can for example be triggered when falling tides lead to the reduction in hydrostatic pressure and thereby cause gases to expand and bubbles to be formed and released (Chanton *et al.*, 1989; Kelley *et al.*, 1995). Most of the gas will pass through the water column into the atmosphere and only a small proportion of the methane will dissolve from the bubble into the water column. Ebullition is a much faster process than molecular diffusion and will thus remove much methane from the sediment, leaving reduced methane concentrations behind. As a consequence of these reduced concentrations, the diffusive flux that is interpreted as the total methane input from the sediment into the water column will also be reduced. When no ebullition occurs, the bubble methane will go back into solution so that the methane concentrations in the sediment increase. Increased concentrations will result in higher diffusive flux rates being calculated.

In conclusion, the observation of gas bubbles emerging from Menai Strait sediments suggests that some of the produced methane does not diffuse by molecular motion from the sediment into the water column but evades at a much faster rate by ebullition. This will reduce the remaining methane concentration so that the diffusive flux calculated from the concentration gradient is also lower. As no information is available neither about the quantitative importance of ebullition in the Menai Strait mudflats nor about the proportion of bubble methane that diffuses into the water column, it is not possible to determine the quantitative effect of methane ebullition from the sediments into the water column.

Horizontal distribution of methane in sediments

There was a significant difference in the methane concentrations and depth distributions between sandy and muddy sediments (Figure 3.5.2.1 A). Methane concentrations in sand are low so that sand is not considered to be an important source of methane for the water column. The major cause for the low methane concentrations in sand is thought to be a shortage of substrate supply. The substrate supply rates to sandy sediments are generally lower than to mudflats because the more turbulent conditions characteristic for sandy areas prevent smaller detritus particles from sedimentation. Sandy sediments can therefore be expected to be less organically rich than muds, so that less substrate is available to methanogens. Also, as the anaerobic layer begins at greater depths in sand than in mud, most substrate materials are thought to be consumed by the aerobic bacterial community, so that very little of the supplied substrates reach the methanogenic zone. The little methane that is produced deep in sandy sediments must then travel a long distance through aerobic layers, in which it might be consumed by aerobic methanotrophs. The lower initial substrate supply, the greater depth of the anaerobic layer, and the larger aerobic layer are thus likely to be responsible for sand being a very much smaller contributor to water column methane than mud. The positive relationship between methane concentrations and porosity when comparing muddy and sandy sediments is thus thought to be a function of both the depth of the anaerobic sediment layer and substrate availability.

The horizontal variability within the mudflats was also extremely high. Station C was nearly two orders of magnitude richer in methane than stations A and B. As different muddy sediments vary so significantly in their methane contents, it is not possible to judge whether the three sampling stations are representative in their concentrations or whether other areas will display much higher or lower concentrations. Porosity cannot account for the differences in methane concentrations at stations A (mean porosity = 0.41, mean concentration = 2.1 μM), B (mean porosity = 0.46, mean concentration = 1.5 μM), and C (mean porosity = 0.42, mean concentration = 106 μM). Although depth profiles of both sandy and muddy sediments suggest a negative relationship between porosity and methane, this was not found to be significant (Figure 4.2.6).

Table 4.2.6 Pearson's correlation coefficient (r), number of paired observations (N), and significance at the 5% level of the relationship between sediment methane concentrations and porosity.

STATION	r	N	5% significant?
A	-0.059	32	No
B	-0.160	56	No
C	0.278	46	No
ALL	0.085	134	No

There was also a significant, but lesser, variability in three neighbouring cores collected from sediments at station B within a distance of less than 1 m (Figure 3.5.2.3). The 15 cm depth-integrated methane content in these triplicate cores varied by more than 100% from 1.2 to 2.6 $\mu\text{mol cm}^{-2}$ and methane concentrations at individual depths varied up to 3.3 fold. Such a high variability in replicate cores could account for much of the variability in flux rates calculated for each site on different dates. A high degree of spatial variability in sediments is common for many biological and chemical parameters, and often causes difficulties in detecting significant trends without exhaustive numbers of replicates. Bange *et al.* (1998) found a significant spatial variability in methane production rates, which they attributed to the differences both in the quantity and quality of organic matter supply. Heyer *et al.* (1990) found a strong dependence of methanogenic rates on the availability of organic matter and argued that the nature of the organic material may be more important for methanogenesis than its quantity. It therefore appears possible that the substrate quantity and quality at station C vary greatly from those at stations A and B. Small scale differences might be caused by a patchy distribution of available substrates within sediments.

Seasonal distribution of methane in sediments

Besides the quantification of the sediment source strength, the major interest in the sediment study is to investigate whether the contribution of methane from the sediment to the water column varies seasonally. In order to investigate whether there is a seasonal pattern in the diffusive flux rates of methane out of the sediments, the percentage flux rates relative to the mean sampling station rates were plotted in Figure 4.2.5.

Maximum methane flux rates had been expected to occur in late summer when the methane concentrations in the water column were at their peak, but the three sampling stations displayed very different patterns in their flux rates over time so that no general seasonal pattern could be detected. The results from similar studies in the literature are conflicting, as seasonal patterns were observed in some investigations (Schmaljohann, 1996) but not in others (Svensson and Rosswall, 1984; Chanton *et al.*, 1989). The results from the seasonal sediment study thus do not suggest an increased methane flux from the sediment into the water column during summer.

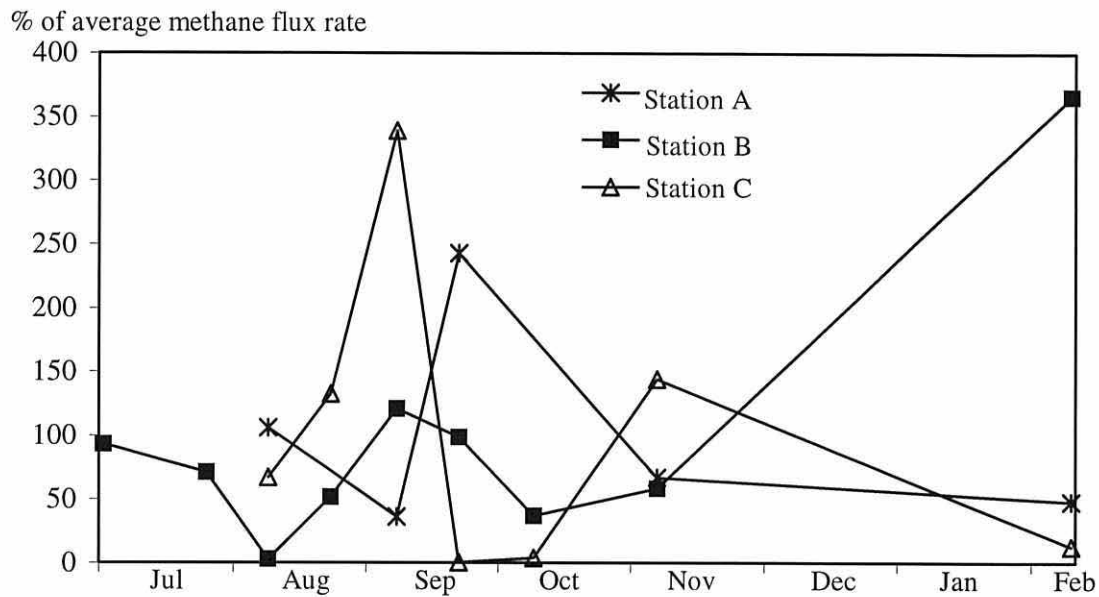


Figure 4.2.5 Seasonal patterns in methane flux rates from muddy sediments at Menai Bridge shown by plotting fluxes as percentages of the mean rate for each station.

In the next few paragraphs the possibility that a seasonal pattern might exist but not be discovered in this study will be explored. Ebullition has been discussed as a major term of uncertainty concerning the rates of methane emission from the sediment into the water column, and might also affect the detection of seasonal patterns as it is primarily a summer phenomenon (Martens *et al.*, 1986). Ebullition is most likely to occur when it is warm because the solubility of gases decreases with increasing temperature. Chanton *et al.* (1989) found that the methane content in the sediments was approximately constant over the year, but that it was predominantly in its gas phase (bubble) during the summer and in its dissolved phase during the winter. Thus, while the total concentrations remained constant, the summer fluxes could be expected to be significantly higher than the winter fluxes as they proceeded largely by the faster process of ebullition. As ebullition occurs at the study sites, it is likely that the flux rates in summer are higher than calculated with the diffusion model. If the flux rates were higher, then the methane productivity of the sediments would also have to be greater in summer than winter. But as it remains unknown how much of the methane that bubbles out of the sediment dissolves into the water column, it is not possible to demonstrate whether the increased sediment production of methane in the summer enhances the concentrations in the water.

It is also possible that there is an increase in the diffusive flux rates in summer that is not detected due to the high degree of horizontal variability in the sediment. This could only be overcome by greatly increasing the number of sediment cores that are collected.

The seasonality of methane in sediments was further investigated by studying the effect of temperature. While methane concentrations correlated positively with temperature in the water

column (Tables 4.2.1 and Figure 4.2.1), this was generally not the case for sediments (Table 4.2.7). A significant - and negative - correlation was only observed at station B as the highest concentration and flux rate were measured on the coldest sampling day. In freshwater sediments, methanogenesis is commonly temperature-limited in winter and substrate-limited in summer (Sorrell and Boon, 1992). A genuine lack of correlation between methane and temperature in the Menai Bridge mudflats could thus be a consequence of a relatively constant substrate supply throughout the year with temperatures that are not limiting to methanogen activity. As methane remained supersaturated in sediments throughout the winter, it seems that the lower temperature limit of methanogens or their substrate-producers was not reached in the study area.

Table 4.2.7 Pearson's correlation coefficient (r), number of paired observations (N), and significance at the 5% level of the relationship between sediment methane concentrations and temperatures.

STATION	r	N	5% significant?
A	0.082	32	No
B	-0.536	56	Yes
C	0.060	46	No
ALL	0.041	134	No

Further, the laboratory experiment that investigated the effect of temperature on sediment methane concentrations did not provide any evidence for increased sediment methane concentrations with temperature and thus for enhanced diffusive fluxes into the water column with higher temperatures (Section 3.6). At all three temperatures methane concentrations decreased significantly over the 64-day incubation period (Figure 3.6.1). At 5°C the methane content began to diminish after the 37th day, at 15°C the reduction was first noted after the first incubation day, and at 25°C concentrations seem to have decreased before the beginning of the experiment, during the seven days of temperature acclimatisation (Table 4.2.8).

Table 4.2.8 Calculated 20 cm depth-integrated methane content (mmol m^{-2}) in cores incubated at different temperatures and for different lengths of time.

DAY	5°C	15°C	25°C
1	28.5	37.7	22.6
20	24.9	14.2	5.3
37	26.5	21.2	7.7
65	12.2	18.0	0.7

This result stands in stark contrast to a ten-day anaerobic slurry incubation experiment of estuarine sediments at 4 and 25°C in which a strong positive dependence of net methane production rates on temperature was noted (Bange *et al.*, 1998).

The results of the sediment incubation experiment suggest that the methane production layer might occur at a depth below 20 cm - although the depth profiles suggest otherwise (Figure 3.6.1) - and might thus not have been included in the sediment cores. In that case the experiment has studied the effect of temperature on the rates either of methane consumption in the sediment or of its evasion from the sediment cores.

Also the diffusive loss of methane from the sediment core into the atmosphere is temperature-dependent and will thus have contributed to the results. At higher temperatures the vertical diffusion coefficient is increased, so that methane will be emitted faster to the atmosphere than at lower temperatures. This may in part explain the reduction in pore water methane concentrations with time at higher incubation temperatures.

In summary, the sediment study provides strong evidence that muddy sediments are a much more significant source of water column methane than either internal water column production or inputs of methane from external sources. The results, however, do not show sedimentary methane fluxes to cause a seasonal increase in methane concentrations in the water column in summer. The observation of gas bubbles evading from mudflats in the Menai Strait suggest that ebullition of methane might be an important transport mechanism for methane out of the sediment that has not been included in this study. It is possible that ebullition enhances the source strength of the sediments beyond the estimates gained with the diffusion model. As ebullition is primarily a summer phenomenon, it could also lead to an increased methane flux rate in the summer.

4.3 Sinks for methane in the Menai Strait

In the first section of the discussion, methane in the Menai Strait was suggested to vary seasonally. The second section discussed the various sources that could contribute to the methane pool and found muddy sediments to be the major source for methane in the water column. The cause for the seasonality, however, could not be attributed to any of the investigated sources. The distribution of methane is not only dependent on its production, but also its consumption and export can significantly influence its spatial and temporal distribution patterns. Reeburgh and Heggie (1977), for example, suggest that consumption processes are more important in controlling methane distribution in the marine environment than production. It is therefore possible that the seasonal signal is not a product of increased summer production but of lower loss rates during the warm season. In this section the importance of biological methane oxidation in the water column will be discussed (Section 4.3.1). Then the loss of methane from the water into the atmosphere will be assessed and quantified (Section 4.3.2).

4.3.1 *In situ* oxidation of methane

Methane concentrations in incubated water were found to decrease no faster in live than poisoned control samples (Figure 3.3.1). This indicates that methanotrophic rates in oxygenated Menai Strait waters are either very small or that they exactly balance methane production rates. Net methane consumption rates in the water column will thus not play an important role in controlling the methane distribution in coastal environments such as the Menai Strait. Published studies of methane consumption rates in oxygenated surface waters support this conclusion.

Methane consumption has been known to occur in the water column of the ocean for a long time but has always been believed to proceed at very low rates. Based on the assumption that no methane production occurs in waters of the deep ocean, and on measurements of methane concentrations and of water mass ages, Scranton and Brewer (1978) calculated a minimum methane oxidation rate in young waters of the deep ocean of around $0.4 \text{ pmol dm}^{-3} \text{ d}^{-1}$ to be responsible for the common methane undersaturation at these depths. Measurements of methane oxidation rates are generally made by first spiking water samples with ^{14}C -labelled methane and by then measuring the rate at which ^{14}C -carbon dioxide evolves from incubated samples. In marine surface waters methane oxidation rates were measured to be higher than the conservative estimates for the deep sea (Scranton and Brewer, 1978).

Table 4.3.1 Aerobic oxidation rates, concentrations, and relative oxidation rates of methane in oxygenated coastal surface sea water at different geographic locations and during different months.

Oxidation ($\text{nM CH}_4 \text{ d}^{-1}$)	Conc. (nM CH_4)	Rel. oxid. ($\% \text{ d}^{-1}$)	Location	Depth (m)	Month	Source
0.3	740	0.04	Upper NY Bay	1-10	March	DeAngelis & Scranton, 1993
10.5	525	2	"	1-12	August	"
0.001	1.6	0.06	Of Puerto Rico	Surface	April	Jones & Amador, 1993
0.001	2.7	0.04		Surface	October	"
0.05	6-10	0.6	Black Sea	top 10	July	Reeburgh <i>et al.</i> , 1991
0.01	3	0.3	W-Cariaco Basin	Surface	Feb/March	Ward <i>et al.</i> , 1987
0.7	215	0.3	Port Moller	3-30	May	Griffiths <i>et al.</i> , 1982
0.03	28	0.1	N-Aleutian Shelf-inshore	Surface	January	"
0.07	11	0.6	"	"	May	"
0.08	31	0.3	"	"	August	"
53	740	7	Cape Lookout Bight	9 m	Summer	Sansone & Martens, 1978

Table 4.3.1 summarises marine aerobic methane consumption rates measured in surface waters at various locations and times. These are seen to range over more than four orders of magnitude from 0.001 to 53 nM d^{-1} . This large range is in part a result of the dependence of consumption rates on substrate availability, *i.e.* on ambient methane concentrations (Griffiths *et al.*, 1982;

Ward and Kilpatrick, 1990; Amaral and Knowles, 1995). Relative methane consumption rates, calculated as the ratio of the oxidation rate to the concentration and expressed as the percentage loss per day, showed a somewhat smaller range from 0.04 to 7% d⁻¹ with a mean of 1 % d⁻¹ and a mode of 0.3 % d⁻¹ (Table 4.3.1). Based on the limited available information on aerobic methane oxidation rates in oxygenated surface sea water, it can thus be concluded that *in situ* methanotrophy is only a minor sink for water column methane in oxygenated coastal waters.

Even as a minor sink for water column methane, methanotrophy could still contribute to the seasonal increase in methane concentrations in summer if it was shown to be higher in winter than summer. In freshwater systems the oxidation rates have been observed to follow a seasonal pattern but with maximum activities in summer (DeAngelis and Scranton, 1993; Jones and Amador, 1993). In sea water the seasonal situation is less clear. Although aerobic oxidation rates at fixed stations in the marine environment vary markedly (Table 4.3.1), and although there appears to be a tendency for increased consumption in summer, no definite seasonal pattern has yet been observed (Griffiths *et al.*, 1982; DeAngelis and Lee, 1994; Jones and Amador, 1993). The varying rates could be caused by various combinations of factors that have been described to influence aerobic methane oxidation rates, such as methane concentrations (Griffiths *et al.*, 1982; Ward and Kilpatrick, 1990; Amaral and Knowles, 1995), oxygen concentrations (Amaral and Knowles, 1995), DIN concentrations (Rudd *et al.*, 1976; Sansone and Martens, 1978), and heterotrophic microbial activity (Griffiths *et al.*, 1982). It can thus be summarised that aerobic methane consumption in the water column is not a fast removal mechanism for methane and cannot be responsible for the seasonal increase in concentrations in summer.

Aerobic oxidation is usually attributed to a variety of different aerobic methanotrophs that have been found to occur in very significant numbers in the surface ocean (Sieburth, 1987; Sieburth *et al.*, 1993a). Johnson *et al.* (1983) and Sieburth (1987) hypothesise that the large abundance of these methanotrophs, combined with a significantly larger daily variation in carbon dioxide than expected from the oxygen equivalent, suggest that the gross rates of methane production and consumption in the water column may be much larger than measured. The high production and consumption rates could be masked by extremely tight cycling mechanisms. Even if this is true, however, it will not significantly influence the methane distribution in the very dynamic coastal waters of the Menai Strait.

Further, anaerobic methane oxidation of rates between 0 and 11,000 nM d⁻¹ have been observed in the water column, but usually in deep anoxic methane-rich bottom water (Lidstrom, 1983; Ward *et al.*, 1987; Reeburgh *et al.*, 1991; Fenchel *et al.*, 1995). As the Menai Strait is fully oxygenated, it is unlikely that anaerobic methanotrophy occurs at appreciable rates.

4.3.2 Loss of methane to the atmosphere

As discussed in section 4.2.1 on atmospheric methane inputs, Menai Strait waters were supersaturated with methane on all occasions so that a diffusive loss of methane from the water into the atmosphere is likely to occur all year round. In this section the evasion rate of methane from the Menai Strait into the atmosphere will be quantified at different times of the year to assess whether variable loss rates can account for the occurrence of a seasonal distribution of water column concentrations. As no measurements of methane fluxes across the sea/air interface were made during this study, flux rates have to be estimated using appropriate gas-exchange models. Before discussing such derived evidence, however, the distribution of methane in air shall be considered.

Partial pressure of methane in the atmosphere

While methane concentrations in Menai Strait waters appear to be higher in summer than winter, an opposite trend can be observed in air (Table 3.1.3). While this tendency was statistically significant only for 1996 in the Menai Strait (Section 3.1), it agrees with the results for northern mid-latitudes from the extensive database collected through the Global Co-operative Flask Sampling Network for the National Oceanic and Atmospheric Administration's (NOAA) Climate Monitoring and Diagnostics Laboratory (CMDL) (Steele *et al.*, 1992) (Figure 1.3). The tendency of lower atmospheric partial pressures in summer was statistically insignificant for the Menai Strait investigation in 1997 and for Point Lynas. It is believed that a high variability in the partial pressures of methane - caused by air being enriched with methane above baseline concentrations - has masked the seasonal trend. The NOAA-CMDL baseline trends for atmospheric methane distributions were established at stations as far removed from large sources of methane as possible. Air sampled above Anglesey, however, is not always as clean as it might have passed over the gas exploration fields in Liverpool Bay or over large areas of land, thereby developing an above-baseline concentration of methane. The variability in the partial pressures of methane above the Menai Strait (Figure 3.1.1 L) might thus be in part a function of wind direction. To confirm that the pre-history of the sampled air, as determined by the prevailing wind direction, was the cause for the large variability in atmospheric methane concentrations would be a major task requiring the analysis of atmospheric partial pressures of methane in relation to trajectories.

The summer minimum in the partial pressure of atmospheric methane can be a result of a) reduced methane fluxes from various sources during summer, and/or b) increased atmospheric methane consumption rates in summer. Reduced summer fluxes from predominantly biogenic methane sources (Table 1.4) are unlikely for three reasons: because a) biological processes such as methanogenesis generally increase with temperature; b) diffusion is positively temperature-dependent and thus occurs faster during summer than winter; and c) increased summer fluxes were measured during methane flux studies (Bange *et al.*, 1994; Hutchin *et al.*, 1996).

While there is thus no evidence for increased methane fluxes during winter, there is ample evidence that chemical methane oxidation in the atmosphere increases in summer (Steele and Lang, 1991). The atmospheric methane consumption rate depends on the availability of hydroxyl radicals, which initiate the oxidation process. As hydroxyl radicals are photochemically produced their abundance increases in summer. It can thus be concluded that the lower atmospheric methane concentrations in summer are caused by increased chemical oxidation rates.

The high water column methane concentrations in summer could be a result of reduced fluxes to the atmosphere, or of increased production, in which case they would result in increased summer fluxes. As the entire marine system at present only contributes about 2% to the atmospheric methane pool (Table 1.4) no conclusions concerning increased or decreased fluxes during summer can be drawn from the atmospheric methane distribution.

Net methane fluxes from the water into the atmosphere

When methane concentrations in surface waters are supersaturated relative to the atmosphere, there will be net methane fluxes across the interface from the sea into the atmosphere. The difference between actual and equilibrium concentrations in the water is thus the driving force for a net diffusive methane flux. The flux rate, however, is not only dependent on the concentration difference but also on the resistance of the water to molecular transport. The transfer velocity of methane through the water, which is the reciprocal of its resistance, therefore also determines the exchange rate. The rate of methane exchange across a boundary layer such as the sea surface is thus calculated as:

$$F_{CH_4} = k_{sw} \times \Delta C = k_{sw} \times (C_w - C_{eq}) \quad (4.7)$$

where F_{CH_4} = methane flux density ($\text{mol cm}^{-2} \text{h}^{-1}$)

k_{sw} = transfer velocity for methane through sea water (cm h^{-1})

ΔC = methane concentration difference between water and atmosphere (mol cm^{-3})

C_w = methane concentration in water (mol cm^{-3})

C_{eq} = methane concentration in water in equilibrium with the atmosphere (mol cm^{-3})

– calculated using equation 2-18 in chapter 2.

While the concentration difference is readily determined, measuring or calculating k_{sw} remains rather problematic. Gas exchange occurs by molecular diffusion of methane along the concentration gradient through a thin boundary or surface film layer at the sea surface (Figure 4.3.1). The molecular diffusion coefficient of the gas, the viscosity of the sea water, and the thickness of the diffusion layer will therefore influence the transfer velocity. Different models have been developed to try and explain the process of gas exchange. They are summarised for example in Liss and Merlivat (1986) and will not be discussed here.

The thickness of the boundary layer is generally assumed to be the most important factor in determining k_{sw} and it varies primarily according to the degree of turbulence at the sea surface. Sea surface turbulence is commonly caused by wind, and in most models k_{sw} is therefore described as a function of wind velocity. Earlier the relationship between wind velocity and methane concentration in the Menai Strait was discussed, and was seen to correlate negatively where daily measurements were available (Figure 4.1.1).

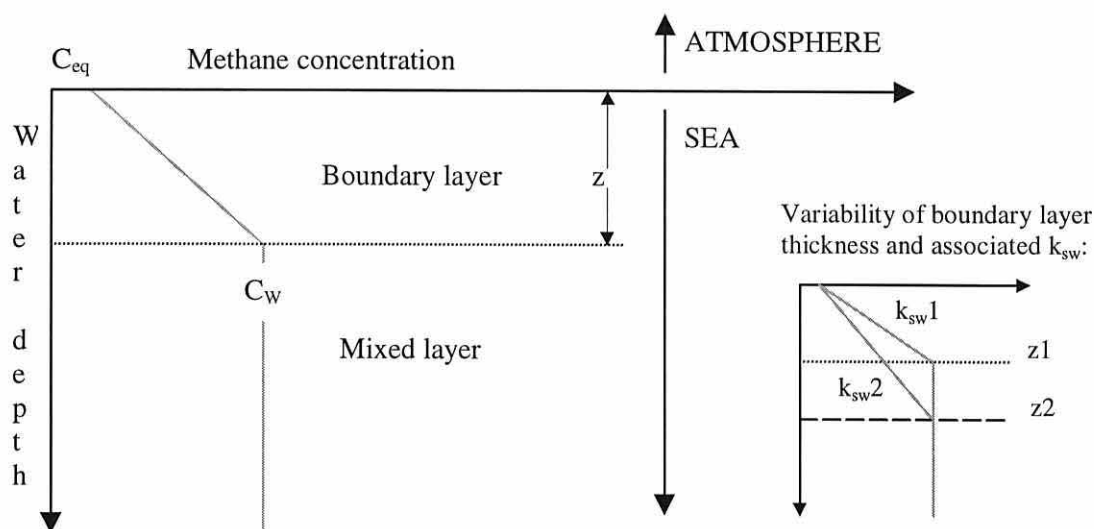


Figure 4.3.1 Model of methane exchange across the sea-atmosphere interface. Over the depth of the sea surface boundary layer (z) the methane concentration decreases along the gradient from mixed layer water concentrations (C_w) to equilibrium concentrations with the atmosphere (C_{eq}). The small diagram on the right hand bottom corner demonstrates how a decrease in boundary layer thickness (z_2 to z_1) causes the transfer coefficient to become steeper (k_{sw2} to k_{sw1}), *i.e.* to numerically increase.

In the following paragraphs the three most common models to derive k_{sw} values from wind velocity are outlined before they are applied to the Menai Strait data. These three models by Liss and Merlivat (1986), Wanninkhof (1992), and Sebacher, Harris and Bartlett (1983) have been used in the literature to predict regional emissions of methane from the oceans into the atmosphere (Table 4.3.2).

There are other models to calculate k_{sw} that are not considered here. Particularly the stability-dependent model by Erickson (1993) has been used recently to calculate marine methane emissions into the atmosphere (Patra *et al.*, 1998). Erickson's model is based on the surface area of sea that is covered by white caps. White caps begin to form at high wind velocities of about 13 m s^{-1} . As no observations on white caps were made in this study, and as wind speeds in the Menai Strait and at Point Lynas remained below 13 m s^{-1} , Erickson's model was not applied.

Table 4.3.2 Reports of methane sea-air flux rate estimates with the model used for studies at a number of sites.

Flux rate ($\mu\text{mol CH}_4 \text{ m}^{-2} \text{ d}^{-1}$)	Model	Study site	Source
2.6 to 1310	Sebacher <i>et al.</i> , 1983	Oregon estuaries	DeAngelis & Lilley, 1987
4.6 to 14	Liss-Merlivat, 1986	Arabian Sea	Owens <i>et al.</i> , 1991
6 to 60000	Liss-Merlivat, 1986	Dutch coast	Scranton & McShane, 1991
9.5 to 14.7	Liss-Merlivat, 1986	Baltic Sea - Feb. 92	Bange <i>et al.</i> , 1994
100 to 1200	"	" - Jul. 92	"
0.1 to 0.4	Wanninkhof, 1992	Pacific ocean	Bates <i>et al.</i> , 1996
3.2	Liss-Merlivat, 1986	N-Arabian Sea	Patra <i>et al.</i> , 1998
5.0	Wanninkhof, 1992	"	"
5.3	Erickson (1993)	"	"

The transfer coefficient shows an approximately quadratic dependence on wind velocity (Kanwisher, 1963; Liss, 1973; Broecker and Peng, 1974; Sebacher *et al.*, 1983; Wanninkhof, 1992). The rate constant of this dependence, however, remains a matter for discussion and research. Flux studies have been conducted both in wind tunnels and in the field to estimate the k_{sw} dependence on wind speed. In the field, a variety of approaches have been employed to measure gas fluxes, which are summarised and discussed comprehensively in Liss (1983), Broecker and Peng (1974), and Liss and Merlivat (1986). Sampling problems at high wind speeds mean that uncertainty remains concerning gas exchange rates during very rough seas.

The Liss-Merlivat model

Liss and Merlivat (1986) formulated the most widely used equations to derive k_{sw} based primarily on data from a tracer experiment with sulphur hexafluoride (SF_6) on a lake (Wanninkhof *et al.*, 1985). They suggest three progressively steeper linear relationships to describe gas transfer coefficients for low wind conditions when the sea surface remains calm, for intermediate wind conditions when capillary waves are formed, and for high wind speeds when waves are breaking and bubbles become entrained. The high wind speed equation (4.10) was originally based on very few measurements but has since been supported by field experiments in rough and stormy seas using a dual-tracer technique (Watson *et al.*, 1991). The empirical Liss and Merlivat (1986) equations, hereafter referred to as the LM model, are:

$$\text{for } u_{10} \leq 3.6 \text{ m s}^{-1} \quad k_{sw} = 0.17 * u_{10} * \left(\frac{Sc}{660} \right)^{\frac{2}{3}} \quad (4.8)$$

$$\text{for } 3.6 \text{ m s}^{-1} > u_{10} \leq 13 \text{ m s}^{-1} \quad k_{sw} = 2.85 * u_{10} - 9.65 * \left(\frac{Sc}{660} \right)^{\frac{1}{2}} \quad (4.9)$$

$$\text{for } u_{10} > 13 \text{ m s}^{-1} \quad k_{sw} = 5.9 * u_{10} - 49.3 * \left(\frac{Sc}{660} \right)^{-\frac{1}{2}} \quad (4.10)$$

where u_{10} = wind speed at 10 m above the sea surface (m s^{-1})

k_{sw} = transfer velocity for methane through sea water (cm h^{-1})

Sc = Schmidt number for methane (dimensionless)

660 = Schmidt number for carbon dioxide in sea water at 20°C (dimensionless)

The Schmidt number in the equations above is the ratio of the kinematic viscosity of sea water to the molecular diffusion coefficient of the gas. As both these parameters are temperature-dependent, and as the diffusion coefficient is gas-specific, the equations for k_{sw} must be corrected by the Schmidt number. The Schmidt number accounts for the temperature effect and allows the transfer of exchange coefficients from carbon dioxide, for which they are usually defined, to other gases. Wanninkhof (1992) developed the following equation to calculate the Schmidt number for methane in sea water as a third-order polynomial function of temperature (t , $^{\circ}\text{C}$):

$$Sc_{CH_4} = 2039.2 - 120.31t + 3.4209t^2 - 0.040437t^3 \quad (4.11)$$

The Wanninkhof model

Wanninkhof (1992) used data from studies of oceanic bomb- and natural- ^{14}C distributions that yielded higher rate constants than the data used for the LM model. Wanninkhof (1992) defined two quadratic equations to account for different averaging periods for wind speed measurements. Averaging wind speeds over long periods has been seen to result in higher transfer coefficients than averaging over short intervals or when winds are steady. For long-term average wind speeds the Wanninkhof model (W model) therefore suggests:

$$k_{sw} = 0.39 * u_{10}^2 * \left(\frac{Sc}{660} \right)^{-\frac{1}{2}} \quad (4.12)$$

And for more instantaneous wind measurements or for conditions of steady winds:

$$k_{sw} = 0.31 * u_{10}^2 * \left(\frac{Sc}{660} \right)^{-\frac{1}{2}} \quad (4.13)$$

The Sebacher, Harris and Bartlett model

Other models have derived their underlying data from controlled wind tunnel experiments in the field or the laboratory. Sebacher, Harris and Bartlett (1983) - hereafter referred to as SHB - derived k_{sw} from methane flux measurements in a small wind velocity controlled chamber placed over a wetland pond. This model is the only model to the author's knowledge that is derived from methane measurements. Corrected to wind velocities at 10 m above the surface, the SHB model proposes:

$$\text{for } u_{10} = 0 \text{ m s}^{-1} \quad k_{sw} = 1.70 * \left(\frac{Sc}{616} \right)^{-\frac{2}{3}} \quad (4.14)$$

$$\text{for } 2.8 \text{ m s}^{-1} \leq u_{10} < 7 \text{ m s}^{-1} \quad k_{sw} = 1.1 + 1.2 \left(\frac{u_{10}}{2} \right)^{1.96} * \left(\frac{Sc}{616} \right)^{-\frac{2}{3}} \quad (4.15)$$

where 616 = Schmidt number for methane in freshwater at 20°C,
calculated with equation 4.11.

The SHB model provides no equation to calculate k_{sw} at wind speeds between 0 and 2.8 m s⁻¹. As wind speeds in this range dominate in the Menai Strait, assumptions had to be made to calculate the exchange coefficients at these low wind velocities. k_{sw} was therefore calculated with equation 4.15, and values of below 1.7 cm h⁻¹ were corrected upwards to 1.7 cm h⁻¹ times the correction factor. This will result in slightly lower k_{sw} values than observed at low wind speeds, and thus produce a conservative estimate of the methane flux from the water into the atmosphere.

Flux rate estimates for methane from the Menai Strait

The wind measurements from the two meteorological stations in the central Menai Strait region were found to vary by a mean factor of 1.65 (Table 3.1.1 and Table 4.3.3). To investigate the dependence of the flux results on wind data, fluxes were calculated for both sets of wind data. To investigate the seasonal distribution of methane loss from the water to the atmosphere, mean fluxes were calculated for two-monthly intervals from mean methane concentration gradients (Figure 4.3.3) and mean k_{sw} values (Figure 4.3.4). The flux results are listed in Table 4.3.5. The standard deviations of the fluxes for different models and wind regimes were calculated using the rules for the propagation of error.

The different models produce flux estimates that vary by a mean factor of approximately 7 from the highest to the lowest estimate for each wind regime (Table 4.3.5). When ignoring the origin of the used wind data, the mean flux estimates vary by up to an order of magnitude. The SHB

flux estimates are consistently the highest and the LM estimates the lowest (Table 4.3.5). These discrepancies are caused by the different relationships between the transfer and the wind velocity, and thus eventually by the variation in empirical data obtained under different conditions. These results suggest that flux rates from different environments should only be compared and combined into models that estimate global greenhouse gas emissions from aquatic environments if the fluxes were calculated with the same model.

Table 4.3.3 Two-monthly mean wind velocities (u_{10} , m s^{-1}) ± 1 SD at the meteorological stations at the School of Ocean Sciences (SOS) and at Pen-y-Ffridd (Ffridd), and mean methane concentration differences (ΔCH_4 , pmol cm^{-3}).

	u_{10} SOS	u_{10} Ffridd	ΔCH_4
1996 Mar-Apr	2.3 ± 1.3	1.4 ± 0.9	7 ± 1.8
May-Jun	2.7 ± 1.3	1.3 ± 0.7	24 ± 10.0
Jul-Aug	1.6 ± 0.8	1.1 ± 0.6	43 ± 7.0
Sep-Nov	2.8 ± 1.7	1.7 ± 1.1	14 ± 6.0
1997 May-Jun	2.3 ± 1.4	1.4 ± 0.9	38 ± 11.8
Jul-Aug	1.7 ± 0.9	1.1 ± 0.8	50 ± 8.6
Sep-Nov	1.9 ± 1.4	1.3 ± 1.0	34 ± 6.6
MEAN	2.2	1.3	29.9

Table 4.3.4 Two-monthly mean methane transfer velocities (k_{sw} , cm h^{-1}) ± 1 SD for the central Menai Strait calculated using the models developed by Sebacher *et al.* 1983 (SHB), and Liss and Merlivat, 1986 (LM), and the long-term average model developed by Wanninkhof, 1992 (W). Two-monthly mean wind velocities from both Pen-y-Ffridd (Ffridd) and the School of Ocean Sciences (SOS) (Table 4.3.3) were used to calculate the transfer coefficient for each model.

	SHB SOS	SHB Ffridd	LM SOS	LM Ffridd	W SOS	W Ffridd
1996 Mar-Apr	1.6 ± 1.8	1.0 ± 1.3	0.2 ± 0.1	0.2 ± 0.1	1.4 ± 1.6	0.5 ± 0.7
May-Jun	2.4 ± 2.3	1.3 ± 1.3	0.4 ± 0.2	0.2 ± 0.1	2.4 ± 2.3	0.6 ± 0.6
Jul-Aug	1.6 ± 1.6	1.5 ± 1.6	0.3 ± 0.1	0.2 ± 0.1	0.9 ± 0.9	0.4 ± 0.5
Sep-Nov	2.6 ± 3.1	1.5 ± 1.9	0.4 ± 0.2	0.2 ± 0.2	2.6 ± 3.1	0.9 ± 1.2
1997 May-Jun	2.0 ± 2.4	1.3 ± 1.6	0.3 ± 0.2	0.2 ± 0.1	1.7 ± 2.1	0.6 ± 0.8
Jul-Aug	1.7 ± 1.7	1.4 ± 2.0	0.3 ± 0.1	0.2 ± 0.1	1.0 ± 1.1	0.4 ± 0.6
Sep-Nov	1.7 ± 2.5	1.3 ± 2.0	0.3 ± 0.2	0.2 ± 0.1	1.2 ± 1.8	0.6 ± 0.9
MEAN	1.9	1.3	0.3	0.2	1.6	0.6

Table 4.3.5 Two-monthly mean methane flux estimates ($\mu\text{mol CH}_4 \text{ m}^{-2} \text{ d}^{-1}$) ± 1 SD for the central Menai Strait as predicted from different models.

	SHB SOS	SHB Ffridd	LM SOS	LM Ffridd	W SOS	W Ffridd
1996 Mar-Apr	3 ± 3	2 ± 2	0.4 ± 0.3	0.2 ± 0.2	2.4 ± 2.8	0.9 ± 1.2
May-Jun	14 ± 14	7 ± 8	2.0 ± 1.3	1.0 ± 0.7	13.4 ± 14.1	3.1 ± 3.6
Jul-Aug	17 ± 17	15 ± 16	2.5 ± 1.3	1.7 ± 1.0	9.5 ± 9.6	4.5 ± 4.9
Sep-Nov	9 ± 11	5 ± 7	1.2 ± 0.9	0.8 ± 0.6	8.5 ± 11.0	3.1 ± 4.3
1997 May-Jun	18 ± 23	12 ± 15	2.8 ± 1.9	1.7 ± 1.2	15.8 ± 19.8	5.8 ± 7.7
Jul-Aug	20 ± 21	17 ± 25	3.0 ± 1.7	2.0 ± 1.5	12.3 ± 13.2	5.2 ± 7.6
Sep-Nov	14 ± 20	11 ± 16	2.1 ± 1.6	1.5 ± 1.2	9.8 ± 14.6	4.6 ± 7.1
MEAN	13.4	9.8	2.0	1.3	10.2	3.9

The LM equations are based on data from lakes, which are fetch-limited when compared to the open ocean from where the data for the W model originate. Reduced fetch has been shown to decrease the rates of gas transfer particularly at higher wind speeds (Upstill-Goddard *et al.*, 1996; Wanninkhof and Bliven, 1991) presumably because the wave fields cannot grow over long distances so that surface turbulence remains lower. As the Menai Strait is likely to be fetch-limited as well, the LM model appears the more appropriate model for the environment. Another reason for the low estimates obtained with the LM model is that the wind data for the LM study were averaged over only 1-2 day intervals. Wanninkhof (1992) discussed that such short intervals result usually in lower k_{sw} values than when longer averaging intervals are applied, so that equations are developed that estimate relatively smaller k_{sw} values. As the flux from the Menai Strait was calculated employing wind velocities that were averaged over two months, the LM equations might underestimate the transfer velocity while the W model appears more appropriate for the wind data.

The SHB flux rates are even higher than the W flux estimates. Wind tunnel studies, which were the sole basis for the SHB model, often create transfer coefficients that are not representative for environmental situations. This is because the shape and size of the chamber influence the wave field and thus the surface turbulence created by a certain wind speed. Most models have therefore used wind tunnel experiments to determine the shape of the curve between transfer coefficient and wind velocity, while field data were used to calibrate these equations (Liss and Merlivat, 1986; Wanninkhof, 1992). The results from the SHB model might thus be overestimates.

The flux calculations based on wind measurements from two different sites in the Menai Strait demonstrate the importance of choosing representative stations. Mean fluxes calculated with wind speeds measured at the School of Ocean Sciences were - depending on the model - between 1.5 and 2.6 times greater than those calculated with Pen-y-Ffridd wind velocities (Table 4.3.5). In general these wind speeds are low when compared *e.g.* to the conditions at Point Lynas (Tables 3.1.1 and 3.1.2), which may be due to the shielding effect of the land. When estimating the mean wind experienced throughout the Menai Strait, the wind speeds measured at both meteorological sites at the narrow central section will be at the lower end so that the flux estimates produced by both sites can be considered as conservative estimates.

All three models show a general increase in flux rates of methane from the sea to the atmosphere during the summer. This is due to the greater concentration differences between the water and the atmosphere in summer (Table 4.3.3). The increase in water column methane concentrations outweighs the reducing effect the calmer summer conditions (Table 4.3.3) have on the transfer coefficients (Table 4.3.4). This observation strongly suggests that the summer increase in Menai Strait methane concentrations is not a result of reduced methane losses to the atmosphere in

summer but of increased production or release during the warmest months, even if such increased production could not be established in the investigation.

The results display that many uncertainties remain about the accuracy of the flux rate estimates from different models and thus also about the dynamics of gas exchange. All three models have used wind velocity as the only determinant for surface turbulence. It is known, however, that other factors - such as the existence of surfactants in the boundary layer (Broecker *et al.*, 1978; Jähne *et al.*, 1987) and perhaps also wind direction (Wanninkhof, 1992) - influence the rate of gas exchange across a boundary layer, and thereby alter the flux rates. The molecular diffusion coefficient through the surface film was already discussed as an influence on gas exchange, and therefore should be corrected for in the Schmidt number. This correction factor, however, is based on the assumption that the surface film consists entirely of seawater, which is not necessarily the case. Surfactants and organic microfilms at the sea surface can reduce the exchange rate of methane (Downing and Truesdale, 1955; Broecker *et al.*, 1978), due to slower diffusion coefficients through more dense matrices and a dampening effect on wave development. It is possible that such a microfilm will be thicker during the summer months due to increased biological activity. A thicker microfilm could reduce the transfer velocity and thus the methane loss rate to the atmosphere. This would mean that the increased summer concentrations of methane were a result of a combination of increased production and reduced diffusive loss. No evidence but the observation of a defined surface film in the summer months, however, exists to support this hypothesis. As the dependence of surface turbulence on wind velocity remains unclear, some workers have started to calculate the transfer velocity based on other parameters which are more closely related to surface turbulence than wind, *e.g.* radar backscatter (Wanninkhof and Bliven, 1991).

Flux rates in 1997 were generally higher than in the previous year (Table 4.3.5). These increased loss rates are a result of higher concentration gradients as the exchange coefficients were lower due to calmer weather conditions (Tables 4.3.3 and 4.3.4). The higher concentration gradients might have been due in part to increased production, but the calmer weather conditions will have also contributed to the concentration increase by reducing the exchange velocities relative to the previous year.

With so many open questions concerning the rate constant to calculate the exchange coefficient from the wind velocity and concerning the mathematically exclusive dependence of k_{sw} on wind, discussion of errors of gas fluxes are difficult. Two major problems for the quantification of errors within the present wind-dependent models are a) the difficulty of obtaining representative wind speed estimates for the region, and b) the strongly non-linear relationship between wind and exchange velocities.

In conclusion, the methane flux to the atmosphere represents the single largest removal term for water column methane. While uncertainties remain about the flux models, there can be little doubt about the general magnitude of this sink. A mean annual removal rate of between 1.3 and 13 $\mu\text{mol CH}_4 \text{ m}^{-2} \text{ d}^{-1}$ from the centre of the Menai Strait requires a source of equal strength to maintain the high degrees of supersaturation.

4.4 Differences between Point Lynas and the Menai Strait

The two main differences observed in this study between Point Lynas and the Menai Strait were the lower methane concentrations and higher wind speeds at Point Lynas (Figure 3.1.1). While no investigation into the methane sources was conducted at Point Lynas, the sink strength was calculated with the exchange models that have also been applied to the Menai Strait data. The results are shown in Tables 4.4.1, 4.4.2, and 4.4.3.

Table 4.4.1 Two-monthly mean wind velocities (u_{10} , m s^{-1}) ± 1 SD and mean methane concentration differences (ΔCH_4 , pmol cm^{-3}) at Point Lynas.

	u_{10}	ΔCH_4
1996 Mar-Apr	6.2 ± 3.1	1.0 ± 0.7
May-Jun	6.4 ± 2.9	1.3 ± 1.0
Jul-Aug	5.6 ± 2.3	3.3 ± 1.4
Sep-Oct	7.4 ± 3.6	1.7 ± 0.4
MEAN	6.4	1.8

Table 4.4.2 Two-monthly mean methane transfer velocities (k_{sw} , cm h^{-1}) ± 1 SD for Point Lynas calculated with the models of Sebacher *et al.* 1983 (SHB), Liss and Merlivat, 1986 (LM), and the long-averaged model of Wanninkhof, 1992 (W).

	SHB k_{sw}	LM k_{sw}	W k_{sw}
1996 Mar-Apr	7.4 ± 7.2	10.8 ± 5.4	10.1 ± 10.1
May-Jun	9.0 ± 8.0	10.5 ± 4.8	12.3 ± 11.2
Jul-Aug	8.5 ± 6.9	7.0 ± 2.9	10.9 ± 9.0
Sep-Oct	13.7 ± 13.0	12.2 ± 5.9	18.8 ± 18.3
MEAN	9.7	10.1	13.1

Table 4.4.3 Two-monthly mean methane flux estimates (F_{CH_4} , $\mu\text{mol CH}_4 \text{ m}^{-2} \text{ d}^{-1}$) ± 1 SD for Point Lynas as predicted from different models.

	SHB F_{CH_4}	LM F_{CH_4}	W F_{CH_4}
1996 Mar-Apr	1.7 ± 1.8	2.5 ± 2.3	2.3 ± 2.6
May-Jun	2.8 ± 2.8	3.2 ± 3.0	3.8 ± 3.8
Jul-Aug	6.7 ± 6.1	5.5 ± 3.3	8.6 ± 7.9
Sep-Oct	5.7 ± 6.1	5.1 ± 2.8	7.9 ± 8.6
MEAN	4.2	4.1	5.6

The results reveal that despite the low concentrations and the relatively small degree of supersaturation at Point Lynas, the emission rate to the atmosphere is of a similar magnitude as for the highly supersaturated Menai Strait (Table 4.4.4). At these higher wind speeds the results from the different flux models are in much better agreement - varying in their mean annual rates between 4.1 and $5.6 \mu\text{mol CH}_4 \text{ m}^{-2} \text{ d}^{-1}$ - than for the low air velocities in the central Menai Strait. Depending on the model used, larger methane flux rates are predicted to emanate either from Point Lynas (LM) or the Menai Strait (SHB and W) (Table 4.4.4).

Table 4.4.4 1996 methane flux rates (F_{CH_4} , $\mu\text{mol CH}_4 \text{ m}^{-2} \text{ d}^{-1}$) \pm SD from the Menai Strait (MS) - using wind measurements from the School of Ocean Sciences - and Point Lynas (PL) calculated with the Liss-Merlivat, 1986 model (LM), the Wanninkhof, 1992 model (W), and the Sebacher, Harris and Bartlett, 1983 model (SHB), and the ratio between the flux rates from the two sites.

MODEL		$F_{\text{CH}_4} \text{ MS } \pm \text{ SD}$	$F_{\text{CH}_4} \text{ PL } \pm \text{ SD}$	RATIO MS/PL \pm SD
LM	Mar-Apr	0.4 ± 0.3	2.5 ± 2.3	0.2 ± 0.2
	May-Jun	2.0 ± 1.3	3.2 ± 3.0	0.6 ± 0.7
	Jul-Aug	2.5 ± 1.3	5.5 ± 3.3	0.5 ± 0.4
	Sep-Oct/Nov	1.2 ± 0.9	5.1 ± 2.8	0.2 ± 0.2
	Average			0.4 ± 0.4
W	Mar-Apr	2.4 ± 2.8	2.3 ± 2.6	1.0 ± 1.7
	May-Jun	13.4 ± 14.1	3.8 ± 3.8	3.5 ± 5.1
	Jul-Aug	9.5 ± 9.6	8.6 ± 7.9	1.1 ± 1.5
	Sep-Oct/Nov	8.5 ± 11.0	7.9 ± 8.6	1.1 ± 1.8
	Average			1.7 ± 2.5
SHB	Mar-Apr	2.7 ± 3.0	1.7 ± 1.8	1.6 ± 2.4
	May-Jun	13.8 ± 14.3	2.8 ± 2.8	4.9 ± 7.0
	Jul-Aug	16.6 ± 16.5	6.7 ± 6.1	2.5 ± 3.4
	Sep-Oct/Nov	8.6 ± 10.8	5.7 ± 6.1	1.5 ± 2.5
	Average			2.6 ± 3.8

This quite intriguing discrepancy in results cannot be resolved with the present knowledge of gas exchange dynamics. Methane emissions were calculated to increase during the summer at Point Lynas. As this had already been observed in the Menai Strait, it is suggested that it is not a chance event but indicates a seasonal pattern. The increased summer emissions are a result of an increased concentration gradient. The source for methane at Point Lynas is unlikely to be local as a survey of the sediments showed these to be made primarily of shell fragments and gravel.

I discovered the secret of the sea in meditation upon the dewdrop.
Kahlil Gibran (1883-1931)

4.5 Methane budget for the Menai Strait water column

In this final discussion section, the results of the study are summarised quantitatively to investigate whether the investigated sources and sinks of methane in the Menai Strait system balance.

The source and sink terms for methane in the water column of the Menai Strait in 1997 are shown and quantified in Figure 4.5.1. The annual strengths of the methane sources and sinks were calculated from the mean annual concentrations and flux rates summarised in Table 4.5.1 and the area, volume, and flow rate estimates for the Menai Strait in Table 4.5.2. The sediment area covered with mud was assumed to be 10% of the total area based on both local knowledge and sediment type descriptions given in the Admiralty Chart. The methane concentration of Liverpool Bay water that advects into the Menai Strait was around 10 nM in summer (Figures 3.2.3 and 3.2.5 B), and is conservatively assumed to be 2 nM in winter. The mean concentration is thus assumed to be around 6 nM.

Table 4.5.1 Mean measured methane concentrations and calculated flux rates in the Menai Strait in 1997. The Liss-Merlivat, 1986 model was used to calculate the loss rate to the atmosphere.

	Concentration (nM)	Rate ($\mu\text{mol CH}_4 \text{ m}^{-2} \text{ d}^{-1}$)
Sources		
Inflowing water	6	-
River water	4.5	-
Raw sewage	476	-
Treated sewage	181	-
Net production in water	-	Negligible
Sediment flux (mud)	-	9.2
Sinks		
Biological oxidation	-	Negligible
Loss to atmosphere	-	2.6

Table 4.5.2 Area, volume and flow rates of Menai Strait water, flow rates of sewage and the River Ogwen and area estimate for muddy sediments.

	Area (m^2)	Volume (m^3)	Flow rate ($\text{m}^3 \text{ d}^{-1}$)
Menai Strait	$20 * 10^6$	$0.1 * 10^9$	$50 * 10^6$
Muddy sediments	$2 * 10^6$	-	-
River Ogwen	-	-	$70 * 10^3$
Treated sewage	-	-	$11 * 10^3$
Raw sewage	-	-	$1 * 10^3$

The only unknown in the budget is an estimate for the methane that is exported with the water into Caernarfon Bay. When adding all sources ($117.7 \text{ kmol y}^{-1}$) and deducting the sinks (19 kmol y^{-1}), 98.7 kmol y^{-1} remain unaccounted for, and can therefore be assumed to be exported into Caernarfon Bay. This is, however, likely to underestimate the real mass of methane that is

annually exported from the Menai Strait. If assuming conservatively that the methane concentrations in the water column remained at Menai Bridge concentrations throughout the south-western part of the Strait, the exported waters would have an annual average concentration of 35 nM. With an annual volume of $18.3 \times 10^{12} \text{ dm}^3$ of water passing through the Menai Strait, the annually exported mass of methane can be calculated to be approximately 640 kmol. As the investigated sources can only account for 98.7 kmol of this, the Menai Strait must produce an extra 541.3 kmol y^{-1} .

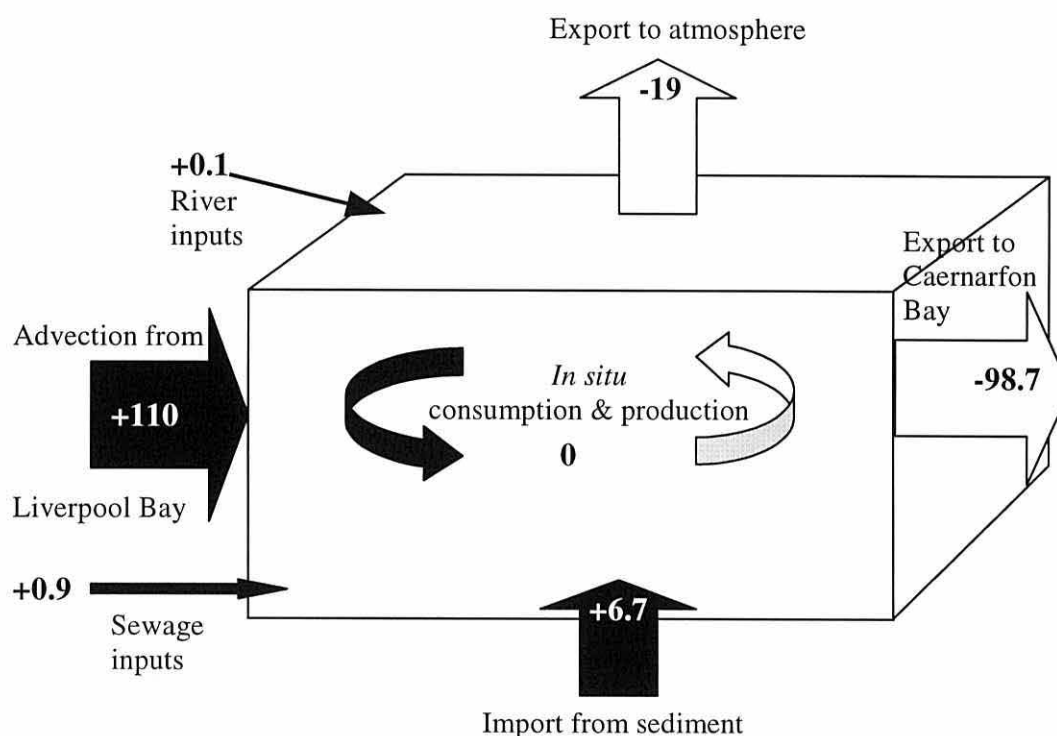


Figure 4.5.1 Total methane budget in kmol y^{-1} for the Menai Strait water column in 1997. Open arrows denote consumption, closed arrows production terms. The export to Caernarfon Bay was calculated by difference between sources and sinks.

The source of this significant mass of methane remains unidentified. The mysterious source is likely to display increased production rates in summer as the seasonal increase in methane was concluded to be caused by an unidentified source. The significant horizontal variability in sedimentary methane concentrations and the unstudied occurrence of gas ebullition suggest that this methane may come from the sediments. If muddy sediments are the principal source for this surplus methane, the estimated $2 \times 10^6 \text{ m}^2$ of mudflats in the Menai Strait will annually produce 548 kmol of methane, or $0.75 \text{ mmol m}^{-2} \text{ d}^{-1}$. Such methane production rates have been reported for other coastal sediments as shown in Table 4.2.5 (page 4-27), and it is thus feasible to suggest that a more detailed sediment study may close the methane budget for the Menai Strait.

*To be without some of the things you want
Is an indispensable part of happiness.*

Bertrand, Lord Russell (1872-1970)

4.6 Conclusions

This project concerns the distribution of methane in temperate coastal waters and the causes of the observed distribution patterns. Methane concentrations, analysed by headspace equilibration followed by gas chromatography, were found to be heterogeneously distributed in space and time. At the two study sites the water column was supersaturated with respect to the atmosphere throughout the year. Although concentrations at the more exposed station at Point Lynas were 2- to 10-fold lower than in the more wind-sheltered Menai Strait, a seasonal pattern of maximum concentrations coinciding with highest water temperatures in the summer were discerned with a fortnightly sampling regime.

The short-term variability at the fixed sampling station in the Menai Strait, however, was found to be so high that it left the seasonal pattern uncertain. In variability studies both the net current direction and the square of the wind velocity were found to be related to methane concentrations. While the current-related variability was reduced by sampling water during the same state of the tide, the variability introduced by the effect of the wind could not be avoided. Despite a tendency for lower wind speeds during the summer, model calculations revealed higher transfer rates during the summer months. Both reduced summer wind speeds and increased summer flux rates suggest the validity of the observed seasonality of methane despite of the large short-term variability. Increased summer flux rates furthermore suggest that there must be seasonally varying net sources for methane in the Menai Strait.

Advection of methane with water flowing into the Menai Strait from Liverpool Bay could only account for at most 20% of the methane measured at the fixed sampling station. Methane contributions from other external sources such as from the River Ogwen and from sewage discharges were quantitatively insignificant. This suggests that approximately 80% of the measured methane must be released from internal sources during the two days the water spends in the Menai Strait.

No significant net methane production could be detected in the water column. Theoretical calculations found no evidence that anaerobic conditions suitable for methanogens would develop or be maintained in particles of widely distributed dimensions in fully oxygenated coastal waters.

Low and quantitatively insignificant rates of water column methane production occurred during a bloom of the heterotrophic dinoflagellate *Noctiluca scintillans*. The agents of this production were speculated to be bacteria described to live intracellularly within these dinoflagellates.

As neither external nor water-column sources of methane can account for the quantity and the seasonal distribution of methane in the Menai Strait, by default it was concluded that the sediments must be the major contributor to water column methane concentrations. Significant concentrations of methane were only measured in muddy sediments, which were estimated to cover approximately 10% of the area of the Menai Strait bottom. Concentrations of methane in muddy sediments were lower than at subtidal coastal sites elsewhere, which was attributed to the effects of periodic aerial exposure of the mudflats during low tide and high occurrence of bioturbation. The source strength of the sediments was calculated with a diffusion flux model, and was found to contribute only approximately 1% of the concentrations measured in the water column. No seasonal pattern in methane concentrations could be demonstrated for the sediments. The horizontal variability of sediments concerning methane, however, was extremely high, and might have masked a seasonal distribution patterns. The observation of gas bubbles emerging from Menai Strait sediments suggests that some of the produced methane does not diffuse by molecular motion from the sediment into the water column but evades at a much faster rate by ebullition.

From mass balance considerations it is concluded that there must thus be an unidentified source for methane in the Menai Strait that produces annually at least 540 kmol of methane with higher production rates in the summer than the winter. The rather gradual increase in methane concentrations in water as it flows through the Strait suggests that this source is not a discreet seep but widespread. The most likely situation is that the sediments produce and release much more methane than has been estimated from the results of the small sediment study.

The atmosphere was identified as the main sink for methane from the water column. The sink strength was determined with three different gas exchange models. All three models calculated a general increase in flux rates of methane from the sea to the atmosphere during the summer. A large discrepancy in flux estimates from the different models - particularly during low wind velocities - demonstrates the holes in our current understanding of the dynamics of gas exchange.

The emission rates of methane from the waters at Point Lynas and the Menai Strait to the atmosphere were calculated to be similar despite the great difference in concentrations between the two sites.

*The outcome of any serious research can only be
To make two questions grow where only one grew before*

Thorstein Keblen (1857-1929)

4.7 Suggestions for future research

Our scientific understanding of methane biogeochemistry is far from complete. Many uncertainties concerning the dynamics of methane in the water column were highlighted in the discussion of this project. These fall into three categories: methane production in the oxygenated water column, the source strength of the sediment, and gas exchange between the water column and the atmosphere.

Methane production in the oxygenated water column

Although *in situ* methane production in the water column was seen to be quantitatively insignificant in coastal areas, it is believed to be important for the open ocean. As the organisms, loci and processes of this production are unknown, research in this field promises to be most exciting.

The experimental design adopted to measure *in situ* methanogenesis in this project proved to be too insensitive. Future incubation experiments should be based on concentrating methane from large volumes of water using a purge-and-trap technique. To ascertain the oxygen status during the incubations, measurements of oxygen concentrations should be conducted. To understand the behaviour of methane concentrations in control samples, fully gas-tight incubation vials should be used, filtered control samples added to investigate the role of adsorption out of or into particles, and the efficiency of mercuric chloride as a poison for methanogens should be tested.

Water in which methane is produced should subsequently be examined to search for the methanogenic organisms and sites. To improve the data applied to physical models that calculate minimum diameters of potentially anoxic particles, measurements of the particle size distribution in the water, of the particle-associated respiration rates and of the methane diffusion rate through the particles should be obtained.

Laboratory experiments should then be conducted with organisms suspected of performing methanogenesis or of harbouring methanogens. This project, for example, suggests that the methanogenic potential of *Noctiluca scintillans* should be examined further. The reported species-specific association of methane production with some herbivorous copepods (DeAngelis and Lee, 1994) should be verified, the list of tested zooplankton species enlarged, and the oxygen-status inside the zooplankton gut should be investigated.

The source strength of the sediment

The quantification of the methane source strength of the sediment remains an unresolved issue. The use of calculated diffusive flux rates to estimate the source strength of the sediment can result in both under- and overestimates of the actual flux rate. Measuring the increase of methane concentrations over time in flux chambers will provide a measure of the actual mass of methane released from the sediment. The flux chamber results, however, will not be a reliable measure for the mass of methane that enters the water column methane pool, as it cannot differentiate between bubble and dissolved methane. Flux chamber measurements will thus have to be accompanied by a study into the importance of ebullition in the investigated sediments. Should ebullition be quantitatively relevant, further work has to concentrate on assessing the dissolution rate of methane from bubbles into the water column to determine the contribution of bubble methane to water column concentrations.

Future sediment sampling strategies for seasonal investigations should aim at minimising the effect of horizontal variability. A thorough study of the spatial distribution of methane in the sediments throughout the study area should precede the seasonal study so that representative sampling sites can be selected. The sampling stations should very narrowly defined.

Also the presence or absence of gas seeps in the sampled area should be investigated by the geotechnical assessment of the bottom.

Gas exchange between the water column and the atmosphere

In the discussion of this project, significant uncertainties associated with the existing gas exchange models have been identified. The discrepancies in the fluxes calculated with different models were found to be particularly high at lower wind speeds, when other parameters that influence surface turbulence and gas exchange rates may become relatively more prominent. It is therefore suggested that a new gas exchange model for low wind speeds be developed. This will be important to estimate emissions of climate gases from all aquatic environments, as emissions at low wind speeds can be as significant as at high wind speeds due to increasing concentration differences across the sea/air interface.

References

- Allredge, A.L. and Cohen, Y. (1987) Can microscale chemical patches persist in the sea? Microelectrode study of marine snow, fecal pellets. *Science*, **235**: 689-691.
- Ali, A. (1992) *Sedimentary, Geophysical and Oceanographic Studies of the NE Menai Strait and Conwy Bay (U.K.)*. Ph.D. Thesis, University of Wales, Bangor.
- Alperin, M.J. and Reeburgh, W.S. (1985) Inhibition experiments on anaerobic methane oxidation. *Applied and Environmental Microbiology*, **50**: 940-945.
- Amaral, J.A. and Knowles, R. (1995) Growth of methanotrophs in methane and oxygen counter gradients. *FEMS Microbiology Letters*, **126**: 215-220.
- Anthony, C. (1982) *The Biochemistry of Methanotrophs*. Academic Press, London.
- Atkinson, L.P. and Richards, F.A. (1967) The occurrence and distribution of methane in the marine environment. *Deep-Sea Research*, **14**: 673-684.
- Badr, O., Probert, S.D. and O'Callaghan, P.W. (1992) Sinks for atmospheric methane. *Applied Energy*, **41**: 137-147.
- Balch, W.E., Fox, G.E., Magrum, L.J., Woese, C.R. and Wolfe, R.S. (1979) Reevaluation of a unique biological group. *Microbiological Reviews*, **43**: 260-296.
- Balch, W.E., Magrum, L.J., Fox, G.E., Wolfe, R.S. and Woese, C.R. (1977) An ancient divergence among the bacteria. *Journal of Molecular Evolution*, **9**: 305-311.
- Bange, H.W., Bartell, U.H., Rapsomanikis, S. and Andreae, M.O. (1994) Methane in the Baltic and North Seas and a reassessment of the marine emissions of methane. *Global Biogeochemical Cycles*, **8**: 465-480.
- Bange, H.W., Rapsomanikis, S. and Andreae, M.O. (1996) The Aegean Sea as a source of atmospheric nitrous oxide and methane. *Marine Chemistry*, **53**: 41-49.
- Bange, H.W., Dahlke, S., Ramesh, R., Meyer-Reil, L.A., Rapsomanikis, S. and Andreae, M.O. (1998) Seasonal study of methane and nitrous oxide in the coastal waters of the southern Baltic Sea. *Estuarine, Coastal and Shelf Science*, **47**: 807-817.
- Barker, H.A. (1936) Studies on methane producing bacteria. *Archives of Microbiology*, **7**: 420-431.
- Barnes, R.O. and Goldberg, E.D. (1976) Methane production and consumption in anoxic marine sediments. *Geology*, **4**: 297-300.
- Baross, J.A., Lilley, M.D. and Gordon, L.I. (1982) Is the CH₄, H₂ and CO venting from submarine hydrothermal systems produced by thermophilic bacteria? *Nature*, **298**: 366-368.
- Bates, T.S., Kelly, K.C., Johnson, J.E. and Gammon, R.H. (1996) A reevaluation of the open ocean source of methane to the atmosphere. *Journal of Geophysical Research*, **101** (D3): 6,953-6,961.
- Bekki, S., Law, K.S. and Pyle, J.A. (1994) Effect of ozone depletion on atmospheric CH₄ and CO concentrations. *Nature*, **371**: 595-597.

- Belyaev, S.S. and Ivanov, M.V. (1983) Bacterial methanogenesis in underground waters. In: R. Hallberg (Editor) *Environmental Biogeochemistry*. Proceedings of the 5th International Symposium on Environmental Biogeochemistry (ISEB). Ecological Bulletin (Stockholm) No. 35. Swedish Natural Scientific Research Council, Stockholm, p. 273-280.
- Bernard, B.B. (1979) Methane in marine sediments. *Deep-Sea Research*, **26**: 429-443.
- Berner, W., Bucher, P., Oeschger, H. and Schauffer, B. (1975) Analysis and interpretation of gas content and composition in natural ice. *Symposium in Isotopes and Impurities in Snow and Ice*. Union géodésique internationale, Grenoble, le 25.08. to 06.09.
- Bianchi, M., Marty, D., Teyssié, J.L. and Fowler, S.W. (1992) Strictly aerobic and anaerobic bacteria associated with sinking particulate matter and zooplankton fecal pellets. *Marine Ecology Progress Series*, **88**: 55-60.
- Blair, N.E. and Aller, R.C. (1995) Anaerobic methane oxidation on the Amazon shelf. *Geochimica et Cosmochimica Acta*, **59**: 3,707-3,715.
- Blight, S.P., Bentley, T.L., Lefevre, D., Robinson, C., Rodrigues, R., Rowlands, J. and Williams, P.J.leB. (1995) Phasing of autotrophic and heterotrophic plankton metabolism in a temperate coastal ecosystem. *Marine Ecology Progress Series*, **128**: 61-75.
- Boehme, S.E., Blair, N.E., Chanton, J.P. and Martens, C.S. (1996) A mass balance of ¹³C and ¹²C in an organic-rich methane-producing marine sediment. *Geochimica et Cosmochimica Acta*, **60**: 3,835-3,848.
- Boone, D.R. (1991) Ecology of methanogenesis. In: J.E. Rogers and W.B. Whitman (Editors) *Microbial Production and Consumption of Greenhouse Gases: Methane, Nitrogen Oxides, and Halomethanes*. American Society for Microbiology, Washington, D.C., p. 57-70.
- Bracke, J.W., Loeb Cruden, D., Markovetz, A.J. (1979) Intestinal microbial flora of the American cockroach, *Periplaneta americana* L.. *Applied and Environmental Microbiology*, **38**: 945-955.
- Bridgman, H.A. (1990) *Global Air Pollution: Problems for the 1990s*. Belhaven Press, London.
- Broecker, H.-C., Peterman, J. and Siems, W. (1978) The influence of wind on CO₂ exchange in a wind-tunnel, including the effects of mono layers. *Journal of Marine Research*, **36**: 595-610.
- Broecker, W.S. and Peng, T.-H. (1974) Gas exchange rates between air and sea. *Tellus*, **26**: 21-35.
- Broecker, W.S. and Peng, T.-H. (1982) *Tracers in the Sea*. Lamont-Doherty Geological Observatory, Palisades, New York.
- Brooks, J.M. and Sackett, W.M. (1973) Sources, sinks, and concentrations of light hydrocarbons in the Gulf of Mexico. *Journal of Geophysical Research*, **78**: 5,248-5,258.
- Brooks, J.M., Fredericks, A.D., Sackett, W.M. and Swinnerton, J.W. (1973) Baseline concentrations of light hydrocarbons in the Gulf of Mexico. *Environmental Science and Technology*, **7**: 639-642.
- Brooks, J.M., Kennicutt, M.C., Fisher, C.R., Macko, S.A., Cole, K., Childress, J.J., Bidigate, R.R. and Vetter, R.D. (1987) Deep-sea hydrocarbon seep communities: evidence for energy and nutritional carbon sources. *Science*, **238**: 1,138-1,142.

- Brooks, J.M., Reid, D.F. and Bernard, B.B. (1981) Methane in the upper water column of the northwestern Gulf of Mexico. *Journal of Geophysical Research*, **86** (C11): 11,029-11,040.
- Bryant, M.P. (1974) Part 13. Methane-producing bacteria. In R.E. Buchanan and N.E. Gibbons (Editors) *Bergey's Manual of Determinative Bacteriology*. 8th edition. The Williams & Wilkins Co., Baltimore, p. 287-304.
- Bryant, M.P., Wolin, E.A., Wolin, M.J. and Wolfe, R.S. (1967) *Methanobacillus omelianskii*, a symbiotic association of two species of bacteria. *Archiv für Mikrobiologie*, **59**: 20-31.
- Burke, R.A. Jr., Martens, C.S. and Sackett, W.M. (1988) Seasonal variations of D/H and ¹³C/¹²C ratios of microbial CH₄ in surface sediments. *Nature*, **332**: 829-831.
- Burke, R.A. Jr., Reid, D.F., Brooks, J.M. and Lavoie, D.M. (1983) Upper water column methane geochemistry in the eastern tropical North Pacific. *Limnology and Oceanography*, **28**: 19-23.
- Burns, S.J. (1998) Carbon isotopic evidence for coupled sulfate reduction – methane oxidation in Amazon Fan sediments. *Geochimica et Cosmochimica Acta*, **62**: 797-804.
- Butler, J.H., Jones, R.D., Garber, J.H. and Gordon, L.I. (1987) Seasonal distribution and turnover of reduced trace gases and hydroxylamine in Yaquina Bay, Oregon. *Geochimica et Cosmochimica Acta*, **51**: 697-706.
- Cantrell, C.A., Shetter, R.E., McDaniel, A.H., Calvert, J.G., Davidson, J.A., Lowe, D.C., Tyler, S.C., Cicerone, R.J. and Greenberg, J.P. (1990) Carbon kinetic isotope effect in the oxidation of methane by the hydroxyl radical. *Journal of Geophysical Research*, **95** (D13): 22,455-22,462.
- Cappenberg, T.E. (1974) Interrelations between sulfate-reducing and methane-producing bacteria in bottom deposits of a freshwater lake. II. Inhibition experiments. *Antonie van Leeuwenhoek*, **40**: 297-306.
- Chanton, J.P. and Martens, C.S. (1988) Seasonal variations in ebullitive flux and carbon isotopic composition of methane in a tidal freshwater estuary. *Global Biogeochemical Cycles*, **2**: 289-298.
- Chanton, J.P., Martens, C.S. and Kelly, C.A. (1989) Gas transport from methane-saturated, tidal freshwater and wetland sediments. *Limnology and Oceanography*, **34**: 807-819.
- Chanton, J.P., Martens, C.S., Kelley, C.A., Crill, P.M. and Showers, W.J. (1992) Methane transport mechanisms and isotopic fractionation in emergent macrophytes of an Alaskan Tundra Lake. *Journal of Geophysical Research*, **97** (D15): 16,681-16,688.
- Cheeseman, P., Toms-Wood, A. and Wolfe, R.S. (1972) Isolation and properties of a fluorescent compound, factor F₄₂₀, from *Methanobacterium* strain M.o.H. *Journal of Bacteriology*, **112**: 527-531.
- Cicerone, R.J. (1988) Greenhouse effect: Methane linked to warming. *Nature*, **334**: 198.
- Cicerone, R.J. and Oremland, R.S. (1988) Biogeochemical aspects of atmospheric methane. *Global Biogeochemical Cycles*, **2**: 299-327.
- Claypool, G.E. and Kaplan, I.R. (1974) The origin and distribution of methane in marine sediments. In: I.R. Kaplan (Editor) *Natural Gases in Marine Sediments*. Plenum Press, New York, p. 99-139.

- Comita, P.B. and Gagosian, R.B. (1983) Membrane lipid from a deep sea hydrothermal vent methanogen: a new macrocyclic glycerol diether. *Science*, **222**: 1,329-1,331.
- Conrad, R. (1989) Control of methane production in terrestrial ecosystems. In: Andreae, M.O. and Schimel, D.S. (Editors) *Exchange of Trace Gases Between Terrestrial Ecosystems and the Atmosphere*. John Wiley & Sons, New York, Chichester, p. 39-58.
- Conrad, R. and Seiler, W. (1988) Methane and hydrogen in seawater (Atlantic Ocean). *Deep-Sea Research*, **35**: 1,903-1,917.
- Craig, H. (1957) Isotopic standards for carbon and oxygen and correction factors for mass-spectrometric analysis of carbon dioxide. *Geochimica et Cosmochimica Acta*, **12**: 133-149.
- Crill, P.M. and Martens, C.S. (1986) Methane production from bicarbonate and acetate in an anoxic marine sediment. *Geochimica et Cosmochimica Acta*, **50**: 2,089-2,097.
- Crutzen, P.J. (1987) Role of the tropics in atmospheric chemistry. In R.E. Dickinson (Editor) *The Geophysics of Amazonia: Vegetation and Climate Interaction*. John Wiley, New York, p. 107-132.
- Crutzen, P.J. (1991) Methane's sinks and sources. *Nature*, **350**: 380-381.
- Cynar, F.J. and Yayanos, A.A. (1991) Enrichment and characterisation of a methanogenic bacterium from the oxic upper layer of the ocean. *Current Microbiology*, **23**: 89-96.
- Cynar, F.J. and Yayanos, A.A. (1992) The distribution of methane in the upper waters of the Southern California Bight. *Journal of Geophysical Research*, **97** (C7): 11,269-11,285.
- Dacey, J.W.H. and Wakeham, S.G. (1986) Oceanic dimethylsulfide: Production during zooplankton grazing on phytoplankton. *Science*, **233**: 1,314-1,316.
- Dando, P.R. and Hovland, M. (1992) Environmental effects of submarine seeping natural gas. *Continental Shelf Research*, **12**: 1,197-1,207.
- Dando, P.R., Austen, M., Burke, R., Kendall, M.A., Kennicutt II, M.C., Judd, A.G., Moore, D.C., O'Hara, S.C.M., Schmaljohann, R., Southward, R. and Southward, A.J. (1991) The ecology of a North Sea pockmark with an active methane seep. *Marine Ecology Progress Series*, **70**: 49-63.
- Dando, P.R., O'Hara, S.C.M., Schuster, U., Taylor, L.J., Clayton, C.J., Baylis, S. and Laier, T. (1994) Gas seepage from a carbonate-cemented sandstone reef on the Kattegat coast of Denmark. *Marine and Petroleum Geology*, **11**: 182-189.
- Daniels, L., Fuchs, G., Thauer, R.K. and Zeikus, J.G. (1977) Carbon monoxide oxidation by methanogenic bacteria. *Journal of Bacteriology*, **132**: 118-126.
- Davis, J.B. and Yarbrough, H.F. (1966) Anaerobic oxidations of hydrocarbons by *Desulfovibrio desulfuricans*. *Chemical Geology*, **1**: 137-144.
- DeAngelis, M.A. and Lee, C. (1994) Methane production during zooplankton grazing on marine phytoplankton. *Limnology and Oceanography*, **39**: 1,298-1,308.
- DeAngelis, M.A. and Lilley, M.D. (1987) Methane in the surface waters of Oregon estuaries and rivers. *Limnology and Oceanography*, **32**: 716-722.

- DeAngelis, M.A. and Scranton, M.I. (1993) Fate of methane in the Hudson River and estuary. *Global Biogeochemical Cycles*, **7**: 509-523.
- DeLaune, R.D., Smith, C.J. and Patrick, W.H. Jr. (1983) Methane release from Gulf coast wetlands. *Tellus Series B*, **35**: 8-15.
- DeRosa, M., DeRosa, S., Gambocorta, A., Minale, L. and Bullock, J.D. (1977) Chemical structure of the ester lipids of thermophilic acidophilic bacteria of the Caldariella groups. *Phytochemistry*, **16**: 1,961-1,965.
- Devol, A.H. (1983) Methane oxidation rates in the anaerobic sediments of Saanich Inlet. *Limnology and Oceanography*, **28**: 738-742.
- Devol, A.H. and Ahmed, S.I. (1981) Are high rates of sulphate reduction associated with anaerobic oxidation of methane? *Nature*, **291**: 407-408.
- Devol, A.H., Richey, J.E., Clark, W.A., King, S.A. and Martinelli, L.A. (1988) Methane emissions to the troposphere from the Amazonian floodplains. *Journal of Geophysical Research*, **93**: 1,583-1,592.
- Dickens, G.R., Paull, C.K., Wallace, P. and the ODP Leg 164 Scientific Party (1997) Direct measurement of *in situ* methane quantities in a large gas-hydrate reservoir. *Nature*, **385**: 426-428.
- Dickinson, R.E. and Cicerone, R. J. (1986) Future global warming from atmospheric trace gases. *Nature*, **319**: 109-115.
- Dlugokencky, E.J., Masaire, K.A., Lang, P.M., Trans, P.P., Steele, L.P. and Nisbett, E.G. (1994) A dramatic decrease in the growth rate of atmospheric methane in the northern hemisphere during 1992. *Geophysical Research Letters*, **21**: 45-48.
- Doddema, H.J. and Vogels, G.D. (1978) Improved identification of methanogenic bacteria by fluorescence microscopy. *Applied and Environmental Biology*, **36**: 752-754.
- Dörr, H., Katruff, L. and Levin, I. (1993) Soil texture parameterization of the methane uptake in aerated soils. *Chemosphere*, **26**: 697-713.
- Downing, A.L. and Truesdale, G.A. (1955) Some factors affecting the rate of solution of oxygen in water. *Journal of Applied Chemistry*, **5**: 570-581.
- Ehhalt, D.H. (1974) The atmospheric cycle of methane. *Tellus*, **26**: 58-70.
- Ehhalt, D.H. (1976) The atmospheric cycle of methane. In: H.G. Schlegel, G. Gottschalk and N. Pfennig (Editors) *Microbial Formation and Utilisation of Gases (H₂, CH₄, CO)*. E. Geltze, Göttingen, Germany, p. 12-22.
- Ehhalt, D.H. and Heidt, L.E. (1973) Vertical profiles of CH₄ in the troposphere and stratosphere. *Journal of Geophysical Research*, **78**: 5,265-5,271.
- Ehhalt, D.H. and Schmidt, U. (1978) Sources and sinks of atmospheric methane. *Pure and Applied Geophysics*, **116**: 452-463.
- Ehrlich, A., (1990) Agricultural contribution to global warming. In J. Leggett (Editor) *Global Warming: The Greenpeace Report*. Oxford University Press, Oxford, p. 400-420.

- Erickson, D.J. (1993) A stability dependent theory for air-sea gas exchange. *Journal of Geophysical Research*, **98**: 8,471-8,488.
- Evans, W.C. (1996) A gold mine of methane. *Nature*, **381**: 114-115.
- Fair, G.M., Geyr, J.C. and Okun, D.A. (1968) *Water and Wastewater Engineering*, Vol. 2. John Wiley & Sons, Inc., New York.
- Fenchel, T., Bernard, T.C., Esteban, G., Finlay, B.J., Hansen, P.J. and Iversen, N. (1995) Microbial diversity and activity in a Danish Fjord with anoxic deep water. *Ophelia*, **43**: 45-100.
- Fenchel, T. and Finlay, B.J. (1991) Synchronous division of an endosymbiotic methanogenic bacterium in the anaerobic ciliate *Plagiopyla frontata* (Kahl). *Journal of Protozoology*, **38**: 22-28.
- Fenchel, T. and Finlay, B.J. (1992) Production of methane and hydrogen by anaerobic ciliates containing symbiotic methanogens. *Archives of Microbiology*, **157**: 475-480.
- Floodgate, G.D. and Judd, A.G. (1992) The origins of shallow gas. *Continental Shelf Research*, **12**: 1,145-1,156.
- Fox, G.E., Magrum, L.J., Balch, W.E., Wolfe, R.S. and Woese, C.R. (1977) Classification of methanogenic bacteria by 16S ribosomal RNA classification. *Proceedings of the National Academy of Science of the United States of America*, **74**: 4,537-4,541.
- Fuglestad, J.S., Jonson, J.E. and Isaksen, I.S.A. (1994) Effects of reductions in stratospheric ozone on tropospheric chemistry through changes in photolysis rates. *Tellus Series B*, **46**: 172-192.
- Fung, I., John, J., Lerner, J., Matthews, E., Prather, M., Steele, L.P. and Fraser, P.J. (1991) Three-dimensional model synthesis of the global methane cycle. *Journal of Geophysical Research*, **96**: 13,033-13,065.
- Giani, D., Giani, L., Cohen, Y. and Krumbein, W.E. (1984) Methanogenesis in the hypersaline Solar Lake (Sinai). *FEMS Microbiology Letters*, **25**: 219-224.
- Gold, K. and Pollinger, U. (1971) Occurrence of endosymbiotic bacteria in marine dinoflagellates. *Journal of Phycology*, **7**: 264-265.
- Gold, T. and Soter, S. (1980) The deep-earth-gas hypothesis. *Scientific American*, **242**: 154-161.
- Green, P.N. (1992) Taxonomy of methylotrophic bacteria. In: J.C. Murrell and H. Dalton (Editors) *Methane and Methanol Utilisers*. Plenum Press, New York, p. 23-84.
- Griffiths, R.P., Caldwell, B.A., Cline, J.D., Broich, W.A. and Morita, R.Y. (1982) Field observations of methane concentrations and oxidation rates in the southeastern Bering Sea. *Applied and Environmental Microbiology*, **44**: 435-446.
- Gutsalo, L.K. (1982) On mantle helium, argon, and methane discharged in thermal spring waters of ocean margin and ridge areas. In: K.A. Fanning and F.T. Manheim (Editors) *The Dynamic Environment of the Ocean Floor*. Lexington Books, Lexington, Toronto, p. 417-437.
- Hahn, J. (1982) Geochemical fossils of a possibly archaeobacterial origin in ancient sediments. *Zentralblatt für Bakteriologie, Mikrobiologie und Hygiene, Abteilung 1, Originale*, **C3**: 40-52.

- Harvey, J.G. (1968) The flow of water through the Menai Straits. *Geophysical Journal. Royal Astronomical Society. London.*, **15**: 517-528.
- Harvey, J.G. (1972) Water temperatures at Menai Bridge pier, 1955-68. *Deutsche Hydrographische Zeitung*, **25**: 202-215.
- Henrichs, S.M. and Reeburgh, S.W. (1987) Anaerobic mineralisation of marine sediment organic matter: rates and role of anaerobic processes in the ocean carbon economy. *Geomicrobiology Journal*, **5**: 191-237.
- Her Majesty's Stationary Office (HMSO) Publication X22.04.22 (1988) *The Determination of Methane and Other Hydrocarbon Gases in Water 1988*. HMSO Books, London.
- Heyer, J., Berger, U. and Suckow, R. (1990) Methanogenesis in different parts of a brackish water ecosystem. *Limnologica*, **20**: 135-139.
- Hilpert, R., Winter, J., Hammer, W. and Kandler, O. (1981) The sensitivity of archaeobacteria to antibiotics. *Zentralblatt für Bakteriologie, Parasitenkunde, Infektionskrankheiten und Hygiene, Abteilung I, Originale*, **C2**: 11-20.
- Hinrichs, K.-U., Hayes, J.M., Sylva, S.P., Brewer, P.G. and DeLong, E.F. (1999) Methane-consuming archaeobacteria in marine sediments. *Nature*, **398**: 802-805.
- Hippe, H., Caspari, D., Fiebig, K. and Gottschalk, G. (1979) Utilisation of trimethylene and other n-methyl compounds for growth and methane formation by *Methanosarcina barkeri*. *Proceedings of the National Academy of Science of the United States of America*, **76**: 494-498.
- Hoehler, T.M., Alperin, M.J., Albert, D.B. and Martens, C.S. (1994) Field and laboratory studies of methane oxidation in an anoxic marine sediment: Evidence for a methanogen-sulfate reducer consortium. *Global Biogeochemical Cycles*, **8**: 451-463.
- Hogan, K.B., Hoffman, J.S. and Thompson, A.M. (1991) Methanogenesis on the greenhouse agenda. *Nature*, **354**: 181-182.
- Holzer, G. and Oró, J. (1979) Gas chromatographic-mass spectrometric analysis of neutral lipids from methanogenic and thermoacidophilic 'archaeobacteria'. *Journal of Chromatography*, **186**: 795-809.
- Houghton, J.T., Jenkins, G.J. and Ephraums, J.J. (Editors) (1990) Introduction. In: *Climate Change. The IPCC Scientific Assessment*, Cambridge University Press, Cambridge, p. xxxv-xxxix.
- Houghton, J.T., Callander, B.A. and Varney, S.K. (1992) *Climate Change 1992. The Supplementary Report to the IPCC Scientific Assessment*. Cambridge. Cambridge University Press.
- Houghton, R.A. and Woodwell, G.M. (1989) Global climate change. *Scientific American*, **260**: 18-25.
- Hovland, M. and Judd, A.G. (1988) *Seabed Pockmarks and Seepages*. Graham and Trotman, London, 293 p.
- Hovland, M., Judd, A.G. and Burke, R.A. (1993) The global flux of methane from shallow submarine sediments. *Chemosphere*, **26**: 559-578.

- Hutchin, P.R., Press, M.C., Lee, J.A. and Ashenden, T.W. (1996) Methane emission rates from an ombrotrophic mire show marked seasonality which is independent of nitrogen supply and soil temperature. *Atmospheric Environment*, **30**: 3,011-3,015.
- Ianotti, E.L., Kafkewitz, P., Wolin, M.J. and Bryant, M.P. (1973) Glucose fermentation products in *Ruminococcus albus* grown in continuous culture with *Vibrio succinogenes*: changes caused by interspecies transfer of H₂. *Journal of Bacteriology*, **114**: 1,231-1,240.
- Iturriaga, R. (1979) Bacterial activity related to sedimenting particulate matter. *Marine Biology*, **55**: 157-169.
- Ivanov, M.V., Lein, A.Y. and Gal'chenko, V.F. (1993) The global methane cycle in the ocean. *Geochemistry International*, **30**: 114-124.
- Iversen, N. (1996) Methane oxidation in coastal marine environments. In: J.C. Murrel and D.P. Kelly (Editors) *Microbiology of Atmospheric Trace Gases*. NATO ASI Series I 39, Springer-Verlag, Berlin, Heidelberg, p. 51-68.
- Iversen, N. and Jørgensen, B.B. (1985) Anaerobic methane oxidation rates at the sulfate-methane transition in marine sediments from Kattegat and Skagerrak (Denmark). *Limnology and Oceanography*, **30**: 944-955.
- Iversen, N. and Jørgensen, B.B. (1993) Diffusion coefficients of sulphate and methane in marine sediments: Influence on porosity. *Geochimica et Cosmochimica Acta*, **57**: 571-578.
- Iversen, N., Oremland, R.S. and Klug, M.J. (1987) Big Soda Lake (Nevada). 3. Pelagic methanogenesis and anaerobic methane oxidation. *Limnology and Oceanography*, **32**: 804-814.
- Jähne, B., Heinz, G. and Dietrich, W. (1987) Measurement of the diffusion coefficients of sparingly soluble gases in water. *Journal of Geophysical Research*, **92** (C10): 10,767-10,776.
- Jannasch, H.W. and Mottl, J. (1985) Geomicrobiology of deep-sea hydrothermal vents. *Science*, **229**: 717-725.
- Johnson, K.M., Davis, P.G. and Sieburth, J.McN. (1983) Diel variation of TCO₂ in the upper layer of oceanic waters reflects microbial composition, variation, and possibly methane cycling. *Marine Biology*, **77**: 1-10.
- Johnson, K.M., Hughes, J.E., Donaghay, P.L. and Sieburth, J.McN. (1990) Bottle-calibration static head space method for the determination of methane dissolved in seawater. *Analytical Chemistry*, **62**: 2,408-2,412.
- Jones, R.D. (1991) Carbon monoxide and methane distribution and consumption in the photic zone of the Sargosso Sea. *Deep-Sea Research*, **38**: 625-635.
- Jones, R.D. and Amador, J.A. (1993) Methane and carbon monoxide production, oxidation, and turnover times in the Caribbean Sea as influenced by the Orinoco River. *Journal of Geophysical Research*, **98** (C2): 2,353-2,359.
- Jones, M. and Spencer, C.P. (1970) The phytoplankton of the Menai Straits. *Journal du Conseil International pour l'Exploration de la Mer*, **33**: 169-180.
- Jones, W.J., Leigh, J.A., Mayer, F., Woese, C.R. and Wolfe, R.S. (1983) *Methanococcus jannaschii* sp. nov., an extremely thermophilic methanogen from a submarine hydrothermal vent. *Archives of Microbiology*, **136**: 254-261.

- Jørgensen, B.B. (1977) Bacterial sulfate reduction within reduced microniches of oxidized marine sediments. *Marine Biology*, **41**: 7-17.
- Jørgensen, B.B. and Revsbech, N.P. (1985) Diffusive boundary layers and the oxygen uptake of sediments and detritus. *Limnology and Oceanography*, **30**: 111-122.
- Judd, A.G. and Hovland, M. (1992) The evidence of shallow gas in marine sediments. *Continental Shelf Research*, **12**: 1,081-1,095.
- Kandler, O. and Hippe, H. (1977) Lack of peptidoglycan in the cell wall of Methanosarcina barkeri. *Archives of Microbiology*, **113**: 57-60.
- Kandler, O. and König, H. (1978) Chemical composition of the peptido-glycan-free cell walls of methanogenic bacteria. *Archives of Microbiology*, **118**: 141-152.
- Kanwisher, J. (1963) On the exchange of gases between the atmosphere and the sea. *Deep-Sea Research*, **10**: 195-207.
- Kaplan, W.A. and Wofsy, S.C. (1985) The biogeochemistry of nitrous oxide: A review. In: H.W. Jannasch and P.J.leB. Williams (Editors) *Advances in Aquatic Microbiology* **3**, Academic Press Inc. (London) Ltd, p. 181-206.
- Karl, D.M. and Tilbrook, B.P. (1994) Production and transport of methane in oceanic particulate matter. *Nature*, **368**: 732-734.
- Kaserer, H. (1905) Die Oxidation des Wasserstoffs durch Mikroorganismen. *Zentralblatt für Bakteriologie, Parasitenkunde und Infektionskrankheiten*, **16**: 618-696.
- Kelley, C.A., Martens, C.S. and Ussler, W. III (1995) Methane dynamics across a tidally flooded riverbank margin. *Limnology and Oceanography*, **40**: 1,112-1,129.
- Kemp, C.W., Curtis, M.A., Robrish, S.A. and Bowen, W.H. (1983) Biogenesis of methane in primate dental plaque. *FEBS Letters*, **155**: 61-64.
- Kenney, J.F. (1995) Comment on 'Mantle hydrocarbons: Abiotic or biotic?' by R. Sugisaki and K. Mimura. *Geochimica et Chosmochimica Acta*, **59**: 3,857-3,858.
- Khalil, M.A.K. and Rasmussen, R.A. (1983) Sources, sinks, and cycles of atmospheric methane. *Journal of Geophysical Research*, **88**: 5,131-5,144.
- Khalil, M.A.K. and Rasmussen, R.A. (1990) Atmospheric methane: recent global trends. *Environmental Science & Technology*, **24**: 549-553.
- Kiene, R.P. (1991) Production and consumption of methane in aquatic systems. In J.E. Rogers and W.B. Whitman (Editors) *Production and Consumption of Greenhouse Gases: Methane, Nitrogen Oxides and Halomethanes*. American Society for Microbiology, Washington, D.C., p. 111-146.
- Kiene, R.P., Ormeland, A.C., Miller, L.C. and Capone, D.G. (1986) Metabolism of reduced methylated sulphur compounds in aerobic sediments and pure culture of an estuarine methanogen. *Applied and Environmental Microbiology*, **52**: 1,037-1,045.
- Kiener, A. and Leisinger, T. (1983) Oxygen sensitivity of methanogenic bacteria. *Systematic and Applied Microbiology*, **4**: 305-312.

- King, G.M. (1984a) Utilisation of hydrogen, acetate and 'non-competitive' substrates by methanogenic bacteria in marine sediments. *Geomicrobiological Journal*, **3**: 275-306.
- King, G.M. (1984b) On the metabolism of trimethylamine, choline, and glycine betaine by sulfate-reducing and methanogenic bacteria in marine sediments. *Applied and Environmental Microbiology*, **48**: 719-725.
- King, G.M. (1990a) Regulation by light of methane emissions from a wetland. *Nature*, **345**: 513-515.
- King, G.M. (1990b) Dynamics and control of methane oxidation in a Danish wetland sediment. *FEMS Microbio Ecol.*, **74**: 309-324.
- King, G.M., Klug, M.J. and Lovley, D.R. (1983) Metabolism of acetate, methanol, and methylated amines in intertidal sediments of Lowes Cove, Maine. *Applied and Environmental Microbiology*, **45**: 1,848-1,853.
- Kling, G.W., Kipphut, G.W. and Miller, M.C. (1992) The flux of CO₂ and CH₄ from lakes and rivers in arctic Alaska. *Hydrobiologia*, **240**: 23-36.
- Klump, J.V. and Martens, C.S. (1981) Biogeochemical cycling in an organic rich coastal marine basin – II. Nutrient sediment-water exchange processes. *Geochimica et Cosmochimica Acta*, **45**: 101-121.
- Kniefel, H. (1979) Amines in algae. In: H.A. Hoppe, T. Levring and Y. Tanaka (Editors) *Marine Algae in Pharmaceutical Science*. De Gruyter, Berlin, p. 365-401.
- Kochevar, R.E., Childress, J.J., Fisher, C.R. and Minnich, E. (1992) The methane mussel: roles of symbiont and host in the metabolic utilisation of methane. *Marine Biology*, **112**: 389-401.
- König, H. and Stetter, K.O. (1982) Isolation and characterisation of *Methanolobus tindarius* sp. nov., a coccoid methanogen growing only on methanol and methylamines. *Zentralblatt für Bakteriologie, Mikrobiologie und Hygiene, Abteilung 1, Originale*, **C3**: 478-490.
- Kosiur, D.R. and Warford, A.L. (1979) Methane production and oxidation in Santa Barbara Basin sediments. *Estuarine and Coastal Marine Science*, **8**: 379-386.
- Kristjansson, J.K., Schönheit, P. and Thauer, R.K. (1982) Different K_S values for hydrogen of methanogen bacteria and sulfate reducing bacteria: an explanation for the apparent inhibition of methanogenesis by sulfate. *Archives of Microbiology*, **131**: 278-282.
- Kross, B.M. (1989) Diffusion loss of light hydrocarbons through caprocks: Part II Experimental studies and theoretical considerations. In: *Shallow Gas and Leaky Reservoirs*. Conference Proceedings, Stavanger, Norway, April 1989.
- Kvenvolden, K.A. (1988) Methane hydrates and global climate. *Global Biogeochemical Cycles*, **2**: 221-230.
- Laier, T., Jørgensen, N.O., Buchardt, B., Cederberg, T. and Kuijpers, A. (1992) Accumulation and seepages of biogenic gas in northern Denmark. *Continental Shelf Research*, **12**: 1,173-1,186.
- Lambert, G. and Schmidt, S. (1993) Reevaluation of the oceanic flux of methane – uncertainties and long term variations. *Chemosphere*, **26**: 579-589.
- Lammers, S. and Suess, E. (1994) An improved head-space analysis method for methane in seawater. *Marine Chemistry*, **47**: 115-125.

- Lammers, S., Suess, E., Mansurov, M.N. and Anikiev, V.V. (1995) Variations of atmospheric methane supply from the Sea of Okhotsk induced by the seasonal ice cover. *Global Biogeochemical Cycles*, **9**: 351-358.
- Lamontagne, R.A., Swinnerton, J.W., Linnenbom, V.J. and Smith, W.D. (1973) Methane concentrations in various marine environments. *Journal of Geophysical Research*, **78**: 5,317-5,324.
- Lamontagne, R.A., Swinnerton, J.W. and Linnenbom, V.J. (1974) C₁-C₄ hydrocarbons in the North and South Pacific. *Tellus*, **26**: 71-77.
- Large, P.J. (1983) *Methylotrophy and Methanogenesis*. Aspects of Microbiology 8, Cole, J.A., Knowles, C. J. and Schlessinger, D. (Series Editors), Van Nostrand Reinhold, Wokingham, U.K. 88 p.
- Lashof, D.A. and Ahuja, D.R. (1990) Relative contribution of greenhouse gas emissions to global warming. *Nature*, **344**: 529-531.
- Lees, V., Owens, N.J.P. and Murrell, J.C. (1991) Nitrogen metabolism in marine methanotrophs. *Archives of Microbiology*, **157**: 60-65.
- Lidstrom, M.E. (1983) Methane oxidation in Framvaren, an anoxic marine fjord. *Limnology and Oceanography*, **28**: 1,247-1,251.
- Lilley, M.D., Baross, J.A. and Gordon, L.I. (1983) Reduced gases and bacteria in hydrothermal fluids: The Galapagos spreading center and 21°N east Pacific rise. In: P.A. Rona, K. Boström, L. Laubier and K.L. Smith Jr (Editors) *Hydrothermal Processes at Seafloor Spreading Centres*. Plenum Press, New York, p. 411-421.
- Lilley, M.D., DeAngelis, M. A. and Gordon, L.I. (1982) CH₄, H₂, CO, and N₂ in submarine hydrothermal vent waters. *Nature*, **300**: 48-50.
- Liss, P.S. (1973) Processes of gas exchange across an air-water interface. *Deep-Sea Research*, **20**: 221-238.
- Liss, P.S. (1983) Gas transfer: Experiments and geochemical implications. In: P.S. Liss and W.G.N. Slinn (Editors) *Air-Sea Exchange of Gases and Particles*. Reidel, p. 241-298.
- Liss, P.S. and Merlivat, L. (1986) Air-sea gas exchange rates: introduction and synthesis. In: P. Buat-Menard (Editor) *NATO ASI Series C Mathematical and Physical Sciences*, **185**: 113-127.
- Lovelock, J.E. (1982) *GAIA, a New Look at Life on Earth*. Oxford University Press, Oxford.
- Lovley, D.R., Dwyer, D. and Klug, M.J. (1982) Kinetic analysis of competition between sulfate reducers and methanogens for hydrogen in sediments. *Applied and Environmental Microbiology*, **43**: 1,373-1,379.
- Lovley, D.R. and Klug, M.J. (1983) Methanogenesis from methanol and from hydrogen and carbon dioxide in the sediments of a eutrophic lake. *Applied and Environmental Biology*, **45**: 1,310-1,315.
- Lowe, D.C., Brenninkmeijer, C.A.M., Manning, M.R., Sparks, R. and Wallace, G. (1988) Radiocarbon determination of atmospheric methane at Baring Head, New Zealand. *Nature*, **332**: 522-525.

- Lucas, I.A.N. (1982) Observations on Noctiluca scintillans McCartney (Ehrenb.) (Dinophyceae) with notes on an intracellular bacterium. *Journal of Plankton Research*, **4**: 401-409.
- MacDonald, G.J. (1983) The many origins of natural gas. *Journal of Petroleum Geology*, **5**: 341-362.
- MacKenzie, A.S. and Quigley, T.M. (1988) Principles of geochemical prospect appraisal. *American Association of Petroleum Geologists (Bulletin)*, **72**: 399-415.
- Mah, R.A. (1980) Isolation and characterisation of Methanococcus mazei. *Current Microbiology*, **3**: 321-326.
- Mah, R.A., Ward, D.M., Baresi, L. and Glass, T. (1977) Biogenesis of methane. *Annual Review of Microbiology*, **31**: 309-341.
- Mann, K.H. and Lazier, J.R.N. (1991) *Dynamics of Marine Ecosystems. Biological-Physical Interactions in the Oceans*. Blackwell Scientific Publications, 466 pp.
- Martens, C.S. (1982) Methane production, consumption, and transport in the interstitial waters of coastal marine sediments. In: K.A. Fanning and F.T. Manheim (Editors) *The Dynamic Environment of the Ocean Floor*. Lexington Books, Lexington, Toronto, p. 187-203.
- Martens, C.S. and Berner, R.A. (1974) Methane production in the interstitial waters of sulfate-depleted marine sediments. *Science*, **185**: 1,167-1,169.
- Martens, C.S. and Berner, R.A. (1977) Interstitial water chemistry of anoxic Long Island Sound sediments. *Limnology and Oceanography*, **22**: 10-25.
- Martens, C.S. and Klump, J.V. (1980) Biogeochemical cycling in an organic-rich coastal marine basin – I. Methane sediment-water exchange processes. *Geochimica et Cosmochimica Acta*, **44**: 471-490.
- Martens, C.S. and Klump, J.V. (1984) Biogeochemical cycling in an organic-rich coastal marine basin - IV. An organic carbon budget for sediments dominated by sulfate reduction and methanogenesis. *Geochimica et Cosmochimica Acta*, **48**: 1,987-2,004.
- Martens, C.S., Blair, N.E., Green, C.D. and Des Marais, D.J. (1986) Seasonal variations in the stable carbon isotopic signature of biogenic methane in a coastal sediment. *Science*, **233**: 1,300-1,303.
- Martens, C.S., Kelley, C.A., Chanton, J.P. and Showers, W.J. (1992) Carbon and hydrogen isotopic characterisation of methane from wetlands and lakes of the Yukon Kuskokwim Delta, Western Alaska. *Journal of Geophysical Research*, **97 (D15)**: 16,689-16,701.
- Martin, W. and Müller, M. (1998) The hydrogen hypothesis for the first eukaryote. *Nature*, **392**: 37-41.
- Marty, D.G. (1993) Methanogenic bacteria in seawater. *Limnology and Oceanography*, **38**: 452-456.
- Matson, J.V. and Characklis, W.G. (1976) Diffusion into microbial aggregates. *Water Research*, **10**: 877-885.
- Mosier, A., Schimel, D., Valentine, D., Bronson, K. and Parton, W. (1991) Methane and nitrous oxide in native, fertilised and cultivated grassland. *Nature*, **350**: 330-332.

- Müller, J.A. (1966) Oxygen diffusion through a pure culture of *Zooglea ramigera*. *Proceedings of the 21st Annual Industrial Waste Conference*, Purdue, p. 962-995.
- Müller, J.F. (1992) Geophysical distribution and seasonal variation of surface emissions and deposition velocities of atmospheric trace gases. *Journal of Geophysical Research*, **97** (D4): 3,787-3,804.
- Müller, V., Blaut, M. and Gottschalk, G. (1993) Bioenergetics of methanogenesis. In: J.G. Ferry (Editor) *Methanogenesis – Ecology, Physiology, Biochemistry and Genetics*. Chapman & Hall, New York, p. 360-406.
- National River Authority (NRA) Bangor (1993) *Menai Strait Catchment Management Plan*. Consultation Report, June 1993.
- Niewöhner, C., Hensen, C., Kasten, S., Zabel, M. and Schulz, H.D. (1998) Deep sulfate reduction completely mediated by anaerobic methane oxidation in sediments of the upwelling area off Namibia. *Geochimica et Cosmochimica Acta*, **62**: 455-464.
- Nisbett, E.G. (1990) The end of the ice age. *Canadian Journal of Earth Science*, **27**: 148-157.
- Nottingham, P.M. and Hungate, R.E. (1968) Isolation of methanogenic bacteria from feces of man. *Journal of Bacteriology*, **96**: 2,178-2,179.
- Novelli, P.C., Masarie, K.A., Trans, P.P. and Lang, P.M. (1994) Recent changes in atmospheric carbon monoxide. *Science*, **263**: 1,587-1,590.
- Odelson, D.A. and Breznak, J.A. (1983) Volatile fatty acid production by the hindgut microbiota of xylophagous termites. *Applied and Environmental Microbiology*, **45**: 1,602-1,613.
- Oke, T.R. (1978) *Boundary Layer Climates*, Methuen, London, New York, 372p.
- Oremland, R.S. (1979) Methanogenic activity in plankton samples and fish intestines: a mechanism for *in situ* methanogenesis in oceanic surface waters. *Limnology and Oceanography*, **24**: 1,136-1,141.
- Oremland, R.S. (1988) Biogeochemistry of methanogenic bacteria. In: Zehnder, A.J.B. (Editor) *Biology of Anaerobic Microorganisms*. John Wiley & Sons, New York, p. 641-705.
- Oremland, R.S. and Culbertson, C.W. (1992) Importance of methane-oxidizing bacteria in the methane budget as revealed by the use of a specific inhibitor. *Nature*, **356**: 421-423.
- Oremland, R.S., Marsh, L.M. and Polcin, S. (1982) Methane production and simultaneous sulphate reduction in anoxic salt marsh sediments. *Nature*, **296**: 143-145.
- Oremland, R.S., Kiene, R.P., Mathrani, I.M., Whiticar, M.J. and Boone, D.R. (1989) Description of an estuarine methylotrophic methanogen which grows on dimethyl sulfide. *Applied and Environmental Biology*, **55**: 994-1,002.
- Owens, N.J.P., Law, C.S., Mantoura, R.F.C., Burkill, P.H. and Llewellyn, C.A. (1991) Methane flux to the atmosphere from the Arabian Sea. *Nature*, **354**: 293-295.
- Panganiban, A.T. Jr., Patt, T.E., Hart, W. and Hanson, R.S. (1979) Oxidation of methane in the absence of oxygen in lake water samples. *Applied and Environmental Microbiology*, **23**: 303-309.

- Patra, P.K., Lal, S., Venkataramani, S., Gauns, M. and Sarma, V.V.S.S. (1998) Seasonal variability in distribution and fluxes of methane in the Arabian Sea. *Journal of Geophysical Research*, **103** (C1): 1,167-1,176.
- Pearman, G.I. and Fraser, P.J. (1988) Sources of increased methane. *Nature*, **332**: 489-490.
- Piccot, S.D., Back, L., Srinivasan, S. and Kersteter, S.L. (1996) Global methane emissions from minor anthropogenic sources and biofuel combustion in residual stoves. *Journal of Geophysical Research*, **101**(D17): 22,757-22,766.
- Priemé, A. (1994) Production and emission of methane in a brackish and a freshwater wetland. *Soil Biology and Biochemistry*, **26**: 7-18.
- Prinn, R.G. (1994) The interactive atmosphere: Global atmospheric-biospheric chemistry. *Ambio*, **23**: 50-61.
- Ramanathan, V. (1988) The greenhouse theory of climatic change: a test by an inadvertent global experiment. *Science*, **240**: 293-299.
- Rasmussen, R.A. and Khalil, M.A.K. (1981a) Increases in the concentration of atmospheric methane. *Atmospheric Environment*, **15**: 883-886.
- Rasmussen, R.A. and Khalil, M.A.K. (1981b) Atmospheric methane (CH₄): Trends and seasonal cycles. *Journal of Geophysical Research*, **86**: 9,826-9,832.
- Rasmussen, R.A. and Khalil, M.A.K. (1984) Atmospheric methane in the recent and ancient atmospheres: concentrations, trends, and interhemispheric gradient. *Journal of Geophysical Research*, **89** (D7): 11,599-11,605.
- Reeburgh, W.S. (1976) Methane consumption in Cariaco Trench waters and sediments. *Earth and Planetary Science Letters*, **28**: 337-344.
- Reeburgh, W.S. (1980) Anaerobic methane oxidation: rate depth distributions in Skan Bay sediments. *Earth and Planetary Science Letters*, **28**: 345-352.
- Reeburgh, W.S. (1982) A major sink and flux control for methane in marine sediments: anaerobic consumption. In: K. Fanning and F. Manheim (Editors) *Dynamic Environment of the Ocean Floor*, Heath, Lexington, p. 203-217.
- Reeburgh, W.S. and Heggie, D.T. (1977) Microbial methane consumption reactions and their effect on methane distributions in freshwater and marine environments. *Limnology and Oceanography*, **22**: 1-9.
- Reeburgh, W.S., Ward, S.C., Whalen, K.A., Sandbeck, K.A., Kilpatrick, K.A. and Kerkhof, L.J. (1991) Black Sea methane geochemistry. *Deep-Sea Research*, **38**: 1,189-1,210.
- Reeburgh, W.S., Whalen, S.C. and Alperin, M.J. (1993) The role of methylotrophy in the global methane budget. In: J.C. Murrell and D.P. Kelly (Editors) *Microbial Growth on C₁ Compounds*. Andover, England, p. 1-14.
- Rice, D.D. and Claypool, G.E. (1981) Generation, accumulation, and resource potential of biogenic gas. *American Association of Petroleum Geologists (Bulletin)*, **65**: 5-25.
- Richey, J.E., Devol, A.H., Wofsy, S.C., Victoria, R. and Riberio, M.N.G. (1988) Biogenic gases and the oxidation and reduction of carbon in Amazon river and floodplain waters. *Limnology and Oceanography*, **33**: 551-561.

- Robertson, A.M. and Wolfe, R.S. (1970) ATP pools in *Methanobacterium*. *Journal of Bacteriology*, **102**: 43-51.
- Robinson, J.A. and Tiedje, J.M. (1984) Competition between sulfate-reducing and methanogenic bacteria for H₂ under resting and growing conditions. *Archives of Microbiology*, **137**: 26-32.
- Rudd, J.W.M. and Hamilton, R.D. (1975) Factors controlling rates of methane oxidation and the distribution of the methane oxidizers in a small stratified lake. *Archives of Hydrobiology*, **75**: 522-538.
- Rudd, J.M.W. and Taylor, C.D. (1980) Methane cycling in aquatic environments. *Advances in Aquatic Microbiology*, **2**: 77-141.
- Rudd, J.W.M., Furutani, A., Flett, R.J. and Hamilton, R.D. (1976) Factors controlling methane oxidation in shield lakes: the role of nitrogen fixation and oxygen concentration. *Limnology and Oceanography*, **21**: 357-364.
- Rudolph, J. (1994) Anomalous methane. *Nature*, **368**: 19-20.
- Sansone, F.J. and Martens, C.S. (1978) Methane oxidation in Cape Lookout Bight, North Carolina. *Limnology and Oceanography*, **23**: 349-355.
- Sansone, F.J. and Martens, C.S. (1981) Methane production from acetate and associated methane fluxes from anoxic coastal sediments. *Science*, **211**: 707-709.
- Schauffler, S.M. and Daniel, J.S. (1994) On the trends of stratospheric circulation changes on trace gas trends. *Journal of Geophysical Research*, **99**: 25,747-25,754.
- Schink, B. and Zeikus, J.G. (1980) Microbial methanol formation: a major endproduct of pectin metabolism. *Current Microbiology*, **4**: 387-389.
- Schmaljohann, R. (1996) Methane dynamics in the sediment and water column of Kiel Harbour (Baltic Sea). *Marine Ecology Progress Series*, **131**: 263-273.
- Schmitt, M., Faber, E., Botz, R. and Stoffers, P. (1991) Extraction of methane from seawater using ultrasonic vacuum degassing. *Analytical Chemistry*, **63**: 529-532.
- Schoell, M. (1980) The hydrogen and carbon isotopic composition of methane from natural gases of various origins. *Geochimica et Cosmochimica Acta*, **44**: 649-661.
- Schoell, M. (1983) Genetic characterisation of natural gases. *American Association of Petroleum Geologists (Bulletin)*, **67**: 2,225-2,238.
- Schomburg, G. (1990) *Gas Chromatography. A practical course*. VCH Verlagsgesellschaft mbH, Weinheim (Germany) and VCH Publishers Inc., New York (USA).
- Schönheit, P., Kristjansson, J.K. and Thauer, R.K. (1982) Kinetic mechanism for the ability of sulfate reducers to out-compete methanogens for acetate. *Archives of Microbiology*, **132**: 285-288.
- Schuster, U. (1994) Microbial methane oxidation in marine sediment around intertidal gas seeps. Ph.D. Thesis. University of Essex. 226 pp.
- Schütz, H., Schröder, P. and Rennenberg, H. (1991) Role of plants in regulating the methane flux to the atmosphere. In: T.H. Sharkey, E.A. Holland and H.A. Mooney (Editors) *Trace Gas Emissions by Plants*. Academic Press, New York, p. 29-63.

- Scranton, M.I. (1988) Temporal variations in the methane content of the Cariaco Trench. *Deep-Sea Research*, **35**: 1,511-1,523.
- Scranton, M.I. and Brewer, P.G. (1977) Occurrence of methane in the near-surface waters of the western subtropical North-Atlantic. *Deep-Sea Research*, **24**: 127-138.
- Scranton, M.I. and Brewer, P.G. (1978) Consumption of dissolved methane in the deep ocean. *Limnology and Oceanography*, **23**: 1,207-1,213.
- Scranton, M.I. and Farrington, J.W. (1977) Methane production in the waters off Walvis Bay. *Journal of Geophysical Research*, **82**: 4,947-4,953.
- Scranton, M.I. and McShane, K. (1991) Methane fluxes in the southern North Sea: The role of European rivers. *Continental Shelf Research*, **11**: 37-52.
- Scranton, M.I., Crill, P., DeAngelis, M.A., Donaghay, P.L. and Sieburth, J.McN. (1993) The importance of episodic events in controlling the flux of methane from an anoxic basin. *Global Biogeochemical Cycles*, **7**: 491-507.
- Scranton, M.I., Donaghay, P. and Sieburth, J.McN. (1995) Nocturnal methane accumulation in the pycnocline of an anoxic estuarine basin. *Limnology and Oceanography*, **40**: 666-672.
- Sebacher, D.I., Harriss, R.C. and Bartlett, K.B. (1983) Methane flux across the air-water interface: air velocity effects. *Tellus Series B*, **35**: 103-109.
- Seiler, W., Conrad, R. and Scharffe, D. (1984) Field studies of methane emission from termite nests into the atmosphere and measurements of methane uptake by tropical soils. *Journal of Atmospheric Chemistry*, **1**: 171-186.
- Shanks, A.L. and Reeder, M.L. (1993) Reducing microzones and sulfide production in marine snow. *Marine Ecology Progress Series*, **96**: 43-47.
- Shine, K.P., Derwent, R.G., Wuebbles, D.J. and Morcrette, J.-J. (1990) Radiative forcing of climate. In: J.T. Houghton, G.J. Jenkins and J.J. Ephraums (Editors) *Climate Change: The IPCC Scientific Assessment*, Cambridge University Press, Cambridge, p. 41-68.
- Sieburth, J.McN. (1979) Protected Microbial Habitats. In: *Sea Microbes*, Oxford University Press, New York, p. 39-69.
- Sieburth, J.McN. (1987) Contrary habitats for redox-specific processes: methanogenesis in oxic waters and oxidation in anoxic waters. In: M.A. Sleight (Editor) *Microbes in the Sea*. Halsted Press, Chichester, England, p. 11-38.
- Sieburth, J.McN. (1988) The nanoplankton peak in the dim oceanic pycnocline: is it sustained by microparticulates and their bacterial consortia? In: C.R. Agegian (Editor) *Biogeochemical Cycling and Fluxes Between the Deep Euphotic Zone and Other Oceanic Realms*. NOAA National Undersea Research Program, Rockville, MD, Research Report 88-1.
- Sieburth, J.McN. (1991) Methane and hydrogen sulfide in the pycnocline: A result of tight coupling of photosynthetic and 'benthic' processes in stratified waters. In J.E. Rogers and W.B. Whitman (Editors) *Microbial Production and Consumption of Greenhouse Gases: Methane, Nitrogen Oxides and Halomethanes*. American Society of Microbiology, Washington D.C., p. 147-174.

- Sieburth, J.McN. (1993) C₁ bacteria in the water column of Chesapeake Bay, USA. I. Distribution of sub-populations of O₂-tolerant, obligately anaerobic, methylotrophic methanogens that occur in microniches reduced by their bacterial consorts. *Marine Ecology Progress Series*, **95**: 67-80.
- Sieburth, J.McN., Johnson, P.W., Church, V.M. and Laux, D.C. (1993a) C₁ bacteria in the water column of Chesapeake Bay, USA. III. Immunologic relationships of the type species of marine monomethylamine- and methane-oxidising bacteria to wild estuarine and oceanic cultures. *Marine Ecology Progress Series*, **95**: 91-102.
- Sieburth, J.McN., Johnson, P.W., Eberhardt, M.A., Sieracki, M.E., Lidstrom, M. and Laux, D. (1987) The first methane-oxidizing bacterium from the upper mixing layer of the deep ocean: *Methylomonas pelagica* sp. nov. *Current Microbiology*, **14**: 285-293.
- Sieburth, J.McN., Johnson, P.W., Macario, A.J.L. and Conway de Macario, E.C. (1993b) C₁ bacteria in the water column of Chesapeake Bay, USA. II. The dominant O₂ and H₂S tolerant methylotrophic methanogens, coenriched with their oxidative and sulphate reducing bacterial consorts, are all new immunotypes and probably include new taxa. *Marine Ecology Progress Series*, **95**: 81-89.
- Siewing, R. (1980) 4.5 Stoffwechsel der Kohlenhydrate. In *Lehrbuch der Zoologie. Band I - Allgemeine Zoologie*. 3. Auflage. Gustav Fischer Verlag, Stuttgart, New York, p. 88-92.
- Simmonds, P.G., Derwent, R.G., McCulloch, A., O'Doherty, S. and Gaudry, S. (1996) Long-term trends in concentrations of halocarbons and radiatively active trace gases in Atlantic and European air masses monitored at Mace Head, Ireland from 1987-1994. *Atmospheric Environment*, **30**: 4,041-4,063.
- Simpson, J.H., Forbes, A.M.G. and Gould, W.J. (1971) Electromagnetic observations of water flow in the Menai Straits. *Geophysical Journal. Royal Astronomical Society. London*, **24**: 245-253.
- Small, L.F., Fowler, S.W. and Ünlü, M.Y. (1979) Sinking rates of natural copepod fecal pellets. *Marine Biology*, **51**: 233-241.
- Smith, G.C. and Floodgate, G.D. (1992) Chemical methods for estimating the concentration of methanogenic bacteria in marine cores. *Continental Shelf Research*, **12**: 1,187-1,196.
- Smith, G.N. and Smith, I.G.N. (1998) *Elements of Soil Mechanics*. Seventh Edition. Blackwell Science, Oxford. 494 pp.
- Smith, R.L. and Oremland, R.S. (1987) Big Soda Lake (Nevada). 2. Pelagic sulfate reduction. *Limnology and Oceanography*, **32**: 794-803.
- Söhngen, N.L. (1906) Über Bakterien, welche Methan als Kohlenstoffnahrung und Energiequelle gebrauchen. *Zentralblatt für Bakteriologie, Parasitenkunde und Infektionskrankheiten, Abstrakt 2*, **15**: 513-517.
- Sørensen, J., Christensen, D. and Jørgensen, B.B. (1981) Volatile fatty acids and hydrogen as substrates for sulfate-reducing bacteria in anaerobic marine sediment. *Applied and Environmental Microbiology*, **42**: 5-11.
- Sorrell, B.K. and Boon, P.I. (1992) Biogeochemistry of Billabong sediments. 2. Seasonal variations in methane production. *Freshwater Biology*, **27**: 435-445.

- Sowers, K.R. and Ferry, J.G. (1983) Isolation and characterisation of a methylotrophic marine methanogen, *Methanococcoides methylmutens* gen. nov., sp. nov. *Applied and Environmental Microbiology*, **45**: 684-690.
- Spiess, F.N., MacDonald, K.C., Atwater, T., Ballard, R., Carranza, A., Cardoba, D., Cox, C., Diaz Garcia, V.M., Francheteau, J., Guerrero, J., Hawkins, J., Haymon, R., Hessler, R., Jutea, T., Kastner, M., Larson, R., Luyendyk, B., MacDougall, J.D., Miller, S., Normark, W., Orcutt, J. and Rangin, C. (1980) East Pacific Rise: Hot springs and geophysical experiments. *Science*, **207**: 1,421-1,433.
- Stanier, R.Y., Ingraham, J.L., Wheelis, M.L. and Painter, P.R. (1987) *General Microbiology*. 5th Edition. Macmillan Education Ltd., Houndsmill & London, 689 p.
- Steele, L.P. and Lang, P.M. (1991) Atmospheric methane concentrations – the NOAA/CMDL global cooperative flask sampling network, 1983-1988. ORNL/CDIAC-42. Springfield, VA: National Technical Information Service.
- Steele, L.P., Fraser, P.J., Rasmussen, R.A., Khalil, M.A.K., Conway, T.J., Crawford, A.J., Gammon, R.H., Masarie, K.A. and Thoning, K.W. (1987) The global distribution of methane in the troposphere. *Journal of Atmospheric Chemistry*, **5**: 125-171.
- Steele, L.P., Dlugokencky, E.J., Lang, P.M., Tans, P.P., Martin, R.C. and Masarie, K.A. (1992) Slowing down of the global accumulation of atmospheric methane during the 1980s. *Nature*, **358**: 313-316.
- Stetter, K.O., Thomm, M., Winter, J., Wildgruber, A., Huber, H., Zillig, W., Jane-Covic, D., König, H., Palm, P. and Wunderl, S. (1981) *Methanothermus fervidus* sp. nov., a novel extremely thermophilic methanogen isolated from an Icelandic hot spring. *Zentralblatt für Bakteriologie, Parasitenkunde, Infektionskrankheiten und Hygiene, Abteilung 1, Originale*, **C2**: 166-178.
- Stevens, C.M. and Engelkemeir, A. (1988) Stable carbon isotopic composition of methane from some natural and anthropogenic sources. *Journal of Geophysical Research*, **93 (D1)**: 725-733.
- Sugimoto, A., Inoue, T., Kirtibutr, N. and Abe, T. (1998) Methane oxidation by termite mounds estimated by the carbon isotopic composition of methane. *Global Biogeochemical Cycles*, **12**: 595-605.
- Sugisaki, R. and Mimura, K. (1994) Mantle hydrocarbons: Abiotic or biotic? *Geochimica et Cosmochimica Acta*, **58**: 2,527-5,242.
- Sugisaki, R. and Mimura, K. (1995) Reply to Comment by J.F. Kenney on 'Mantle hydrocarbons: Abiotic or biotic?' *Geochimica et Cosmochimica Acta*, **59**: 3,859-3,861.
- Sugisaki, R., Mimura, K. and Kato, M. (1994) Shock synthesis of light hydrocarbon gases from H₂ and CO: Its role in astrophysical processes. *Geophysical Research Letters*, **21**: 1,031-1,034.
- Svensson, B.H. and Rosswall, T. (1984) *In situ* methane production from acid peat in plant communities with different moisture regimes in a subarctic mire. *Oikos*, **43**: 341-350.
- Swinnerton, J.W., Linnenbom, V.J. and Cheek, C.H. (1962) Determination of dissolved gases in aqueous solutions by gas chromatography. *Analytical Chemistry*, **34**: 483-485.
- Swinnerton, J.W., Linnenbom, V.J. and Cheek, C.H. (1969) Distribution of methane and carbon monoxide between the atmosphere and natural water. *Environmental Science and Technology*, **3**: 836-838.

- Tett, P. (1987) Plankton. In J.M. Baker and W.J. Wolff (Editors) *Biological Surveys of Estuaries and Coasts*. Cambridge University Press, Cambridge, p. 328-335.
- Thompson, A.M. and Cicerone, R.J. (1986) Possible perturbations to atmospheric CO, CH₄, and OH. *Journal of Geophysical Research*, **91**: 10,853-10,864.
- Tilbrook, B.D. and Karl, D.M. (1995) Methane sources, distributions and sinks from California coastal waters to the oligotrophic North Pacific Gyre. *Marine Chemistry*, **49**: 51-64.
- Topp, E. and Hanson, R.S. (1991) Metabolism of radiatively active trace gases by methane-oxidising bacteria. In: J.E. Rogers and W.E. Whitman (Editors) *Microbial Production and Consumption of Greenhouse Gases: Methane, Nitrogen Oxides and Halomethanes*, American Society for Microbiology, Washington, D.C., p. 71-90.
- Tornabene, T.G., Langworthy, T.A., Holzer, G. and Oró, J. (1979) Squalenes, phytanes and other isoprenoids as major neutral lipids of methanogenic and thermoacidophilic 'archaeobacteria' *Journal of Molecular Evolution*, **13**: 73-83.
- Traganzo, E.D., Swinnerton, J.W. and Cheek, C.H. (1979) Methane supersaturation and ATP zooplankton blooms in near-surface waters of the Western Mediterranean and the subtropical North Atlantic Ocean. *Deep-Sea Research*, **26A**: 1,237-1,245.
- Tyler, S.C. (1991) The global methane budget. In: J.E. Rogers and W.B. Whitman (Editors) *Microbial Production and Consumption of Greenhouse Gases: Methane, Nitrogen Oxides, and Halomethanes*. American Society for Microbiology, Washington, D.C., p. 7-38.
- Uhlig, G. and Sahling, G. (1990) Long-term studies on *Noctiluca scintillans* in the German Bight: Population dynamics and red tide phenomena 1968-1988. *Netherlands Journal of Sea Research*, **25**: 101-112.
- Ullman, W.J. and Aller, R.C. (1982) Diffusion coefficients in nearshore marine sediments. *Limnology and Oceanography*, **27**: 552-556.
- Upstill-Goddard, R.C., Rees, A.P. and Owens, N.J.P. (1996) Simultaneous high-precision measurements of methane and nitrous oxide in water and seawater by single phase equilibration gas chromatography. *Deep-Sea Research*, **43**: 1,669-1,682.
- Vaghjiani, G.L. and Ravishankara, A.R. (1991) New measurement of the rate coefficient for the reaction of OH with methane. *Nature*, **350**: 406-409.
- Valentine, D.W., Holland, E.A. and Schimel, D.S. (1994) Ecosystem and physiological controls over methane production in northern wetlands. *Journal of Geophysical Research*, **99 (D1)**: 1,563-1,571.
- Van Bruggen, J.J.A., Stumm, C.K. and Vogels, G.D. (1983) Symbiosis of methanogenic bacteria and sapropelic protozoa. *Archives of Microbiology*, **136**: 89-95.
- Wakeham, S.G. and Lee, C. (1993) Production, transport, and alteration of particulate organic matter in the marine water column. In: M.H. Engel and S.A. Macko (Editors) *Organic Geochemistry*. Plenum Press, New York, p. 145-169.
- Wanninkhof, R.H. (1992) Relationship between wind speed and gas exchange over the ocean. *Journal of Geophysical Research*, **97**: 7,373-7,382.
- Wanninkhof, R. and Bliven, L. (1991) Relationship between gas exchange, wind speed and radar backscatter in a large wind-wave tank. *Journal of Geophysical Research*, **96**: 2,785-2,796.

- Wanninkhof, R., Ledwell, J.R., and Broecker, W.S. (1985) Gas exchange-wind speed relationship measured with sulfur hexafluoride on a lake. *Science*, **227**: 1,224-1,226.
- Ward, B.B. (1992) The subsurface methane maximum in the Southern California Bight. *Continental Shelf Research*, **12**: 735-752.
- Ward, B.B. and Kilpatrick, K.A. (1990) Relationship between substrate concentration and oxidation of ammonium and methane in a stratified water column. *Continental Shelf Research*, **10**: 1,193-1,208.
- Ward, B.B. and Kilpatrick, K.A. (1993) Methane oxidation associated with mid-depth methane maxima in the Southern Ocean. *Continental Shelf Research*, **13**: 1,111-1,122.
- Ward, B.B., Kilpatrick, K.A., Novelli, P.C and Scranton, M.I. (1987) Methane oxidation and methane fluxes in the ocean surface layer and deep anoxic waters. *Nature*, **327**: 226-229.
- Ward, D.M. and Winfrey, M.R. (1985) Interactions between methanogenic and sulfate-reducing bacteria in sediments. *Advances in Aquatic Microbiology*, **3**: 141-179.
- Watanabe, S., Higashitani, N., Tsurushima, N. and Tsunogai, S. (1995) Methane in the western North Pacific. *Journal of Oceanography*, **51**: 39-60.
- Watson, A.J., Upstill-Goddard, R.C. and Liss, P.S. (1991) Air-sea exchange in rough and stormy seas measured by a dual-tracer technique. *Nature*, **349**: 145-147.
- Watson, R.T., Rodhe, H., Oeschger, H. and Siegenthaler, U. (1990) Greenhouse gases and aerosols. In J.T. Houghton, G.J. Jenkins, and J.J. Ephraums (Editors) *Climate Change: The IPCC Scientific Assessment*. Cambridge University Press, Cambridge, p. 1-40.
- Weiss, R.F. and Price, B.A. (1980) Nitrous oxide solubility in water and seawater. *Marine Chemistry*, **8**: 347-359.
- Whalen, S.C. and Reeburgh, R.S. (1990) Consumption of atmospheric methane by tundra soils. *Nature*, **346**: 160-162.
- Whiticar, M.J. (1982) The presence of methane bubbles in acoustically turbid sediments of Eckernförder Bay, Baltic Sea. In: K.A. Fanning and F.T. Manheim (Editors) *The Dynamic Environment of the Ocean Floor*. Lexington, USA, p. 219-235.
- Whittenbury, R., Phillips, K.C. and Wilkinson, J.F. (1970) Enrichment, isolation and some properties of methane-utilising bacteria. *Journal of General Microbiology*, **61**: 205-218.
- Wiesenburg, D.A. and Guinasso, N.L. Jr. (1979) Equilibrium solubilities of methane, carbon monoxide, and hydrogen in water and sea water. *Journal of Chemical and Engineering Data*, **24**: 356-360.
- Wilkness, P.E., Lamontagne, R.A., Larson, R.E. and Swinnerton, J.W. (1978) Atmospheric trace gases and land and sea breezes at the Sepic River coast of Papua New Guinea. *Journal of Geophysical Research*, **83**: 3,672-3,674.
- Williams, P.J.leB. and Jenkinson, N.W. (1982) A transportable microprocessor-controlled precise Winkler titration suitable for field station and shipboard use. *Limnology and Oceanography*, **27**: 576-584.
- Williams, R.T. and Bainbridge, A.E. (1973) Dissolved CO, CH₄, and H₂ in the Southern Ocean. *Journal of Geophysical Research*, **78**: 2,691-2,694.

- Willett, J.E. (1987) *Gas Chromatography: Analytical Chemistry by Open Learning (ACOL)*. John Wiley & Sons, Chichester, U.K.
- Wolfe, R.S. (1993) An historic overview of methanogenesis. In J. G. Ferry (Editor) *Methanogenesis. Ecology, Physiology, Biochemistry & Genetics*. Chapman & Hall, London, p. 1-32.
- Woltemate, I., Whiticar, M.J. and Schoell, M. (1984) Carbon and hydrogen isotopic composition of bacterial methane in a shallow freshwater lake. *Limnology and Oceanography*, **29**: 985-992.
- Yamamoto, S., Alcauskas, J.B. and Crozier, T.E. (1976) Solubility of methane in distilled water and seawater. *Journal of Chemical and Engineering Data*, **21**: 78-80.
- Zehnder, A.J.B. (1978) Ecology of methane formation. In: R. Mitchell (Editor) *Water Pollution Microbiology* **2**, John Wiley, New York, p. 349-376.
- Zehnder, A.J.B. and Brock, T.D. (1979) Methane formation and methane oxidation by methanogenic bacteria. *Journal of Bacteriology*, **137**: 420-432.
- Zehnder, A.J.B. and Brock, T.D. (1980) Anaerobic methane oxidation: occurrence and ecology. *Applied and Environmental Microbiology*, **39**: 194-204.
- Zehnder, A.J.B., Huser, B.A., Brock, T.D. and Wuhrmann, K. (1980) Characterisation of an acetate-decarboxylating, non-hydrogen-oxidizing methane bacterium. *Archives of Microbiology*, **124**: 1-11.
- Zehnder, A.J.B. and Wuhrmann, K. (1977) Physiology of a *Methanobacterium* strain AZ. *Archives of Microbiology*, **111**: 199-205.
- Zeikus, J.G. (1977) The biology of methanogenic bacteria. *Bacteriological Reviews*, **41**: 514-541.
- Zeikus, J.G. and Ward, J.C. (1974) Methane formation in living trees: a microbial origin. *Science*, **184**: 1,181-1,183.
- Zeikus, J.G. and Wolfe, R.S. (1972) *Methanobacterium thermoautotrophicus* sp. nov., an anaerobic, autotrophic, extreme thermophile. *Journal of Bacteriology*, **143**: 432-440.
- Zimmermann, P.R., Greenberg, J.P., Wandiga, S.O. and Crutzen, P.J. (1982) Termite: a potentially large source of atmospheric methane, carbon dioxide, and molecular hydrogen. *Science*, **218**: 563-565.

Appendix 2-1

Wind speed profiles: calculating speeds at 10 m height

The earth's surface imposes a frictional drag on horizontal wind and thereby causes the wind speed (u) to decrease the closer it is to the ground. The frictional drag is larger where the earth's surface is rough (*e.g.* woodlands or cities) than in smooth open country or over calm waters. Also the wind speed itself affects the strength of the frictional drag. The greater the drag is, the smaller is the wind speed gradient with height and thus the deeper is the boundary layer. The vertical profile of wind speed with height above ground has been found to follow a logarithmic decay curve in the boundary layer under conditions of neutral atmospheric stability and can be described by the following logarithmic wind profile equation (Oke, 1978, p. 47):

$$u_z = \frac{u_f}{k} * \ln \frac{z}{z_0} \quad (\text{A1-1})$$

where u_z is the mean wind speed (m s^{-1}) at height z (m), u_f the friction velocity (m s^{-1}), k the von Kármán constant ($\cong 0.40$) and z_0 the roughness length (m). z_0 - the height at which the neutral wind profile extrapolates to a zero wind speed - is a measure of the surface roughness. It is related to the actual size, shape and density of the roughness elements. Typical values for z_0 were used. Pen-y-Bonc and Pen-y-Ffridd measure wind over grass that is kept short (height $h \cong 0.05$ m). Under these circumstances the roughness length is calculated to be 0.005 m (using the equation $\log z_0 = \log h - 0.98$) (Oke, 1978 p. 119). At the School of Ocean Sciences the wind is measured on top of the Westbury Mount building at around 20 m. The estimated value for a building of that size is after Oke (1978, p. 263) approximately 0.7 m.

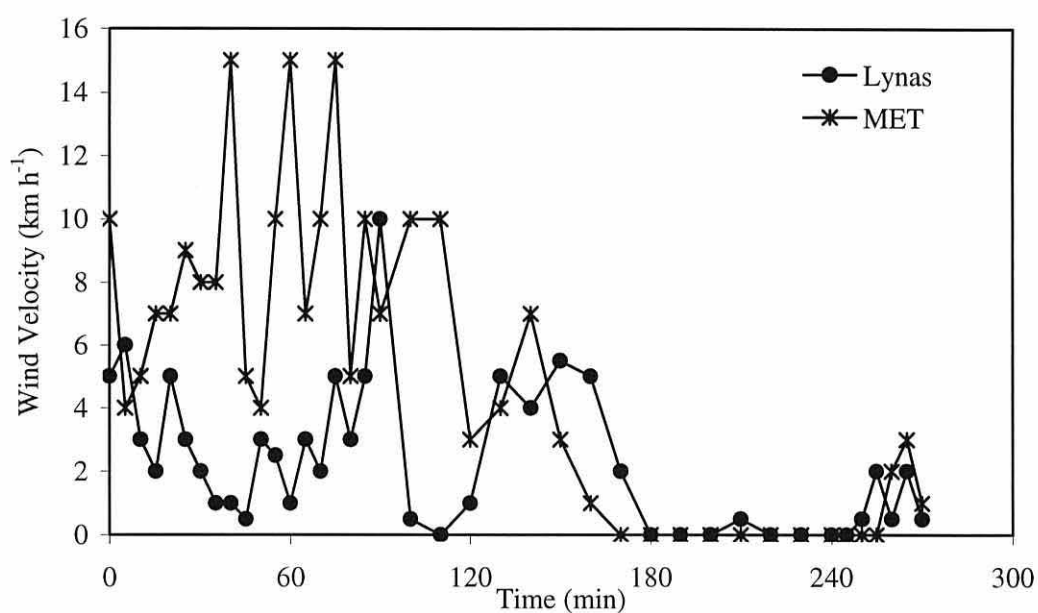
The friction velocity is the only unknown in the equation for the height at which the measurements were taken and is thus calculated by rearranging equation A1-1.

Assuming that the friction velocity remains constant the wind speed at $z = 10$ m can now be calculated.

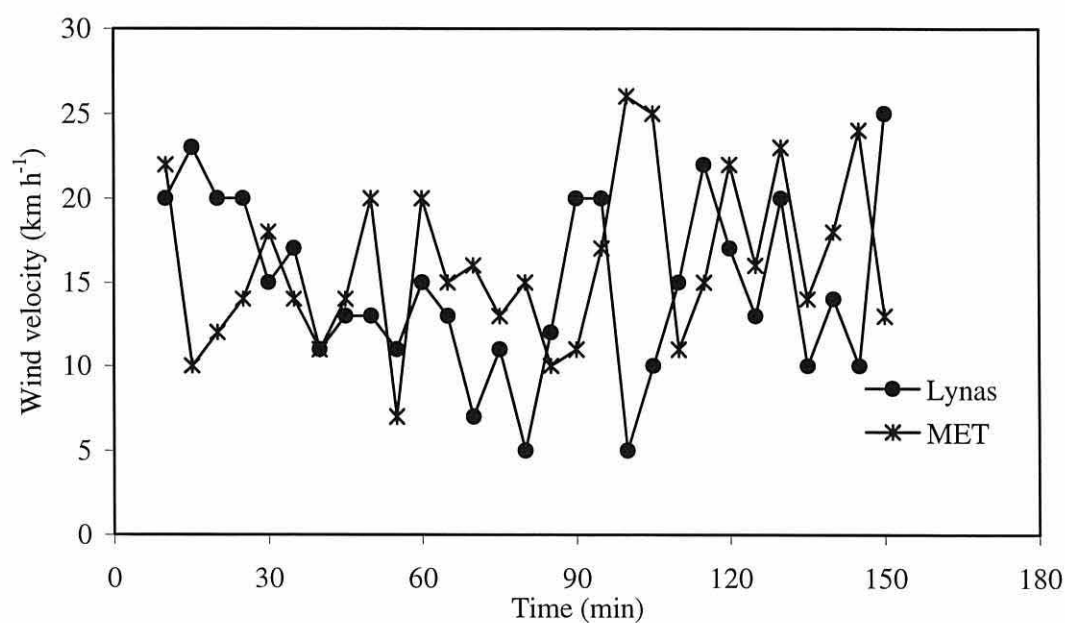
Appendix 2-2

Cross calibration of wind velocities at Point Lynas and the meteorological station at Pen-y-Bonc

A. 08.10.1997: A calm day



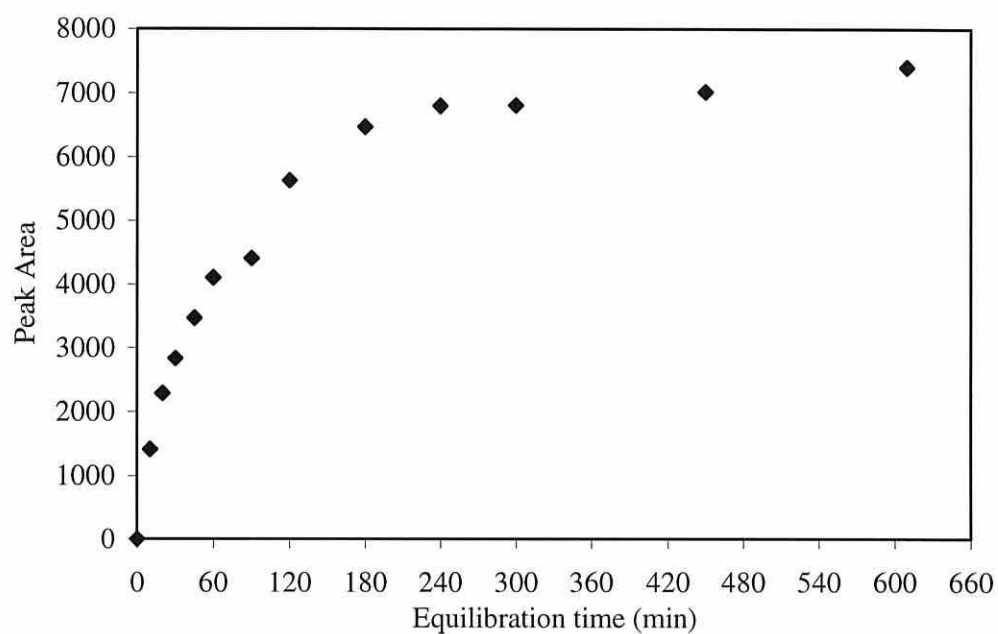
B. 10.10.97: A windy day



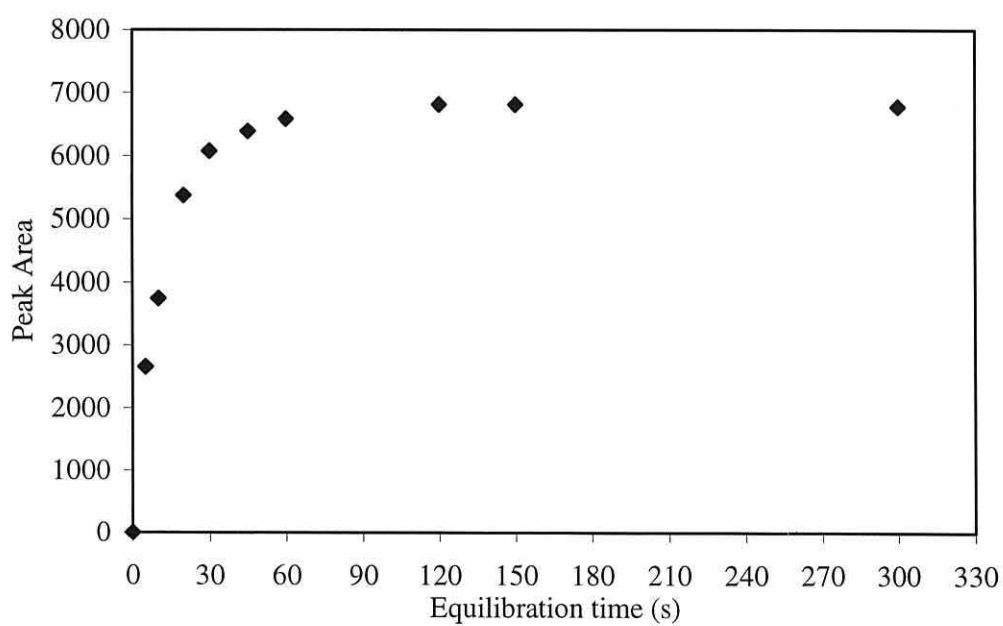
Appendix 2-3

Calibrations for methane headspace equilibration times using passive (A) and active (B) mixing

A. Passive equilibration



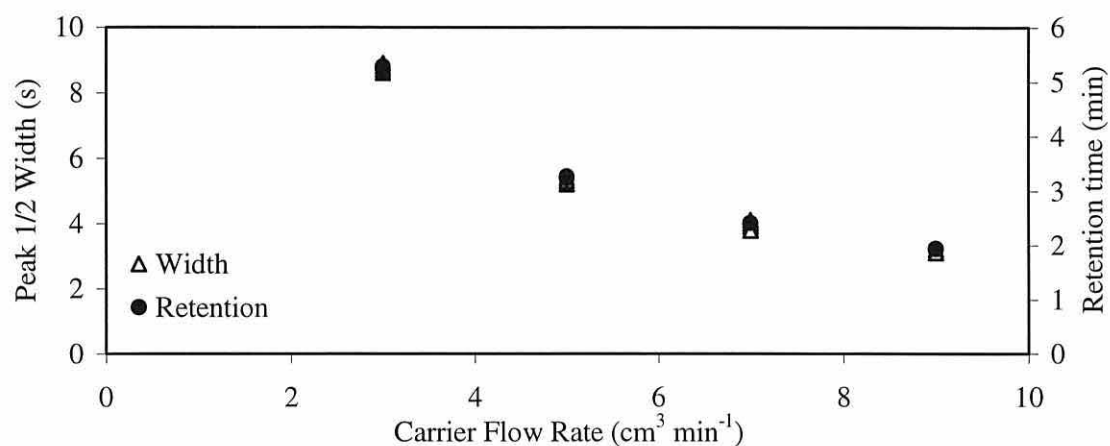
B. Active equilibration



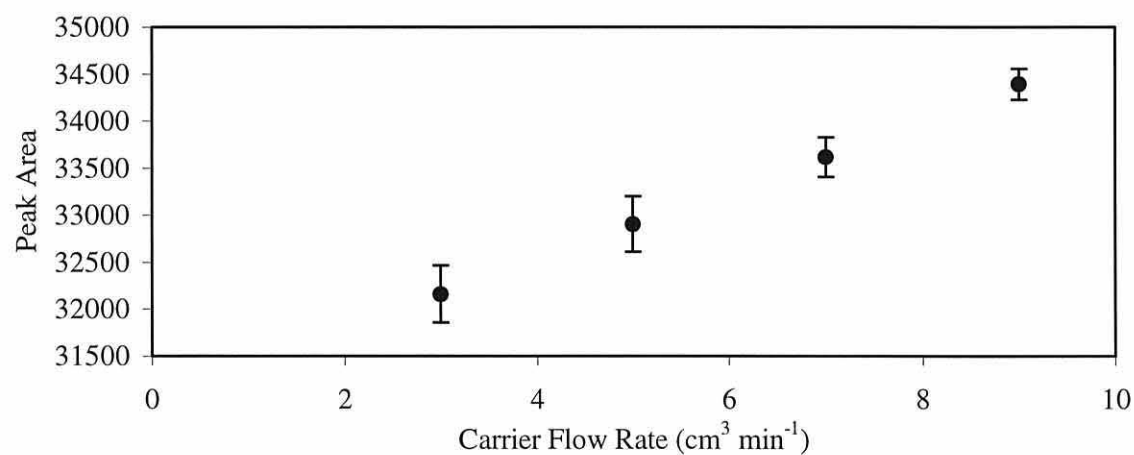
Appendix 2-4

GC calibration: carrier flow (A, B) and temperatures (C)

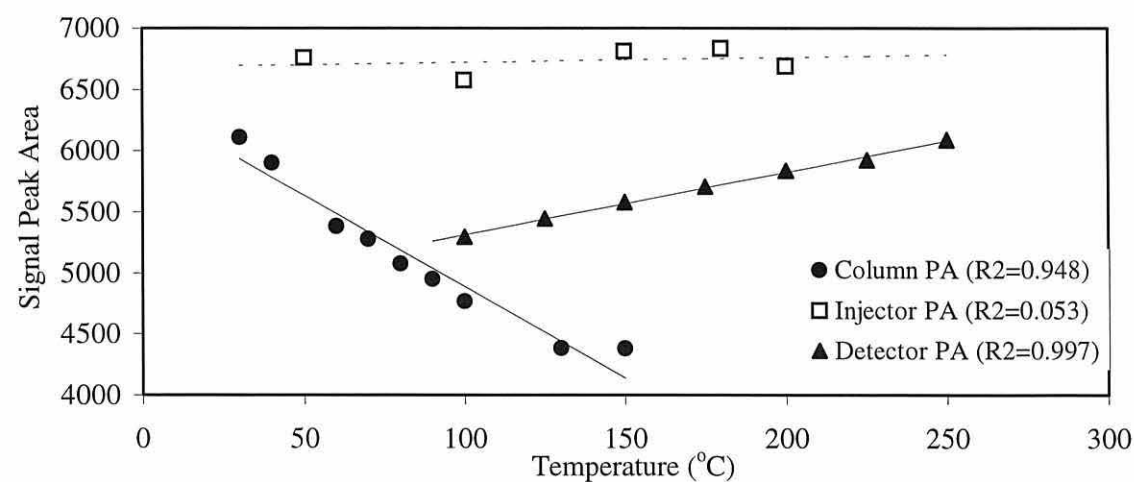
A. Carrier gas flow rate: Effect on signal sharpness and retention time



B. Carrier gas flow rate: Effect on signal intensity



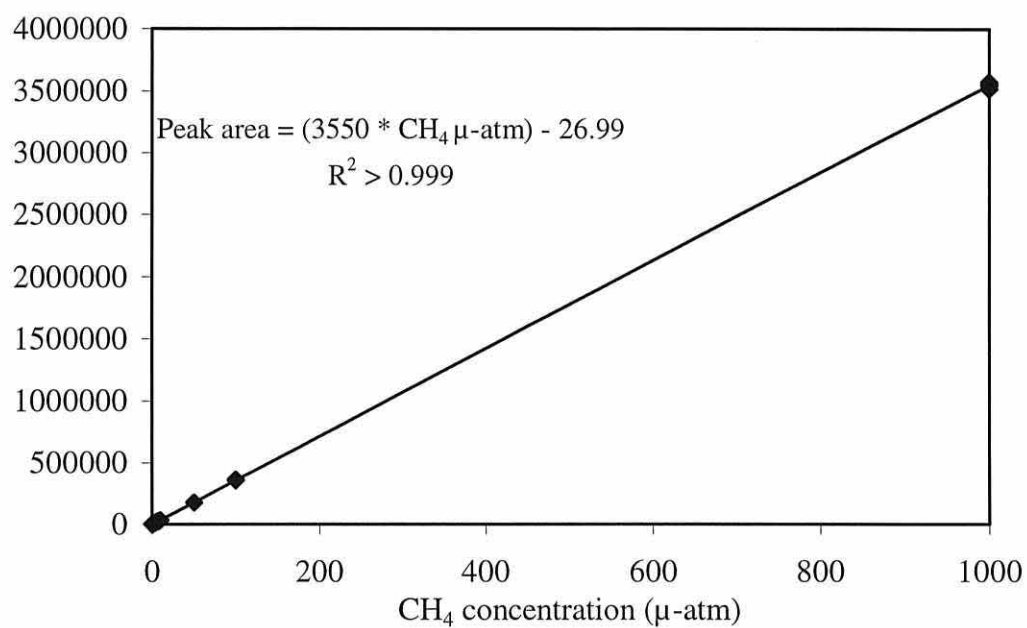
C. Column, injector and detector temperatures: Effect on signal intensity



Appendix 2-5

GC calibration curve for methane

Peak area



Appendix 2-6

Precision in dependence of signal intensity

CH ₄ (μ-atm)	Mean PA	SE	CV (%)
0.25	1054	23	4.94
0.5	1984	31	2.67
1	3091	12	0.85
2.5	9369	31	0.74
5	17205	34	0.44
7.5	25922	38	0.33
10	34951	54	0.31
50	175260	58	0.07
100	359000	125	0.06

Appendix 3-1

Raw data of the seasonal pelagic study (Chapter 3.1)

1996 Menai Strait

Date	CH ₄	SE	Temp	Sal.	Chl a	Phaeo	O ₂	POC	PON	NCP	DCR	Atm. CH ₄	Wind	SD
	nM		°C		µg/dm ³	µg/dm ³	µM	µM	µM	µmol/l/d	µmol/l/d	µ-atm	m/s	
05.03.	10.0	0.25	5.2	33.25	0.48	0.90	320.5	29.7	3.9	1.54	1.33	1.86		
16.03.	9.1	0.07	5.3	33.28	1.11	2.16	321.5	20.0	3.4	1.74	1.20	1.92		
03.04.	9.0	0.12	6.7	33.42	3.25	2.51	339.0	38.6	4.6	18.52	4.51	1.95		
17.04.	9.8	0.23	8.0	33.70	2.63	3.30	328.3	35.6	4.3	6.43	4.28	1.87	0.80	0.93
30.04.	13.2	0.36	9.4	33.95	6.92	1.38	333.9	47.3	5.9	21.43	8.85	1.91	1.48	1.33
13.05.	13.7	0.21	10.8	33.41	12.79	7.69	336.6	113.7	12.4	28.42	12.11	1.90	1.93	0.39
28.05.	26.2	0.39	11.6	33.54	13.13	6.55	303.6	335.6	12.6	41.16	17.73	1.87		
13.06.	20.3	0.21	13.6	33.35	3.35	2.81	246.1			-9.55	14.86	1.88		
25.06.	33.4	0.20	15.0	34.08	1.03							1.88		
27.06.	38.2	0.84	15.2	34.19	1.15	2.47	214.6			-1.68	5.22	1.90		
11.07.	41.7	1.29	15.8	34.10	4.23	4.32	268.8			34.19	14.20	1.75	2.19	0.70
29.07.	53.0	2.31	18.7	33.87	3.39	2.06	232.0			9.65	6.62		1.08	0.61
27.08.	40.2	0.07	17.8	33.76	1.56	1.87	235.8	73.6	3.7	16.41	3.82	1.75	1.31	0.49
12.09.	19.6	0.36	16.3	33.79	4.82							1.80	1.64	0.95
17.09.	21.6	0.17	16.3	33.66	1.50	1.09	249.3			9.65	5.31	1.84	1.93	1.08
19.09.			16.3					122.0	5.4				5.29	1.98
23.09.	20.5	0.54	15.6	33.50									1.04	0.93
30.09.	17.9	0.28	15.0	33.11									2.30	1.04
16.10.	6.3	0.22	13.0	33.5	1.50	1.61	263.0		5.4	0.08	2.3	1.83	3.50	1.88
13.11.					1.05	3.10	289.1	234.5	10.5				0.77	0.38
21.11.	13.1	0.27	6.5	33.2	0.60	1.82	297.5	178.5	5.9	0.13	0.92	1.94	1.39	0.82

1997 Menai Strait

Date	CH ₄	SE	Temp	Sal.	Chl a	Phaeo	O ₂	POC	PON	Atm.	Wind	SD
	nM		°C		µg/dm ³	µg/dm ³	µM d ⁻¹	µM	µM	CH ₄ µ-atm	m/s	
05.02.					1.71	2.03		70.9	8.5		1.90	0.93
21.02.					0.54	0.63		112.0	4.9		4.85	1.34
10.03.					2.41	2.09		487.7	11.4		0.93	0.78
16.04.				33.68	1.65	0.42		145.8	4.5		1.71	1.20
01.05.	21.5	0.77	11.1	33.31	12.93	5.05	391.3			1.87		
09.05.			9.7	32.71								
12.05.	22.8	0.36	10.5	32.62	12.63	2.59	293.5	431.0	15.4	1.98		
19.05.	36.0	1.76	11.3	32.79						2.30	1.49	1.60
25.05.			12.0	32.54							1.41	1.34
27.05.	38.3	0.09	12.7	32.32			296.2			1.94	2.32	1.60
28.05.	43.0	0.60	13.3	32.20	6.92	0.35		314.7	9.0	2.01	2.07	1.32
29.05.	40.4	0.79	13.8	32.08						1.98	1.31	1.11
30.05.	52.3	0.91	14.3	32.00						1.92	1.33	1.11
31.05.			14.1	31.97							2.05	2.07
01.06.			14.1	31.92							5.54	1.74
02.06.	22.2	0.48	14.0	31.42						1.87	6.60	1.50
03.06.	35.2	0.40	14.0	31.35						1.93	4.57	1.84
04.06.	44.6	0.30	14.3	31.34						1.88	1.30	0.91
05.06.	51.8	0.88	14.2	31.55						1.94	2.76	2.70
06.06.	39.6	0.23	14.1	31.77						1.88	4.50	1.53
07.06.	28.3	0.47	14.2	30.70						1.84	5.86	1.10
08.06.	34.7	0.20	14.1	31.75						1.87	3.95	1.37
09.06.	40.8	0.10	14.2	30.91	0.51	0.46	237.3	175.1	5.3	1.89	2.57	0.99
10.06.	49.5	0.35	14.0	30.94						2.09	1.78	1.34
11.06.	54.5	0.14	14.2	30.86						1.89	2.48	1.92
12.06.	61.1	0.15	14.3	30.73						1.93	1.65	0.90
20.06.	56.7	0.18	13.8	32.53						1.85	1.46	1.08
23.06.					0.75	1.84		125.6	3.0		1.02	0.40
01.07.	52.5	0.50	13.7	32.15						1.86	1.12	0.33

1997 Menai Strait cont.

Date	CH ₄	SE	Temp	Sal.	Chl a	Phaeo	O ₂	POC	PON	Atm.	Wind	SD
	nM		°C		µg/dm ³	µg/dm ³	µM d ⁻¹	µM	µM	CH ₄ µ-atm	m/s	
02.07.			14.0	32.68	12.78	5.38					1.04	0.48
03.07.	59.6	0.38	14.0	32.74						1.91	0.58	0.52
04.07.			14.0	33.09							0.64	0.35
07.07.	53.6	0.61	15.7	33.36	7.52	2.51		426.6	9.3	1.85	1.26	0.92
09.07.	59.8	1.01	16.4	33.42							1.30	0.98
19.07.			16.5	32.99			257.9				1.08	0.88
22.07.					3.61	1.23	239.2	518.2	7.0		0.94	0.84
28.07.	41.3	0.36	17.3									
30.07.	39.4	0.27	17.1		3.89	1.42						
05.08.					5.41	1.50	210.5	160.5	6.7			
11.08.	63.2	0.88	19.2		2.63	1.04						
19.08.			18.2		6.92	1.04	260.6	260.9	6.8			
22.08.	58.0	2.07	18.1									
26.08.	46.4	0.23	18.1		0.68	0.69	235.6					
01.09.			17.3		1.65	1.11	235.4	154.7	6.0			
04.09.	29.0	0.69	16.8									
16.09.					1.05	0.85	247.1	122.7	4.3			
23.09.	35.3	0.23	16.5									
29.09.	44.0	0.37	15.6		0.83	1.35						
30.09.					0.75	0.84	241.4	113.1	3.5			
13.10.	41.8	0.76	13.4		1.86	1.10				1.85	1.25	0.64
17.10.			14.1	33.48	1.96	2.37	256.7	184.6	5.1			
28.10.			12.7	33.15								
01.11.	31.1	0.08	11.6	33.48	1.86	1.12				1.99	0.31	0.27
06.11.			10.9	33.05	1.65	1.46	266.8				0.34	0.34

1998 Menai Strait

Date	CH ₄	SE	Temp	Sal.	Chl a	Phaeo	POC	PON	Atm.	Wind	SD
	nM		°C		µg/dm ³	µg/dm ³	µM	µM	CH ₄ µ-atm	m/s	
07.02.	12.7	0.18	7.5						2.03		

1996 Point Lynas

Date	CH ₄	SE	Temp	Sal.	Chl a	Phaeo	POC	PON	O ₂	NCP	DCR	Atm.	Wind	SD
	nM		°C		µg/dm ³	µg/dm ³	µM	µM	µM	µmol/l/d	µmol/l/d	CH ₄ µ-atm	m/s	
07.03.	3.2	0.20	4.8	34.05	0.88	1.67	633.1	69.5	304.3			1.83	7.32	1.70
14.03.	4.6	0.16	4.9	33.93	1.68	3.79	1655	159.4	320.5				9.25	5.03
20.03.	4.2	0.23	5.5	33.95	1.57	1.82	607.0	64.8	321.7	2.41	0.87	2.10	10.53	1.68
28.03.			5.7		1.19	1.36	393.6	45.2	323.9	0.38	0.88	1.96	7.84	1.94
05.04.	5.1	0.13	6.3	34.21	3.10	2.70	551.3	64.6	330.0	19.0	0.67	2.12	5.31	2.17
11.04.	5.3	0.10	7.0	34.33	4.19	3.25	491.4	66.9	343.6	25.96	0.41	2.03	1.62	0.96
18.04.	3.4	0.07	7.1	34.29	2.99	3.52	434.0	61.9	326.3	6.86	2.32	1.86	1.64	0.69
04.05.	3.5	0.09	8.5	34.00	13.88	7.46	792.2	109.3	329.2	56.74	2.5	1.87	2.74	1.77
11.05.	4.2	0.05	9.3		22.81	12.57	1677	132.3	372.1	47.7	10.46	1.90	2.83	0.83
17.05.	4.0	0.05	11.1	34.30	21.95	12.27	1580	135.7	347.0	38.1	15.73	1.45	7.11	1.29
04.06.	2.5	0.17	11.0	34.37	23.76	14.21	1989	154.0	337.0	33.44	16.47	1.60	3.00	0.39
17.06.	5.6	0.07	12.7	34.45	0.58	0.69	386.9	56.6	253.7	-6.87	8.33	1.97	7.71	1.95
02.07.	3.7	0.09	13.0	34.48	1.23	1.11	477.0	62.6	249.9	-62.04	70.21	1.92	10.48	2.62
17.07.			16.6		1.06	1.22	1644	375.2	250.1	6.28	4.5		2.40	2.03
19.07.	6.5	0.90	16.6	34.25								1.95	7.58	3.19
01.08.	6.1	0.86	16.8	34.24	2.46	1.46	452.3	56.1	251.2	9.79	4.43	1.95	6.51	2.52
15.08.	7.1	0.35	17.1	34.28	1.11	0.82	366.8	52.3	260.3	22.69	4.74	1.96	1.80	0.89
30.08.	5.8	0.22	17.0	34.31	2.07	2.38	391.6	54.4	258.0	10.85	1.85	1.74	8.99	2.27
13.09.	4.7	0.43	16.1	34.19	1.04	1.81	329.3	39.7	254.8	4.86	1.68	1.84	7.19	5.65
27.09.	4.2	0.09	15.4	33.75	1.81	2.66	447.2	56.2	254.8	-0.56	3.26	1.81	8.22	1.26
13.10.	3.9	0.10	14.8	34.12	0.74	1.90	374.7	42.5	262.7	2.48	2.28	1.83	8.48	3.88

Appendix 3-2

Raw data for short-term variability study (Chapter 3.2)

A) FIXED STATION VARIABILITY

Variability of various parameters over a spring-neap tidal cycle between 27 May to 12 June 1997 at St. George's Pier (Figure 3.2.1).

Date	CH ₄ nM	SE	Mean wind m/s	SD	Sea temp. °C	Mean air temp °C	Atm. CH ₄ μ-atm	HW height * m
27.05.	38.30	0.09	2.321	1.598	12.9	16.3	1.94	6.63
28.05.	43.02	0.60	2.071	1.322	13.5	16.0	2.01	6.3
29.05.	40.40	0.79	1.313	1.105	14.1	16.7	1.98	6.03
30.05.	52.26	0.91	1.330	1.113	14.7	19.1	1.92	5.97
31.05.			2.047	2.068		19.8		6.14
01.06.			5.538	1.742		17.0		6.53
02.06.	22.23	0.48	6.599	1.500	14.8	15.6	1.87	6.78
03.06.	35.19	0.38	4.566	1.836	14.3	15.6	1.93	7.00
04.06.	44.59	0.30	1.299	0.911	14.5	18.0	1.88	7.13
05.06.	51.80	0.88	2.758	2.696	14.5	17.8	1.94	7.15
06.06.	39.61	0.23	4.499	1.529	14.6	17.9	1.88	7.06
07.06.	28.29	0.47	5.860	1.104	14.6	17.4	1.84	6.89
08.06.	34.67	0.20	3.946	1.366	14.4	14.7	1.87	6.66
09.06.	40.78	0.16	2.571	0.987	14.4	14.7	1.89	6.39
10.06.	49.48	0.35	1.780	1.341	14.6	16.6	2.09	6.12
11.06.	54.50	0.14	2.485	1.922	15.0	16.5	1.89	5.86
12.06.	61.13	0.15	1.654	0.903	14.6	14.2	1.93	5.65

* Sea height above chart datum during day time high tide (time of sampling)

Variability of various parameters over a diurnal tidal cycle on 7 July 1997 at St. George's Pier (Figure 3.2.2).

Time GMT	CH ₄ nM	SE	Mean wind m/s	SD	Sea Temp °C	Air Temp °C	Atm. CH ₄ μ-atm	Current speed &dir -m/s	Tidal height m
0725	61.44	1.08	0.53	0.28	15.7	21.8	1.85	0.66	1.43
0825	64.23	0.52	0.78	0.52	15.7	24.2	1.85	0.66	2.30
0925	52.75	0.19	1.85	0.22	15.6	25.2	1.85	0.29	3.57
1025	51.96	0.14	2.30	0.24	15.5	25.6	1.85	-0.31	5.22
1125	53.32	0.26	2.35	0.32	15.4	26.0	1.84	-0.76	6.28
1225	53.63	0.61	2.54	0.25	15.6	25.7	1.85	-0.74	6.71
1325	49.76	1.18	2.47	0.24	15.7	24.9	1.84	-0.56	6.22
1425	44.06	0.66	2.64	0.24	15.9	23.8	1.83	-0.34	5.31
1525	44.81	0.50	2.78	0.17	15.9	22.8	1.81	-0.12	4.17
1625	46.36	0.66	2.70	0.37	15.9	22.2	1.84	0.18	3.03
1725	42.71	0.19	1.57	0.45	16.0	20.8	1.90	0.30	2.06
1825	41.86	0.05	1.29	0.70	15.8	17.9	1.88	0.40	1.46
1925	72.85	0.86	1.40	0.74	15.6	16.2	1.88	0.67	1.47

Variability of various parameters over half a tidal cycle on 22 August 1997 at the NE entrance of the Menai Strait (Figure 3.2.3).

Time GMT	CH ₄ nM	Sea Temp °C	Atm. CH ₄ μ-atm	Current speed m/s
0742	51.42	17.8	1.91	-0.527
0752		18.1		-0.509
0802	51.96	18.3		-0.330
0812		18.5		-0.229
0822	48.02	18.9		-0.099
0832		18.3		0.142
0842	41.31	18.4	1.82	0.425
0852		18.3		0.507
0902	36.41	18.3		0.649
0912	35.43	18.0		0.529
0922		18.1		0.536
0932	19.82	18.0		0.474
0942		18.0		0.542
0952	17.33	18.0	1.82	0.647
1002		17.9		0.784
1012	25.02	18.1		0.904
1022		18.5		0.810
1032	13.11	18.3		0.602
1042		18.7		0.667
1052	17.35	18.8		0.564
1102		18.6	1.84	0.639
1112	13.60	18.3		0.652
1122		18.9		0.539
1132	13.57	18.0		0.498
1142		18.3		0.410
1152	9.81	18.1	1.84	0.363
1202		18.2		0.315
1212	10.87	18.0		0.171
1222		18.3		0.156
1232	10.09	17.9		0.113

B) SPATIAL VARIABILITY

Aquatic methane concentrations (CH₄), water temperatures and atmospheric methane concentrations along transect stations from Telford Bridge to Bangor Pier on 19 May 1997 (Figure 3.2.5 A).

Station No.	CH ₄ (nM)	SE	Sea temp (°C)
1	35.10	0.59	12.1
2	37.71	0.03	12.1
3	53.33	0.55	12.5
4	47.80	1.50	12.5
5	56.03	0.08	12.5

Aquatic methane concentrations (CH₄), water temperatures and atmospheric methane concentrations along transect stations from Puffin Island to St. George's Pier on 05 June 1997 (Figure 3.2.5 B).

Station No.	CH ₄ (nM)	SE	Sea temp (°C)	Atm.CH ₄ (μ-atm)
6	16.62	0.11	13.2	2.08
7	20.05	0.42	13.2	2.05
8	18.10	0.51	13.4	2.01
9	18.98	0.86	13.4	1.99
10	22.34	0.69	13.9	1.99
11	29.48	0.53	13.9	1.96
12	28.04	1.08	13.7	1.96
13	43.62	1.44	14.0	1.97
14	49.34	2.3	14.1	1.96
15	50.52	1.47	14.5	1.94

Aquatic methane concentrations (CH₄), water temperatures and atmospheric methane concentrations along transect stations across the Lavan Sands on 20 June 1997 (Figure 3.2.5 C).

Station No.	CH ₄ (nM)	SE	Sea temp. (°C)	Atm.CH ₄ (μ-atm)
16	32.10	7.00	18.4	1.93
17	18.45	0.70	18.4	
18	21.26	0.84	18.5	1.93
19	47.89	0.84	18.4	
20	26.89	0.54	18.5	
21	41.68	0.91	18.6	2.03
22	85.62	8.69	18.6	

Depth profiles of aquatic methane concentrations (CH₄) and water temperatures at three mid-stream stations in the central Menai Strait on 28 July 1997 (Figure 3.2.6).

Station No.	Depth (m)	CH ₄ (nM)	Sea temp (°C)
23	0.2	38.38	19.4
23	1	43.32	19.3
23	2	42.17	19.3
23	4	39.79	19.4
23	7	41.88	19.4
23	10	41.11	19.4
23	13	40.30	19.4
24	0.2	44.00	19.4
24	1	41.65	19.5
24	2	40.94	19.5
24	4	10.45	19.5
24	7	41.66	19.5
24	10	43.25	19.5
24	12	41.70	19.5
25	0.2	46.54	19.3
25	1	42.98	19.1
25	2	42.85	19
25	4	41.66	19
25	7	42.43	18.9
25	10	42.88	18.9
25	13	42.75	18.9

Depth profile of aquatic methane concentrations (CH₄) at St. George's Pier on 13 June 1996 (Figure 3.2.6).

Depth (m)	CH ₄ (nM)	SE
0.5	21.23	0.44
1	20.48	0.24
2	24.15	0.83
3	28.12	1.28
4	28.82	0.84
5	28.30	0.14

C) TEMPORAL VARIABILITY

Aquatic (CH₄) and atmospheric (Atm. CH₄) methane concentrations at different times during drifting from Bangor to Port Dinorwic on 09 July 1997 (Figure 3.2.7).

Drifting time (min)	CH ₄ (nM)	SE	Atm. CH ₄ (μ-atm)
0	51.38	1.53	1.985
10	49.28	0	
20	51.29	1.02	
30	52.79	1.06	1.949
40	52.09	1.55	
50	54.14	0.7	
60	52.73	1.74	1.961
70	52.32	1.55	
80	52.26	1.78	
90	57.68	0.84	1.946
95	57.08	0	
100	55.99	1.83	
105	57.68	0.78	
110	59.59	0.06	1.939
120	62.57	2.6	
130	60.62	1.83	
140	61.56	2.37	1.868
150	59.95	1.73	

Appendix 3-3

Raw data for Menai Strait water incubations (Chapter 3.3)

Dates of sampling, incubation times and results of incubations of unconcentrated (Unconc.) and concentrated (Conc.) water samples from the Menai Strait for aquatic methane (CH₄) including the HgCl₂ poisoned control results (Figure 3.3.1).

Date	Incub. time h	Unconc. nM CH ₄	Unconc. control nM CH ₄	Conc. nM CH ₄	Conc.control nM CH ₄
01.05.1997	0	20.6	19.9		
	0	25.1	20.4		
	0	22.7	17.6		
	24	20.2	18.6		
	24	21.0	18.4		
	24	21.8	19.1		
	48	17.3	18.5		
	48	18.5	15.0		
	48	16.5	15.3		
12.05.1997	0	21.5	20.7		
	0	20.8	20.5		
	0	20.9	20.9		
	24	16.0	15.7		
	24	17.2	16.3		
	24	18.7	16.7		
	48	13.2	16.9		
	48	16.0	12.4		
	48	14.3	14.8		
27.05.1997	0	38.1	37.6		
	0	35.7	39.3		
	0	41.3	39.5		
	24	36.1	39.9		
	24	37.4	38.2		
	24	38.9	36.7		
	48	30.3	28.8		
	48	31.8	31.7		
	48	32.9	32.8		
09.06.1997	0			41.1	38.5
	0			41.6	38.2
	0			40.5	38.9
	24			45.0	31.1
	24			43.5	32.2
	24			45.2	32.9
	48			41.8	33.1
	48			54.9	34.1
	48			53.3	33.4
02.07.1997	0	42.5	43.2	32.6	32.5
	0	40.1	42.7	31.4	30.8
	9	36.9	38.7	29.2	28.4
	9	37.3	38.4	30.5	28.6
	18	35.8	36.7	28.0	27.5
	18	35.0	37.3	27.3	26.9
	27	33.3	33.2	30.9	27.7
	27	33.5	30.2	27.5	25.8
	36	32.3	30.1	30.2	27.5
	36	32.0	33.4	33.7	26.6

(Figure 3.3.1) cont.

Date	Incub. time	Unconc.	Unconc. control	Conc.	Conc. control
	h	nM CH ₄	nM CH ₄	nM CH ₄	nM CH ₄
30.07.1997	0	40.7	39.0	34.7	34.7
	0	40.9	40.3	34.6	34.6
	0	41.3	41.5	34.6	34.6
	24	31.8	31.7	35.2	31.0
	24	31.1	31.7	31.0	32.8
	24	31.2	31.9	32.8	35.2
	48	30.8	31.3	35.0	28.7
	48	32.8	31.9	34.8	29.5
	48	36.6	30.1	36.7	26.4
11.08.1997	0	65.3	60.4	46.1	41.4
	0	67.3	60.0	47.0	42.0
	0	64.4	61.9	46.5	41.6
	24	48.1	45.5	36.8	32.3
	24	49.3	45.3	40.0	31.7
	24	47.2	45.5	40.4	32.9
	48	52.0	36.1	33.6	29.3
	48	46.8	37.5	32.1	26.8
	48	42.2	42.7	35.7	27.0
26.08.1997	0	47.9	50.4	40.8	42.8
	0	47.9	51.4	41.0	44.8
	0	47.2	50.8	42.4	43.1
	24	35.1	36.2	41.5	42.7
	24	34.2	40.4	36.7	34.6
	24	34.1	38.8	37.8	39.2
	48	32.1	36.1	48.1	36.7
	48	31.3	36.7	52.0	35.0
	48	32.0	36.3	48.8	36.3
29.09.1997	0	45.0	45.5	37.7	37.3
	0	45.2	46.8	37.2	39.3
	0	46.1	46.0	37.6	39.4
	24	34.0	32.6	31.1	31.4
	24	34.8	35.9	29.7	30.0
	24	35.1	34.4	30.3	30.8
	48	31.0	29.1	33.0	26.4
	48	31.2	31.2	31.7	26.4
	48	31.4	30.5	32.2	25.9
13.10.1997	0	43.7	41.7	24.8	24.1
	0	42.3	42.8	24.9	26.2
	0	41.2	44.6	25.3	25.8
	24	31.1	33.1	22.6	23.0
	24	31.5	35.3	23.1	24.4
	24	33.5	33.9	21.3	22.7
	48	32.8	32.8	21.2	22.1
	48	32.1	33.8	22.9	21.9
	48	33.9	32.3	24.9	23.2
01.11.1997	0	32.0	33.9	31.3	32.8
	0	32.3	34.6	30.2	29.5
	0	32.1	38.9	31.5	29.2
	24	25.6	28.7	26.9	25.3
	24	26.0	33.9	23.4	23.2
	24	27.5	30.1	25.3	23.8
	48	25.5	27.3	30.2	24.2
	48	25.7	29.2	23.4	24.5
	48	23.9	25.6	27.0	24.0

Sea temperature, natural chlorophyll and phaeopigment concentrations and the concentration factor for the concentrated sample on the dates when water for incubations was collected.

Date	Sea Temp °C	Natural Chl a $\mu\text{g dm}^{-3}$	Natural Phaeo $\mu\text{g dm}^{-3}$	Conc. Factor*
01.05.1997	11.1	12.93	5.05	
12.05.1997	10.7	12.63	2.59	
27.05.1997	12.9	6.92	0.35	
09.06.1997	14.4	0.51	0.46	N/A
02.07.1997	14.3	12.78	5.38	51.3
30.07.1997	17.1	3.38	1.42	56.9
11.08.1997	19.2	2.63	1.04	18.4
26.08.1997	18.0	0.68	0.69	37.4
29.09.1997	15.6	0.83	1.35	58.6
13.10.1997	13.4	1.86	1.10	35.1
01.11.1997	11.6	1.86	1.12	26.1

*Concentration factor = volume of water concentrated by passing through 53 μm plankton net as estimated from POC and PON analyses. Values are means of triplicate POC and PON samples.

Appendix 3-4

Raw data for sewage incubations (Chapter 3.4)

Methane concentration incubation of treated sewage from Treborth on 03 July 1997

Time h	Live nM CH ₄	Control nM CH ₄
0	87.3	84.0
0	86.5	85.5
11	73.1	73.5
11	72.4	72.7
24	65.9	67.1
24	69.2	67.7

Methane concentration incubation of raw Menai Bridge sewage on 22 July 1997

Time h	Live nM CH ₄	Control nM CH ₄
0	117.2	107.9
0	102.0	111.0
12	94.0	89.5
12	94.1	85.4
24	90.1	80.0
24	84.0	78.6
48	77.3	72.6
48	78.6	67.1

Appendix 3-5

Raw data for sediment study (Chapter 3.5)

3.5.1 Seasonal distribution of pore water methane, water content (% by weight) and temperature in sediments at stations A, B and C in the Menai Bridge mud flats in 1997

Station	Date	Depth cm	CH ₄ μM	Pore water % by weight	Sed. Temp °C
A	07/08/97	0	0.16	25.95	20.0
A	07/08/97	5	0.50	24.45	18.6
A	07/08/97	10	1.30	29.08	17.6
A	07/08/97	15	2.31	23.99	16.9
A	07/08/97	20	2.80	29.79	16.8
A	05/09/97	0	0.32	28.72	15.8
A	05/09/97	5	0.46	27.26	16.0
A	05/09/97	10	0.75	29.59	16.3
A	05/09/97	15	1.65	25.4	16.3
A	05/09/97	20	1.64	23.7	16.3
A	05/09/97	25	1.22	27.28	16.3
A	05/09/97	30	1.71	29.18	16.3
A	19/09/97	0	0.28	24.61	13.9
A	19/09/97	5	1.17	22.23	14.3
A	19/09/97	10	1.17		14.7
A	19/09/97	15	5.43	23.64	14.9
A	19/09/97	20	6.74	28.12	15.1
A	19/09/97	25	6.83	24.2	14.6
A	19/09/97	30	10.99	23.16	14.4
A	03/11/97	0	0.23	22.24	11.4
A	03/11/97	5	0.45	24.32	11.8
A	03/11/97	10	0.91	24.05	11.8
A	03/11/97	15	1.41	22.71	11.8
A	03/11/97	20	2.26	22.46	11.9
A	03/11/97	25	3.15	27.59	12.0
A	03/11/97	30	3.48	27.38	12.1
A	04/02/98	0	0.02	22.58	8.3
A	04/02/98	5	0.39	29.16	8.1
A	04/02/98	10	1.19	23.91	8.0
A	04/02/98	15	1.45	22.72	7.8
A	04/02/98	20	1.61	22.45	7.8
A	04/02/98	25	2.20	25.56	7.9
A	04/02/98	30	2.11	23.88	7.7
B	01/07/97	0	0.17	40.9	14.6
B	01/07/97	5	0.14	31.71	15.0
B	01/07/97	10	0.32	34.16	15.6
B	01/07/97	15	0.41	29.79	15.3
B	01/07/97	20	1.87	32.63	16.5
B	01/07/97	25	1.80		16.6
B	24/07/97	0	0.35	37.83	18.3
B	24/07/97	5	1.15	30.14	18.1
B	24/07/97	10	1.12	26.98	18.0
B	24/07/97	15	1.17	30.24	17.9
B	24/07/97	20	1.71	22.89	18.0

3.5.1 Cont.

Station	Date	Depth cm	CH ₄ μM	Pore water % by weight	Temp °C
B	07/08/97	0	0.15	37.78	19.1
B	07/08/97	5	0.14	33.24	18.0
B	07/08/97	10	0.10	29.14	17.0
B	07/08/97	15	0.08	27.36	16.6
B	07/08/97	20	0.20	31.03	16.4
B	21/08/97	0	0.21	39.57	18.5
B	21/08/97	5	0.31	32.48	18.5
B	21/08/97	10	0.38	31.22	17.9
B	21/08/97	15	1.03	31.15	17.9
B	21/08/97	20	1.15	24.06	17.8
B	21/08/97	25	0.88	29.60	17.8
B	05/09/97	0	0.35	35.61	16.2
B	05/09/97	5	0.46	33.36	15.5
B	05/09/97	10	0.94	34.91	16.2
B	05/09/97	15	1.50	24.75	16.2
B	05/09/97	20	3.07	28.5	16.2
B	05/09/97	25	3.25	32.27	16.2
B	05/09/97	30	2.91	28.71	16.1
B	19/09/97	0	0.09	37.22	14.3
B	19/09/97	5	0.52	34.06	14.6
B	19/09/97	10	1.06	37.07	15.0
B	19/09/97	15	1.46	34.78	15.1
B	19/09/97	20	1.20	34.15	15.2
B	19/09/97	25	0.78	29.94	15.2
B	19/09/97	30	1.00	29.13	15.2
B	06/10/97	0	0.11	37.54	14.9
B	06/10/97	5	0.36	33.37	14.7
B	06/10/97	10	0.31	30.95	14.7
B	06/10/97	15	0.67	29.45	14.9
B	06/10/97	20	0.40	24.16	14.5
B	06/10/97	25	0.18	27.25	14.5
B	06/10/97	30	0.06	29.9	14.4
B	03/11/97	0	0.08	39.82	11.3
B	03/11/97	5	0.15	30.77	11.8
B	03/11/97	10	0.16	29.52	11.8
B	03/11/97	15	0.49	37.14	11.7
B	03/11/97	20	0.97	33.8	12.1
B	03/11/97	25	1.13	28.61	12.0
B	03/11/97	30	1.93	29.55	12.0
B	04/02/98	0	0.16	34.57	8.3
B	04/02/98	5	0.37	33.54	8.2
B	04/02/98	10	2.07	32.33	7.6
B	04/02/98	15	5.15	32.77	7.8
B	04/02/98	20	13.05	26.49	7.8
B	04/02/98	25	12.92	28.76	7.8
B	04/02/98	30	13.27	35.51	7.6

3.5.1 Cont.

Station	Date	Depth cm	CH ₄ μM	Pore water % by weight	Temp. °C
C	07/08/97	0	2.28	34.87	20.5
C	07/08/97	5	21.74	23.98	19.7
C	07/08/97	10	106.12	21.67	18.7
C	07/08/97	15	134.30	20.58	17.5
C	07/08/97	20	90.53	20.10	17.1
C	21/08/97	0	35.99	44.45	18.8
C	21/08/97	5	106.42	27.02	18.5
C	21/08/97	10	183.23	26.08	17.9
C	21/08/97	15	153.20	22.72	17.9
C	21/08/97	20	131.58	28.46	17.9
C	21/08/97	25	126.43	33.53	17.8
C	05/09/97	0	35.85	48.17	15.4
C	05/09/97	5	315.48	24.3	16.1
C	05/09/97	10	393.09	22.87	16.1
C	05/09/97	15	237.39	44.29	15.4
C	05/09/97	20	240.91	34.23	16.2
C	05/09/97	25	334.88	34.68	16.2
C	05/09/97	30	301.03	37.19	16.0
C	19/09/97	0	0.80	40.25	14.7
C	19/09/97	5	0.98	24.63	16.8
C	19/09/97	10	0.81	27.06	16.8
C	19/09/97	15	0.66	27.17	15.3
C	19/09/97	20	0.59	26.71	15.3
C	19/09/97	25	1.48	26.53	15.2
C	19/09/97	30	2.00	22.73	14.9
C	06/10/97	0	0.24	31.28	15.1
C	06/10/97	5	3.42	14.9	14.9
C	06/10/97	10	0.57	20.46	14.9
C	06/10/97	15	0.45	21.72	15.0
C	06/10/97	20	0.48	21.03	15.0
C	06/10/97	25	0.19	16.84	15.0
C	06/10/97	30	0.28	20.43	14.9
C	03/11/97	0	79.26	30.83	11.5
C	03/11/97	5	188.81	35.77	11.4
C	03/11/97	10	273.50	33.51	11.4
C	03/11/97	15	227.73	35.27	11.8
C	03/11/97	20	440.31	23.87	11.8
C	03/11/97	25	305.52	34.73	12.1
C	03/11/97	30	257.94	36.98	12.2
C	04/02/98	0	0.73	38.03	9.2
C	04/02/98	5	1.68	25.29	8.1
C	04/02/98	10	1.42	24.43	7.3
C	04/02/98	15	5.62	22.24	7.1
C	04/02/98	20	29.95	21.55	7.3
C	04/02/98	25	58.24	20.35	7.3
C	04/02/98	30	37.91	20.26	7.3

3.5.2 Spatial variability of sedimentary methane and water content

Effect of sediment type on methane concentrations (nM) and water content (% by weight) in sediment depth profiles on 1 July 1997 (mud) and 11 July 1997 (sand) (Figure 3.5.2.1).

Depth	Sand	Sand	Mud	Mud
cm	nM CH ₄	% water	nM CH ₄	% water
0	34.6	23.6	168.6	40.9
5	26.0	23.3	142.7	31.7
10	64.7	23.2	322.7	34.2
15	181.4	22.2	408.3	29.3
20	132.8	22.2	1868.0	29.8

Effect of tidal exposure on sedimentary methane concentration on 24 July 1997 (Figure 3.5.2.2).

Depth	High shore	High shore	Mid shore	Mid shore	Low shore	Low shore
cm	μM CH ₄	% water	μM CH ₄	% water	μM CH ₄	% water
0	0.145	32.24	0.362	32.6	0.295	37.83
5	0.162	33.01	0.387	31.9	0.980	30.14
10		39.06	0.330	33.1	0.965	26.98
15	0.356	37.51	0.495	29.2	1.016	30.23
20	0.724	27.75	0.507	26.6	1.462	22.89
25	0.747	33.05	0.609	26.7		

Heterogeneity in pore water methane (μM) and water content (% by weight) in triplicate sediment cores from Menai Bridge mudflats station C on 21 August 1997 (Figure 3.5.2.3).

Depth	Rep 1	Rep 1	Rep 2	Rep 2	Rep 3	Rep 3
cm	μM CH ₄	% water	μM CH ₄	% water	μM CH ₄	% water
0	18.84	47.45	63.07	45.68	26.07	40.24
5	73.99	27.37	121.25	29.36	124.00	24.35
10	101.96	30.66	154.07	26.94	293.67	20.65
15	102.01	22.66	182.49	21.79	175.10	23.73
20	126.78	22.93	136.38	29.19		31.79
25	117.62	28.71	135.24	35.56		34.7

Appendix 3-6

Raw data for sediment incubation experiment (Chapter 3.6)

21 August 1997: Interstitial methane and % water in sediments (by weight) in triplicate cores – see Appendix 3.5.1

28 August 1997: Interstitial methane and % water in sediments incubated at 5, 15 and 25°C

Depth cm	5°C μM CH ₄	5°C % water	15°C μM CH ₄	15°C % water	25°C μM CH ₄	25°C % water
0	15.5	27.00	19.7	34.81	9.8	41.75
5	143.9	27.95	226.4	23.88	130.5	26.86
10	178.3	26.60	224.2	24.13	153.1	28.18
15	173.6	29.62	215.6	24.87	114.1	20.24
20	131.9	31.83	163.8	26.19	99.8	24.52

16 September 1997: Interstitial methane and % water (by weight) in sediments incubated at 5, 15 and 25°C

Depth cm	5°C μM CH ₄	5°C % water	15°C μM CH ₄	15°C % water	25°C μM CH ₄	25°C % water
0	2.6	30.03	1.3	35.87	4.5	28.70
5	79.9	26.15	19.4	23.07	21.8	29.41
10	159.7	24.46	52.0	24.66	31.0	21.88
15	185.8	25.00	178.7	27.76	32.8	24.91
20	143.1	27.81	67.1	27.02	35.6	30.96

03 October 1997: Interstitial methane and % water (by weight) in sediments incubated at 5, 15 and 25°C

Depth cm	5°C μM CH ₄	5°C % water	15°C μM CH ₄	15°C % water	25°C μM CH ₄	25°C % water
0	2.6	39.47	3.9	34.52	2.0	42.53
5	113.2	34.30	33.3	24.45	22.1	23.83
10	187.2	28.86	111.9	21.77	42.8	25.67
15	172.0	27.03	179.1	24.81	76.6	22.10
20	112.5	22.82	196.3	30.08	23.2	19.51

31 October 1997: Interstitial methane and % water (by weight) in sediments incubated at 5, 15 and 25°C

Depth cm	5°C μM CH ₄	5°C % water	15°C μM CH ₄	15°C % water	25°C μM CH ₄	25°C % water
0	1.2	32.05	3.9	28.81	0.3	26.59
5	18.0	26.37	28.4	24.95	2.6	20.23
10	91.1	28.53	76.0	24.59	3.8	22.25
15	125.4	20.74	173.5	23.63	5.9	23.02
20	16.1	23.02	161.8	26.50	3.0	26.34

Appendix 4-1

Diffusion into spherical particles: Derivation of equation 4.1

The oxygen concentration (O_b) at distance b from the centre of a particle with radius ra or at the centre of the particle itself (O_c) can be calculated from the rate of oxygen influx into the particle by molecular diffusion (diffusion coefficient D_o) from the external seawater matrix with oxygen concentration O_{ex} , and the rate of internal oxygen removal (c) by aerobic respiration by heterotrophic bacteria living in and on the particle.

Figure A 4-1 visualises these processes.

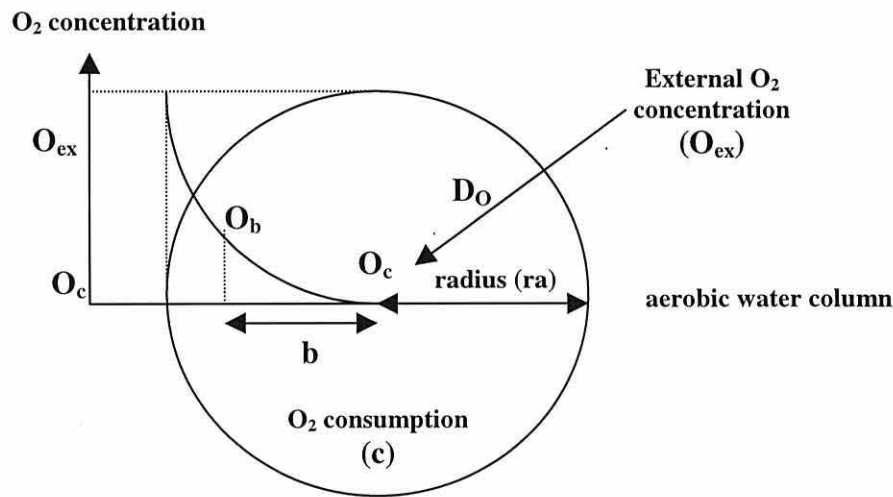


Figure A 4-1 Diagram showing the oxygen distribution in a spherical particle as produced by the interaction of oxygen influx and removal. Explanation of symbols can be found in text (after Jørgensen, 1977).

Under steady state conditions the supply of oxygen via diffusion into the particle is equal to the rate of oxygen removal. Mathematically, this can be expressed as:

$$\frac{\delta O}{\delta t} = D_o \times V^2 O - c = 0 \quad (\text{A 4-1})$$

where O is the oxygen concentration, t is time and $V^2 O$ is the Laplace operator which describes the not constant gradient of change.

For conditions of radial symmetry of the particle, $V^2 O$ is expressed as:

$$V^2 O = \frac{1}{ra^2} \times \left(ra^2 \times \frac{\delta^2 O}{\delta ra^2} + 2ra \frac{\delta O}{\delta r} \right) \quad (\text{A 4-2})$$

Combining equations A 4-1 and A 4-2 in a differential equation results in:

$$D_o \times \frac{1}{ra^2} \times \frac{\delta}{\delta ra} \times \left(ra^2 \times \frac{\delta O}{\delta ra} \right) - c = 0 \quad (\text{A 4-3})$$

Integrating and solving equation A 4-3 to calculate the oxygen concentration in the centre of the spherical particle:

$$O_c = O_{ex} - \frac{c}{6D_o} \times ra^2 \quad (\text{A 4-4})$$

or the oxygen concentration (O_b) at distance b from the particle centre:

$$O_b = O_{ex} - \left(\frac{c}{6D_o} \right) \times (ra^2 - b^2) \quad (\text{A 4-5})$$

Thus, the radius of a spherical particle in which the only the very centre achieves anaerobiosis ($O_c=0$) can be calculated from:

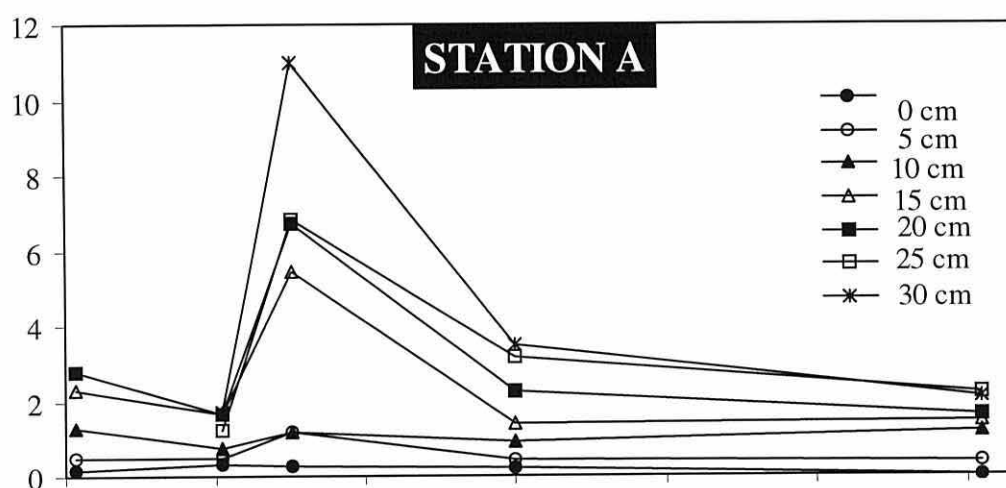
$$ra = \sqrt{\frac{O_{ex} \times 6D_o}{c}} \quad (\text{A 4-6})$$

Appendix 4-2

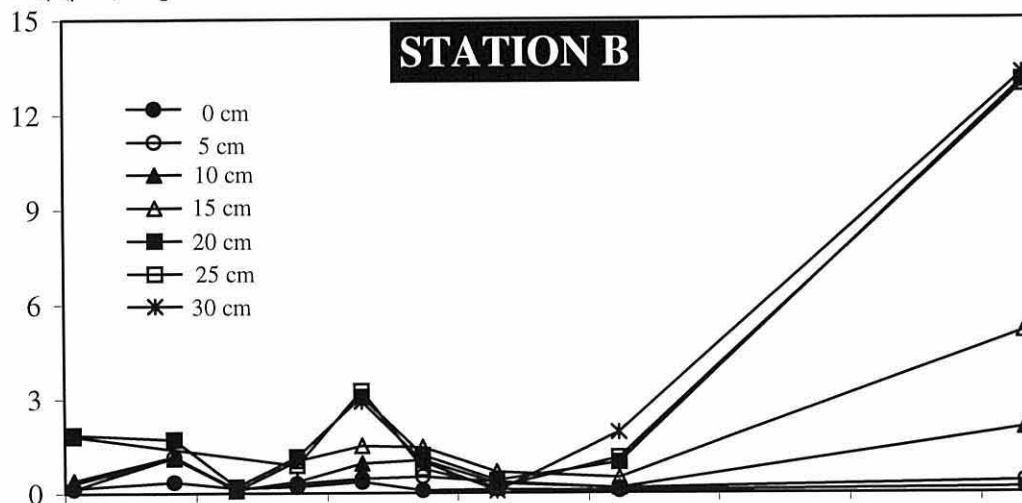
Distribution of methane at several sediment depths with time at stations A, B and C in the Menai Bridge mudflats

The following figures represent the seasonal sediment data in Figures 3.5.1.1 A, 3.5.1.2 A, and 3.5.1.3 A plotted against time instead of sediment depth.

CH₄ (uM) in pore water



CH₄ (μM) in pore water



CH₄ (μM) in pore water

